Cranfield University

Cranfield Health

PhD

Damion K Corrigan

Analytical technology for cleaning verification and analysis of drug purity in pharmaceutical production.

Supervisors: Professor Sergey Piletsky and Dr Sean McCrossen

February 2008

This thesis is submitted in fulfilment of the requirements for the Degree of Doctor of Philosophy

Abstract

Production of pharmaceuticals is a complex process which goes beyond the synthetic reactions undertaken to produce the final drug product. In multi purpose manufacturing facilities the equipment used in the processes must be proven to be sufficiently free of residue from the previous compound so that safe manufacture of the next compound can commence. Cross contamination can pose serious health risks so cleaning verification is a process of extreme importance.

Pharmaceutical products may contain impurities that originate from the synthetic stages of production, the starting materials or from *in situ* reactions taking place in the final drug. Some of these impurities may be genotoxic. Genotoxic impurities are a class of impurities for which awareness is currently growing in the pharmaceutical industry.

Traditional analytical chemistry methods such as HPLC are currently employed for the detection and quantification of cleaning residues and genotoxic impurities. These methods can be extremely time consuming. The aims of this project are to investigate swab sampling in cleaning verification, to develop alternative analytical methods which speed up and enhance knowledge of the cleaning verification process and to begin the development of an assay system for commonly occurring genotoxic impurities.

Acknowledgements

I would firstly like to thank my supervisors Professor Sergey Piletsky and Dr Sean McCrossen for their supervision, advice and encouragement with this project. I would like to thank Dr Michael Whitcombe for his help and support throughout the study. Dr Kal Karim, Dr Elena Piletska and Dr Iva Chianella for their help and guidance. Dr Michael Cauchi for his help with Principal Component Analysis. Also the other members of my laboratory for their help.

I would like to thank my friends and family for their support and encouragement throughout the course of the study and in particular my girlfriend Amy Rawlins.

Nomenclature and abbreviations

IR – infrared

NIR – near infrared

SERS – surface enhanced Raman spectroscopy

ACN – acetonitrile

DMF – n,n-dimethylformamide

THF – tetrahydrofuran

NMR – nuclear magnetic resonance

PCA - Principal Component Analysis

Table of Contents

List of Figures

List of tables

1 Introduction

1.1 Pharmaceutical production: cleaning verification and genotoxic impurities.

Pharmaceuticals are produced in specialist manufacturing facilities. Some facilities are dedicated to the production of a particular drug but some facilities may be multi purpose. In multi purpose plants the equipment must be proven to be sufficiently free of the previous drug in order for production of the next drug to commence. This means the machinery must be appropriately clean with residue from the previous drug proven to be at a predetermined target level. The process by which the plant is determined as clean is known as cleaning verification and the process involves sampling from equipment surfaces and subsequent analysis of those samples.

The quality of pharmaceutical product is critically affected by a production step which is neither productive, nor in a sense pharmaceutical. This production step is the cleaning of pipes, equipment and containers bearing pharmaceutical products (Zeller, 1993). Its planning, performance and validation are important in the production of pharmaceuticals.

Figure 1.1. Photographic example of a pharmaceutical pilot plant. The presence of large surface area, plus pipes, valves etc means that cleaning is an arduous process and it must be done rigorously to ensure that residues are eliminated. Source:http://www.ittallaght.ie/science/nationalpharmaceuticaleducationcentre/pharmaceuticalpilotplant/

The development of rigorous cleaning verification systems is critical to companies involved in the manufacture of pharmaceuticals. Responsibility lies with the manufacturer to develop robust cleaning procedures and to demonstrate that the execution of the cleaning procedure was successful. Success of cleaning is shown by analytical testing of the equipment involved in manufacture for both residual drug ingredients and cleaning agents introduced during the cleaning process itself (Shifflet and Shapiro, 2002).

Impurities can accumulate in drug products as by products from either the synthetic reactions/intermediates involved in the manufacturing process, impurities from the starting materials or from *in situ* reactions taking place in the drug product involving classes of compounds such as residual solvents. Some of these impurities may have

unwanted toxicities such as genotoxicity or carcinogenicity and therefore have an effect on a product's risk assessment (Muller *et al.,* 2006).

Pharmaceutical companies are under pressure to limit impurities and therefore cleaning verification and measuring genotoxic impurities are two areas of interest. Both represent emerging areas of research; the reason being analytical technology improving to a point where residuals on manufacturing equipment are much more apparent and awareness of impurities and their potential toxicological effect is greater than in the past. Cleaning verification also represents a significant cost factor to the pharmaceutical industry and this is because the process currently relies on chromatographic methods such as HPLC for sample analysis. Sampling must be representative of the equipment train used to produce a particular drug and this can lead to the generation of a significant number of samples for analysis. Manufacturing downtime can be significant because HPLC analysis is a lengthy process particularly when the number of samples is so high. The failure of one sample can trigger a recleaning of the equipment and so change over or release of the plant as it sometimes known can take weeks. This period of downtime represents a significant incursion of costs because the plant is effectively standing idle.

Genotoxic impurities represent an unwanted class of impurities which the pharmaceutical industry is becoming increasingly aware of. Genotoxic impurities can be reduced or eliminated by selecting appropriate synthetic routes, solvents and intermediates but it is acknowledged by the regulatory bodies of the pharmaceutical industry that the presence of impurities and therefore potentially genotoxic impurities

in pharmaceutical products is almost inevitable. The industry's aim is to control the types and quantities of impurities in their drugs.

1.1.1 Aims and objectives

The aims and objectives of this project are: to enhance the understanding of aspects of the cleaning verification process, to investigate potential analytical technologies that could be implemented to speed up the process of cleaning verification and to develop an analytical technique to detect the presence of genotoxic impurities in drug samples.

The characteristics of different commercially available swabs were tested in order to identify the best swabs for swab sampling. The investigation shed light on aspects of the sampling process that are important within the field of cleaning verification. The work is presented in chapter 3 and the outcome was an increased understanding of the issues associated with swab sampling.

Alternative cleaning verification technologies were introduced and tested. The introductory section of the thesis contains information on optical spectroscopies and chapter 4 will present results on the investigations of the chosen techniques and their potential use within cleaning verification.

Optically active dyes were investigated with the aim of developing an assay or sensor for the presence of genotoxic impurities in drug products. The results of these investigations are presented in chapter 5. Chapter 6 contains an overall discussion of the work undertaken during this programme of research.

2 Literature Review

2.1.1 Cleaning – definitions and outline

Cleaning validation and cleaning verification are two terms used in the area of cleaning pharmaceutical equipment. A cleaning process must be validated before it can be implemented on the industrial scale. The strategy of validation should be defined, often validating from the worst case of cleaning so subsequent reductions can be made. Personnel should be trained in terms of plant operations, processes and cleaning methods for the drug of interest and standard operating procedures are written for, plant operations, plant processes, method of cleaning and sampling and testing methods. The cleaning method should be optimised where necessary during the development of the cleaning procedure. The work should highlight potential problems such as poor solubility, scale build up, critical parts of the plant which may require testing and any affinities of the products to stick to manufacturing equipment. The analytical method should be chosen appropriately and validated so that accuracy and sensitivity are known. The sampling plan should be designed so that it is representative of the manufacturing equipment train, particularly any curved pipes or valves where material can accumulate and then documented in the validation protocol. Toxicological and medical data should be documented so that cleaning limits can be agreed (Pharmaceutical Quality Group, 1999).

Sampling, analysis and limits are vital aspects of both cleaning validation and verification. Verification and validation mean slightly different things but sometimes their use in the literature isn't always clear. Cleaning validation refers to the validation of the cleaning processes to be used in a plant and covers the aspects of

setting up a validated cleaning programme. All aspects of the validated cleaning programme should be documented as this is subject to regulatory scrutiny. The overall aim of cleaning validation is to design a valid cleaning protocol. Cleaning verification refers primarily to the process of cleaning and checking the plant for contamination once production has begun and the appropriate cleaning protocol is in place. The two definitions are loose and used interchangeably in the literature but from henceforward the term cleaning verification will be used in this thesis unless specifically referring to the process of validating a cleaning regime.

2.1.2 Cleaning Verification – background and regulatory expectations

The US Food and Drug Administration (FDA) has noted that US drug products are of a generally high quality, however there is an increasing trend towards manufacturing related problems leading to recalls and disruption of manufacture (Urbas & Lodder, 2003). Jenkins & Vanderwielen, 1993 presented evidence that the number and severity of FDA citations over cleanliness was increasing and this showed that regulatory authorities were placing greater emphasis on cleaning. Low manufacturing process efficiency has also led to an increased cost of drugs and emphasis on good manufacturing practices (GMP) as the means of controlling drug quality has led to a widespread reluctance amongst companies to innovate within the manufacturing sector of their business. Such problems have led the FDA to conclude that a new scientific understanding of the drug production process achieved through the use of new technologies should be used to provide science-based approaches to improving the quality of the manufacturing process (FDA, 1993).

Attention to cleaning procedures from the regulatory bodies of the pharmaceutical industry is increasing. Increased levels of scrutiny from the authorities make it necessary for companies to better understand their cleaning verification processes. The mandate of cleaning verification is very simple, the idea is to reduce the levels of contaminants to below those deemed acceptable before commencing the manufacture of another drug. The greatest concerns are associated with instances where equipment is used to manufacture multiple active pharmaceutical ingredients (APIs) and where cross contamination can have potentially deleterious effects.

Regulation of cleaning verification is not a rigid process and the individual cleaning programmes need to be tailored to suit the pharmaceutical product manufactured. In it's 1993 document, entitled Guide to Inspections Validation of Cleaning Processes the FDA lists its expectations.

FDA expects firms to have written procedures (SOP's) detailing the cleaning processes used for various pieces of equipment. FDA expects firms to have written general procedures on how cleaning processes will be validated. FDA expects the general validation procedures to address who is responsible for performing and approving the validation study, the acceptance criteria, and when revalidation will be required. FDA expects firms to prepare specific written validation protocols in advance for the studies to be performed on each manufacturing system or piece of equipment which should address such issues as sampling procedures, and analytical methods to be used including the sensitivity of those methods. FDA expects firms to conduct the validation studies in accordance with the protocols and to document the results of studies. FDA expects a final validation report which is approved by

management and which states whether or not the cleaning process is valid. The data should support a conclusion that residues have been reduced to an "acceptable level." (FDA 1993).

2.1.3 Cleaning

Cleaning personnel should have clean room garments including: boots, cover alls (normally woven polyester), masks, hoods and gloves for cleanliness and safety (Cooper, 1997). The recommended steps for wiping are:

Fold the wiper into quarters, obtaining several clean wiper surfaces (figure 2.1). Folding helps to better distribute the pressure of the fingers and the hand. Wipe on a pattern of parallel strokes with some overlap, changing the surface of the wiper on every stroke. Start each stroke at the cleaner end of the path to be cleaned. Change the wiper after approximately every ten wiper lengths of surface. This should be done more frequently if the surface is visibly dirty (figure 2.2). To disinfect, use a saturated wiper and leave a visible film of disinfectant. (Cooper, 1997)

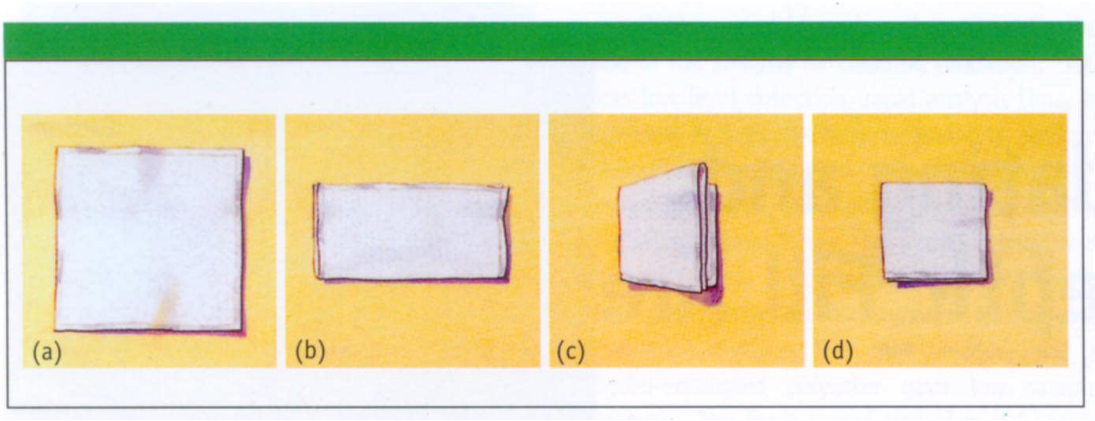

Figure 2.1. Showing how the wiper should be folded prior to cleaning. Folding into quarters helps the worker to better distribute pressure from their hand. Source: Cooper, 1997.

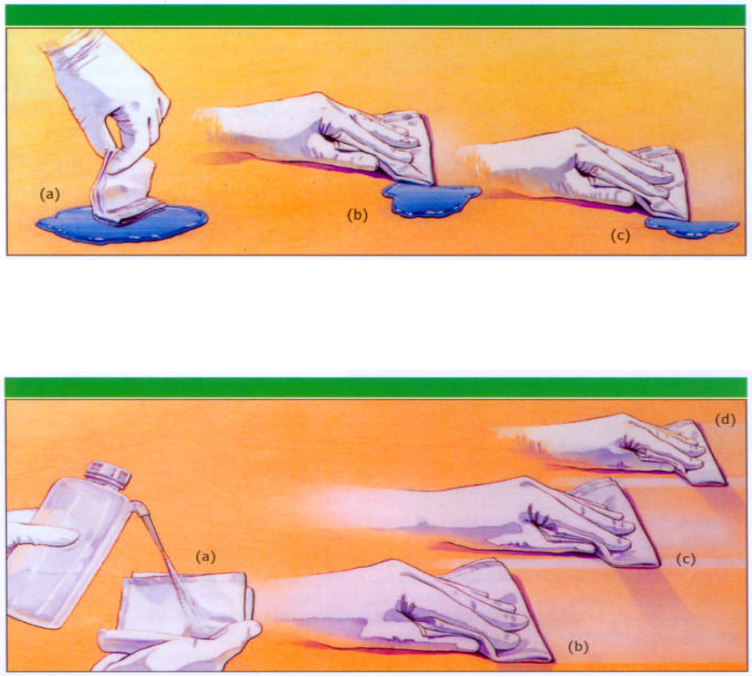

Figure 2.2. Showing the recommended method for cleaning surfaces by hand. It is recommended that the worker start from the cleaner end of the path and wipe in overlapping strokes. Source: Cooper 1997.

The success of cleaning has been evaluated by adding dye to product surrogates and then swabbing the surfaces and analysing the swabs for traces of the dye (Gavlick *et al.,* 1995). A similar procedure can be carried out where the drug itself or cleaning residues are tested for rather than the dye (Zeller, 1993). Cleaning validation needs to take into account the nature of the surfaces being tested. Flat surfaces are relatively easy to analyse and it is also easy to calculate the area of surface being analysed. There can be a tendency to avoid corners and depressions with some people recommending the use of pointed swabs to recover residues from hard to reach areas (Zeller, 1993). Others recommend using rinse analysis for sampling in hard to reach areas such as corners, depressions and around valves (Gavlick *et al.,* 1995). However, as will be stated there are problems associated with rinse analysis.

Understanding the removal of sample from the swab for analysis is another important part of the cleaning validation and verification processes (see figure 2.3). Usually swabs are employed to remove materials from the surface of interest. The swabs are immersed in liquid and then agitated or sonicated in order to liberate as much material as possible. Three of the most important criteria when choosing the correct swabbing material for cleaning verification are:

1) Minimal background - background is the amount of contamination on the swab. The procedure must be validated to take this into account. Blank contribution from the swab must be minimal.
2) High recovery rate - this is essentially the percentage of contaminant actually measured by the analytical technique when the swab is spiked with a known

quantity of the species of interest. Sixty per cent recovery rates are acceptable, however, higher recovery rates are desirable.

3) Low particle generation - it is critical that as little material as possible from the swab be left behind on the surface of interest. These particles would further contaminate the surface (Miscoscio, 1997)

Figure 2.3. Showing the removal of samples from surfaces with a swab for subsequent analysis. Source: Miscoscio, 1997.

Nozal *et al.,* (2000) described a method where the removal of acetylsalicylic acid from glass, vinyl and steel surfaces was validated. They were able to achieve recovery rates of 86 per cent, 90 per cent and 94 per cent from glass, vinyl and steel by using moistened cotton swabs to recover the compound from the surface. Mirza *et al.,* (1999) carried out a study where they were able to use cotton swabs to achieve 87.5 per cent and 89.0 per cent recoveries of meclizine hydrochloride from stainless steel plates. Nozal *et al.,* (2002) again used their procedure of swabbing to achieve recovery rates of 88.5 per cent, 94.2 per cent and 95.2 per cent for vinyl, glass and steel for the drug sumatriptan succinate. Klinkenberg *et al.,* (2003) used cotton swabs

moistened with methanol to achieve a recovery rate of 90 per cent for amlodipine from stainless steel. All of these methods outlined used HPLC as the analytical technique. As is often stated in the literature, HPLC is the most widely used analytical technique for cleaning verification sample analysis within the pharmaceutical industry.

Equipment and facility design is a vitally important aspect of the cleaning process. Material selection depends upon the characteristics of the product to be handled. Materials should be smooth surfaces for which the product does not have any affinity such as glass, inert plastic and stainless steel. Tests to determine the absorption of chemicals by the surfaces of materials and desorption of chemicals from the materials into the drug formulation should be done at the development stage. This problem is of relevance to rubber and plastic. For example, preservatives from the drug can absorb into silicone rubber and mould release lubricants from plastic can enter the drug formulation (Pharmaceutical Quality Group, 1999).

Parts for cleaning should be easily dismantled, connections should be easily dismantled, dead legs should be avoided and in no case should extend beyond a length equivalent to six diameters of the pipe, tight bends in pipe work should be avoided, pumps should be easily dismantled, valves with easy clean designs should be selected and adequate drainage should be ensured (Pharmaceutical Quality Group, 1999).

Considerations such as those just outlined from the Pharmaceutical Quality Group 1999 are elements of understanding for the sampling process and must be considered when devising a sampling regime that is representative of the equipment train.

2.1.4 How clean is clean?

No standards for selecting safety margins or establishing cleanliness criteria exist within the industry. As a result, each company develops its own guidelines on cleaning requirements for the various compounds they manufacture. For example, one such approach uses daily intake as the basis for such determinations (Jenkins *et al.*, 1995). Acceptable daily intake for humans is normally calculated by applying a hazard risk factor to toxicological and pharmacological data which establishes a "no effect level" for humans. Typical hazard risk factors range between 1/100 and 1/10000 and usually vary in an inversely proportional manner relative to the potency of a substance and completeness of available toxicology/pharmacology data. A common practice observed in most companies today involves the use of three basic formulae:

1) The 10 ppm formula. This formula allows the presence of no more than 10 ppm of product A into the next products (B) maximum potential daily dose. Given the production scale of product B, the acceptance level is calculated as milligrams of product A per litre of cleaning solution.
2) The acceptable daily intake formula. This formula allows no more of product A into product B than what the acceptable daily intake dictates. The acceptable daily intake can be based on the eight hour acceptable worker exposure limit (AWEL).
3) The 1/1000 of therapeutic level formula. This formula allows no more than 1/1000 of product A's minimum therapeutic daily dose into product B's daily

maximum dose. Calculation requires knowledge of product B's production scale. (Jenkins *et al.,* 1995)

Depending on data availability, cleaning criteria are frequently based on the formula that results in the lowest number – most typically the 1/1000 of therapeutic level formula. It is apparent that the more active a particular drug is the lower the cleaning criteria would be and therefore the cost of maintaining product quality and personnel safety would be higher. This results in cleaning and decontamination being a serious concern and a major cost contributor to the manufacturing process (Valvis & Champion, 1999).

The first step when initiating a cleaning validation program is to define the strategy and make sure that the cleaning methods to be employed have themselves been validated (Gavlick *et al.,* 1995). The strategy must account for the range of products and types of equipment employed in the manufacturing process. The procedure must have minimum acceptance levels determined by acceptable numbers of trials and appropriate levels of sampling. The continuous improvement of analytical techniques means that the limit of quantification no longer represents the standard of cleanliness. Instead acceptable levels of impurities have to be set (Zeller, 1993). A number of publications have proposed acceptance levels for tolerable concentrations of contaminating substances. Nearly all of the proposed acceptance levels have one disadvantage in common; their definition is very rigid. Either a theoretical concentration is increased by a set value or an existing concentration such as the daily therapeutic dose gets reduced by a set percentage or a logarithmic value. Both of these methods create problems (Zeller, 1993).

The method of cleaning employed is related to the types of residue/material that must be removed from the manufacturing surface. This means that acceptable residue limits should be based on information related to the drug toxicological profile and its relative potency. The biggest problems are caused by highly potent drugs, or drugs with relatively high toxicities. Cleaning verification needs to be sufficiently sensitive in order to confirm that acceptable levels of cleanliness have been attained. In addition, more frequent validations and follow up monitorings may be necessary in the case of more potent drugs (Zeller, 1993). Other areas of difficulty for cleaning verification and therefore potentially in need of special attention are filling needles and tablet punches. Residue left behind on these devices can lead to significant contamination because of the critical role the equipment plays in the manufacturing process (Jenkins & Vanderweilen, 1994).

2.1.5 Sample collection

There are two major methods employed for collecting samples for analysis, these are residue collection by swabbing surfaces and residue collection by rinse analysis (Kaiser *et al.,* 1999).

Surface swabbing and rinse analysis have been fairly successful, but there are disadvantages associated with both methods. Swabbing is the more prevalent of the two procedures and some of the problems associated with it include: the requirement to physically collect samples from the surface, partial recovery of residues, problems associated with the recovery of residues from the swab itself and it is a lengthy procedure resulting in significant amounts of downtime. Rinse analysis can be used

in its own right or as a complementary procedure to swab analysis. Limitations with this approach include difficult method validation and residue solubility/detachment issues. Both methods present the additional difficulty of still having to ascertain the amount of residue remaining on the surface of interest (Gavlick *et al.*, 1995). In swab analysis, water is the most commonly used agent when dislodging material from the swab itself, although organic solvents such a methanol or hexane can be employed. In rinse analysis, the solvent could be organic, e.g. methanol or it could be the final water rinse that commonly marks the terminal step of the cleaning process.

The sampling technique plays an important role in determining which analytical method is to be employed. Some techniques are more compatible with swabbing and others more compatible with rinse analysis. An important factor to be taken into account when trying to select an analytical method is the nature of the sample itself. Residues can be: drug actives, formulation components, cleaning agents, organic, inorganic, water soluble, particulate, microbial and/or endotoxins (Zeller, 1993). In addition, it must be recognised that the chemical structure of the active ingredient can be altered by cleaning agents. If the cleaning agent is going to have an effect upon the chemical structure of the active ingredient, the worker needs to be aware of this so that the correct chemical structure is actually investigated (Gavlick *et al.*, 1995).

2.1.6 Sample analysis – requirements, options and constraints

In advance of selecting an analytical method, some definitions need to be considered. The limit of detection (LOD) is the lowest amount of a particular compound that can be detected. The limit of quantitation (LOQ) is defined as the lowest amount of a particular compound that can be quantified. The residue acceptance limit should be

above the LOQ so that it can be accurately quantified. (Kaiser *et al.,* 2001). The analytical methods involved in cleaning verification can be divided into two broad groups. Some are specific and some are non specific. Specific methods include: High Performance Liquid Chromatography (HPLC), ion chromatography, infrared spectroscopy, inductively coupled plasma, capillary electrophoresis and the other chromatographic methods. It must however be noted that not all of these methods are specific in that they will identify the potential contaminant without additional information. For example, HPLC can be used to separate out potential contaminants by manipulating the conditions within the HPLC instrument. Non specific methods will highlight the presence of particular types of compounds that produce a defined response. Some examples include total organic carbon (TOC), pH, titrations and conductivity (Kaiser *et al.*,1999). Titrations can be for acids or bases but not particular acids or bases. There are however specific titrations for classes of surfactants (Jenkins & Vanderweilen, 1994).

Deciding upon which analytical technique to use is obviously a multifaceted decision. Many of the articles within the literature describe HPLC and TOC as favourable approaches (Kaiser *et al.,* 1999). Other groups have looked at column liquid chromatography coupled to Fourier transform-infrared spectroscopy (Somsen *et al.*, 1998). Gas chromatography and Fourier transform-infrared spectroscopy is a well established system and commercially available units are in existence (Somsen et al., 1998).

The analytical methods chosen should also reflect an optimisation between practicality and reliability (Zeller, 1993). To achieve this optimisation, it is useful to

denote one ingredient in the formulation as a “guiding substance”. The criteria upon which the analytical technique is selected are: concentration of the concerned substance within the product, its UV absorption, its pharmacological potency, the existence of an analytical assay method and its solubility.

Another important element of cleaning verification is making sure that there are no residuals left from the cleaning agents employed. If a cleaning agent effectively removes the drug/product residues but leaves behind its own residue, then one type of contamination has been exchanged for another and the equipment has not been cleaned effectively. Thus, the analytical strategy must consist not only of assays for the determination of pharmaceutical product and cleaning agent residues, but also a clear rationale for choosing a particular assay (Gavlick *et al.*, 1995).

2.1.7 Analytical techniques associated with cleaning verification

Almost every pharmaceutical company has an HPLC instrument. HPLCs utilise a variety of detectors and these include: ultraviolet (UV), fluorescence, electrochemical, refractive index, conductivity and evaporative light scattering. The ultraviolet detector is by far the most common, however evaporative light scattering may well be the most appropriate detector for cleaning agents (Kaiser & Minowitz, 2001).

There are a number of advantages to using UV detectors and these include: the fact that many compounds contain chromophore groups, usually no additional reagents or pre-column or post column reactions are necessary, the technique is generally inexpensive and molar absorptions are generally not affected by temperature and therefore there is no need for heating or cooling the detector. Many instruments are

equipped with diode array spectral capabilities allowing for easy identification of impurities or potential contaminants. A disadvantage with UV detection is the fact that not all compounds have chromophores and this is particularly true of some surfactants used in the pharmaceutical industry (Kaiser & Minowitz, 2001).

Under the technique of evaporative light scattering detection the compound is separated on an HPLC column as usual, moved to a nebulizer that is combined with a gas stream and then passed through a heated column. The heated column incorporates the mobile phase leaving the solid analyte in the column. The solid phase then passes through a detector that consists of a laser or light source. The laser or light source is scattered when it hits the solid analyte. The detector then picks up this scattering. There are many advantages associated with evaporative light scattering detectors. The technique is described as universal because it can detect any sort of compound. Evaporative light scattering is simple, versatile, rugged in use and since it is a mass detector all compounds produce similar responses. The two main disadvantages are that there is a very limited choice of buffer salts (buffers that evaporate are necessary so that they do not remain behind and interfere with the solid phase). The second disadvantage is that the nebulizer and detector must produce a consistent particle size, careful cleaning and monitoring of the nebulizer is required (Kaiser & Minowitz, 2001).

Many different residues can be detected by HPLC techniques, including drugs and detergents. When dealing with detergent residues it is important to clearly identify what is being analysed because the separation and quantitation of these particular compounds is especially difficult (Kaiser & Minowitz, 2001).

Total organic carbon (TOC) analysis is determined by the oxidation of an organic compound into carbon dioxide. This oxidation can occur through a number of mechanisms depending on the instrument being used. Some typical methods are persulfate, persulfate/UV detectors and direct combustion. The carbon dioxide produced from these reactions is either measured by conductivity or infrared spectroscopy. Instruments generally measure the inorganic carbon content of a sample. The total carbon content of a sample is then determined and the inorganic portion deducted to yield the levels of total organic carbon. There are two primary advantages associated with total organic carbon analysis. Firstly, it does not take long to develop a method as there are not a lot of variables in the actual analysis. Secondly, the method is a very quick one (Jenkins *et al.,* 1996).

A significant disadvantage with total organic carbon analysis is the fact that the compound must be water soluble. Organic solvents cannot be used because they contribute to the final measurement. Another potential problem is that contamination can be an issue, the atmosphere, the swab itself, personnel and other sources can cause contamination. When a total organic carbon method is developed appropriate blanks and controls should be elucidated in order to ensure the correct levels of organic carbon are measured (Kaiser & Minowitz, 2001).

Jenkins *et al.,* 1996 showed ppm and ppb detection of pharmaceuticals and biopharmaceuticals and also discussed the potential for significant time savings with total organic carbon analysis but as discussed above there are widely known disadvantages with total organic carbon analysis. At this point it is pertinent to say

that HPLC remains the dominant analytical technique employed by the pharmaceutical industry for analysis of cleaning verification. Much of this is because of regulatory viewpoints and because companies for sound commercial reasons will follow the regulatory view point in terms of pharmaceutical production whilst maintaining an interest in cleaning verification research and analysis methods. Total organic carbon analysis will be discussed again further in the section on commercially available cleaning verification systems.

2.1.8 Helpful strategies

In many ways it is easier to dedicate a facility to the manufacture of one drug rather than having to clean to such stringent levels. Already there are certain drugs that must be manufactured in dedicated facilities. Penicillin and beta-lactam antibiotics are examples of drugs where an isolated facility is required for production. Another approach that can be taken by pharmaceutical companies is to try and group the manufacture of certain drugs to certain facilities in order to aid the cleaning process. When this occurs, the groupings are based on scientific data such as product type, product family and equipment type (Gavlick *et al.,* 1995). A potential mistake is to focus attention on the high volume or higher money making drugs when the lower volume drugs may be more potent and thus place the higher volumes at risk. Therefore, when looking at cleaning verification strategies the nature of all the products being manufactured in a particular facility must be taken into account (Gavlick *et al.,* 1995).

Clean in place (CIP) operations are becoming increasingly important within the pharmaceutical industry. The technologies were initially implemented within the

food and dairy industries. CIP systems offer significant benefits including automation and the ability to consistently produce uniform levels of cleanliness. Manually based systems are subject to operator based error and sometimes result in equipment not reaching the desired level of cleanliness. CIP systems are used mainly for cleaning tanks and transfer lines and they have a variety of designs ranging from a simple high pressure flush to a multiprocessor controlled multi task batch-type system (Myers *et al.*, 1997). Another method of obtaining a final sample for establishing cleanliness is that of conducting a boil out (Valvis & Champion, 1999). A boil out involves the refluxing of a solvent inside a closed vessel system in order to clean its interior surfaces and produce a representative sample. The cleaning effectiveness of a boil out relies on the combined actions of the dissolution, mixing shear and vapour extraction all resulting in an exponential dilution cleaning profile (Valvis & Champion, 1999). Clean in place systems can be used to facilitate the cleaning of hard to reach areas in a boil out procedure.

The potency and toxicological profile of a drug are extremely important factors when considering cleaning verification. Understandably, the pharmaceutical industry is the most heavily regulated of the industries of this type (paints, foods etc). The narrow concentration range over which compounds are therapeutically active dictates that the final concentration must be as accurate as possible. Also, people taking these drugs are often in a weakened state because of illness and are therefore less likely to tolerate excessive amounts of impurities. A result of this strict regulation is that the pharmaceutical industry is at the cutting edge of cleaning verification technology (Ciurczack, 1998). The cleaning verification process and its key check points are depicted in figure 2.4.

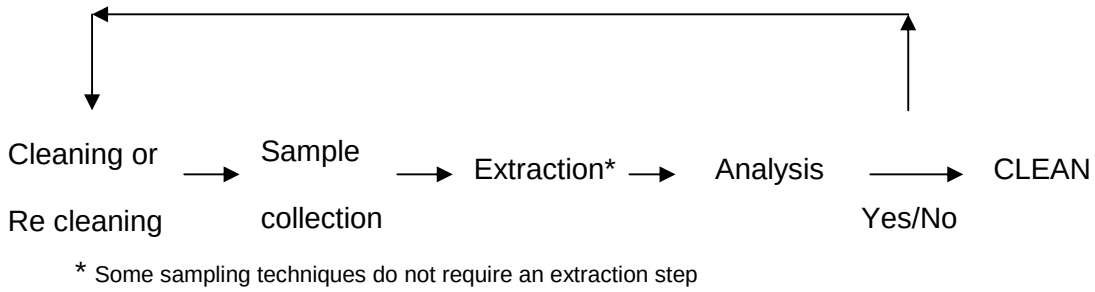

Figure 2.4. The key points in the cleaning verification process.

2.1.9 Commercially available cleaning verification systems.

Companies such as Texwipe provide commercially available swabs for cleaning verification. A variety of specific designs are available. Texwipe lists the benefits of their standard Alpha™ swab as: made from ultra low non volatile residue, gives low particle and fibre generation, good sorbency, contains no contaminating adhesives and has excellent chemical resistance. This standard swab is described as being suitable for cleaning verification, cleaning with solvents, applying lubricants and other liquids and removing excess materials. Long handled varieties can be purchased. The rationale behind the long handled design is that they improve the workers ability to carry out sampling in difficult to reach areas. Other designs include swabs with a variety of head shapes including triangular, pointed and rectangular, foam covered swabs that are designed to have improved absorbency for use in difficult to sample areas, mini compressed swabs with a micro tip head designed to clean grooves and channels. All of these different head designs can be purchased in a variety of handle lengths. Swabs are available that have been processed using a proprietary treatment

allowing the measurement of extremely low total organic carbon levels and are sold as part of a specialist total organic carbon kit. A variety of swab designs are shown in figure 2.5.

Figure 2.5. Four different designs of swab. The first is a standard swab, the second has a larger rectangular head, the third swab has a foam covering and is designed to be extra absorbent and the fourth is a microswab designed for sampling in grooves and channels. Source: www.texwipe.com

One of the focuses of this project is on developing a sensor or system aimed at speeding up the cleaning verification process. There would be little point in carrying out work on sensor technology when a commercially produced alternative is already available or imminent and so the current market has been reviewed and an assessment made on the worth of proceeding along the line of enquiry. Cleaning verification equipment breaks down into a small number of analytical technologies and approaches to cleaning verification taken by manufacturers of commercial products include: on-line UV monitoring, surface monitoring fluorimetry, total organic carbon

analysis, ion mobility spectrometry, and surface NIR. Any sensor system would have to offer the same low levels of detection that HPLC is capable of but offer advantages in terms of simplicity and time taken to carry out testing.

As a technology, UV monitoring offers a number of commercially available systems. UV technology is based around the fact that many of the compounds under investigation during the cleaning verification process contain chromophores. UV technology can be divided into two groups, the first group includes technologies that monitor the surface of interest directly and the second group comprises technologies that monitor the contents of the equipment train directly by being “on-line”.

The surface monitoring fluorimeter SMF2 manufactured by Safe Training Systems is a direct reading spectrofluorimeter that employs a xenon flash lamp in order to excite materials on the surfaces of interest. The resulting excitation is detected and a result produced. The technique is not suitable for full time use in a cleaning verification scenario for two main reasons, these are; making the device intrinsically safe is far too costly and the data produced from steel and glass surfaces is not of the required accuracy.

The Cleanscan system produced by Clairet Scientific was evaluated with cleaning verification in mind. The system is designed for on-line monitoring and consists of a UV diode array spectrometer and windows NT computer which has been enclosed in a stainless steel air purged cabinet thus providing intrinsic safety and making the device suitable for use in a plant environment. A fibre optic flow cell is located on the outside of the enclosure and is attached to the reactor via a series of hoses and

recirculation pumps. The system has advantages and disadvantages. The disadvantages include the fact that engineering difficulties arise because of the extra plumbing and there are problems with the software package provided. SpectrAlliance sell a more suitable software package along with hardware that is very similar to that of the Cleanscan system. A significant advantage of the SpectrAlliance system is that the data can be transmitted in a wireless fashion and the operator is not obliged to take a blank solvent reference spectrum before data collection can commence. A stored reference spectrum of the cleaning solvent is used, reducing the need for access to the flow cell and reduces the requirement to bring solvent bottles into the plant area. The system offers a series of significant advantages in terms of data storage, data management and protocol storage.

Expo Technologies market two products for cleaning verification the ePAT 631 (figure 2.6) and the ePAT 731 (figure 2.7). The ePAT 631 is designed for monitoring surface cleanliness and is based on a diode array UV spectrometer with a portable analyzer and detection limits of µg/cm2 can be achieved.

Figure 2.6. The ePAT 631 analyser manufactured by Expo technologies.

Figure 2.7. The ePAT 731 analyser manufactured by Expo technologies.

In comparison to the ePAT 631, the ePAT 731 operates from a different perspective in that it offers monitoring of rinsate. The system is based upon a diode array based UV/NIR spectrometer, designed to measure cleaning and final rinse solutions during the cleaning of API and drug product vessels. The system monitors cleaning based on a pre developed method for the active pharmaceutical ingredient of interest down to low levels and then the manufacturing equipment can be swabbed for off line analysis by HPLC. The system offers benefit by not ever triggering a re-clean because it monitors elimination of the compound and then subsequent verification of cleanliness can take place with swabbing and HPLC meaning there are no incidents where recleaning has to take place. With this product, there is no need to swab sample the equipment in a speculative fashion to find out if it is clean because the ePAT671 has shown elimination of the active pharmaceutical ingredient and therefore speeds up release of the plant.

Another technique for which many commercially available systems are in existence is ion mobility spectrometry. The technique involves the introduction of a sample into the machine which is then volatilised and accelerated down a drift tube to a detector. Different ions have different migration times and a series of plasmagrams (spectra) are generated. The technique is employed in situations where explosive or drug detection is needed such as airports or ports. The technique has limitations associated with it and these include the fact that it is extremely sensitive and therefore can either be swamped or cause cleaning to levels below those required. The linearity and reproducibility are often not as good as that seen in liquid chromatographic methods.

One company beginning to strongly market ion mobility detection for cleaning verification is Smiths detection (figure 2.8). The company state that technologies delivering low level, specific, high speed detection will become the leading technologies in the field of cleaning verification. They state that with ion mobility spectrometry a company can reduce their analysis time and speed up release of the plant, speed up the validation of cleaning protocols and reduce the cost per sample. The company claim the limit of detection for their system is typically between 10 pg and 1 ng or 1 ppb for a 10 µl injection or 1 ppm for a 1 µl injection, the limit of quantitation is usually three times higher than the limit of detection and that R^2 values typically exceed more than 0.999. In combination with their high pressure injection technique, Smiths have shown sensitive detection of active pharmaceutical ingredient down to 1 µg/ml.

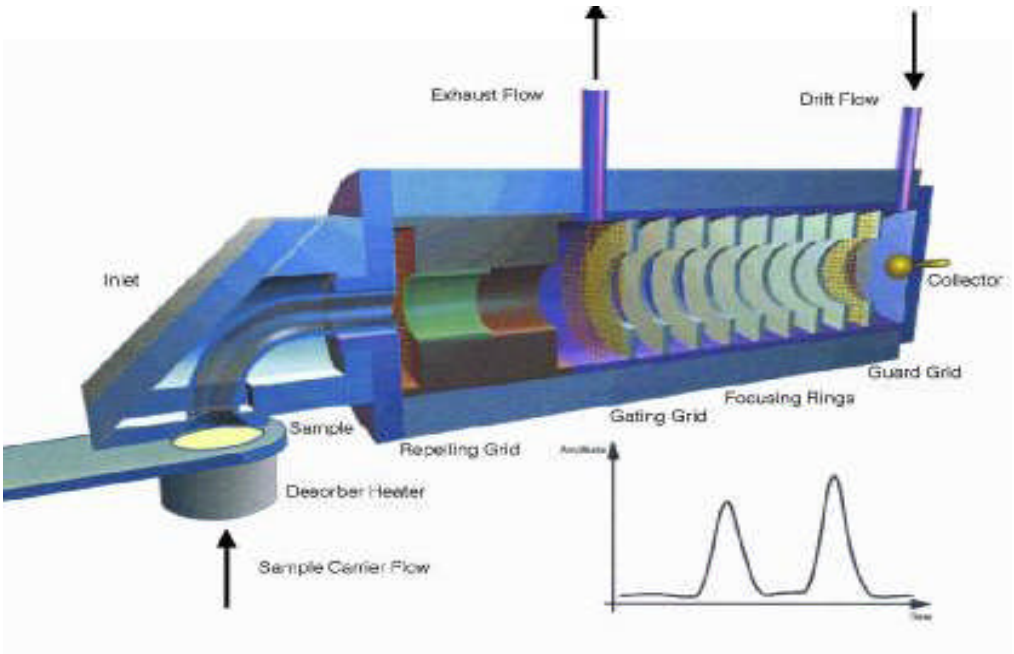

Figure 2.8. Summarising the Smiths Ionscan system. The sample is introduced after deposition on a Teflon filter and ions are accelerated down the drift tube before hitting a detector. The system can also be coupled to a high pressure injection device that introduces sample for analysis.

NIR is a technology that has shown some promise for cleaning verification. Improvements in fibre optic technology coupled with improvements in data handling are continually making NIR a more feasible option for cleaning verification. Additionally, improved signal to noise ratios have enabled the technique to be taken seriously as one capable of detecting at low levels. An example of a commercially available NIR system is the Iso-Pharm™ manufactured by LT industries. As well as offering the usual features associated with a NIR material analysing system machine the Iso-Pharm™ has a patented system that facilitates the safe transfer of data from one plant to another. This is particularly important because it allows raw material calibration libraries to be transferred. Another example of a commercially available product is the SpotView manufactured by Bruker Optics. The product is capable of *in*

situ analysis with the speed and sensitivity required for cleaning verification and consists of the Bruker Optics IRCube coupled with a patented grazing angle probe.

NIR is an emerging technology and there are advances still to be made. One of the current problems is that of sampling. Most machines work well on flat stainless steel surfaces but do not produce data of the same quality when working on curved surfaces, glass and vinyl. At present there would not appear to be a NIR technology capable of taking on the cleaning verification workload.

Two press releases by the Strategic Environmental Research and Development Program entitled "Cleaning Verification Techniques Based on Infrared Optical Methods" and "Visual Cleaning Performance Indicators for Cleaning Verification" provided examples of the direction in which thought regarding cleaning verification is heading. The project on visual cleaning performance indicators involved the use of commercially available and environmentally safe dyes and a coupling agent so that the binding of dye to surface contaminants could be visually detected (Strategic Environmental Research and Development Program: Pollution Prevention PP-1138). The other project, based on infrared optical methods involves measuring grazing incidence infrared reflectance on the surface and sought to build two devices, one based on a widely tunable infrared laser with high speed surface imaging capability that is limited to the detection of organic compounds and the second capable of high sensitivity detection of organic and inorganic compounds but at slower speeds and therefore incapable of real time analysis (Strategic Environmental Research and Development Program: Pollution Prevention PP-1117).

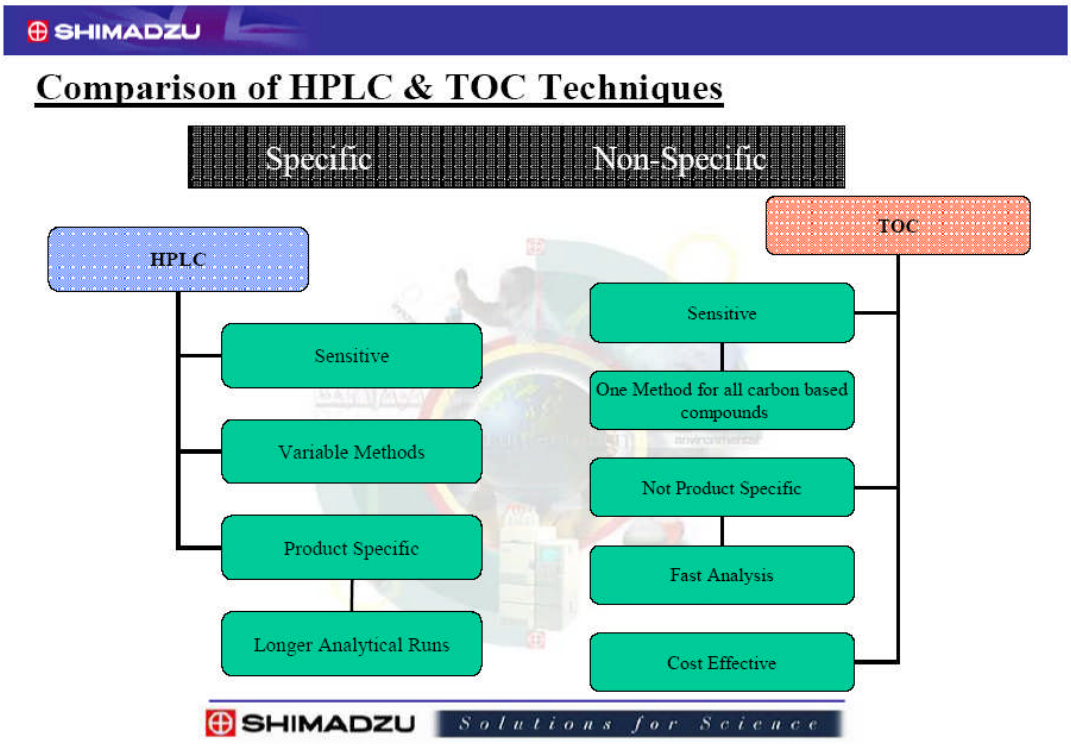

Figure 2.9. Companies such as Shimadzu market their Total Organic Carbon analysis systems for cleaning verification. This diagram illustrates that Total Organic Carbon analysis is a quick and cost effective method but also highlights that it is non specific. Source: www.ssi.shimadzu.com

Shimadzu point out that Total Organic Carbon analysis is suitable for cleaning verification because of its high levels of sensitivity provided the sample contains carbon and is soluble at the levels needed for the assay. The FDA perspective on Total Organic Carbon analysis for cleaning verification has changed since the 1993 Inspection Guide on Cleaning Verification. In the 2005 questions and answers on good manufacturing practice, level 2 guidance, the FDA stated that since the publication of the 'Inspection Guide on Cleaning Validation' in 1993, a number of studies have been published to demonstrate the adequacy of TOC in measuring contaminant residues.

To summarise, it can be seen that there is a wide range of commercially available cleaning verification products. Many of the technologies are still at a developmental stage and cannot offer the same quality of information currently offered by HPLC. Techniques such as NIR still have to overcome some sampling difficulties encountered when trying to take measurements on a variety of different surfaces. Problems will always arise when trying to implement a new technology within a company but the supplier and purchasing company can often tailor the technology to meet the technical demands of the purchasing company.

With the FDA perspective on cleaning verification still clear it is potentially dangerous for manufacturing firms to deviate away from existing validated cleaning protocols and technologies. Not one of the technologies outlined in this section has seen significant take up and this underlines the point about how reliable and trusted the HPLC method has become. Companies manufacturing alternative cleaning verification technologies need to be able to demonstrate sensitivity and specificity and whilst techniques such as Total Organic Carbon analysis have the required sensitivity, they lack the specificity.

From the technologies outlined, the ePAT 731 looks promising because it does not take over from HPLC but eliminates the need for speculative sampling. A firm can know that their equipment is sufficiently clean and then carry out direct sampling and HPLC analysis. Also, the Ionscan system manufactured by Smiths detection represents a move towards ion mobility spectrometry being more widespreadly

adopted by the pharmaceutical industry. The emergence of technology such as ion mobility spectroscopy has been until now driven by the security industry.

Surface enhanced Raman spectroscopy (SERS) is an optical spectroscopic technique which will be introduced in the section on optical spectroscopies. A major point from this section in terms of the project aims is that companies are not currently seriously marketing optical and in particular SERS based technologies for cleaning verification. Explosive/narcotic detection systems based on SERS exist but no company is currently marketing a SERS based system for cleaning verification work. SERS has the potential for cleaning verification analysis because of its high levels of sensitivity, lack of sample preparation and quick detection time and therefore it will be a good technique to investigate with respect to cleaning verification..

2.2 Spectroscopic techniques

Optical spectroscopic techniques are technologies that could be put to use within the field of cleaning verification. The following section of the thesis discusses infrared, Raman and fluorescence spectroscopy and cites instances where application into the field of cleaning verification has been attempted. Figuire 2.10 presents a summary of infrared, near infrared and Raman spectra on one axis for the purposes of comparison.

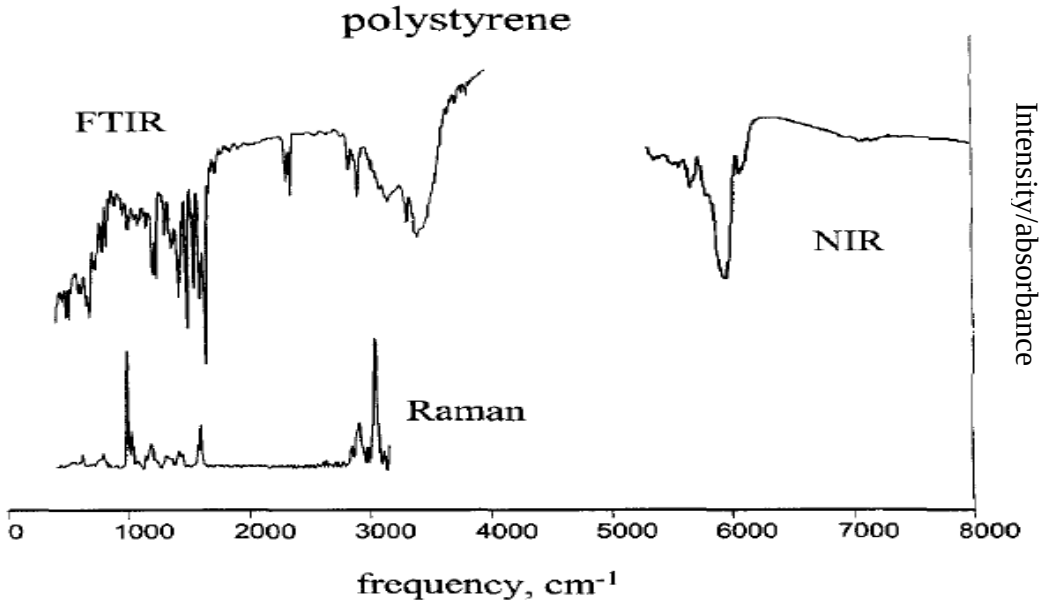

Figure 2.10. A representative diagram showing infrared transmission, near infrared transmission and Raman scattering on the same energy scale (x-axis) for polystyrene. The intensity on the y-axis is changed for infrared and near infrared because near infrared normally has a weaker absorption (McCreery, 1999).

2.2.1 Infrared Spectroscopy

The infrared region of the electromagnetic spectrum is normally divided into three sections. In the direction of longer wavelengths there are: the near, the mid and the far infrared regions. The standard mid infrared region used in infrared spectroscopy extends from the wavelength 2.5 μm to 25 μm. This region is often expressed in wavenumbers and extends from 4000 cm^{-1} to 400 cm^{-1} (Hollas, 2002). Wavenumber is a convenient tool of expression because the number is directly proportional to the amount of energy. Therefore a higher wavenumber equals a higher amount of energy.

Nearly all compounds with covalent bonds absorb radiation within the infrared region of the electromagnetic spectrum. As is seen with other types of absorption, infrared absorption causes the molecule to be excited into a higher energy state. Again, as is seen with the absorption of other types of radiation the process is quantised. The absorption of infrared radiation corresponds to energy changes of the order 8 to 40 kJ/mole (Stuart, 2004). Radiation of this energy bracket matches that of the vibrational frequencies of most covalent molecules. During the absorption process, the frequencies of infrared that match the natural vibrations of the molecule of interest will be absorbed. This absorption process is characterised by an increase in the amplitude of the vibrational motion of the bonds in the molecule.

An important point to make note of is the fact that not all bonds in a molecule are capable of absorbing infrared radiation, even if the frequency of the radiation matches that of the bond motion. Only bonds with a dipole moment that changes as a function of time are capable of absorbing infrared radiation (Gunzler & Gremlich, 2002). A bond must present an electrical dipole that is changing at the same frequency as the incoming radiation in order for energy to be transferred. The changing electrical dipole of the bond can couple with the sinusoidally changing electromagnetic field of the incoming radiation (Gunzler & Gremlich, 2002). Thus, a symmetric bond that has identical or nearly identical functional groups will not absorb in the infrared region.

The fact that every type of bond has a different natural frequency of radiation, coupled with the fact that two identical bonds in different compounds are in different environments results in the fact that no two molecules have the same infrared absorption patterns (Williams & Flemming, 1995). Therefore, to use a basic analogy,

the infrared spectrum provides us with a fingerprint of the molecule. The infrared absorption spectrum gives scientists extremely important information about a particular molecule's functional groups and an example spectrum is presented in figure 2.11.

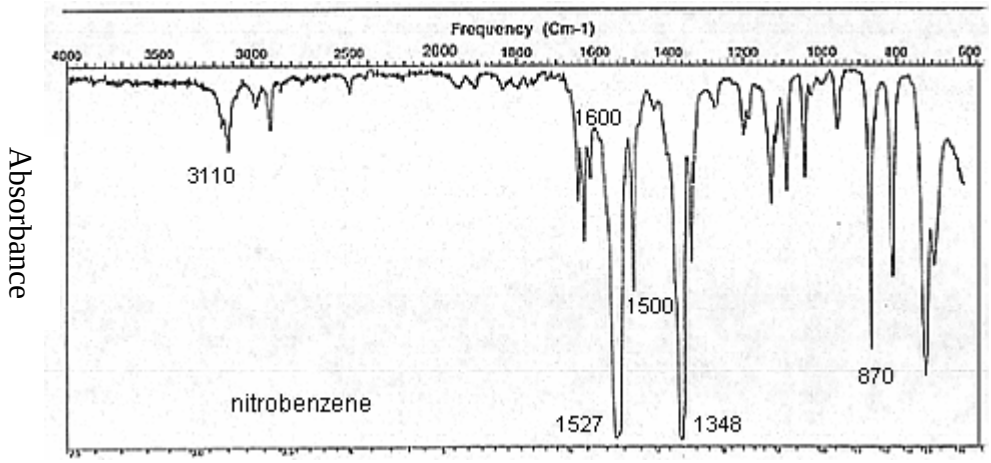

Figure 2.11. An example of an infrared spectrum for nitrobenzene. Source: www.chem.csustan.edu

2.2.2 Modes of stretching and bending induced by absorption of infrared radiation.

The most elementary modes of motion that are infrared active and can therefore be induced by infrared radiation are stretching and bending. In addition, there are more complex types of stretching and bending. Asymmetric stretching vibrations generally occur at higher frequencies than symmetric stretching vibrations and in general stretching vibrations occur at higher frequencies than bending vibrations (Hollas, 2002). The terms scissoring, rocking, wagging and twisting are commonly used in the literature to describe the origin of infrared bands. These vibrations are referred to as "fundamental absorptions" and are caused by the excitation from the ground state to

the lowest energy excited state. The different molecular vibrations are depicted in figure 2.12.

In any group of three or more atoms, where at least two are identical there are two modes of stretching, symmetric and asymmetric. Examples of such groupings are: -CH_3, -CH_2, -NO_2, –NH_2 and anhydrides. The methyl group gives rise to a symmetric stretching vibration at about 2872cm^{-1} and an asymmetric stretch at about 2962cm^{-1} (Gunzler & Gremlich, 2002) The anhydride functional group gives two absorption bands in the C≡O region because of the symmetric and asymmetric modes of stretch. A similar phenomenon occurs in the amine group where a primary amino (NH_2) usually has two absorptions in the N-H stretch region, whilst a secondary amine (RNH_2) has only one absorption peak. Amides exhibit similar bonds. There are two strong N=O stretch peaks for a nitro group, with the symmetric stretch appearing at about 1350cm^{-1} and the asymmetric stretch appearing at about 1550cm^{-1} (Gunzler & Gremlich, 2002).

Types of Molecular Vibrations

- Stretching
- Bending
  - scissoring
  - bending
  - twisting
  - wagging

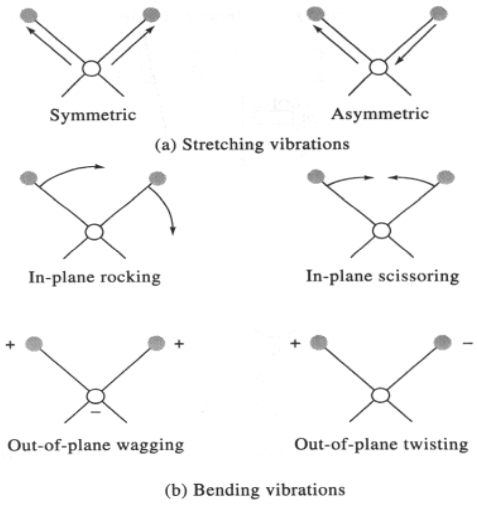

Figure 2.12. Showing different modes of stretching and bending in molecules exposed to infrared radiation. Source: www.tntech.edu/mcwells/ppt

Often the spectrum is complicated because of the presence of weak overtones, combination bands and difference bands. Overtones are caused by excitations from the ground state to higher energy states that correspond to integral multiples of the frequency of the fundamental (v). A suitable example is that of weak overtone bands being observed at 2v, 3v etc. Any type of physical vibration will result in the generation of overtones. Two vibrational frequencies can couple together and cause a frequency within a molecule. This is called a combination band and such bands are the sum of the two interacting bands. Not all possible combinations can occur.

Difference bands are similar to combination bands and the observed frequency results from the difference between the two interacting bands.

Overtone, combination and difference bands can be calculated directly by manipulating frequencies in wavenumbers via multiplication, addition and subtraction. When a fundamental vibration couples with an overtone or combination band, the coupled vibration is called Fermi resonance (Stuart, 2004). Rotational frequencies for the whole molecule are not infrared active, they will often couple with the stretching and bending vibrations in the molecule giving fine structure to the absorptions and thus complicating the spectrum (Stuart, 2004). This process of rotational coupling is one of the reasons why the bands in an infrared spectrum are broad and not sharp and can lead to a large amount of fine structure being unresolved.

2.2.3 The infrared spectrometer

There are two types of infrared spectrometer in common use, the dispersive infrared spectrometer and the Fourier transform-infrared spectrometer. Both machines yield spectra in the 4000-400 cm^{-1} range.

A general explanation of the dispersive infrared spectrometer starts with the fact that the instrument produces two equally intense beams of infrared radiation. The sample of interest is placed in the path of one beam and a reference in the path of the other beam. The beams then pass through the monochromator, dispersing each one into a continuous spectrum of infrared frequencies. The monchromator alternately passes the beams to a diffraction grating. The diffraction grating rotates slowly and varies the frequency or wavelength reaching the thermocouple detector. The detector itself

is able to determine which frequencies have been absorbed by comparing the beam that has been passed through the sample with the reference beam. The signal from the detector is then amplified, allowing the apparatus to produce the spectrum.

Most modern infrared spectrometers in use throughout laboratories operate on a different principle. The optical pathway produces a pattern called an interferogram. This is a complex signal but it contains all the infrared frequencies in a wave like pattern. An interferogram is essentially a plot of intensity against time. This is called a time dispersive spectrum, dispersive spectrometers are said to record the frequency domain (Williams & Flemming 1995). A mathematical operation called a Fourier transformation separates the individual absorption frequencies from the interferogram producing spectra virtually identical to that of the dispersive spectrometer. The advantages associated with Fourier transform-infrared spectroscopy are that it takes not much longer than a second to produce an interferogram. Therefore many interferograms can be collected and used to obtain a spectrum by applying the Fourier transformation.

Fourier transform spectrometers can be computer interfaced and operate in a single beam mode. The operator obtains interferograms for the background and then interferograms for the sample of interest. The background interferogram is then subtracted from the sample interferogram and the Fourier transformation carried out to yield spectra virtually identical to those produced by the dispersive machine. The most significant advances in infrared spectroscopy have come about as a result of the introduction of Fourier transform-infrared spectroscopy. The procedure has dramatically improved the quality of infrared spectra and minimised the time required

to obtain data. Additional improvements in computing power and software. have also allowed the field to make great improvements.

One of the greatest challenges for the infrared spectroscopist can be sample preparation. A number of sampling techniques have become available since the introduction of Fourier transform-infrared spectroscopy with its increased sensitivity and improved signal to noise ratio. The classic infrared sampling technique is the alkali halide pellet preparation. This technique involves mixing the solid state sample of interest with an alkali halide (typically KBr or KCl) at 1-2% (w/w) sample/alkali halide ratio, pulverising into a finely ground homogenous mixture, placing the mixture into a die (typically stainless steel) and subjecting it to approximately 10,000 psi of pressure for a period of time to produce a glass pellet (Bugay, 2000). The resulting pellet has the sample finely dispersed throughout the glass and can be placed into the spectrometer for analysis. This method of sampling is best in cases when simple compound identification is the goal. The pressure required to form the pellet and possible halide exchange can lead to transformation of the sample (Bugay, 2000).

The mineral oil mull technique is an alternative means of preparing samples. The sample is mixed in an agate mortar with a small amount of mineral oil. The sample is placed into an infrared window and then placed into a spectrometer. Unfortunately the mineral oil has a number of intense spectral peaks associated with it and these bands may overlap important peaks from the sample (Bugay, 2000). The diffuse reflectance method (DR) is probably one of the most important sampling techniques from the point of view of pharmaceutical problem solving. The technique is non intrusive.

When Fourier transform-infrared spectroscopy is applied to solid surfaces, three different techniques of reflectance spectroscopy can be used, specular reflectance, diffuse reflectance and reflection-absorption spectroscopy. Specular reflectance is used on flat, clean surfaces and spectra are readily obtained from comparatively small samples at incidence angles of about fifteen to seventy-five degrees. Diffuse reflectance spectra are commonly obtained from rough surfaces, or from the surfaces of powdered samples, often using specially designed accessories or spectrometers. The third type of reflectance spectrum, commonly called a reflection-absorption spectrum is fairly easily obtained from surfaces coated with thick fibres in the range of 0.2 to 2.0 μm. Simple reflectance spectra obtained from such surfaces are in effect transmission spectra obtained while the spectrometer radiation passes through the fibre before and after being reflected from the surface. However, in the cases of extremely thin layers such as monomolecular layers, the path length through the film may be too short to produce a useable spectrum. In practice, layers less than 10 μm in thickness cannot be successfully detected or characterised using conventional specular or diffuse reflectance geometries. The problem has been acknowledged and the method commonly known as grazing angle Fourier transform-infrared spectroscopy has been developed (Melling *et al.*, 2001).

Infrared microspectroscopy can be seen as the natural method of investigation for solid state samples. Ultimately, only one sample particle is needed but limitations with diffraction dictate that the particle needs to be bigger than 10 x 10 μm. The sample is placed in an infrared optical window and the slide is then placed into the microscope and visually inspected. When a sample of interest is located, the viewing

field is reduced and depending on morphology, thickness and transmittance properties, a reflectance and/or transmission infrared spectrum may be obtained by the infrared microscope accessory (Aldrich & Smith, 1999).

2.2.4 Infrared spectroscopy and cleaning verification

Fourier transform-infrared spectroscopy is now a well known and approved method for quantitative and qualitative analysis within the pharmaceutical industry (Severdia, 1995). As previously stated, swab analysis is the prominent method employed for sample recovery but is has several limitations that include incorrect estimations depending on the physical characteristics of the surface being investigated and excessive consumption of time. Traditionally, conventional Fourier-transform infrared spectroscopy has been used as a method to investigate the nature of samples recovered from swabs.

Bley and Behnring (2001) successfully implemented a system to carry out quantitative and qualitative evaluation of residual contamination on machine surfaces (see figure 2.13). The measurement system was based around Fourier transform-infrared spectroscopy with a specially designed flexible mid infrared fibre optic probe. They found that the residues recovered from the surfaces mainly resulted from: drugs, cooling lubricants hydraulic and guide way oils as well as machining chips and pigments. The installed fibre optic probe system connected to a conventional Fourier transform-infrared spectrometer proved capable of carrying out qualitative and quantitative residue recognition tests on contaminated work pieces. The qualitative tests (mainly used to determine the kind and composition of the residues) can be done

easily whereas the quantitative tests require a more prolonged planning stage to ensure accuracy.

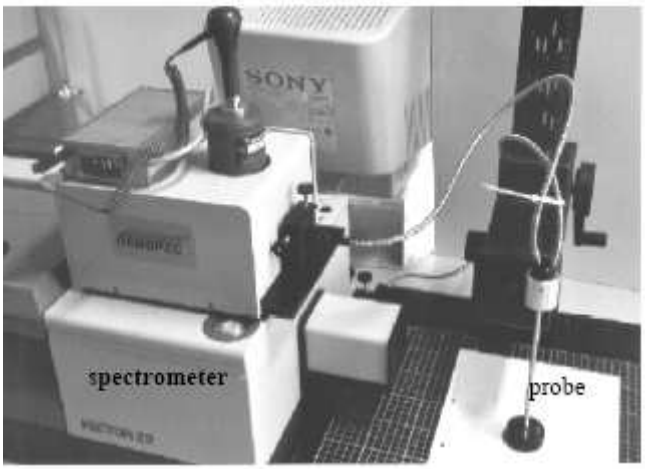

Figure 2.13. Flexible Fourier transform monitoring system devised by Bley and Behrning (2001).

Reflectance spectroscopy is a well known technique for obtaining Fourier transform-infrared spectra from powdered samples and surfaces (Sommer & Hardgrove, 2000). Mid infrared grazing-angle spectroscopy is the most sensitive optical absorption technique available for measuring low chemical concentrations on reflective materials (Mehta *et al.*, 2002). The disadvantage of conventional spectroscopic methods for applications such as cleaning verification is that samples must be physically placed within the sample compartment of the spectrometer for measurement. This limitation is not desirable for sampling reactor surfaces and around valves during the cleaning verification process. It is becoming increasingly possible to use Fourier transform-infrared spectroscopy to sample outside the compartment of the spectrometer. This has been facilitated by the emergence of fibre optic cables that transmit in the mid

infrared range. The result is that it is becoming increasingly feasible to carry out *in situ* spectroscopic testing (Mehta *et al.,* 2002).

Mehta *et al.,* (2002) designed a grazing angle head with a long fibre optic lead which allows a large surface area to be analysed at a great distance. These factors significantly improve the sensitivity and signal to noise ratio when compared to other methods using a mid infrared beam to sample the surface. The machine was used is a second experiment that compared it to swab testing combined with HPLC analysis. The mid infrared machine compared favourably showing that the low levels of residue could be detected accurately. The authors believed that by coupling it with chemometric methods, they would have a suitably sensitive method of measuring contamination on surfaces.

An ideal method for cleaning verification would be a rapid, automated, *in situ*, multi component analysis of the entire surface. A system of this nature would have eliminated the inadequacies associated with surface sampling. Advances in mid infrared fibre optics are beginning to yield instruments for *in situ* testing.

2.2.5 The near infrared region

The near infrared energy band is defined as 780 to 2500 nm, the mid infrared 2500 to 4000 nm and the far infrared region from 40000 to 1000000 nm. Even though official standards, textbooks and the scientific literature generally state that the near infrared spectral region extends from 780-2500 nm, a simple set of hydrocarbon spectra demonstrate that the vibrational information characterised by the harmonic vibrations of the C-H stretch fundamental and their corresponding combination bands occur

approximately from 690 to 2000 nm (Workman *et al.,* 2003). The predominant near infrared spectral features include the methyl C-H stretching vibrations, methylene C-H stretching vibrations, aromatic C-H stretching vibrations and O-H stretching vibrations. Minor but still important features include: methoxy C-H stretching, carbonyl associated C-H stretching, N-H from primary amides, secondary amides, N-H from primary, secondary and tertiary amino acids and N-H from amino salts (Workman *et al.,* 2003).

Pharmaceutical applications of near infrared include: identification of raw materials and product quality, moisture and solvent content in drying or solvent removal processes, residual drug carryover in manufacturing facilities, mixing quality evaluation and imaging of tablets and packaging systems (Wargo & Drennen, 1995).

There are a number of advantages associated with probing in the near infrared region and these include: C-H associated vibrational information is repeated eight times from 690 to 3000 nm. Sample harmonics may be selected or more information from rich combination regions may be seen. Low cost instruments with high signal to noise ratios are simply made and typically exhibit signal to noise ratios of 25,000-100,000 to 1. High near infrared throughput is possible even when employing low cost fibre optics. Variable pathlengths for individual use are possible, typically from 1 mm to 10 cm or more using different near infrared spectral regions (Ciurczak, 1998).

The ability to discriminate between components, the rapidity and the *in situ* capabilities make near infrared appealing. However, there are problems with sample size that need to be addressed. Implementation of near infrared into cleaning

verification is still a work in progress. Instruments that have already been developed require lots of validation work. As with conventional infrared, an ideal machine would be rapid, sensitive and able to sample a variety of surfaces (Yoon *et al.*, 2004).

When routinely analysing a pharmaceutical product with near infrared, two basic procedures are involved. The first is the determination of one of several components (quantitative analysis), using a suitable calibration step based on algorithms, these are step wise linear regression or partial least squares. In order to carry out calibration, it is necessary to use production samples, but this has the disadvantage of having a very narrow concentration range. It has now been suggested that laboratory samples be used to widen the concentration ranges of different types of molecules (Ciurczak, 1998). Quantitative methods are possible when changes in the response of the near infrared spectrometer are proportional to changes in the concentration of chemical components or changes in the physical characteristics of the sample undergoing analysis (scattering/absorptive properties).

The second procedure (qualitative analysis) consists exclusively of determining whether the product is within specification limits. This can be done by using pattern recognition techniques. Qualification involves comparing the spectrum of the sample with the spectra of products contained within the library that correspond to samples fitting within the specifications. The spectra of the samples contained within the library are represented by a certain tolerance in the wavelength domain that is due to a natural variability in the manufacturing process. The qualification process checks if the spectrum of the sample fits within the tolerance limits. The qualification is produced by computing the distance at each wavelength between the sample and the

average spectrum of the library. If the maximum distance computed does not pass a certain threshold the sample is qualified (Workman *et al.,* 2003).

The near infrared spectrum depends on the chemical and physical characteristics of the product all of which affect the qualification, whereas in the quantitative analysis only the parameters for which the calibration has been carried out can be checked. The near infrared spectrum may change slightly due to small variations in the manufacturing process or in the characteristics of any of the raw materials (Gonzalez & Prous, 1995). Recent refinements of the near infrared technique include the emergence of chemometrics and the diminishing distinction between near infrared and infrared as measuring techniques (Ciurczak, 1998). Some would still maintain the difference and see the two methods as complimentary, with each spectral region providing unique advantages for the analyst. Tremendous advances have been made in recent years in the use of near infrared spectroscopy for the analysis of pharmaceuticals. Just fifteen years ago near infrared was used in a way that offered relatively few advantages over other existing analytical methods. Advances in instrumentation, software and data handling mean that rapid sample characterisation is now possible. The pharmaceutical industry is beginning to develop near infrared methods to monitor many phases of the manufacturing process (Ciurczak, 1998).

Over the past several years there has been a great deal of interest placed on the development of attenuated total internal reflectance (ATR) infrared accessories possessing a variety of sampling configurations (Sommer & Hardgrove, 2000). These devices allow near infrared spectroscopy to be practiced in process control environments and quality control laboratories where the method is not only robust,

but has the benefits of little sample preparation and the ability to analyse highly absorbing species and/or aqueous species. The development of attenuated total reflectance devices has increased the use of infrared spectroscopy but interest is mainly focused on the study of trace quantities and materials in aqueous solution. Sommer & Hardgrove, (2004) described a method for the study of solutes in aqueous solution using a micro-attenuated total ATR accessory. The device they implemented employed a single bounce internal reflection element (IRE) which focuses the radiation to a 10-pl volume element (see figure 2.14). By microscopic condensation they were able to record parts per million levels of poly ethylene glycol (PEG) and polyacrylic acid (PAA).

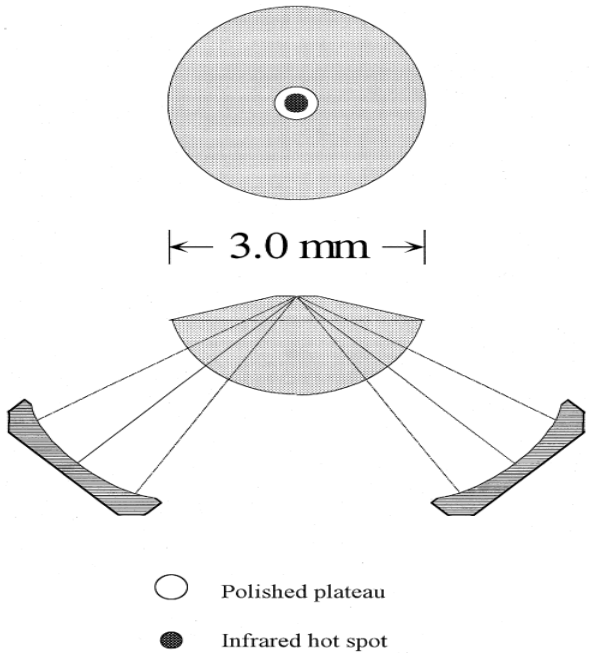

Figure 2.14. An optical diagram of the internal reflection element (IRE) which focuses infrared radiation to a 10-pl element (Sommer & Hardgrove 2000).

2.2.6 Raman Spectroscopy

The phenomenon of inelastic light scattering is known as Raman radiation and was first documented in 1928 by Raman and Krishnan. When a substance is irradiated with monochromatic light, most of the scattered energy comprises radiation of the incident frequency (Rayleigh scattering). In addition a very small quantity (0.0001 %) of photons with shifted frequency are observed (figure 2.15). The fraction of photons scattered from molecular centres with less energy than they had before the interaction are said to be Stokes scattered. The anti Stokes scattered photons have greater energy than the exciting radiation (Vankiersblick *et al.,* 2002).

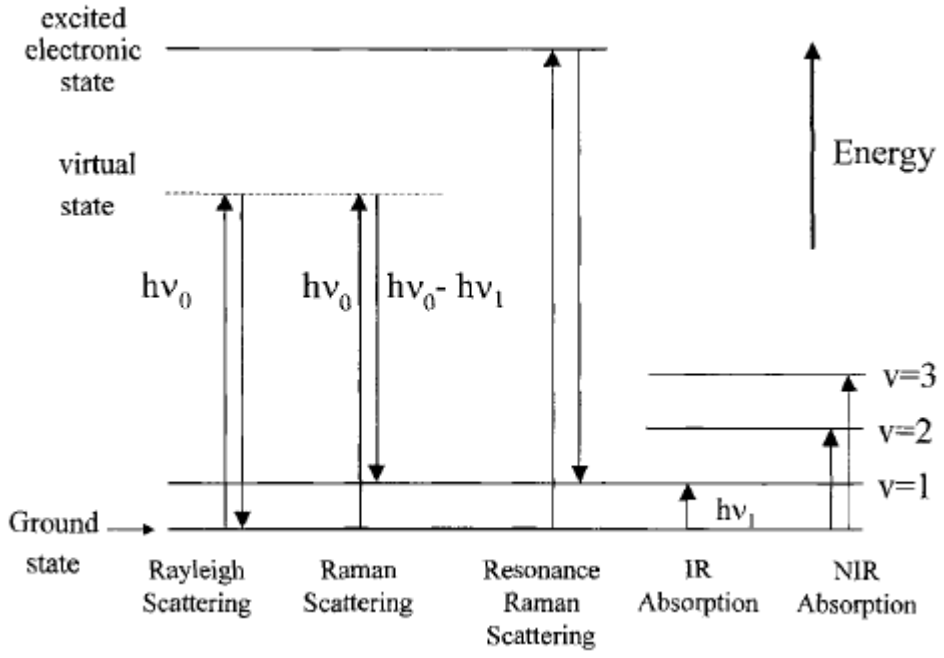

Figure 2.15. Spectroscopic transitions underlying several types of vibrational spectroscopy. v_o indicates laser frequency, v is the vibrational quantum number. The virtual state is a short-lived distortion of the electron distribution by the electric field of the incident light. McCreery, 2000.

When light and matter interact with one and other the following things may occur: the photons of light may be absorbed, scattered, not interact with the sample and simply pass through the material. If the energy of an incident photon corresponds to the energy gap between the ground state and the excited state of the molecule then an excited photon may be absorbed and the molecule promoted to a higher energy state. It is this change that gets measured in absorption spectroscopy by detecting the loss of radiation from the light. However, it is also possible for the photon to interact with the molecule and scatter from it. In this case there is no need for the photon to have an energy that matches that of the difference between the ground and excited states of the molecule. The scattered photons can be observed by collecting light at an angle to the incident light beam and provided there is no absorption from any electronic transitions which have similar energies to that of the incident light, the efficiency increases as the fourth power of the frequency of the incident light. Scattering is a commonly used technique, for example it is employed when measuring particle size and size distributions down to 1 μm. The main scattering technique employed at the molecular level is Raman scattering. The way in which radiation is employed in Raman and infrared spectroscopy is different. In infrared spectroscopy, the sample is irradiated and absorption occurs when the frequency of the incident radiation matches that of a vibration so that the molecule is promoted to a vibrationally excited state. The loss of radiation from the beam is detected. In Raman spectroscopy a single frequency of light is employed to irradiate the sample. The electron cloud of the molecule can be perturbed by molecular vibrations and it is possible for the optical oscillation from the incident light and the vibrational oscillations of the molecule to interact which leads to Raman scattering. In Raman scattering, light interacts with the molecule and distorts (polarises) the cloud of electrons around the nuclei to form a

short lived state called a “virtual state”. The state is unstable and the photon is rapidly re-radiated. A Raman spectrum consists of scattered intensity on the y-axis against energy in the form of wavenumbers on the x-axis (see figure 2.16). The peaks correspond to a given Raman shift from the energy of the incident light. The molecule can be in an excited vibrational state and if it is in such a state when an incident photon is scattered, the photon will have more energy. This is known as anti-Stokes scattering. Stokes and anti-Stokes peaks appear symmetrically about the y-axis as shown in figure 2.17 but their intensities vary with the Stokes shifted photons producing peaks with a greater intensity (McCreery, 1999).

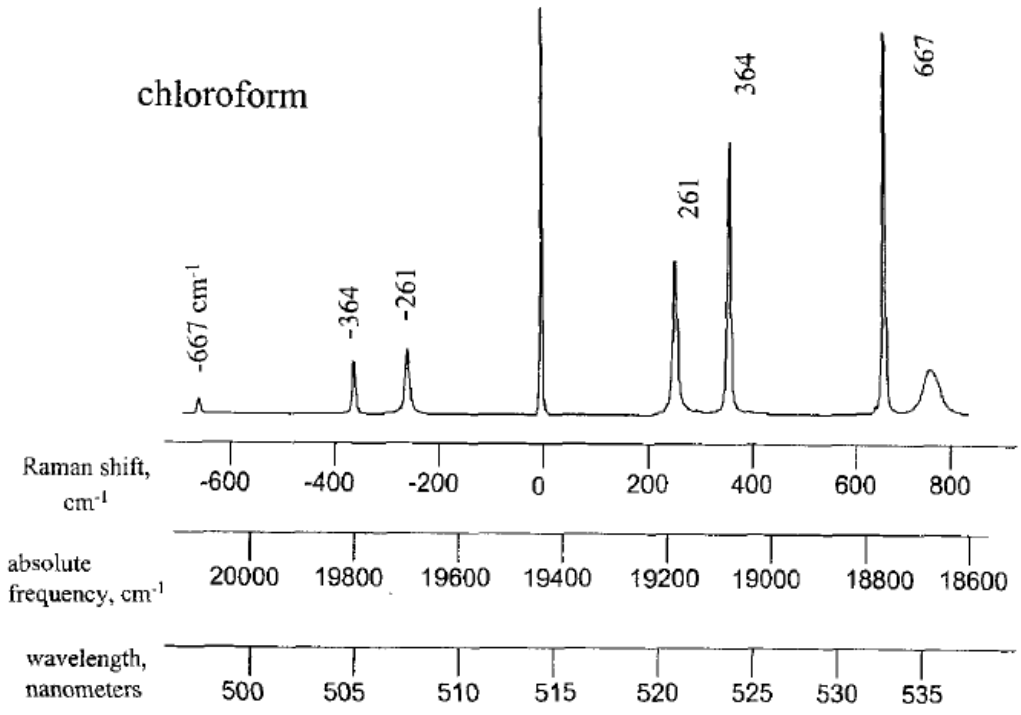

Figure 2.16. Showing the Raman spectrum of chloroform at room temperature using a 514.5 nm laser. The peak observable at 0 is the Rayleigh scattering which is several orders of magnitude more intense but is reduced in a Raman spectrum by the use of a band reject filter. The different ways in which the x-axis can be plotted are shown but

convention is to plot the x-axis as Raman shift in reciprocal centimetres from the laser line which is designated as 0. Additionally, convention assigns Stokes scattering to the right and anti-Stokes scattering to right in spite of anti-stokes scattered photons having more energy. McCreery, 2000.

When electron cloud distortion is the only factor involved in scattering, the photons will be scattered with very small frequency changes because the electrons are comparatively light. This scattering process is called elastic light scattering and is the dominant process. If nuclear motion is induced during the scattering process, energy will be transferred from the incident photon to the molecule or from the molecule to the scattered photon. In these cases the process is inelastic and the energy of the scattered photon is different from that of the incident photon by one vibrational unit. This Raman scattering is an inherently weak process where every one in 10^6-10^8 photons that scatter will Raman scatter. This does not cause the process to be insensitive because modern lasers and microscopes possess very high power densities. A disadvantage is that high laser intensities can leave the sample vulnerable to degradation.

Both infrared and Raman spectroscopy are concerned with measuring associated molecular vibrations and rotational energy changes. However, the requirement for vibrational activity in Raman spectra is not a change in dipole as in infrared spectra but is a change in the polarisability of the molecule (it is therefore possible to obtain Raman spectra from homonuclear molecules). The energy resulting from the shift is equal to the vibrational energy gap that is excited in infrared spectroscopy (Vankiersbick *et al.*, 2002).

Two major technologies are used to obtain Raman spectra: dispersive Raman and Fourier-transform Raman. Each technique has unique advantages and the method that best suits the sample should be preferred. Related techniques are important in the pharmaceutical area, one being confocal Raman spectroscopy which is a useful technique for non destructively probing depths of a sample without cross sectioning. Confocal Raman spectroscopy can selectively probe any given X,Y,Z location in a sample with spatial resolution in the micron range. It is best done by dispersive Raman spectroscopy with short wavelengths.

A potential problem with Raman spectroscopy is fluorescence. Even weak fluorescence is a stronger effect that Raman scattering and therefore fluorescence has the potential to overwhelm the Raman signal. Fluorescence can originate from the analyte of interest or from impurities in the sample and is typically a problem associated with visible lasers. The effect of fluorescence can be reduced by using a laser of longer wavelength such as a 1064 nm laser but these lasers have less power and so the Raman signal reduces. There is always a trade off involved in laser selection but the use of a longer wavelength laser has helped to get around some of the problems associated with background fluorescence in biological samples.

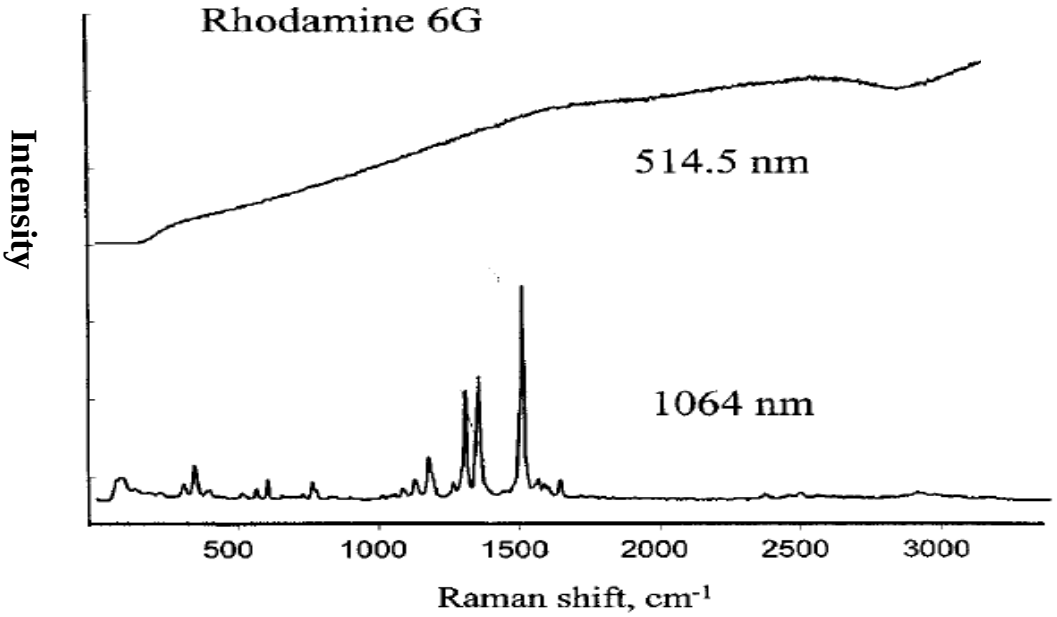

Figure 2.17. Raman spectra of Rhodamine 6G acquired with the use of a 514.5 nm laser and 1064 nm laser. Intensity scales differ with the upper spectrum having a very high intensity but showing the broad unresolved spectrum typical of fluorescing samples. McCreery, 2000.

2.2.7 Surface Enhanced Raman Spectroscopy

In surface enhanced Raman spectroscopy (SERS) the Raman scattering from a compound or ion absorbed on a structural metal surface can be 10^3-10^6 times greater than that in solution. Surface enhanced Raman scattering is greatest on silver but is observable on gold and copper as well. SERS arises from two mechanisms, the first is an enhanced electromagnetic field produced at the surface of the metal. The second is the enhanced formation of a charge transfer complex between the surface and the analyte molecule (chemical enhancement). Molecules with lone pairs of electrons or π clouds show the strongest surface enhanced Raman scattering. Even single molecule detection has been reported by SERS. The technique has the big advantage

of permitting *in situ* studies and allows work to be carried out in situations previously not thought possible (Campion & Kambhampandi, 1998).

As a field of research, SERS is approximately twenty five years old. Much discussion has taken place during those years about the basis of the enhancement and a consensus is emerging that the electromagnetic mechanism is responsible for the bulk of the enhancement with the chemical enhancement playing only a small part. The basic idea behind the electromagnetic theory is that a small metallic sphere with dimensions smaller than the wavelength of illuminating light will sustain oscillating surface plasmon multipoles induced by the time varying electric field vector of the light. Under these conditions the intensity of light at certain portions near the metal particle is enhanced (Moskovits, 2005).

For SERS to occur, the particles or metal features responsible for its operation must be small with respect to the wavelength of the incoming light (Moskovits, 2005). Most SERS active substrates in size terms fall between 5 and 100 nm. The majority of SERS active systems are made up of multiple particles. Nanoparticle aggregates, roughened metal surfaces and island films are examples of SERS active substrates (Moskovits, 2005). When nanoparticles are aggregated the nature of the enhancement is through the space electromagnetic coupling of particles. Xu and Kall, 2003 demonstrated an increase in signal from a SERS system when two particles are brought in close proximity to one and other. For molecules in the gap between two particles in close proximity to each other the enhancement factor can be as great as 10^{11} for silver nanoparticles aggregated with haemoglobin.

There is no doubt about the sensitivity offered by SERS and its potential use in sensors across a whole variety of fields. One disadvantage is inconsistency and this lies in the production of good substrates. The nature of the electromagnetic effect dictates that for an enhancement of signal to be achieved, the SERS hotspots must be in close proximity to each other and for that enhancement to be consistent from substrates to substrate the SERS architecture must be reproducibly produced.

2.2.8 Substrates

A method for the preparation of gold colloid was outlined by G Frens in 1972. The method involves the reaction of $HAuCl_4$ with trisodium citrate to produce gold colloid and is commonly known as the citrate reduction method. This basic method still persists but refinements and alternative techniques have been published in the wake of the initial paper. In the general sense, colloids for SERS are prepared by the reduction of metal cations from their salts. For silver these would commonly be $AgNO_3$ and Ag_2SO_4 and in the case of gold $HAuCl_4$ and $KAuCl_4$ with sodium citrate or sodium borohydride (Aroca *et al.,* 2005). Other factors in colloid preparation such as aggregation have been studied with reference to SERS in order to develop an understanding of how to create effective and consistent SERS structures.

Dou *et al.,* 1999 investigated the effect of aggregation for studying glycine solutions in conjunction with gold and silver colloids. It was found that the emergence of the SERS effect occurred in concert with the coagulation of gold particles. Kneipp *et al.,* 1998 showed large enhancement of signal was possible for molecules on gold colloidal clusters. An overall enhancement of 10^{14} was observed for molecules attached to colloidal gold clusters. Aggregation into 250 nm clusters gave optimal

enhancement of signal and sodium chloride was added to enhance aggregation. In SERS experiments perchlorates, nitrates and chlorides are most commonly employed as aggregating agents (Aroca *et al.*, 2005). Munro *et al.*, 1995 characterised the surface of citrate reduced silver colloid for use as a SERS substrate. It was found that colloid with a wavelength maximum absorption between 402 and 404 nm gave the best enhancement of the Raman signal.

There is a very large variety of SERS substrates other than colloids including roughened electrodes and metal island films. However, wet chemistry provides an inexpensive and versatile approach to metal nanoparticle fabrication. Colloidal nanoparticles are commonly used for SERS studies in a suspension or a sol, or the analyte-colloid system is cast onto a sustaining surface such as glass and left to dry, forming particles of a variety of shapes (Aroca *et al.*, 2005).

The hallmark of SERS is selectivity, potential for remote sampling through fibre optics and capability for detection of analytes in aqueous solutions. Despite these advantages the widespread use of SERS based analytical technologies has been slow. Before SERS based sensors can find broad applications in routine chemical analysis new SERS materials must be developed that yield consistently high signals and provide detection generality towards a wide range of chemical and environmental analytes. The major requirements for the SERS substrate materials include controlled nanoscale structure, periodicity and chemical selectivity (Kuncicky *et al.*, 2006)

Other methods of producing SERS substrates are reported in the literature. Sun *et al.*, 2005 outlined a method were a highly concentrated well stable gold colloid was

prepared from a direct mix of a amino bearing polyelectrolyte and $HAuCl_4$ in aqueous solutions. Branched polyethylenimine (BPEI) is mixed with $HAuCl_4$ at room temperature and over time the solution reaches a purple colour. The size of colloidal particles was found to be variable as the molar ratio of BPEI- HAuCl4 was altered. Pal *et al.*, 2003 outlined a method for the photochemical preparation of gold nanoparticles. The method involves the photoirradiation of $HAuCl_4$ in poly (oxyethylene) isooctylphenyl ether (Triton X-100). After irradiation the Triton X-100 acts as a stabilising agents, yielding a method that produces a colloid that is stable for several months.

Freeman *et al.*, 1996 prepared silver colloid clad gold nanoparticles for SERS. Substantial SERS increases were found for pyridine, BPE and p-NMDA. When silver was deposited on the surface of the gold nanoparticle in small amounts the enhancement was greatest but if the layer of silver is made thicker the enhancement diminishes. Cao & Li, 1999 demonstrated a new approach for producing surface roughness on silver substrates for SERS. After adding the molecule of interest and allowing it to adsorb onto the silver surface the etchants potassium ferricyanide (III) potassium thiocyanate are added. The SERS spectra for the molecule of interest is not present to begin with but as the etching reaction proceeds the SERS spectra appears as the surface gains increasing amounts of roughness.

Wang *et al.*, 2002 used silver hydrosols to generate SERS spectra for water insoluble drugs such as salicylic acid and acetaminophen. Hossain *et al.*, 2006 were able to fabricate a 2D nanostructure of gold nanoparticles on glass. Using crystal violet they were able to achieve a 10^8 enhancement of signal.

Kuncicky *et al.,* 2006 used a convective assembly method to deposit films from chemically unmodified metallic nanoparticles on plain non functionalized glass substrates. The substrates produced showed excellent SERS properties and the enhancement varied as nanoporosity and substrate structure was varied so the optimum configuration of hot spots could be created for optimised SERS.

2.2.9 Applications

Surface enhanced Raman spectroscopy provides a technique for measuring extremely low concentrations of chemical species. The technique has been applied across many fields and has potential uses in the area of cleaning verification. A suitable example is that of work done by Quagliano, 2004 where it was demonstrated as possible to study surface contaminants on semiconductors with SERS. By spraying the surface with a silver island film to create a discontinuous film, an enhanced Raman effect was observed. This technique is applicable across a whole range of fields where it is desirable to probe a surface.

Work has been carried out with surface enhanced Raman spectroscopy to investigate low levels of chemical species. Sanchez-Cortes *et al.,* 1998 carried out a study with dithiocarbamate fungicides adsorbed onto aqueous silver colloids. They were able to use surface enhanced Raman spectroscopy to obtain good quality spectra from very low aqueous concentrations and found it possible to detect the fungicide thiram at a concentration of 10^{-7} M with after excitation with a 1054 nm laser. Bazzaoui *et al.*, 2001 used surface enhanced Raman spectroscopy to obtain spectra for polyalkylthiopenes on gold electrodes and in silver colloids. They found that the

spectra of polalkylthiophenes taken on silver colloids were very similar to those taken on a gold electrode but with a large signal amplification. Bazzaoui *et al.,* 2001 pointed out that these findings were of significance to the study of trace quantities in any field.

Brolo *et al.,* 1997 were able to use surface enhanced Raman spectroscopy to obtain spectra for pyridine and pyrazine on a gold electrode. The two species were adsorbed onto the electrode by their nitrogen lone pairs. The authors compared the SERS data to electrochemically determined concentrations for both pyridine and pyrazine adsorbed onto a gold electrode. They found no correlation between surface coverage and intensity for concentrations that were greater than a monolayer but found that when surface coverage was incomplete SERS intensity did follow surface coverage. Fabriciova *et al.,* 2004 used surface enhanced Raman spectroscopy to investigate the adsorption and chemical behaviour of the anthroquinone drugs Quinizarin and Danthron. From the differences in their spectral behaviour it was possible to draw important conclusions about the biological significance of anthraquinone drugs (Fabriciova *et al.,* 2004). Wang *et al.,* 2002 presented a study where surface enhanced Raman spectroscopy was employed in conjunction with silver hydrosols to obtain spectra for drugs such as aspirin, salicylic acid, acetaminophen and vitamin A acid. The high sensitivity of surface enhanced Raman spectroscopy coupled with the linear calibration curve made the trace quantification of the drugs feasible. Wang *et al.,* 2002 stated that the low levels of detection they achieved made the method comparable or better than currently existing calorimetric or spectrophotometric methods.

Faulds *et al.,* 2001 investigated SERS in solutions of amphetamine sulfate dried in wells made on aluminium blocks. They looked at gold/silver colloids and gold/silver thin films. It was possible to detect amphetamine sulphate down to concentrations of 10^{-5} mol dm^{-3}. It was found that gold films gave the most reproducible results but it was not possible to make the system quantitative because of the inability to focus the laser on the entire sample. Lee & Farquharson, 1999 produced a silver doped sol-gel for use in SERS. The gel was evaluated using p-aminobenzoic acid which is a common contaminant in ground water supplies. Detection at the level of parts per million was achieved for p-aminobenzoic acid but the authors stated that parts per billion levels of detection would be possible with improved equipment and with modifications to the sol-gel. Trachta *et al.,* 2004, combined HPLC and SERS to the analysis of drugs in human blood and urine by using a homemade gelatine based silver halide dispersion to coat the wells of a microtiter plate. It is advantageous to couple SERS to HPLC in when attempting to identify illicit drugs in human blood and urine because of the matrix effect of those two bodily fluids. Mass spectrometry, NMR and electrochemical detection have been applied with HPLC for identification but SERS has potential because families of drugs have characteristic band patterns and so with the emergence of differing forms of the same drug, identification is made very easy due to the presence of characteristic bands. Trachta *et al.,* 2005 found that in most cases of the drugs they analysed, 10 µl of eluent taken at the time of peak appearance was enough to obtain a SERS spectrum for the drug.

Chen *et al.,* 2005 applied SERS to the study of anthraquinone dyes used in the study of works of art. Two methods were developed, the first one involved coating dyes already stained with the dyes of interest with silver nanoparticles and the second

involved the use of Ag-Al_2O_3 that had been spin coated onto glass slides. The dye alizarin was identified from madder root extract using the Ag-Al_2O_3 substrate. With a silver coating of 50nm it was possible to detect the dye down to a limit of 7 x 10-15g. This is an extremely good result but the method included careful removal of a small amount of fibres for further processing so it could not be said to be a completely non-destructive process.

SERS can be used to gain additional information about a molecule and the way in which it is adsorbed onto the SERS substrate. Leopold *et al.*, 2005 showed that SERS spectra of thiamine molecules adsorbed onto colloidal gold particles at pH values of 3, 4 and 5 revealed the presence of protonated and unprotonated versions of the thiamine molecule.

SERS has also been evaluated with respect to application in the field of detecting low levels of excitatory amino acids. The ability to detect these excitatory amino acids at low concentrations would be beneficial because they amino acids are often released from damaged neurons in head trauma victims. O'Neal *et al.*, 2003 looked at SERS for the quantification of excitatory amino acids with aqueous silver colloids. In aqueous solutions they were able to detect glutamate and aspartate at low levels with them being able to quantify glutamate between 0.4 and 5 μmol/L. Glutamate was also detectable from clear biological microdialysis solutions. The results compared extremely well to HPLC and so SERS could be applied as a system for rapid detection of potential neuron damage in head trauma victims.

The work outlined above is a small sample of a field in which many applications are being found for SERS. The limit of detection will reduce as SERS substrates and their production are improved. Applications for SERS are constantly being found in the fields of: environmental analysis, law enforcement, textiles, medicine, drug testing and in the field of pharmaceuticals. One aim of this project is to investigate the potential application of SERS in cleaning verification. The body of work that exists on SERS shows that it can detect at the levels necessary for cleaning verification work and it has the advantages of producing a characteristic spectra for each compound investigated whilst being potentially non destructive.

2.2.10 New SERS technologies

The enhancement gained in SERS is a most impressive one and with it comes the potential to sense molecules at extremely low levels. Single molecule detection has been reported with SERS. Kneipp *et al.,* 1997 showed SERS detection for single molecule crystal violet in aqueous silver colloid and Maruyama *et al.,* 2001 showed single molecule detection for Rhodamine and adenine. These potential levels of sensitivity make SERS an attractive technology on which to base sensor and detection systems. SERS is sensitive and readily achievable under laboratory conditions with favourable combinations of nanoparticle and substrate. A challenge is to make the technique generic and so much work is being carried out on turning SERS into a reproducible and versatile technique that can be put to use in every day situations.

A promising area of research is “Tip Enhanced Raman Spectroscopy” TERS. The principle behind TERS is to coat a fibre optic cable or glass tip with silver or gold particles or island films to create a probe capable of producing a SERS effect on the

surface which it is probing. Stokes *et al.,* 2004 showed the SERS effect was possible from a silver island based SERS nanoprobe. A tapered nanoprobe as small as 100 nm in diameter with 10 nm silver islands at the tip was fabricated and used to investigate glass surfaces coated with brilliant cresyl blue and p-aminobenzoic acid. The tip was integrated into a microscope set up and it was shown that the SERS effect was present when the tip was brought into close contact with the substrate. Stokes *et al.,* 2004 concluded that the observation of contact induced SERS analysis of dry surfaces was important because it demonstrates the feasibility of probing dry samples on solid surfaces.

Viets & Hill 2004, carried out a study of fibre optic SERS sensors and compared three methods of preparing sensor tips. The types of probe compared in the study were silver island films, silver films over nanoparticles and silver films over a roughened or sand blasted fibre tip. Thiophenol was used as the reference chemical and the SERS effect was found to be similar for all three tips. The durability and potential to regenerate the roughened or sandblasted tips meant that they emerged from the study as the tip with most promise. Pettinger *et al.,* 2005 demonstrated the potential of TERS when studying the dye malachite green isothiocyanate by achieving enhancements of signal from the dye molecule of approximately 6×10^6 adsorbed on a gold substrate in a region within a 50 nm radius underneath the tip

TERS has potential for inducing a localised enhancement of Raman signal that can be used for detection of target molecules. The main disadvantage with TERS at present is reproducibility of the tips and breakage of tips. When these initial difficulties have been overcome, TERS may emerge as a useful variant of SERS.

2.2.11 Cleaning limits and SERS

There are no hard and fast rules concerning the levels to which pharmaceutical manufacturing equipment must be cleaned before the plant can be released for production of a new compound. The 10 ppm formula, the acceptable daily intake formula based on the eight hour acceptable worker exposure limit and the 1/1000 of therapeutic level formula have been introduced as potential methods by which the level to clean can be calculated. As has already been discussed, cleaning verification is often based on the formula that yields the lowest value and this is most typically the 1/1000 of therapeutic level. (Valvis & Champion, 1999).

For the purposes of this study it is important to discuss the information for calculating cleanliness levels relates to in terms of detection levels. Chapter four mainly deals with SERS and attempts to implement it as a cleaning verification technology. Therefore it is important to be working at levels of contamination appropriate for cleaning verification.

From the literature it is apparent that there is quite a wide range of concentrations over which detection of active pharmaceutical ingredient has been attempted. The explanation for this is the variation in pharmacological potency between different drug compounds with lower levels of detection a requirement for more potent compounds where carry over of drug into the next product presents an even greater risk to patient health.

Zeller 1993, in validating a cleaning system applied several concentrations of product dissolved in methanol to swabs and allowed the methanol to evaporate dry. Linearity was found over the range 0.02 –0.1 µg/ml and quantitation possible with the sampling procedure to 0.98 ng/cm^2. These levels turned out to be much lower than the actual levels of detection and quantitation needed based on the product's 1/1000 of therapeutic dose. Shifflet & Shapiro (2002) discussed a theoretical calculation in which it was calculated as necessary to detect at levels equivalent to 25 µg/ml. Valvis & Champion 1999, discussed cleaning validation work for a potent anticancer agent in which it was necessary to detect down to 10 ppm in 50 L of cleaning solvent in order to classify the equipment as clean. Ultimately validation went down to 0.1 ppm and it was possible to clean the equipment to 2 ppm for the compound of interest.

Liu & Pack, 2007 validated a cleaning verification assay for a highly potent compound at levels of 50ng/cm^2 and 50 ng/100cm^2 which equated to 5 ng/ml or 3 ng/ml when losses were allowed for. It was pointed out that for drugs where the therapeutic dose is in the low micrograms per day, the cleaning verification acceptance limit is going to be driven down into the nanogram range. The authors were able to validate an LC/MS method for the determination of residues for their target compounds which were new chemical entities belonging to Eli Lilly.

2.3 Fluorescence spectroscopy

Luminescence is the emission of light from any substance and occurs from electronically active states. The phenomenon of luminescence can be divided into two groups; fluorescence and phosphorescence depending on the nature of the excited

state. In excited singlet states, the electron in the excited orbital is paired (of opposite spin) to the second electron in the ground state orbital. Consequently, a return to the ground state is spin allowed and occurs rapidly by emission of a photon. Typical emission rates of fluorescence are $10^8 s^{-1}$ meaning that a typical fluorescence lifetime is around 10 nanoseconds (Sharma & Schulman, 1999). The lifetime of a fluorophore is the average time between its excitation and its return to the ground state. The short time scales involved mean that measuring time resolved fluorescence requires sophisticated optics and electronics. Whilst time resolved fluorescence presents technical difficulties, it is used more often than the steady state measurements because the data provided can yield greater amounts of information.

In recent years there has been a great proliferation in the use of fluorescence spectroscopy in the sciences. The proliferation has come about because advances in optical technology mean that the fluorescence technique can be used within a large number of disciplines. Fluorescence spectroscopy and time resolved fluorescence were primarily research tools used in biochemistry and biophysics. Fluorescence is now used in a wide range of disciplines including environmental monitoring, clinical chemistry, DNA sequencing and genetic analysis. Fluorescence presents such a potentially useful tool because of the high sensitivity of detection that can be achieved and because it is much safer than other techniques such as the use of radioactive tracers.

Fluorescent probes are the most important aspect of fluorescence spectroscopy. Obviously the instrumentation is important but the wavelengths and time resolution required of the machine are determined by the fluorescent properties of the

fluorophores. In addition, the properties of the probe determine what sort of results the experiment can achieve. For example, only probes sensitive to pH changes can be used to measure pH. There are two major groups of fluorophore, intrinsic and extrinsic. Intrinsic fluorophores are those that occur naturally and include the aromatic amino acids, NADH, flavins and include derivatives of pyridoxal and chlorophyll. Extrinsic fluorophores have to be added to a sample of interest and include dansyl chloride, fluoroscein, rhodamine and numerous other substances (Valeur, 2002).

In protein, the dominant fluorophore is the indole group of tryptophan. Indole absorbs near 280 nm and emits near 340 nm (Lackowicz, 1999). The emission spectrum of indole is highly sensitive to solvent polarity. The emission of indole may be blue shifted if the group is buried within native proteins and its emission may shift to longer wavelengths (red shift) when the protein is unfolded (Lakowicz, 1999).

The problem associated with many analytical techniques are high consumption of reagents and a long time for analysis (Moreira *et al.*, 2004). Moreover, the need for sample preparation prior to determination makes them cumbersome thus less attractive for large scale analyses. In this respect fluorescent detection is a simple and rugged technique that does not require the use of reagents and solvents, is non destructive and does not generate residues. The technique makes it possible to carry out easy and fast determination of solid samples. The total analysis time could be as short as couple of minutes.

2.4 Relevant patents and commercially available equipment

Information pertinent to the area of infrared spectroscopy and cleaning verification can be found by looking at patents and commercial websites. The major area of patent activity at the moment with respect to infrared spectroscopy is the registration of devices for *in situ* spectroscopic analysis. As has already been said, the ability to sample directly the surface of interest would be hugely advantageous and so work is being done in that area to produce reliable instrumentation.

Melling *et al.*, 2001 patented a spectroscopic accessory for examining films and coatings on solid surfaces. The accessory is designed for a Fourier transform-infrared spectrometer and is composed of fibre optic cables that are connected to a framework within which two mirrors are sited. The mirrors are off axis parabolas and are positioned with respect to one and other and with respect to the fibre optic cables. The beam from the first cable is reflected by the first mirror onto the sample surface at or near the grazing angle, after which it is captured by the second mirror and focused onto the end of the return cable which transmits it back to the spectrometer. Very thin films and coatings can be spectroscopically detected and characterised using the accessory.

The aim of the invention was to reconcile the spectroscopic advantages of the grazing angle approach with the ease of use presented by a fibre optic cable. The desired outcome is to permit spectroscopic testing on surfaces such as metals without having to remove sample and place it within the sample compartment of the spectrometer (Melling *et al.*, 2001).

Berard *et al.,* (1992) filed a patent for optical fibre coupled devices for infrared spectroscopy. The invention is directed to a probe operative in the infrared region of the electromagnetic spectrum for *in situ* sensing of the absorption of infrared energy in a sample. The probe comprises an attenuated total reflection element (ATR) having an input and an output end respectively for receiving infrared radiation and transmitting attenuated infrared radiation. The attenuated total reflectance element has wall portions disposed about a central or long axis thereof for reflecting infrared energy transverse to the central axis. A bundle of infrared transmitting fibres is located at the input end of the attenuated total reflectance element for transmitting and receiving infrared radiation into and out of the element. The fibres have end faces proximate the attenuated total reflectance element lying in a plane perpendicular to the central element (Berard *et al.,* 1992).

The aim of the invention was to provide a convenient means of coupling an attenuated total reflectance element to a spectrometer so that good spectra may be obtained in moderate times from samples including those that are inconvenient or dangerous to measure in a spectrometer.

2.5 Genotoxins and limits for genotoxic impurities in drug substances

Impurities accumulate in pharmaceuticals as a result of starting impurities and as by products of the reactions taking place during the synthetic steps involved in a drug's production. *In situ* reactions often involving residual solvents can also be responsible for the origin of impurities found in pharmaceutical formulations. Many of the impurities found in pharmaceutical formulations after synthesis can be genotoxic.

Figure 2.18 provides a representative scheme which illustrates the routes by which genoxotoxic impuities may enter pharmaceutical products.

The International Conference on Harmonization (ICH) Guidelines Q3A(R), Q3B(R) and Q3C are a set of documents that deal with many of the issues surrounding genotoxic impurities in pharmaceutical formulations.

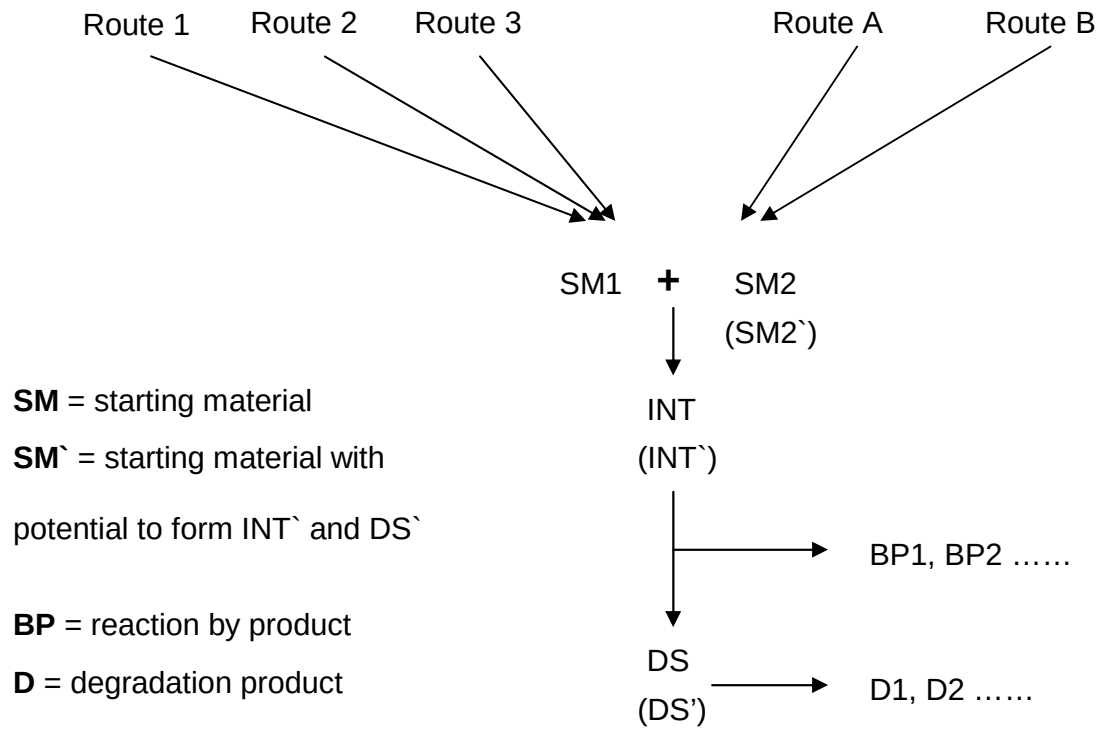

Figure 2.18. A representative scheme showing how genotoxic impurities can potentially accumulate in the end product of a drugs' synthesis. Adapted from Kirkland & Snodin 2004.

Degradation product impurities are of primary concern while process related impurities are both necessary to control in APIs. Many potential impurities result

from the pharmaceutical manufacturing process including starting materials, isomers, intermediates, reagents, solvents, catalysts and reaction by products (Argentine *et al.*, 2007).

The classification of a genotoxic impurity is an impurity that presents clear evidence for its genotoxicity. Usually this is from positive findings in an *in vivo* mammalian test (e.g. the rodent bone marrow micronucleus test) with supporting evidence from *in vitro* tests (e.g. Ames bacterial mutation test, *in vitro* chromosomal aberration test, mouse lymphoma tk mutation test). These tests form the recommended battery of tests for new pharmaceuticals. Tests such as those previously outlined may not detect certain tissue specific, sex specific or species specific carcinogens and so non standard or modified tests may be required (Kirkland & Snodin, 2004).

Compounds that are genotoxic *in vivo* are usually animal carcinogens and therefore suspect human carcinogens. Genotoxins have traditionally been assumed to cause DNA damage that can potentially lead to tumour initiation and progression. It is becoming increasingly acknowledged that genotoxic events may result from threshold mediated processes (Kirkland & Snodin, 2004).

Genotoxic and carcinogenic properties may be acceptable for some active pharmaceutical ingredients such as cytotoxic cancer chemotherapies; where as impurities in most drug substances and products have limited, if any, beneficial effects and therefore carry risk without significant associated benefit (McGovern & Jacobson-Kram, 2006). Scrutiny of genotoxic impurities in pharmaceutical formulations has increased significantly in the recent past for two major reasons and

these are improvements in analytical technology meaning it has become much easier to identify impurities and an increased awareness towards the dangers of many compounds and the associated risk to human health.

Regulatory documentation addressing the issues of impurities and residual solvents exist and the ICH guidelines ICH Q3A(R), Q3B(R) and Q3C(R) represent a consensus on how impurities should be controlled in marketed products. However important issues are not addressed in the guidelines, for example, acceptable levels of impurities in drugs in development and control of genotoxic impurities (Jacobson-Kram & McGovern, 2007).

In December 2002, the Safety Working Party (SWP) of the European Committee for Proprietary Medicinal Products (CPMP) published a position paper on the limits for genotoxic impurities. The European Union intended to supplement the gap in the International Conference on Harmonization guidelines on qualification of impurities, as it was deemed that impurities with genotoxic potential where a special case not specifically covered in terms of qualification by the Q3A and Q3B guidelines. The SWP's proposed approach follows a safety factor based risk assessment process similar to that in ICH guidelines Q3C limits for residual solvents rather than a qualification process described in ICH Q3A and Q3B (Kirkland & Snodin, 2004).

The SWP acknowledge threshold mechanisms and in their paper recommend that genotoxic impurities should be avoided if at all possible and particularly if there is no threshold mechanism known. If genotoxic impurities are unavoidable then they should be reduced to the lowest feasible levels and/or alternative reagents/synthetic

routes used. Based on the ICH guidelines for exposure to residual solvents, the "permitted daily exposure" PDE for a genotoxic impurity with a threshold mechanism of genotoxicity is calculated using the No Observed Effect Limit (NOEL) or Lowest Observed Effect Limit (LOEL) from the most relevant animal studies and incorporation of safety factors (Jacobson-Kram & McGovern, 2007).

For genotoxic impurities without evidence for a threshold mechanism of genotoxicity the guidelines set out by the SWP propose a policy of controlling levels to as "low as reasonably practicable" (ALARP principle). The SWP assert that in the case of compounds lacking evidence for a threshold mechanism during production of the compound every effort must be made to reduce the genotoxic impurities through technical efforts such as purification steps. Compounds that fall into this group of not having clear evidence for a threshold mechanism include alkylating agents and intercalating agents. Regulatory agencies perform risk assessments to calculate the increased levels of adverse events resulting from exposure to the genotoxic impurity and set exposure levels which result in "acceptable risks". This is often a chance of 10^{-5} or 10^{-6} of additional cancers from lifetime exposure (Jacobon-Kram & McGovern, 2007).

A white paper was presented at a public meeting of the Pharmaceutical Research and manufacturing Association (PhRMA) after development by a task force. The document outlines a procedure for testing, classification, qualification and toxicological risk assessment of potentially genotoxic impurities in pharmaceutical products. A staged threshold of toxicological concern approach was proposed by the task force with respect to genotoxic impurities since some medicines, particularly

those in development were only administered for limited time spans. The proposed short term limits are based on a 10^{-6} risk of additional lifetime cancers and the limits for greater than twelve months are based on a 10^{-5} risk. The limits of exposure result from a linear extrapolation of the threshold of toxicological concern for a lifetime daily exposure to shorter term daily exposures. (McGovern & Jacobson-Kram, 2006).

Table 2.1. PhRMA Genotoxic Impurity Task Force Proposal, (McGovern & Jacobson-Kram, 2006).

Duration of clinical trial exposure (months).	<1	1-3	3-6	6-12	>12
Allowable daily intake (µg/day) for all phases of development	120	60	20	10	1.5

The FDA perspective on this matter is an acknowledgment that complete removal of genotoxic impurities may not always be possible and that pharmaceutical companies should strive to reduce genotoxic impurities to the lowest possible levels where they represent an insignificant risk to patients or clinical trial subjects. The exact level should be based on compound specific data and a staged implementation of the threshold of toxicological concern is acceptable for developmental products. In some cases the thresholds may be increased if the drug is of significant therapeutic potential. The FDA Center for Drug Evaluation and Research (CDER) is currently developing guidance to address the issue of genotoxic impurities in pharmaceutical products (Jacobson-Kram & McGovern, 2007)..

In summary, whilst no official legislation exists, the daily limit agreed upon for a genotoxic impurity is 1.5 µg/day when the drug in question is one prescribed for a period greater than twelve months. The levels of genotoxic impurities may increase for drugs taken for shorter periods of time and for drugs still in the developmental stage.

2.5.1 Examples of impurity formation and analytical techniques for detection of genotoxic impurities.

The development of analytical technology and methodologies for the determination of genotoxic impurities in active pharmaceuticals is of great importance because it allows for the development of a greater understanding of synthetic processes and degradation pathways and is a key aspect in establishing regulatory controls.

Analytical specificity and sensitivity are primary considerations for the determination of genotoxic impurities in pharmaceuticals. Techniques with appropriate selectivity are necessary to avoid false positives caused by interferences and detectability requirements are usually lower than for other impurities, sometimes extending down to the low parts per million range. The potential specification limit for an impurity is a key factor in determining the sensitivity requirement for the analytical method and in certain cases could dictate the analytical technique required for control (Argentine *et al.*, 2007).

Sulfonic acids such as methane sulfonic acid, benzene sulfonic acid and ρ-toluene sulfonic acid are routinely employed to produce conjugates with active pharmaceutical ingredients in order to improve pharmacological properties. The

formation of these conjugate salts usually improves the solubility, absorption and physical properties of APIs and thus increases the feasibility of a successful formulation. The use of these sulfonic acids can potentially lead to the formulation of trace levels of sulfonic acid esters in the final API (Calon & Richoll, 2005).

There are two main means by which sulfonic acid esters can enter the final API.

1) As a process related impurity carried over into the API
2) Formed *in situ* by the reaction of these acids with residual solvents used during synthesis.

The likelihood of formation of sulfonic acid esters is increased if alcohol groups are present in the formulation or used in any stage during synthesis (Taylor *et al.*, 2005).

The potential toxicity of sulfonic acid esters has been documented. Methyl methane sulfonate and ethyl methane sulfonate can alkylate cellular DNA. Methods have been developed to quantitate the degree of alkylation by measuring ethylated and methylated DNA adducts, mostly by HPLC methods. Gas chromatography has been used for the determination of S – methylcysteine and other alkylated amino acids as a marker of exposure to methyl methane sulfonate and other alkylating agents (Calon & Richoll, 2005).

Calon & Richoll 2005 developed a sensitive detection system for methyl and ethyl esters or methane sulfonic acid, benzene sulfonic acid and ρ–toluene sulfonic acid based on solid phase microextraction to prepare the sample and then GC/MS in the SIM mode for analysis. They were able to validate the system down to 5 ppm.

Taylor *et al.,* 2005 were able to carry out low level determination of ρ-toluenesulfonate and benzenesulfonate esters by HPLC/MS and GC achieving detection at less than 0.1 ppm. The authors stated that their method had the advantage of not being coupled to solid phase extraction, solid phase micro extraction or liquid phase micro extraction.

Carbonic acid chloromethyl tetrahydro-pyran-4-yl ester (CCMTHP) is commonly used as an alkylating reagent in the synthesis of APIs. As specified in the European Agency for the Evaluation of Medicinal Products (EMEA) position paper on the limits of genotoxic impurities, alkylating agents are considered to be the archetypal class belonging to the group of genotoxic impurities. Therefore, the CCMTHP content in the final drug product should be as low as technically feasible (Li & Slugget, 2005)

Detection of CCMTHP requires sensitive trace analysis techniques (method should be sensitive, selective and robust). The GC-MS SIM method they developed and described is a relatively simple analytical procedure for the accurate determination of trace levels of CCMTHP down to 10 ppm in an API. The method requires no extraction, derivitization or cleanup and can be readily adapted for the analysis of other halogen containing alkylating agents used in the manufacture of pharmaceutical products (Li & Slugget, 2005).

Regulatory authorities recognise the fact that analysis of genotoxic impurities is not without its challenges, however in most cases current analytical chemistry techniques are adequately sensitive and available to industry. Various LC/GC methods either

alone or coupled to MS should in most cases provide the necessary technological platforms for appropriate method development (McGovern & Jacobson-Kram, 2006).

Separation, identification and quantification may be more challenging in certain cases when the impurities of interest are degradants that form only in the presence of excipients, residual solvents or from contact with container closure components i.e. leachables. Also, separation of the impurity from the matrix of the drug product may pose analytical challenges regarding the development of routine methods for the assessment of drug products (McGovern & Jacobson-Kram, 2006).

3 Characterisation of commercially available swabs for cleaning verification

This chapter presents recovery and debris generation data for seven commercially available swabbing materials. The difference in recovery rate from a stainless steel surface and after direct spiking is also examined for two of the better performing swabs. Recovery rates and debris generation are compared and conclusions on swab performance are made.

3.1 Introduction

As discussed in the introductory section of the thesis, there are many important aspects of swab sampling. Within the cleaning verification field there is currently little published work comparing commercially available swabs for cleaning verification work. For this chapter it was decided to undertake experimental work aimed at investigating the swabbing properties of seven commercially available swabs or swab materials. Claims are made about the suitability of different swabbing products for cleaning verification but little data exists and so this chapter is aimed at comparing different commercially available swabs. The ability of the swab to recover compound is a crucial element in its suitability for cleaning verification and this is something we decided to investigate. Recovery rates of 60 per cent are acceptable but higher rates are desirable (Miscoscio, 1997). The tendency of the swab to leave behind debris on the sampled surface is another factor that should be taken into account when selecting a swab for cleaning verification work (Miscoscio, 1997) and it was decided to investigate this process too.

With the knowledge gained from experiments on the swabbing process we gain a better understanding of swabs and their properties with relevance to cleaning

verification and are in a position to draw conclusions about the best combinations of swab and solvent for cleaning verification work. Sampling is a vital aspect of the cleaning verification process and this work will enhance the understanding of it. As well as gaining an understanding of what recoveries are achievable it will also be possible to see what sort of levels of variation are inherent in the process. For the experiments presented in the section of the thesis all swab sampling is done by one person but in a pharmaceutical company, swab sampling is done by a number of different employees and ensuring reproducibility of results across the entire workforce is something pharmaceutical companies invest a lot of time and money in. Good consistency of results is also important from the point of view of safety of the final product. Underestimating the amount of residue left on the equipment could result in the plant being released before it is sufficiently clean and therefore leading to the manufacture of an overly contaminated batch of new product. Overestimation is more of an economic problem in that it means the plant will be re-cleaned when further cleaning is unnecessary.

The experiments will be conducted with water and ethanol as the solvents. Water is polar and is often used in the pharmaceutical industry during the cleaning process. Ethanol is less polar and is an example of an organic solvent that might be used for cleaning verification. The drugs or drug like compounds for which recoveries will be measured are: acetaminophen, nicotinic acid, diclofenac and benzamidine. Acetaminophen is a drug compound that readily dissolves in both water or ethanol. Benzamadine is a drug like compound which is also readily dissolved in water or ethanol. In this study, acetaminophen was dissolved in water and benzamidine ethanol. Diclofenac is a hydrophobic drug molecule. It's log p value is 3.42 and was

used as an example of a hydrophobic compound. It was dissolved in ethanol. Nicotinic acid is a polar compound (log p = 0.56) with structural and functional similarities to many drug compounds and was dissolved in water for the experiments in this study.

3.2 Materials and methods

The swabs under investigation were either purchased from the supplier or received as gifts. The seven swabs used in the study were: Absorbond™, MiracleWipe™, Technicloth™, Betawipe™, Alphawipe™, Super Polx 1200™ and Texwipe ™. All of the swabs apart from the Super Polx 1200™ are manufactured by Texwipe (New Jersey, US). Super Polx 1200 is manufactured by Berkshire (Surrey, UK).

Table 3.1. Swabbing materials investigated (information supplied by manufacturer).

Absorbond™	100% hydroentangled polyester
MiracleWipe™	100% continuous filament nylon
Technicloth™	Hydroentangled, non woven 55% cellulose & 45% polyester
Betawipe™	Polypropylene and cellulose wiper
Alphawipe™	100% continuous filament polyester
Super Polx 1200™	100% continuous filament polyester
Texwipe™	100% cotton woven wiper.

Acetaminophen, nicotinic acid, diclofenac and benzamidine were purchased from Sigma (Poole, Dorset, UK). Isopropyl alcohol was analytical grade and purchased from Fisher Scientific (Loughborough UK)

A stainless steel surface was thoroughly washed with isopropyl alcohol and then left to dry prior to use. A known amount of compound was spread across the surface in 1 ml of solvent (water or ethanol). The solvent was then allowed to evaporate. The surface was wiped clean with swabbing material soaked in solvent (water or ethanol).

The swabbing material was placed into an 18 ml vial with a further 5 ml of solvent, ultrasonicated for 10 minutes and then vortexed for 2 minutes. UV-vis spectroscopy was carried out in 1 ml sample quartz cuvettes using a UV 2100 spectrophotometer (Shimadzu, Milton Keynes, UK). Calibration curves were made for each of the compounds under investigation. Acetaminophen was measured at 245 nm, nicotinic acid at 245 nm, diclofenac at 269 nm and benzamidine at 284 nm. The calibration curve for acetaminophen was linear over the range of 0 - 0.2 mg/ml ($R^2 = 0.998$). The calibration curve for nicotinic acid was linear over the range of 0 – 0.2 mg/ml ($R^2 = 0.996$). The calibration curve for diclofenac was linear over the range of 0 - 0.04 mg/ml ($R^2 = 0.999$). The calibration curve for benzamidine was linear over the range of 0 – 0.3 mg/ml ($R^2 = 0.999$). All UV measurements were carried out three times and each contamination and subsequent extraction was performed four times for each compound in order to produce reliable results

In order to examine debris generation, a stainless steel surface was pre cleaned with isopropyl alcohol and allowed to dry. The surface was then loaded with 1 ml of acetaminophen solution at a concentration of 1 mg/ml. The surface was allowed to dry and then wiped clean with a swab soaked in water. The surface was allowed to dry and then investigated with the aid of a microscope (Karl Zeiss (UK) Axioskop – Welwyn Garden City, Herts, UK). Debris generation per square cm was measured after the swabbing materials had been used to clean a stainless steel surface. Five counts were performed in order to produce reliable results.

Images of swabs were also captured by microscope (Karl Zeis (UK) Axioskop).

The metal surface was swabbed as described below.

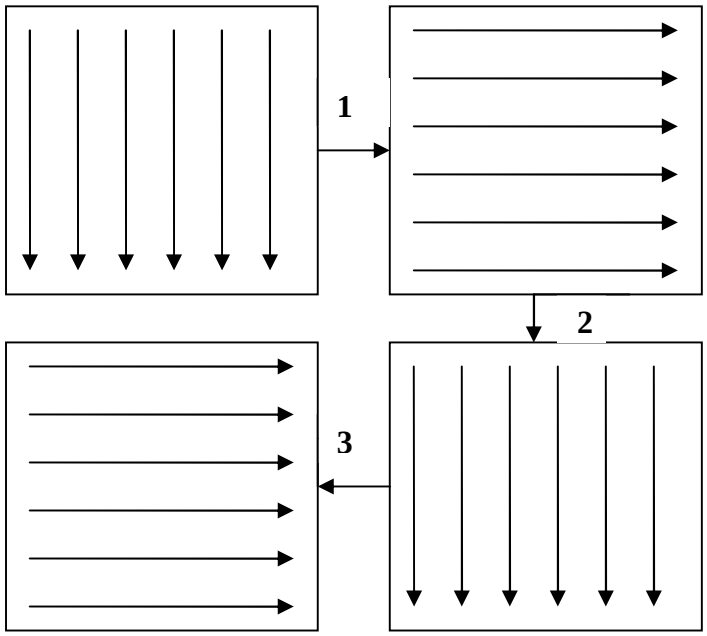

Figure 3.1. Showing the swabbing procedure for one sample collection.

3.3 Results

3.3.1 Images of swabs

The swabs were imaged under a microscope and their properties summarised in order to aid characterisation.

3.3.2 Absorbond™

To the hand the swab had a soft feel with no stretching ability and to the eye the swab was found to have a glossy appearance. Under the microscope a filamentous arrangement of fibres was observed.

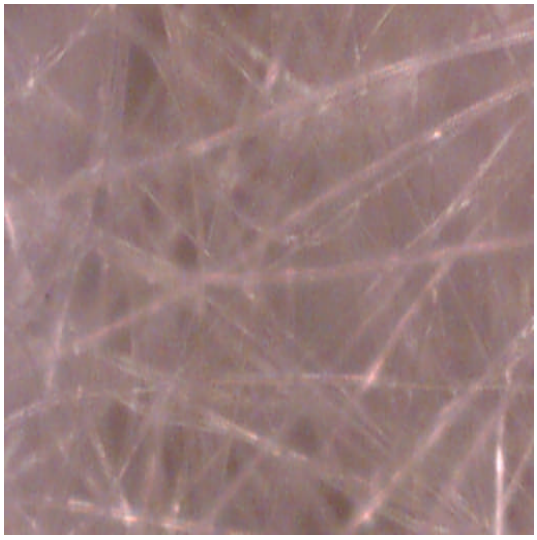

Figure 3.2. Image taken of fibres from an Absorbond™ swab (x 20). The swab had a filamentous appearance under the microscope.

3.3.3 MiracleWipe™

The fibres were found to have a bundled appearance under the microscope.

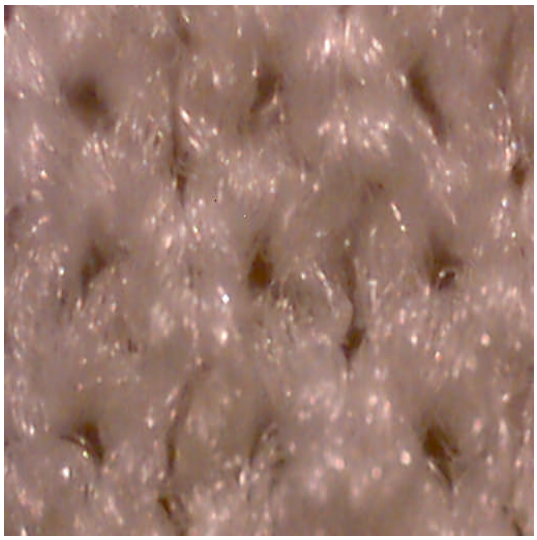

Figure 3.3. Image of fibres from a MiracleWipe™ swab (x 40).

Figure 3.4. Showing the MiracleWipe™ swab at x 4 magnification.

The pattern revealed the bundled nature and inherent stretching ability of the swab. To the hand MiracleWipe™ had a soft feel and was able to be stretched.

3.3.4 Technicloth™

The Technicloth™ was similar to Absorbond™ under the microscope with a filamentous appearance apparent. To the hand Technicloth™ had a coarse feel and had no noticeable stretching ability.

Figure 3.5. Showing fibres from a Technicloth™ swab (x 20).

3.3.5 Betawipe™

Like Absorbond ™ and Technicloth™, the Betawipe™ had a filamentous appearance under the microscope.

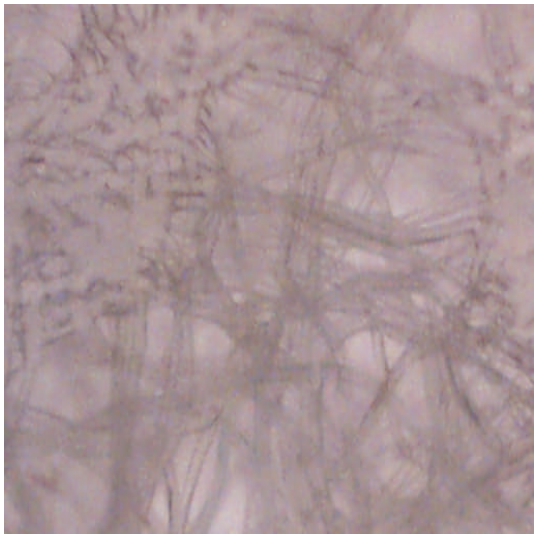

Figure 3.6. Images of fibres from a Betawipe™ swab (x 20).

Figure 3.7. Image of the Betawipe™ swab at x 4 magnification.

Visible as white circles on the swab, Figure 3.7 shows the depressions that were apparent on the Betawipe™ swab surface.

Betawipe™ had a sponge like feel to the hand. It was thicker than all the other swabs and had small depressions on its surface (visible to the eye but shown under x 4 magnification in Figure 3.7).

3.3.6 Alphawipe™

Like MiracleWipe™, Alphawipe™ had bundled fibres. To the hand, Alphawipe™ had a soft feel and possessed the ability to stretch.

Figure 3.8 Image of fibres from Alphawipe™ (x 20).

3.3.7 Super Polx 1200™

The fibres were bundled in appearance and showed similarity to MiracleWipe™ and Alphawipe™. To the hand Alphawipe™ had a soft feel and possessed the ability to stretch.

Figure 3.9. Images of fibres from a Super Polx 1200™ swab (x 20).

3.3.8 Texwipe™

The fibres had a filamentous appearance and showed similarity to Absorbond™, Technicloth™ and Betawipe™. To the hand Texwipe™ had a coarse feel and did not possess the ability to stretch.

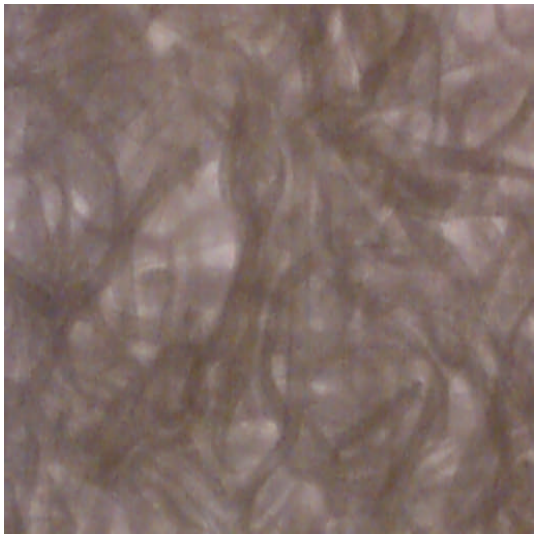

Figure 3.10. Image of fibres from a Texwipe™ swab (x 20).

3.3.9 Summary of swab properties

Table 3.2. Summarising the physical properties of the investigated swabs.

Wiper	Microscopic appearance	Macroscopic appearance	General Comments
Texwipe™	Filamentous	Coarse	N/A
Absorbond™	Filamentous	Soft	Glossy appearance
MiracleWipe™	Bundled	Soft	Stretchy
Technicloth™	Filamentous	Coarse	N/A
Betawipe™	Filamentous	Foam like	Contains small holes
Alphawipe™	Bundled	Soft	Stretchy
Super Polx 1200™	Bundled	Soft	Stretchy

In summary, the swabs fell into two broad categories. MiracleWipe™, Alphawipe™ and Super Polx 1200™ had fibres with a bundled appearance under the microscope. These swabs had a soft feel to the hand and had the ability to stretch. Technicloth™ and Texwipe™ had a filamentous appearance under the microscope. These two swabs had a coarse feel to the hand and no discernable stretchiness. Betawipe™ and Absorbond™ were slightly anomalous. Both had a filamentous appearance under the microscope but unlike Technicloth™ and Texwipe™ they did not have the coarse feel. Absorbond™ had a very smooth feel and glossy appearance but did not possess any stretching ability. Betawipe™ felt thick to the hand in spite of being found to have a slightly rough feel. The Betawipe™ swab also had a spongy quality.

3.3.10 Compound recovery

Acetaminophen and nicotinic acid were dissolved in water before contamination and recovered in water. Diclofenac and benzamidine were dissolved in ethanol before contamination and recovered in ethanol.

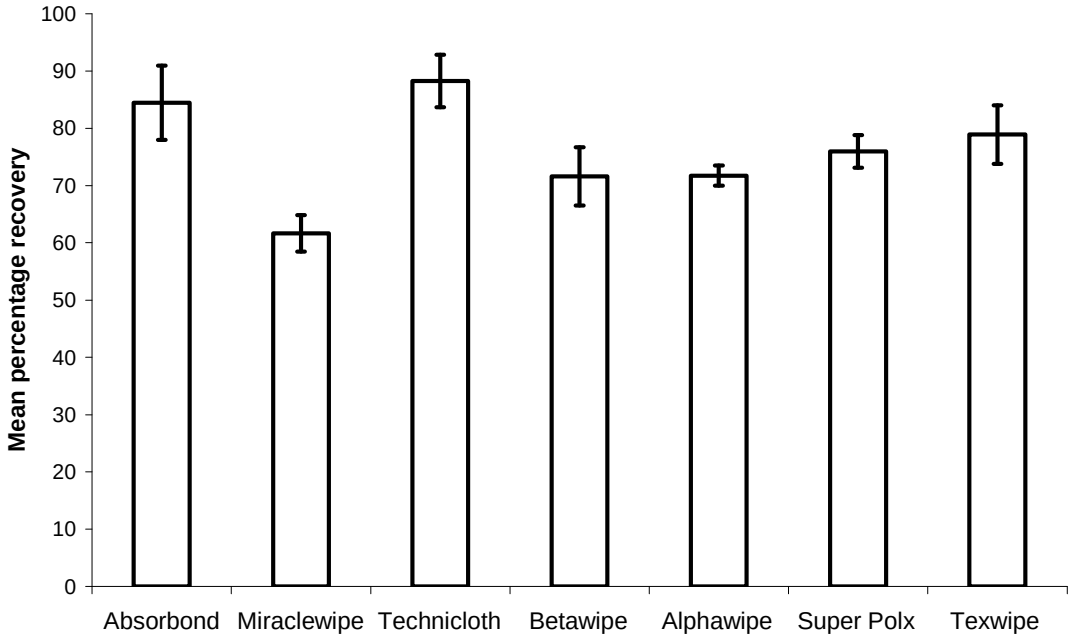

Figure 3.11. Mean percentage recovery of compound from seven commercially available swabbing materials used to wipe clean a stainless steel surface pre loaded with 0.1 mg of acetaminophen. The bars represent standard deviation.

The mean percentage recovery of acetaminophen in the overall sense was high with highest recovery of 88.2% achieved with the Technicloth™. The lowest mean percentage recovery was 61.6% and from the MiracleWipe™. This amounted to a wide disparity. Betawipe™, Alphawipe™, Super Polx 1200™ and Texwipe™ all had recovery rates in the 70-80% range and they were 71.6%, 71.7%, 76.0% and 78.9% respectively. The Absorbond™ wiper was the only other one to achieve an above 80% recovery rate at 84.5%.

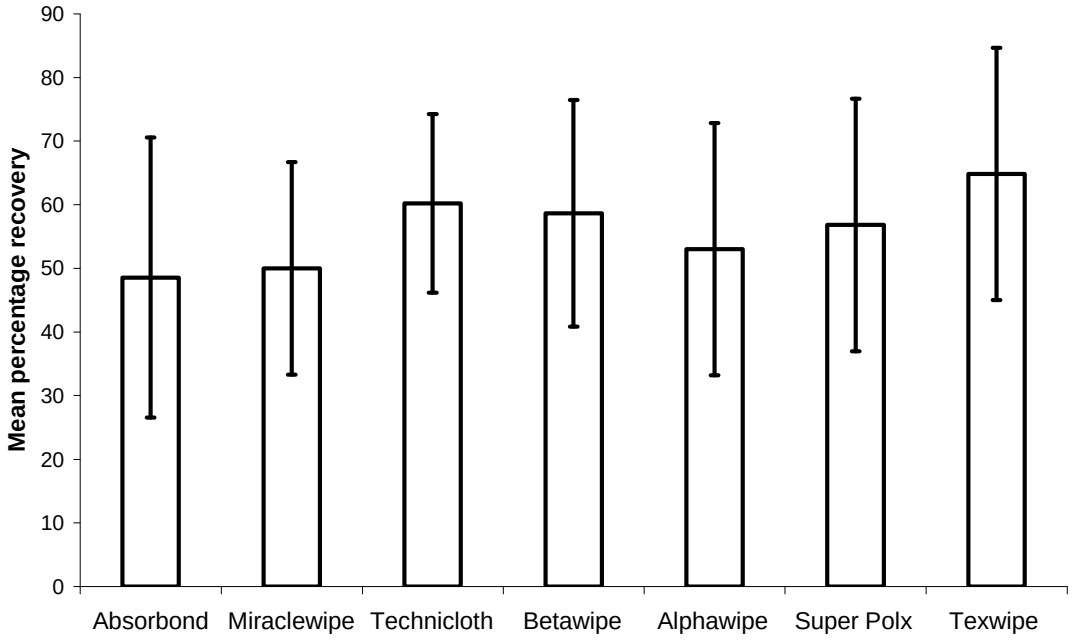

Figure 3.12. Mean percentage recovery of compound from seven commercially available swabbing materials used to wipe clean a stainless steel surface pre loaded with 0.1 mg of nicotinic acid. The bars represent standard deviation.

When compared to acetaminophen, much lower rates of recovery were achieved on stainless steel surfaces pre loaded with nicotinic acid. Texwipe™ had the highest observed recovery rate at 64.8%. Technicloth™ had the second highest recovery rate at 60.2%. MiracleWipe™, Betawipe™, Alphawipe™ and Super Polx 1200™ all displayed recovery rates in the 50-60% range with precise rates of 50.0%, 58.7%, 53.0% and 56.8% respectively. Absorbond™ had the lowest recovery rate for nicotinic acid at 48.6% and this was in fact the lowest recovery seen throughout the study. The high variations observed in measurement are worth noting. Since nicotinic acid is the most polar compound of all tested in this work a potential conclusion could

be that the low recovery is a result of enhanced affinity of a polar species to polar steel surface.

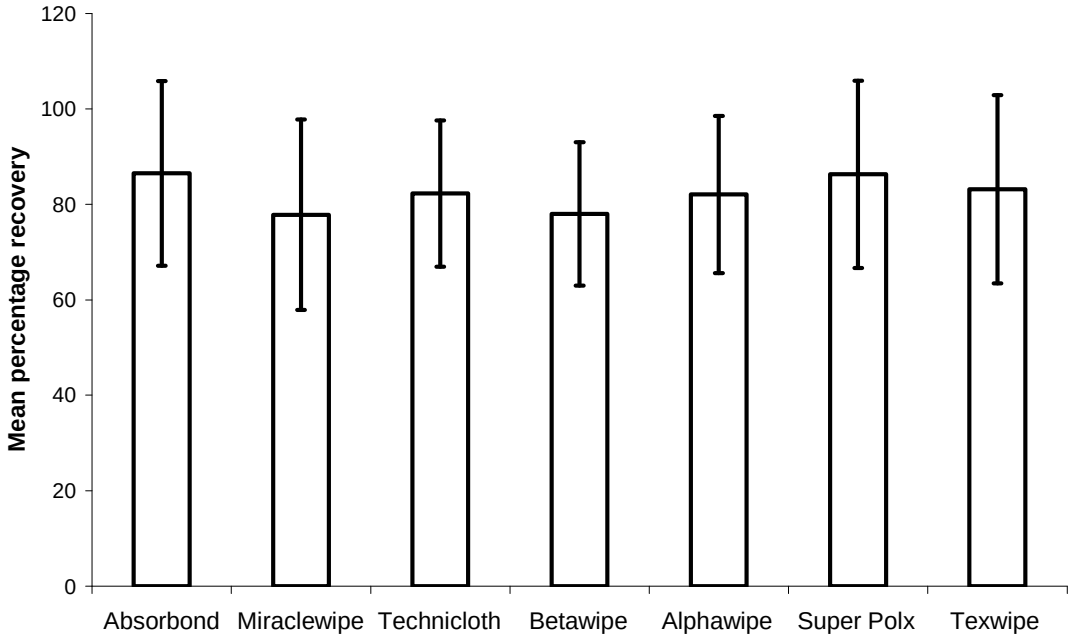

Figure 3.13. Mean percentage recovery of compound from seven commercially available swabbing materials used to wipe clean a stainless steel surface pre loaded with 0.1 mg of diclofenac. The bars represent standard deviation.

Diclofenac recovery rates were good with all swabbing materials, achieving a recovery of above eighty per cent apart from with MiracleWipe™ and Betawipe™ (77.8% and 78.0% respectively). Absorbond™ and Super Polx 1200™ had the highest recoveries at 86.5% and 86.3% respectively. Technicloth™, Alphawipe™ and Texwipe™ achieved recoveries of 82.3%, 82.1% and 83.2% respectively.

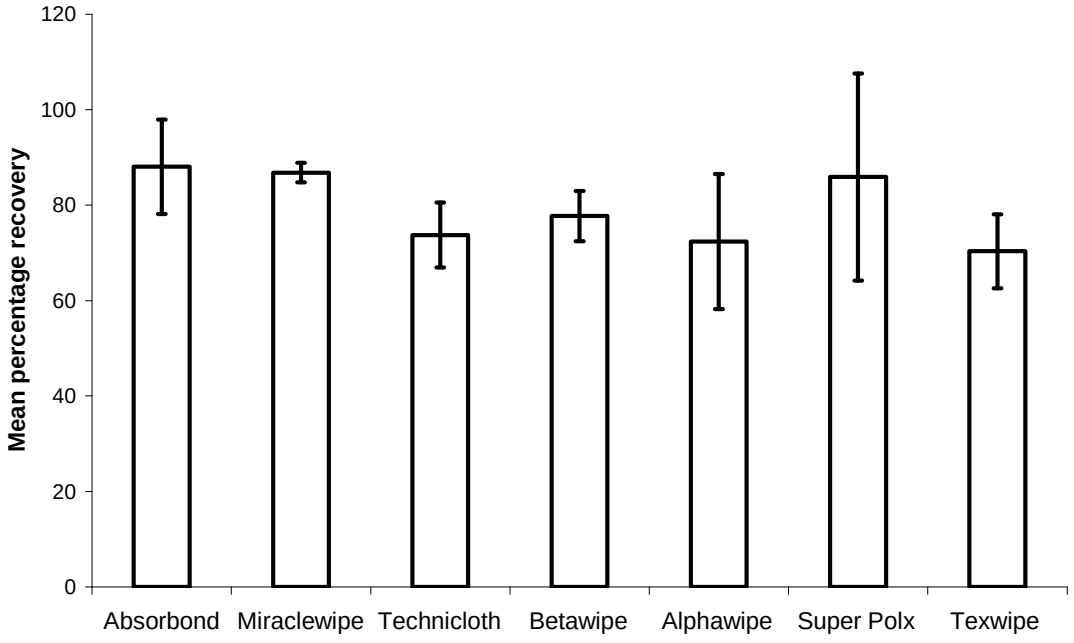

Figure 3.14. Mean percentage recovery of compound from seven commercially available swabbing materials used to wipe clean a stainless steel surface pre loaded with 1 mg of benzamidine. The bars represent standard deviation.

Recoveries for benzamidine were again generally high. The lowest recovery observed was for Texwipe™ at 70.3%. Technicloth™, Betawipe™ and Alphawipe™ showed recoveries in the 70-80% range, more precisely achieving recovery rates of 73.7%, 77.7% and 72.3% respectively. Absorbond™, MiracleWipe™ and Super Polx 1200™ achieved recovery rates of 88.0%, 86.8% and 85.8% respectively.

3.3.11 Debris generation

This section presents a series of images of fibres and particles found on a stainless steel surface after wiping with the various swab materials.

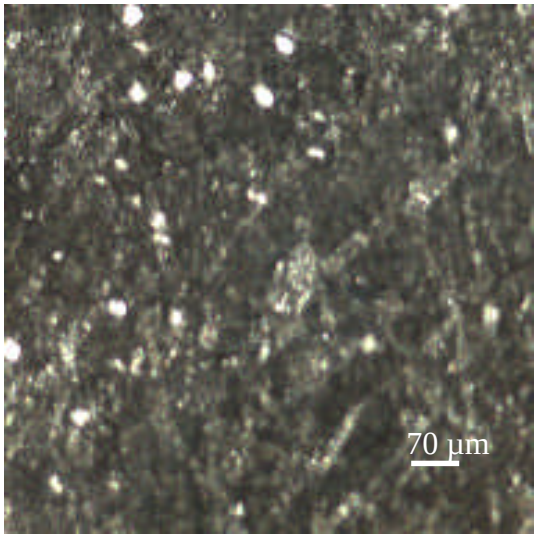

Figure 3.15. Residual particles deposited by a Betawipe™ (x10)

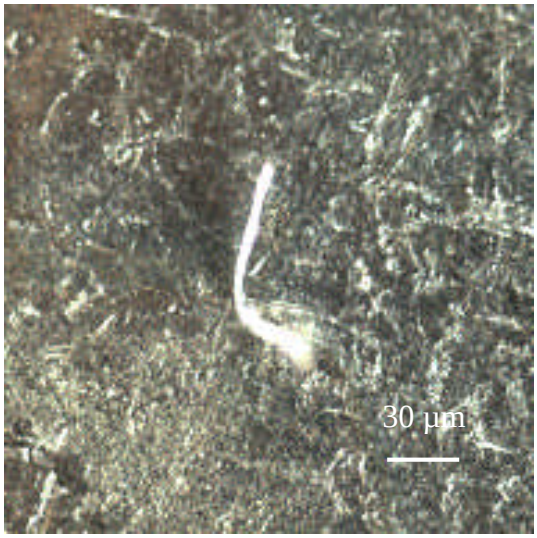

Figure 3.16. A fibre deposited by a Texwipe™ (x10).

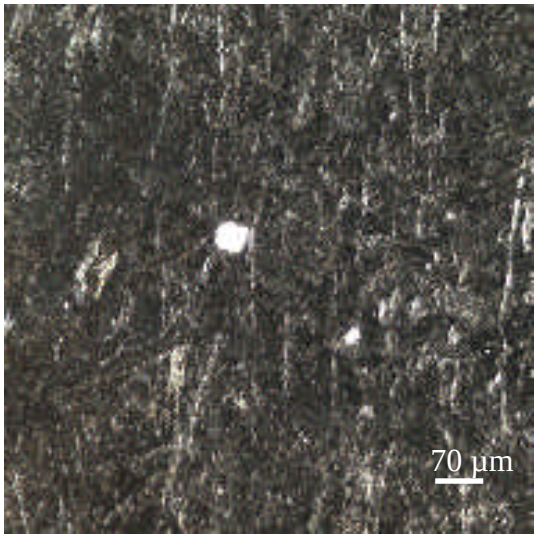

Figure 3.17. Residual particle deposited by an Alphawipe™ (x10)

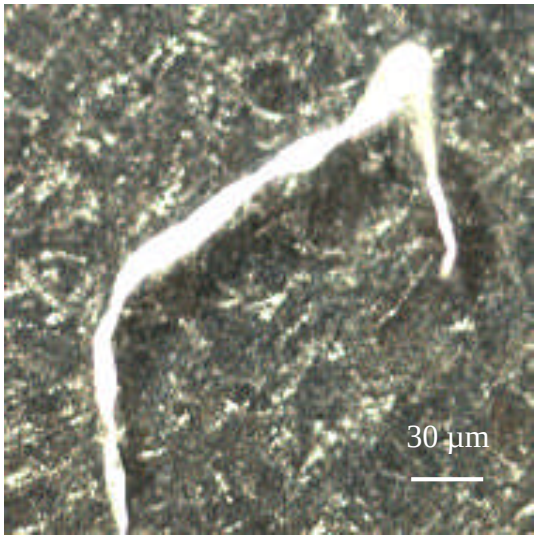

Figure 3.18. A fibre deposited by a Technicloth™ (x40).

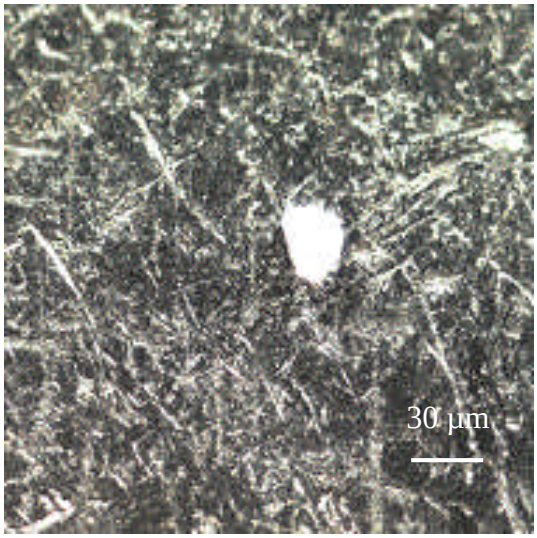

Figure 3.19. Residual particle deposited by a MiracleWipe™ (x40).

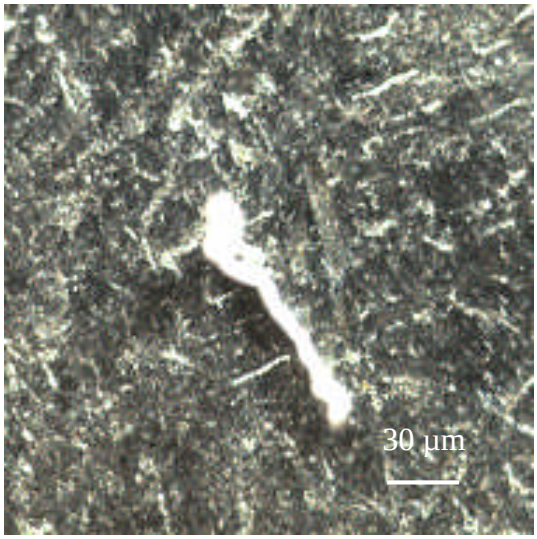

Figure 3.20. A fibre deposited by an Absorbond™ (x40)

Counts were made of fibre and particle generation as debris on wiped surfaces. The results were collated and a presented in figure 3.21.

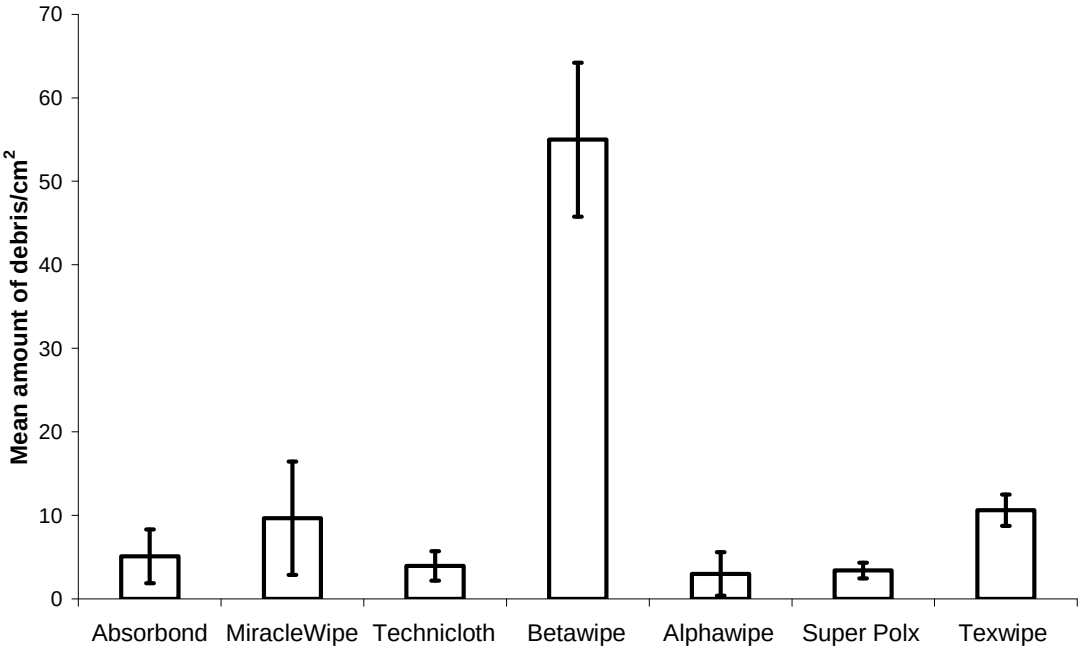

Figure 3.21. Mean amount of debris left behind on a stainless steel surface after wiping clean with seven different commercially available swabbing materials.

Debris generation fell between the range of 3.0 pieces/cm^2 and 10.6 pieces/cm2 for six of the seven swabs. Debris generation for Betawipe™ was high at 55 pieces/cm^2.

3.3.12 Compound recovery from spiked swabs in comparison to compound recovery from contaminated surfaces.

In order to obtain some additional information on the swabbing process Technicloth™ and Absorbond™ were selected to be spiked directly with compound. Technicloth™ was selected because it had good recoveries for all compounds. Absorbond™ was selected because it had good recoveries for acetaminophen, diclofenac and benzamidine but showed the lowest recovery in the entire study for nicotinic acid. Therefore it would be particularly interesting to compare the recovery of nicotinic acid from Absorbond™ when spiked directly and when used to sample a

contaminated surface. Once spiked the compound was recovered using the procedure employed for swabs used to wipe the metallic surface.

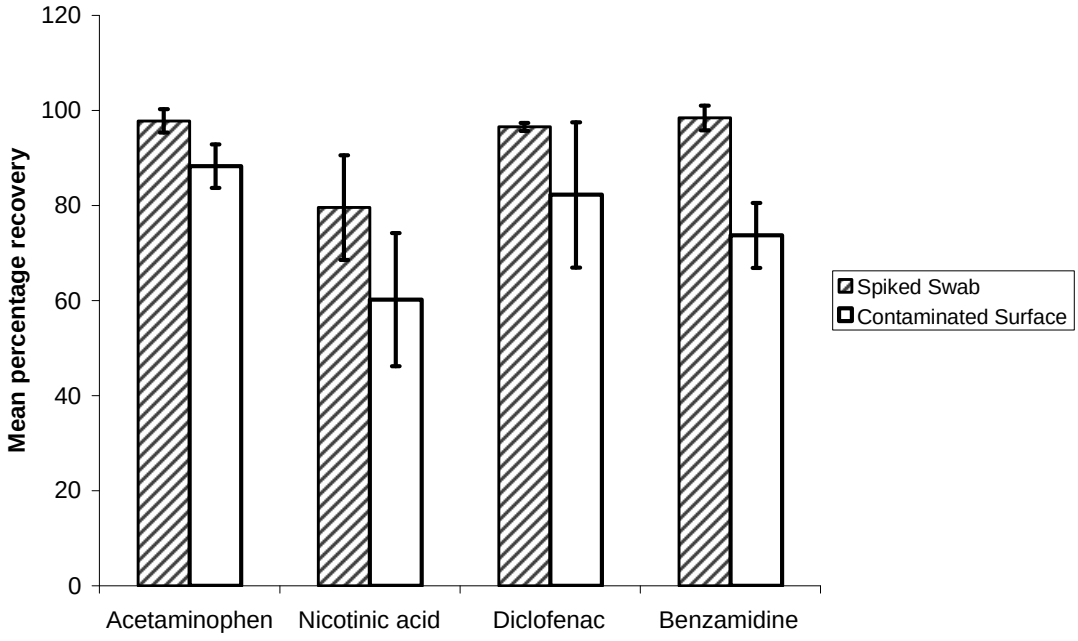

Figure 3.22. Recovery of all four compounds from a directly spiked Technicloth™ swab(black) and from a contaminated steel surface (white) wiped with the Technicloth™ swab. The bars represent standard deviation.

Technicloth™ showed increased recoveries and smaller variation after direct spiking with compound. The most significant gain was with nicotinic acid where recovery increased from 60.2% to 79.6%. Benzamidine also increased significantly from 73.7% to 98.5%. This increase in compound recovery indicated that for acetaminophen, diclofenac and benzamidine on a contaminated surface; the major loss of compound occurred through the compounds remaining present on the steel surface. Spiking the swab improved recovery for nicotinic acid markedly but a significant amount of compound (approx 20%) remained unaccounted. Another point

worth noting is that unlike acetaminophen, diclofenac and benzamidine where direct spiking of the swab caused a reduction in standard deviation, the high standard deviation for nicotinic acid remained when the swab had been spiked directly. Acetaminophen, diclofenac and benzamidine all showed high recoveries and small standard deviations where as nicotinic acid still showed a large standard deviation in spite of the recovery improving.

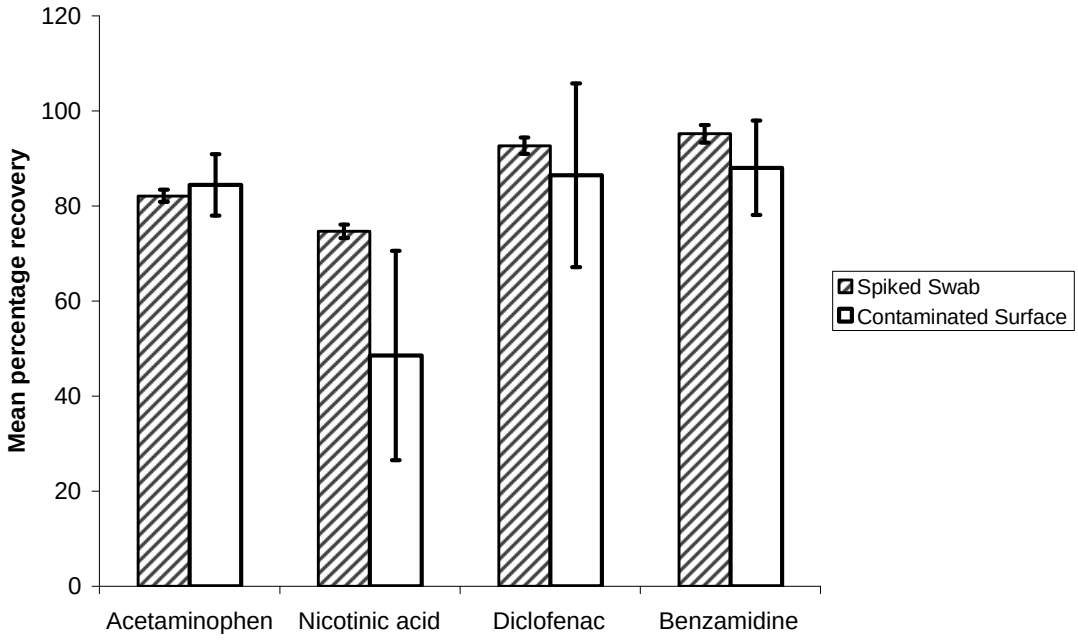

Figure 3.23. Recovery of all four compounds from a directly spiked Absorbond™ swab (black) and from a contaminated steel surface (white) wiped with the Absorbond™ swab.

Absorbond™ showed increased recoveries and much smaller variations after direct spiking with compound for nicotinic acid, diclofenac and benzamidine with nicotinic acid again displaying a marked increase from 48.6% to 74.7%. Acetaminophen recovered slightly less well from a spiked swab, falling from 84.5% to 82.1%. As

with the data where a contaminated steel surface had been wiped, better performances (92.7% for diclofenac and 95.2% for benzamidine) for compounds dissolved in ethanol than in water (82.1% for acetaminophen and 74.7% for nicotinic acid) were observed. For Absorbond™, when spiking the swab directly, the standard deviation of nicotinic acid was similar to those of acetaminophen, diclofenac and benzamidine.

Table 3.3. Summarising recovery rates and their standard deviations from the combinations of compounds and swabs used in the study.

Wiper	Acetaminophen	Nicotinic Acid	Diclofenac	Benzamidine
Absorbond™	84.5 ± 6.5	48.6 ± 22.0	86.5 ± 19.3	88.0 ± 9.9
Miraclewipe™	61.6 ± 3.2	50.0 ± 16.7	77.8 ± 20.0	86.8 ± 2.1
Technicloth™	88.2 ± 4.6	60.2 ± 14.0	82.3 ± 15.3	73.7 ± 6.8
Betawipe™	71.6 ± 5.1	58.7 ± 17.8	78.0 ± 15.0	77.7 ± 5.3
Alphawipe™	71.7 ± 1.7	53.0 ± 19.8	82.1 ± 16.5	72.3 ± 14.1
Super Polx 1200™	76.0 ± 2.8	56.8 ± 19.8	86.3 ± 19.6	85.8 ± 21.7
Texwipe™	78.9 ± 5.1	64.8 ± 19.8	83.2 ± 19.7	70.3 ± 7.7

Table 3.4. Summarising debris generation for the swabs used in the study.

	Mean	S.D.
Absorbond	**5.1**	**3.2**
MiracleWipe	**9.7**	**6.8**
Technicloth	**4.0**	**1.8**
Betawipe	**55.0**	**9.2**
Alphawipe	**3.0**	**2.6**
Super Polx	**3.4**	**0.9**
Texwipe	**10.6**	**1.9**

Table 3.5. The overall average recoveries and standard deviations for the swabs used in the study.

Wiper	Mean percentage recovery for entire study	Mean S.D.
Absorbond™	76.9	14.4
Miraclewipe™	69.1	10.5
Technicloth™	78.3	10.2
Betawipe™	71.5	10.8
Alphawipe™	75.2	15.7
SuperPolx 1200™	76.3	16.0
Texwipe™	74.3	13.1

Table 3.6. Recoveries and standard deviations for spiked Technicloth™ and Technicloth™ used to wipe a contaminated steel surface.

Technicloth™	Spiked Swab	S.D.	Contaminated Surface	S.D.
Acetaminophen	97.8	2.5	88.2	4.6
Nicotinic acid	79.6	11.0	60.2	14.0
Diclofenac	96.6	0.9	82.3	15.3
Benzamidine	98.5	2.6	73.7	6.8

Table 3.7. Recoveries and standard deviations for spiked Absorbond™ and Absorbond™ used to wipe a contaminated steel surface.

Absorbond™	Spiked Swab	S.D.	Contaminated Surface	S.D.
Acetaminophen	82.1	1.3	84.6	6.5
Nicotinic acid	74.7	1.4	48.6	22.0
Diclofenac	92.7	1.7	86.5	19.3
Benzamidine	95.2	1.9	88.0	9.9

3.4 Discussion

All of the swabs used in the study achieved overall recoveries in excess of 70% apart from MiracleWipe™ which achieved an overall recovery of 69.1% (see table 2.4). The figure quoted from the literature of 60% (Miscoscio, 1997) was met in the overall sense if the sets of data for each swab are averaged. For reference purposes, recovery data is tabulated in tables 3.3-3.7.

Acetaminophen recovered well for all seven swabs within a range of 61.6% – 88.2%. Again all recoveries from the swabs were in the 70-90% range apart for MiracleWipe™ which achieved 61.6%. The combination of Technicloth™, acetaminophen and water as the recovery solvent achieved 88.2%. This is a high recovery and demonstrates that high recoveries can be achieved with particular combinations of swab, compound and extraction solvent.

Diclofenac recovered well from all seven swabs with a range of 77.8 - 85.6 %. The standard deviations were on the whole higher with diclofenac than with acetaminophen and benzamidine. Absorbond™ and Super Polx 1200™ both performed well in combination with diclofenac and ethanol as the extraction solvent achieving recoveries of 86.5 and 86.3% respectively. Again this demonstrated that high recoveries were achievable with a particular combination of swab, compound and extraction solvent.

Benzamidine recovered well for all seven swabs with a range of 70.3 – 88.0 %. Absorbond™ performed well in combination with ethanol as the extraction solvent to

achieve the rate of 88.0%. Standard deviations were on the whole lower for benzamidine than diclofenac but the Super Polx 1200™ had a noticeably large standard deviation of 21.7 (the largest in the entire study) where as the other swabs in combination with benzamidine fell between 2.1 and 14.1.

Of the four compounds investigated in the study, nicotinic acid performed least well in terms of recovery. The range of recoveries fell between 48.6% (Absorbond™) and 64.8% (Texwipe™). Only Technicloth™ and Texwipe™ were able to achieve the satisfactory milestone of a 60% recovery as quoted by Miscoscio, 1997. Standard deviations were high too, showing that variability of recovery was also an issue with the combination of swabs, compound and extraction solvent.

To help gain further understanding of recoveries and the swabbing process, Absorbond™ and Technicloth™ were spiked directly with compound and then subjected to the same extraction process as the swabs used in the previous section of the study focused on recoveries from a contaminated steel surface. It was observed that recoveries increased in all cases except for Absorbond™ where the recoveries fell from 84.5 to 82.1%. This was a small drop that fell within the standard deviation of 6.5 for the recovery found with acetaminophen from the contaminated surface. All other recoveries increased and in particular nicotinic acid showed a marked increase going from 48.6% and 60.2% in Absorbond™ and Technicloth™ respectively to 74.7 and 79.6% respectively. These gains in recovery are significant and show that somewhere in the process of sampling with and extracting from a contaminated swab be it Absorbond™ or Technicloth™, a significant amount of nicotinic acid is lost.

The other three compounds tested showed increases in recovery when the swab was directly spiked. Recoveries of 97.8, 96.6 and 98.5% were observed for acetaminophen, diclofenac and benzamidine respectively in combination with the Technicloth™ swab. These were up from 88.2, 82.3 and 73.3 for acetaminophen, diclofenac and benzamidine when recovering from a steel surface. The fact that such high recoveries were achievable when the swab was spiked would suggest that for acetaminophen, diclofenac and benzamidine in combination with the Technicloth™ swab, a significant amount of compound was left behind on the steel surface. This statement can be made because it is known that when the swab was directly spiked the recoveries were close to one hundred percent.

For the Absorbond™ swab a minor decrease in recovery for acetaminophen (84.5 to 82.1%.) was observed but it fell within one standard deviation of the mean recovery from the contaminated surface. Nicotinic acid, diclofenac and benzamidine all showed increased recoveries when the swab was spiked directly, 48.6, 86.5 and 88.0 % respectively to 74.7, 92.7 and 95.2 % respectively. From this data we can draw the conclusion that when in combination with diclofenac and benzamidine the Absorbond™ swab does not absorb all of the contaminating compound because recoveries of greater than 90 percent are observed when the swab is directly spiked with the two compounds. For acetaminophen and nicotinic acid the same conclusion cannot be drawn because a proportion of compound is still unaccounted for. When the swab was spiked directly, recoveries of 82.1 and 74.7 were observed. In the case of acetaminophen there is a high degree of similarity between the recoveries from a contaminated steel surface and from a spiked Absorbond™ swab. This may suggest that a certain amount of acetaminophen remains bound to the Absorbond™ swab

fibres in spite of the extraction process. The fact that the swab is spiked means that a known amount of compound is present to begin with and so it cannot be said that some is left behind on the surface.

The increased recoveries for nicotinic acid are not so easily explained. Recoveries of 74.7 and 79.6% respectively from directly spiked Absorbond™ and Technicloth™ swabs are a significant improvement on recoveries from a contaminated steel surface but approximately 20-25% of the compound is still unaccounted for. A possible explanation is that nicotinic acid has a different affinity for the swab fibres to the other compounds tested. The extraction process would be less efficient if the affinity between compound and fibres was high and would result in more nicotinic acid remaining bound within the swab after extraction. Another possible explanation is a lower affinity between the swab fibres and nicotinic acid meaning a smaller amount of compound is recovered from the metallic surface. Thirdly, nicotinic acid might have a higher affinity for the steel surface than the other compounds tested.

The Super Polx 1200™ and Absorbond™ swabs showed excellent recoveries when in combination with the two compounds dissolved in ethanol. Super Polx 1200™ was found to have recoveries of 86.3 and 85.8% for diclofenac and benzamidine and Absorbond™ had recoveries of 86.5 and 88.0% for diclofenac and benzamidine. Neither swab is unique, both are made from polyester and they differ in that Absorbond™ has a fibrous appearance under the microscope and Super Polx 1200™ has a bundled appearance under the microscope. Absorbond™ has a soft finish and a glossy appearance where as Super Polx 1200™ has a soft feel and is stretchable.

To summarise, the data on recoveries showed that high recoveries from a stainless steel surface can be achieved with the correct combination of swab, compound and extraction solvent., e.g. 88.2% for acetaminophen, Technicloth™ and water, 88.0% for benzamidine, Absorbond™ and ethanol. Low recoveries can also be achieved, 48.6% for nicotinic acid in combination with Absorbond™ swab and water. Analytical scientists within pharmaceutical companies need to be aware that an incorrect match in compound, swab and solvent can lead to low recoveries and should choose and validate combinations of compounds, swab and extraction solvent appropriately.

Debris generation produced more uniform levels of performance apart from Betawipe™ which produced a much higher amount of debris than the other swabs. Betawipe™ generated a mean amount of debris of 55.0 pieces.cm^2. The other six swabs generated debris in the range of 3.0 to 10.6 pieces/cm^2. Betawipe was particularly spongy and so extra pressure can be applied during the wiping process. The slightly abrasive nature of the swab combined with the spongy quality may account for the generation of higher amounts of debris. The debris was mainly small particles as shown in Figure 3.15 where as the other swabs tended to leave behind fibres and particles. Fibres and particles were rarely apparent to the eye and the low and consistent levels of particle generation back up the manufactures claims about low particle generation from their swabs.

A significant factor in this work on swabbing is the problem of sampling. The data sets quite often showed large standard deviations and some of this variation must be introduced during the wiping process. This is going to be true for both the recoveries

and debris generation. The data from swabs spiked directly showed less variation and this will be partly due to there not being a sampling step involved. Some of the variation in the recovery data from sampled surfaces as shown by standard deviation will result from the compound remaining on the steel surface but it is inevitable that some error will be introduced by the individual carrying out the wiping. In this study, all wiping was carried by one person and so this will have helped to reduce operator based error. Pharmaceutical companies work hard to make sure that their operatives can swab consistently because it is vital to show that your swabs are representative of the actual levels of contamination on the manufacturing equipment. A point of importance to come out of this study is that of variation and that the swab sampling process has a certain amount of error inherent in it.

3.5 Conclusions

From the data it can be argued that in the overall sense Technicloth™ performed best with its recovery rate of 78.3% (highest in the study) and average standard deviation of 10.2 (lowest in the study). For cleaning verification sampling it can be argued that Technicloth™ represents the best all purpose choice. However, the data presented in this chapter shows that recovery rates of up to 88.2% can be achieved with a favourable combination of compound, swab and extraction solvent and that an unfavourable combination such as that seen with nicotinic acid and Absorbond™ can result in a recovery as low as 48.6%.

Debris generation was low for six of the swabs but Betawipe™ produced a significantly higher amount of debris.

Spiking swabs directly produced improved recoveries thus demonstrating that in the case of swabbing experiments, some compounds remain behind in significant amounts on the steel surface.

Analytical scientists working in this area need to be mindful of the problems associated with swab sampling. This study has shown significant differences in recoveries for different swab/compound/solvent combinations and emphasised the levels of variation in the recoveries produced when just one individual is responsible for sampling. Studies of this nature do not exist within the academic domain and most data on this topic is held within companies as part of their individual cleaning regimes. Some of the problems associated with swab sampling have been highlighted by this study as well as the achievability of high recoveries of drugs when particular combinations of solvent and swab are employed.

4 Raman spectroscopy and SERS for Cleaning Verification in the Pharmaceutical Industry.

Having introduced Raman spectroscopy and SERS in chapter 2, this chapter introduces and discusses the rationale for testing SERS with relevance to cleaning verification and the necessary levels of detection for cleaning verification work are introduced. Results are presented that show the difficulties associated with using SERS to detect contamination from the swab directly and that provide a support for the use of solid SERS substrates for the identification of residual compounds on a pre contaminated stainless steel surface at concentrations relevant to cleaning verification.

4.1 Introduction

As stated in the introductory section of the thesis, SERS is a highly sensitive spectroscopic technique, potentially capable of detecting chemical species at the levels necessary for cleaning verification work. There are difficulties associated with spectroscopic probing methods for direct measurements on manufacturing equipment in pharmaceutical facilities that include the requirement to make all devices intrinsically safe so that can be used in the solvent rich plant atmosphere and the problems of sampling curved surfaces and pipes with spectroscopic sampling accessories, therefore the swab is a potentially useful point in the cleaning verification process that could be investigated with the aim of speeding the process up.

The main aims of the chapter is to show that Raman spectroscopy can detect contamination on swabs and find the level of contamination at which the signal is lost, to show that SERS can be carried out on the Raman microscope, to obtain SERS spectra for compounds of interest at concentrations relevant to cleaning verification

work and to modify the swab so that a SERS signal can be obtained and contamination determined directly from the swab surface by SERS. Should it not prove possible to detect contamination directly from the swab by SERS, alternative SERS methods will be tested.

As has already been pointed out, SERS is an evolving technology and some problems exist regarding the consistency of signal and reproducibility of results. Obtaining the correct SERS chemistry is of paramount importance and this is another initial aim of the chapter. By demonstrating SERS as possible and generating SERS spectra for various compounds on our Raman system it will then be possible to employ the technique to look at the cleaning verification problem.

As pointed out in the literature review, the wide disparity in levels to which it is necessary to clean adds some difficulty to the experiments with SERS. The initial Raman spectroscopy work with steel surfaces will employ a contamination level of 111µg/100 cm^2 or 1.1µg/cm^2. Additionally, some of the work will be carried out in the ppm range and for the purposes of comparison to cleaning verification this will be mainly around the 10 ppm range. When trying to implement SERS as a cleaning verification technology the contamination levels investigated will be from approximately 100 ng.cm^2 to 1 ng/cm^2.

4.2 Materials and Methods

Raman spectroscopy and SERS were carried out with a Horiba Olympus BX40 Raman microscope (Horiba Jobin-Yvon, Stanmore, UK). Images presented in this chapter were taken through the camera attachment of the Raman microscope.

Gold colloid was prepared by mixing 1 ml of a 0.1% sodium citrate solution with 40 mls of 1% hydrogen tetrachloroaurate trihydrate (gold chloride) solution at 60 ^{o}C. The reaction mixture was then heated up to boiling point and cooled in ice when the mixture had taken on a red colour. The method was taken from a paper by Frens, 1973 and is a frequently cited method of preparing gold colloid in the SERS literature.

SERS experiments performed in liquid were carried out by attaching the Horiba liquid sampling accessory to the microscope. Liquid samples were pipetted into a 1 ml quartz cuvette, placed into the sampling accessory and then a spectrum was recorded. The solutions were made up by mixing in the ratio of 100 µl analyte, 900 µl gold colloid and 50 µl of 3% NaCl solution (Faulds *et al.*, 2002).

Solutions for SERS experiments were prepared by mixing the analyte solution with gold colloid and 3% wt NaCl solution in a 10 µl, 100 µl, 5 µl fashion. In a typical experiment, a solution was prepared by mixing 10 µl of analyte with 100µl of gold colloid and 5 µl of 3% wt NaCl solution. A 5 µl drop of solution was placed on a glass microscope and allowed to evaporate dry before inspection under the Raman microscope. Gold colloid for these experiments had a mean particle size of 5 or 20

nm and was purchased from Sigma (Poole, Dorset, UK). The method was adapted from a paper by Li *et al.,* 2003.

Swabs were impregnated with gold colloid by folding the wiper into a 15 ml funnel and then pouring the gold colloid solution prepared using the citrate reduction method through. The filtrate was collected and poured through a further two times. The swabs were left on the bench over night to dry before use in experiments.

Swabs were sputter-coated using an Agar Scientific Automatic Sputter Coater (Stanstead, Essex, UK). The device was used on the routine sample coating setting. After loading the swab into the chamber, the argon supply was opened and the regulator valve set to at 0.3 bar. The manual mode was then selected and the "flush" button pressed. After 3 – 5 seconds the "leak" button was pressed and the pressure was allowed to stabilise at 0.08 mb. The auto mode was selected and then the "cycle" button was pressed resulting in a forty second gold coating of the swab. The duration of the coating time was changed to twenty seconds in order to produce partially coated sputter coated swabs.

In experiments where a contaminated stainless steel surface was swabbed, prior to contamination the surface was cleaned with isopropyl alcohol. Once dry the compound of interest was deposited onto the surface in 1 ml of solvent, spread across the surface and subsequently allowed to evaporate dry. The surface was then wiped with a moistened swab.

One set of gold substrates were prepared by Dr Jin Sung Kim in the Department of Engineering and Computer Science at the University of Michigan. The diagram of the preparation method can be found in Appendix 1.

Klarite substrates were purchased from Mesophotonics Ltd (Southampton, UK) and in this project used by pipetting a 5 µl drop of liquid onto the roughened gold surface and allowing to dry. Once the solvent evaporated the surface was inspected with the Raman microscope and a spectrum recorded.

Acetaminophen, nicotinic acid, ibuprofen, diclofenac, trichloroacetic acid, maleic acid, ascorbic acid, citric acid, thiamine, sodium citrate, hydrogen tetrachloroaurate trihydrate were purchased from Sigma (Poole, Dorset, UK). Methanol, ethanol and isopropyl alcohol were purchased from Fisher Scientific (Loughborough, UK).

Principal component analysis

When interpretation of a spectrum becomes difficult, statistical analysis methods such as Principal Component Analysis (PCA) can be used to help interpret the data. PCA provides an approximation of a data table, data matrix (X) in terms of the product of two small matrices (T & P). The matrices capture the essential data patterns of X. Almost any data matrix can be simplified by PCA and it estimates the correlation structure of the variables. In a principle component model the importance of a variable is indicated by the size of it residual variance (Wold. S, 1987). A basic assumption in the use of PCA is that the score and loading vectors corresponding to the largest eigenvalues contain the most information relating to the specific problem and that the remaining ones comprise noise. Therefore the vectors are usually written

in terms of their eigenvalues (Wold. S, 1987). In this study PCA was used on the SERS spectra for acetaminophen and ibuprofen. A 3-D plot was produced showing PCA scores on all three axes for spectra of acetaminophen and ibuprofen. PCA was carried out using the computer software Matlab.

4.3 Results

4.3.1 Raman spectroscopy of commercially available swabs

Raman spectroscopy was carried out on commercially available swabs so that the spectra for the swabs could be compared. It would be potentially useful if one swab or certain swabs were found to possess a minimal Raman spectrum as this would make it easier to distinguish peaks owing to contamination.

Texwipe™

Texwipe™ was made from cotton which is cellulose based. The spectrum showed two large characteristic peaks at 1612 and 1725 cm^{-1} and significant activity in the "fingerprint" region between 1250 cm^{-1} and 250 cm^{-1}. The swab had a filamentous appearance but many of the individual fibres were obscured because of the swab having depth. The Raman spectrum above in Figure 4.1 was taken by focusing the laser onto the fibre pointed out by the arrow in Figure 4.2.

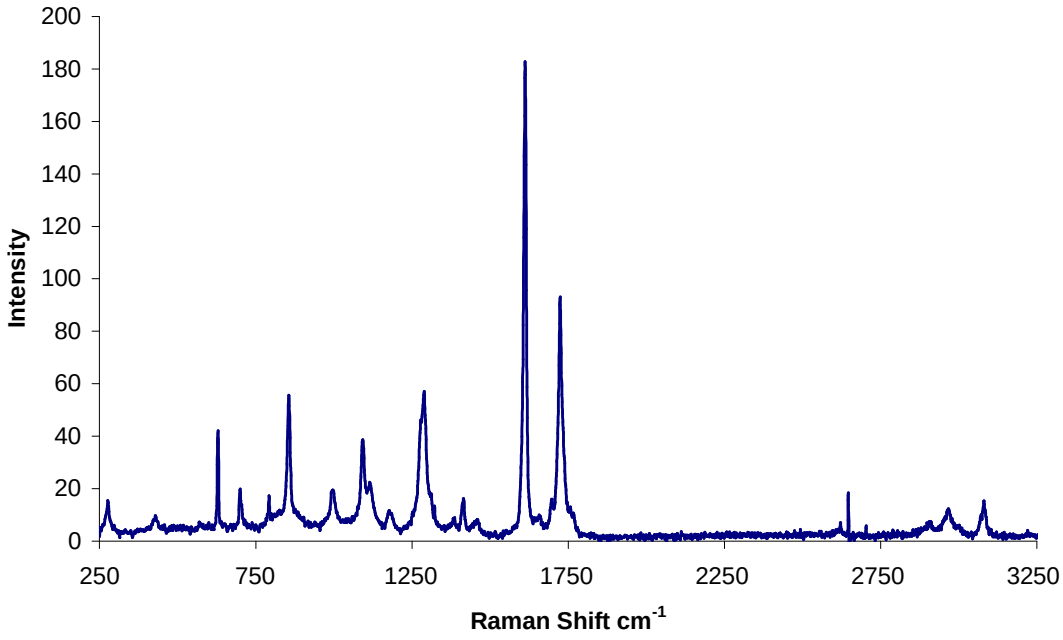

Figure 4.1. Raman spectrum from the surface of a Texwipe™ swab.

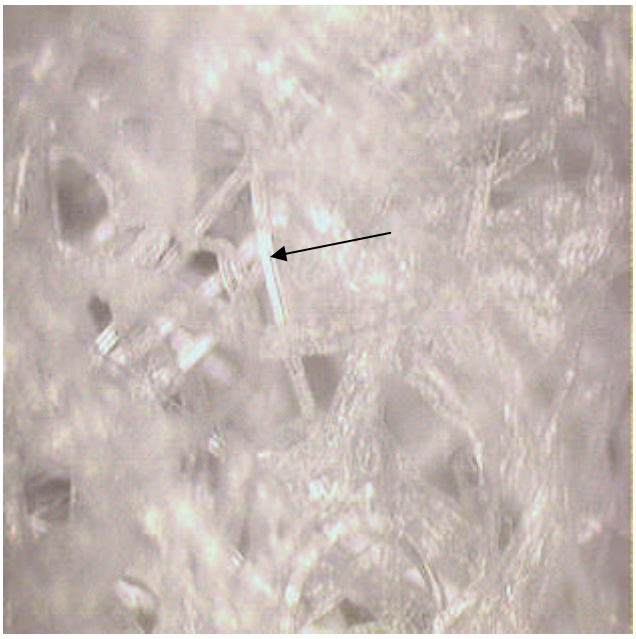

Figure 4.2. Image taken on the Raman microscope of the surface of a Texwipe™ swab (x10).

Absorbond™

The Absorbond™ swab showed a very similar Raman spectrum to Texwipe™. The two large peaks at 1612 and 1725 cm^{-1} observed with Texwipe™ were also apparent with Absorbond and identical patterning of bands in the fingerprint region was also apparent.

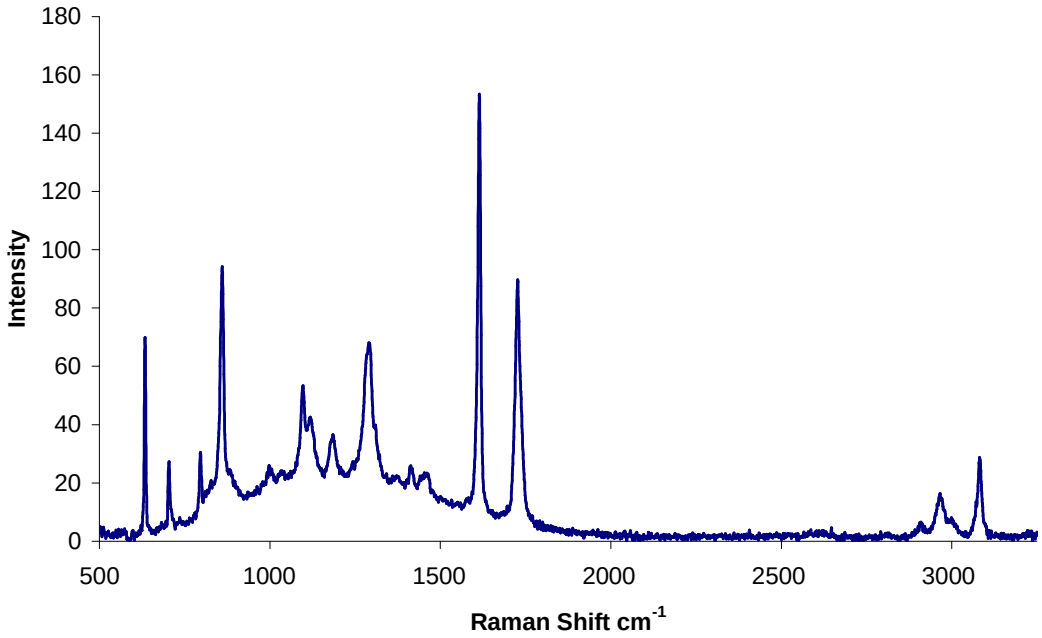

Figure 4.3. Raman spectrum from the surface of an Absorbond™ swab.

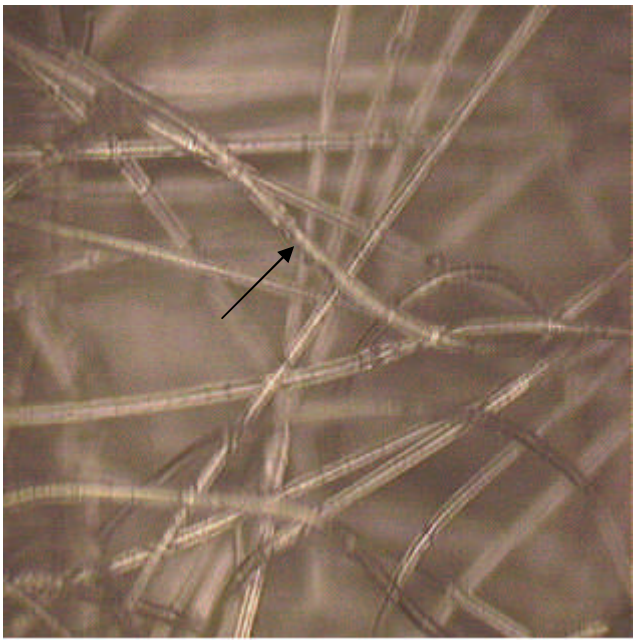

Figure 4.4. Image taken on the Raman microscope of the surface of the Absorbond™ swab (x 10).

Absorbond™ was found to have a filamentous appearance under the microscope and the swab having depth meant that a number of fibres were out of focus when sampling. The Raman spectrum in Figure 4.3 was taken by focusing the laser onto the fibre indicated by the arrow in Figure 4.4.

MiracleWipe™

MiracleWipe™ was constructed from nylon and so a totally different Raman spectrum was found. The patterning in the fingerprint region was different to the spectra for Absorbond™ and Texwipe™ and additionally much more activity apparent in the 2800 cm^{-1} to 3200 cm^{-1} range. The MiracleWipe™ swab had a bundled appearance and this made a Raman spectrum more difficult to acquire because individual fibres upon which to focus the laser are less apparent. The Raman spectrum in Figure 4.5 was acquired by focusing the laser onto the spot indicated by the arrow in Figure 4.6.

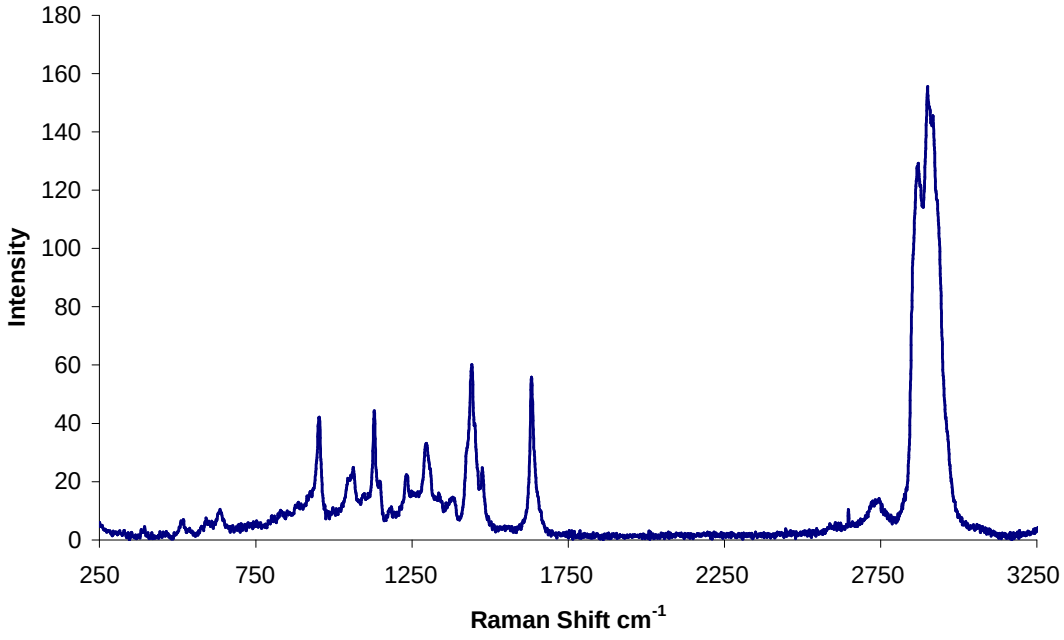

Figure 4.5. Raman spectrum from the surface of a MiracleWipe™ swab.

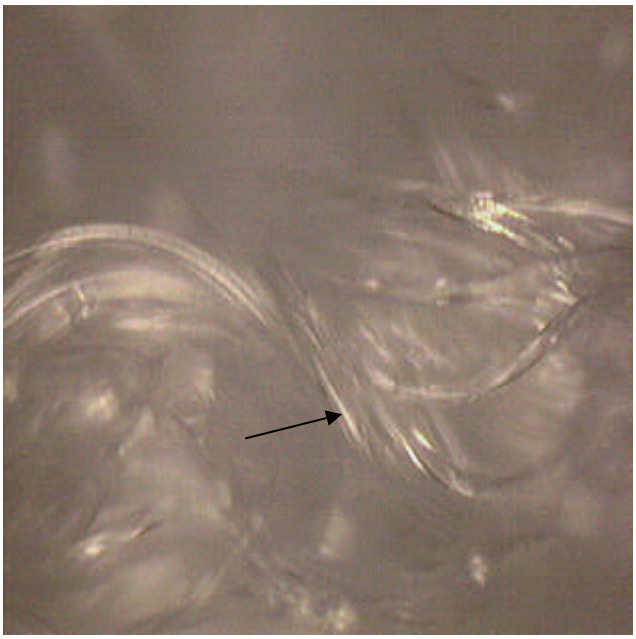

Figure 4.6. Image taken on the Raman microscope of the surface of a MiracleWipe™ swab (x10).

Technicloth™

This spectrum was identical to the spectra acquired for Absorbond™ and Texwipe™ except that the small peaks at 2971 and 3081 cm^{-1} were not present. The Technicloth™ swab was made from a blend of cellulose and polyester whilst the Absorbond™ swab was made from polyester and the Texwipe™ swab made from cotton. A high similarity in Raman spectra was observed from three swabs (Texwipe™, Absorbond™ and Technicloth™) that were of different polymeric materials.

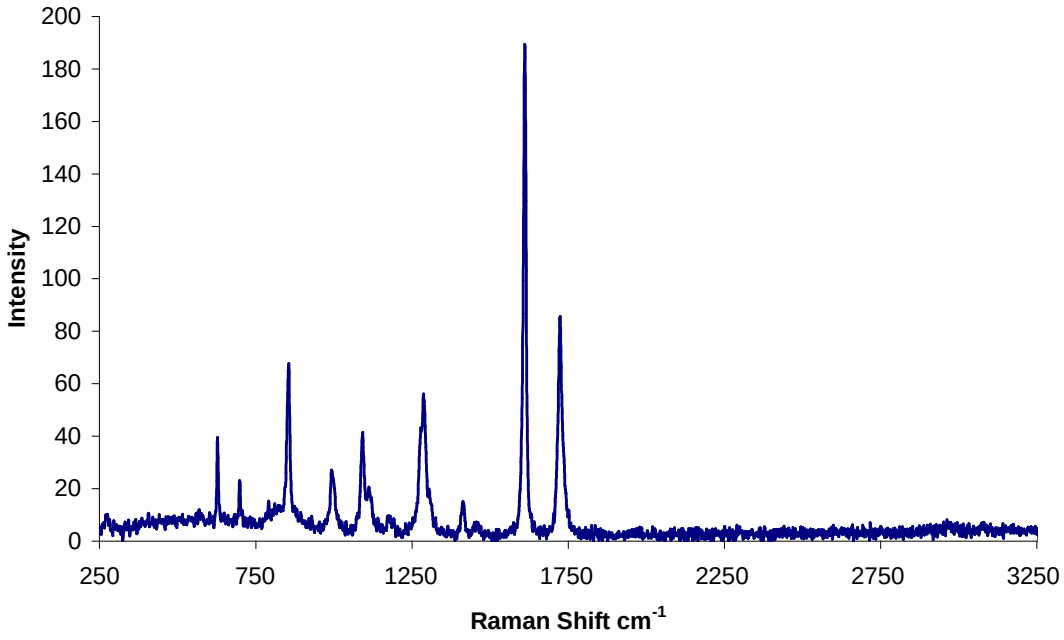

Figure 4.7. Raman spectrum from the surface of a Technicloth™ swab.

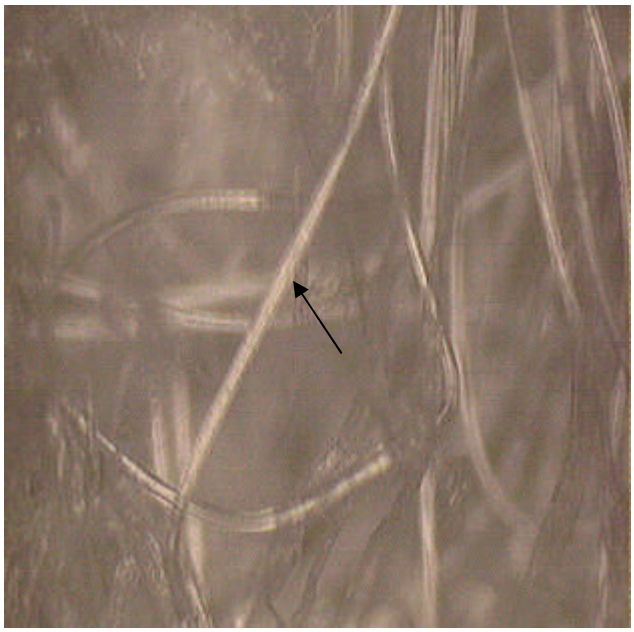

Figure 4.8. Image taken on the Raman microscope of the surface of a Technicloth™ swab (x10).

The Technicloth™ swab had a filamentous appearance under the Raman microscope and the Raman spectrum in Figure 4.7 was taken by focusing the laser onto the spot indicated by the arrow in Figure 4.8.

Betawipe™

Betawipe™ was made from polypropylene and consequently a different Raman spectrum was acquired. No activity beyond 1458 cm^{-1} was apparent until reaching the 2750 to 3250 cm^{-1} range where six peaks between 2840 $.cm^{-1}$ and 2960 cm^{-1} were apparent.

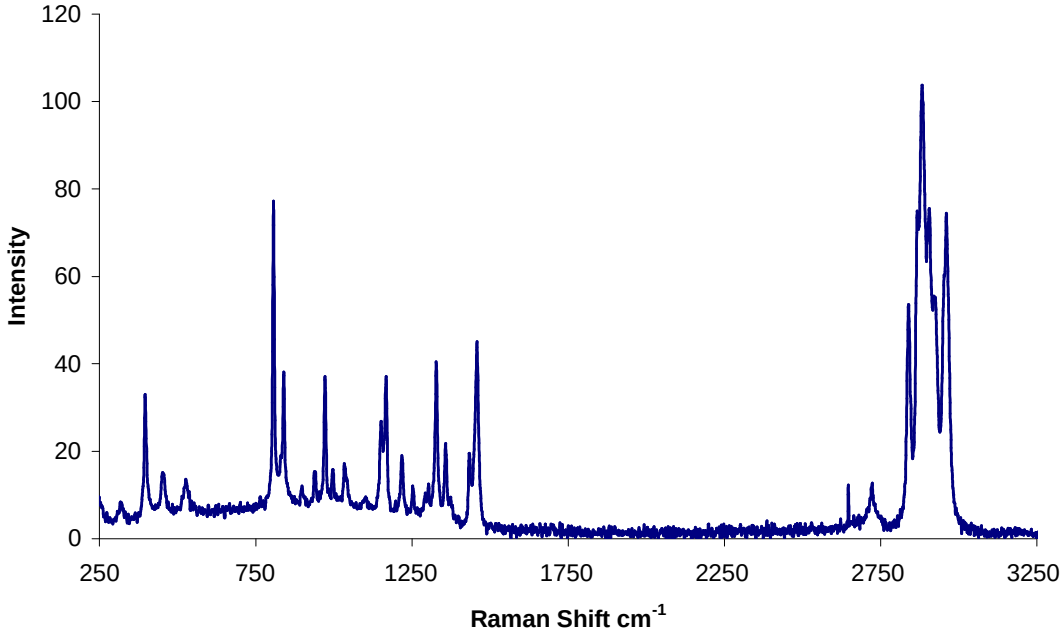

Figure 4.9. Raman spectrum from the surface of a Betawipe™ swab.

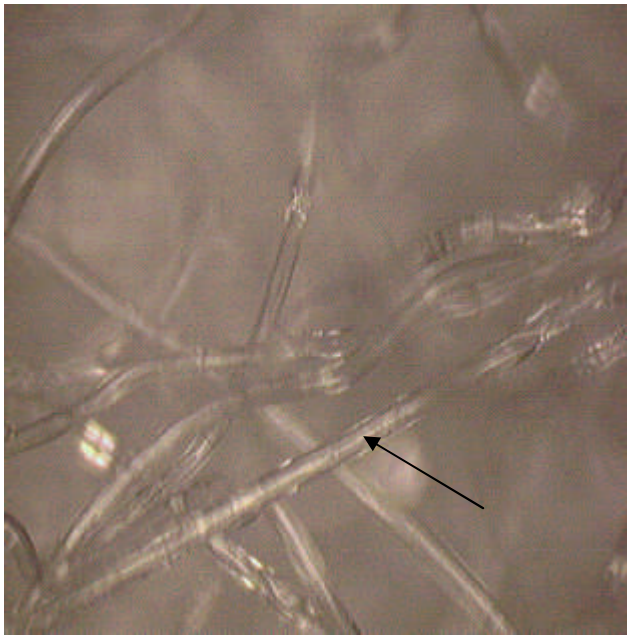

Figure 4.10. Image taken on Raman microscope of the surface of the Betawipe™ swab (x10).

The image above taken using the Raman microscope revealed a filamentous appearance for the Betawipe™ swab. The Raman spectrum in Figure 4.9 was acquired by focusing the laser spot on the point indicated by the arrow in Figure 4.10.

Alphawipe™

Alphawipe was made from polyester and a similar Raman spectrum to that acquired for Absorbond™ and Technicloth™ which also contain polyester was acquired. The two peaks at 1612 and 1725 cm^{-1} were particularly apparent.

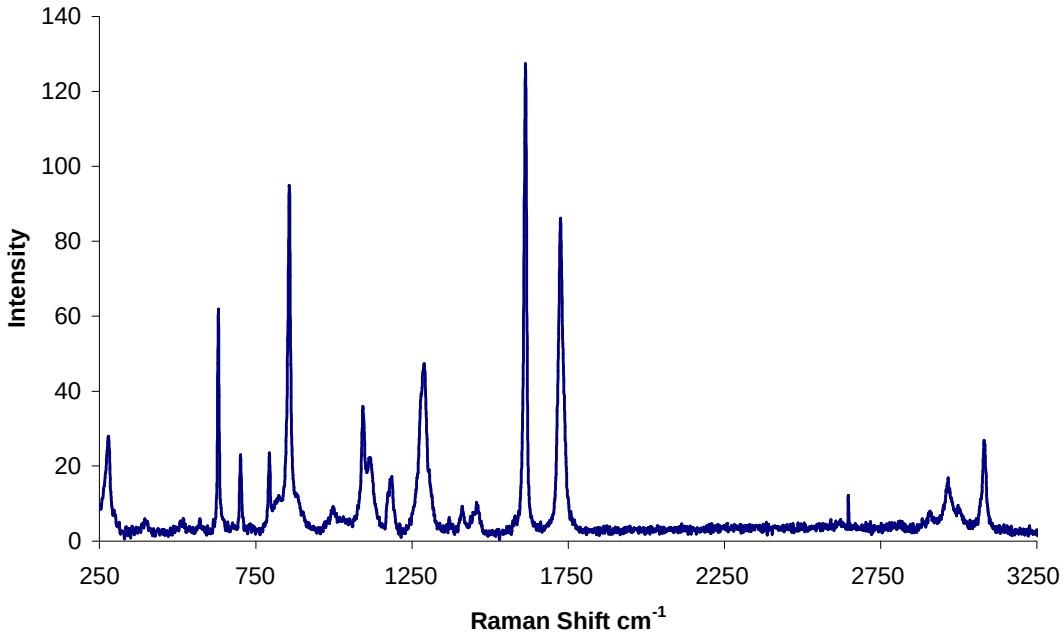

Figure 4.11. Raman spectrum for the surface of an Alphawipe™ swab.

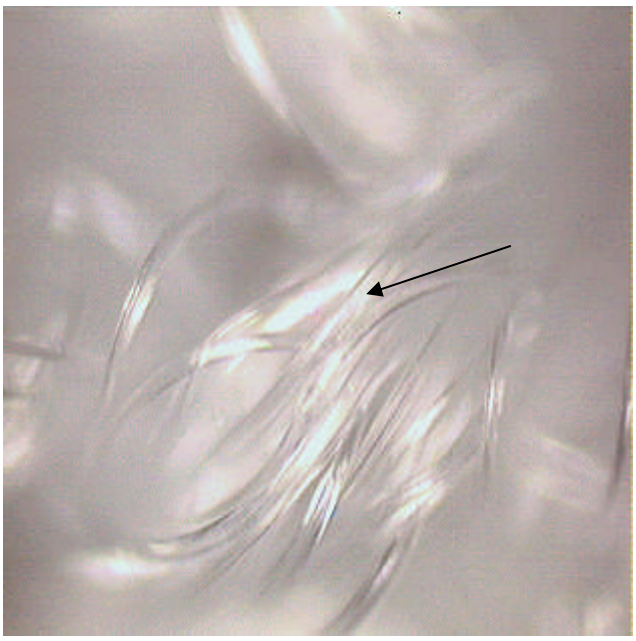

Figure 4.12. Image taken on Raman microscope of the surface of the Alphawipe™ swab (x10).

Alphawipe™ had a bundled appearance under the Raman microscope and the Raman spectra above was acquired by focusing the laser onto the spot indicated by the arrow.

Super Polx 1200

Super Polx 1200™ was made from polyester and the spectrum was the same as those acquired from Absorbond™, Technicloth™ and Alphawipe™ which were all polyester containing swabs. Again, the two peaks at 1612 and 1725 cm^{-1} were particularly apparent.

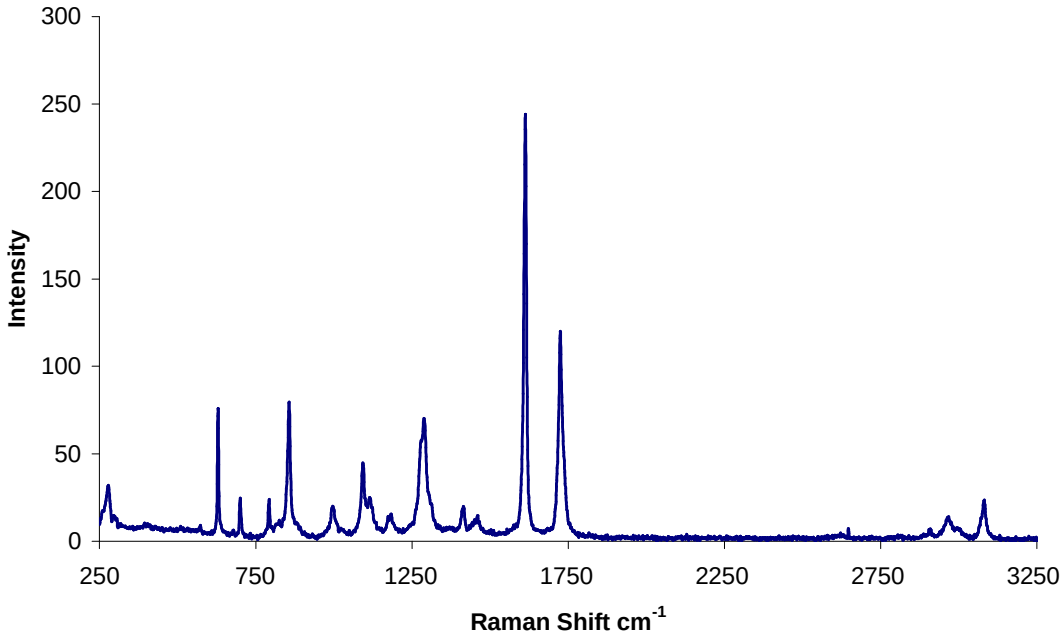

Figure 4.13. Raman spectrum for the surface of a Super Polx 1200™ swab.

Super Polx 1200™ was made from polyester and the spectrum was the same as those acquired from Absorbond™, Technicloth™ and Alphawipe™ which were all polyester containing swabs. Again, the two peaks at 1612 and 1725 cm^{-1} were particularly apparent.

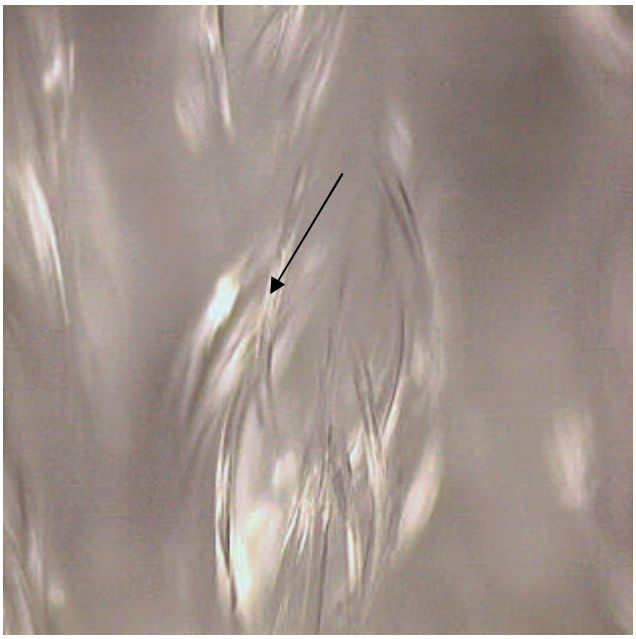

Figure 4.14. Image taken on Raman microscope of the surface of the Super Polx 1200 swab (x10).

Super Polx™ was found to be similar to Alphawipe™ under the Raman microscope because it had a bundled appearance and spectroscopically because it is constructed from polyester. The Raman spectrum for Super Polx 1200™ was acquired by focusing the laser onto the spot indicated by the arrow.

Summary of swab spectra

Absorbond™, Technicloth™, Alphawipe™, Super Polx™ and Texwipe™ all had extremely similar Raman spectra. The main characteristic peaks were found at 1612 and 1725 cm^{-1} and these were due to a carbonyl group, with one of the bands resulting from an asymmetric combination These swabs were made from polyester, polyester/cellulose or cotton. A well defined chemical structure for the swabs from the proprietary companies was lacking but significant amounts of similarity in the Raman spectra for these five swabs was apparent.

MiracleWipe™ was made from nylon and had a markedly different Raman spectrum from the swabs just discussed. Again nylon is only a general description because there are a number of variants of nylon but the peak at 1633 cm^{-1} is due to a carbonyl group. Increased activity in the C-H region was observed compared to the five swabs previously mentioned.

Betawipe™ was made from polypropylene and had a Raman spectrum different from that of the swabs previously mentioned. There was increased activity in the 2750 – 3250 cm^{-1} range. The polymer polypropylene contains a number of C-H, CH_2 and methyl groups which gave rise to the total of six peaks found between 2840 and 2925 cm^{-1}.

These investigations revealed that the swabs all had well defined Raman spectra. The information gained in this section can be used to distinguish between peaks due to contamination and peaks originating from the swab itself. No one particular swab was less active with Raman spectroscopy and therefore no particular swab could be labelled as useful for looking for signs of contamination because of its minimal Raman contribution.

Sampling from the swab surface.

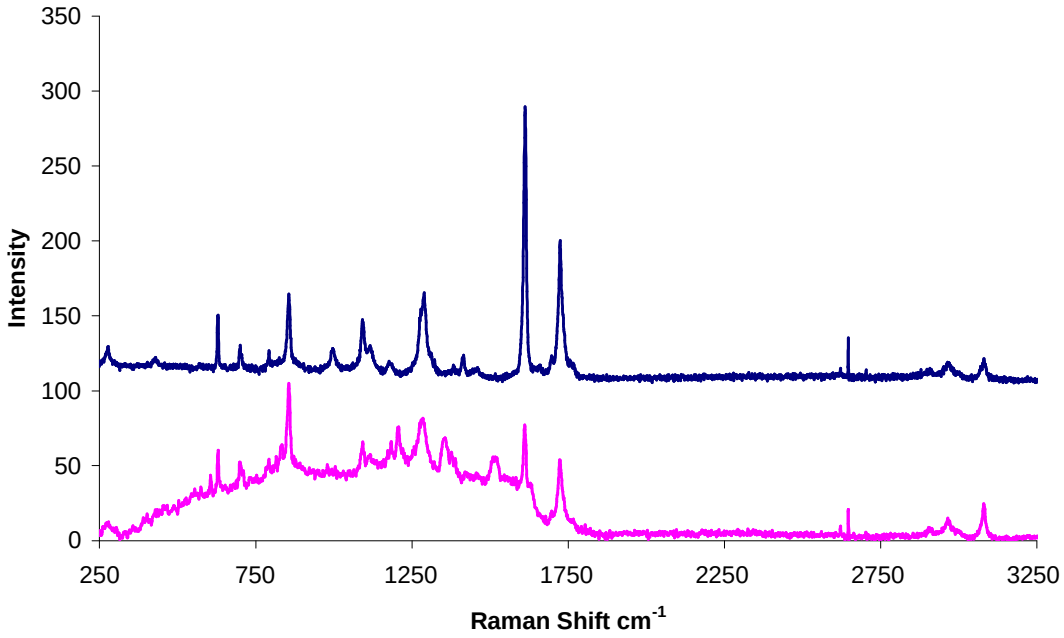

Figure 4.15. Two Raman spectra from different areas of the same Texwipe™ swab. Blue – fibre from top ofswab. Pink – fibre within swab.

Figure 4.15 shows how the area sampled can have an effect on the intensity of signal and resolution of peaks. These two spectra were from the same swab but different fibres. The blue spectrum was taken from an individual fibre onto which the laser spot could be easily focused. The pink spectrum was from a less prominent fibre, partially obscured by others and less able to be covered by the laser spot. Surface detail and the actual spot sampled can have an effect on the quality of the spectrum acquired.

From experiments carried out in the previous section it became apparent that a Raman spectrum with good peak amplitude and a favourable signal to noise ratio was more easily acquired from a swab of filamentous appearance under the microscope than

from a swab of bundled appearance. Texwipe™, Absorbond™, Technicloth™ and Betawipe™ produced more consistent Raman spectra with good peak amplitude and a favourable signal to noise ratio.

4.3.2 Raman spectra from contaminated swabs

Swabs were contaminated with acetaminophen, ibuprofen and diclofenac at a theoretical level of 111 µg/cm2 by wiping a contaminated stainless steel surface as outlined in the Materials and Methods section before analysis by Raman microscope.

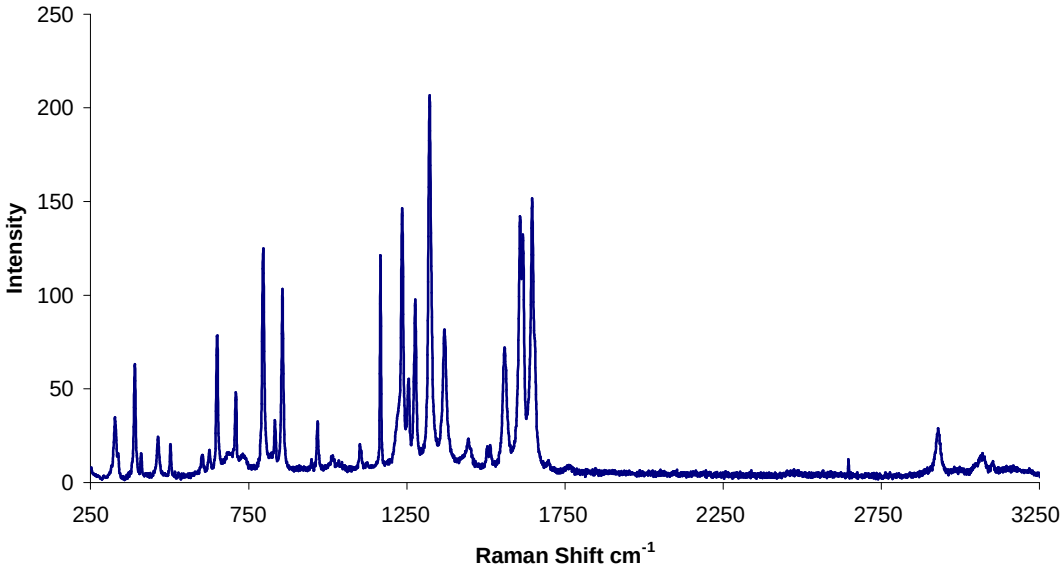

Figure 4.16. Raman spectrum from a Texwipe™ used to clean a stainless steel surface contaminated to 111.1 µg/cm^2 of acetaminophen.

Figure 4.16 shows the spectrum of acetaminophen absorbed onto a Texwipe™ swab. The spectrum showed none of the characteristic peaks associated with the Texwipe™ swab and compared well to a reference spectrum for acetaminophen.

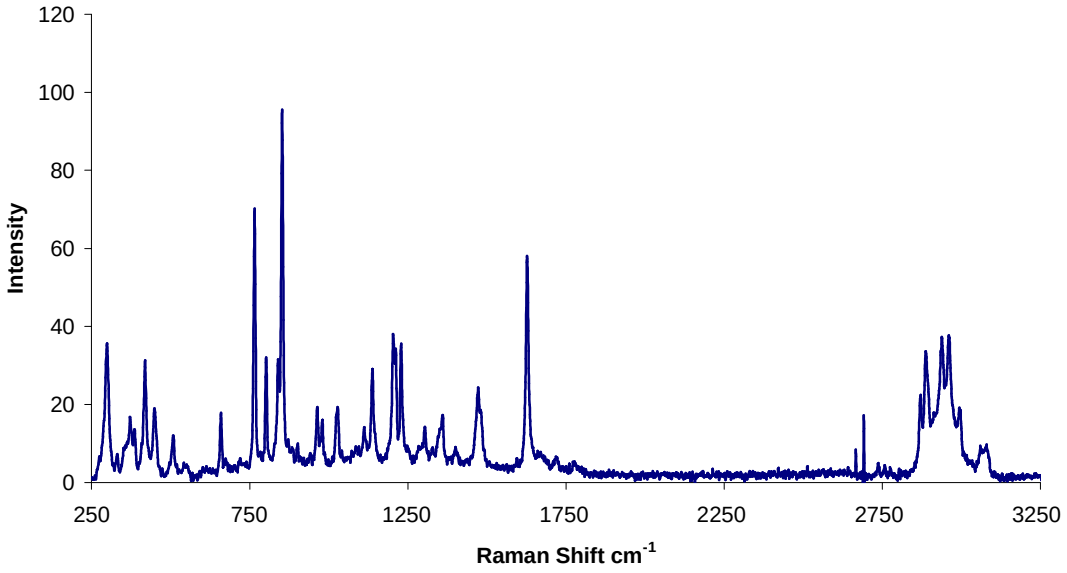

Figure 4.17. Raman spectrum from a Texwipe™ used to clean a stainless steel surface contaminated to 111.1 µg/cm^2 of ibuprofen.

Similarly, when contaminated with ibuprofen, the spectrum showed none of the characteristic peaks associated with the Texwipe™ swab and compared well to a reference spectrum for ibuprofen.

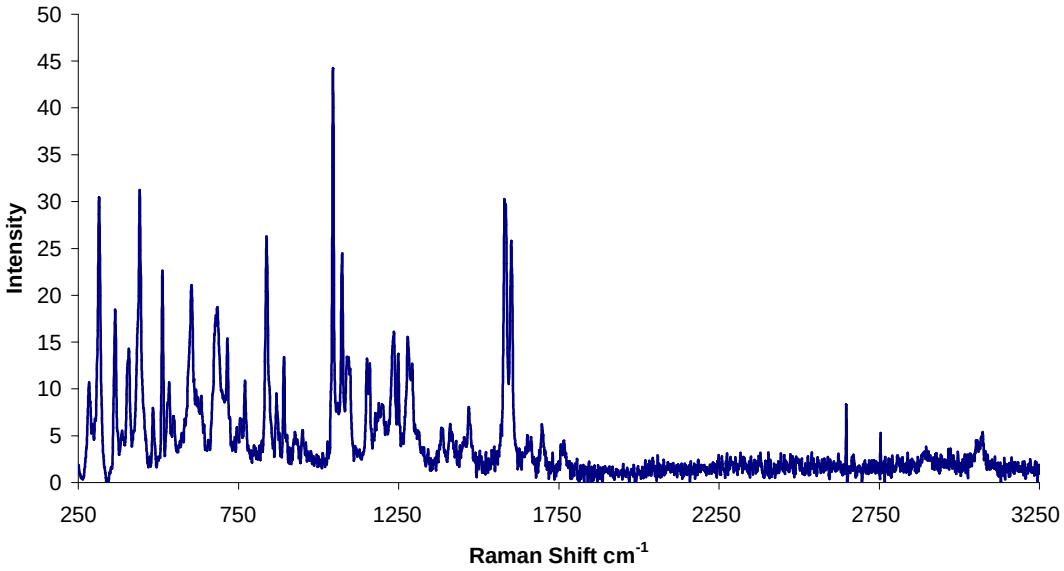

Figure 4.18. Raman spectrum from a Texwipe™ used to clean a stainless steel surface contaminated to 111.1 µg/cm^2 of diclofenac.

The spectrum presented in figure 4.18 showed none of the characteristic peaks associated with the Texwipe™ swab and compared well to a reference spectrum for diclofenac.

Figures 4.16, 4.17 and 4.18 showed that it was possible to non-destructively sample the swab surface for signs of contamination. A large number of attempts were made to detect contamination and therefore the levels of sensitivity required improvement so that detection can take place at levels encountered during cleaning verification.

4.3.3 SERS

As pointed out in the introductory section of this thesis, SERS is a very sensitive technique and if successfully applied enables the detection of residues at low

concentrations. Here the initial aim was to detect contamination from the surface of the swab itself.

SERS with gold colloid

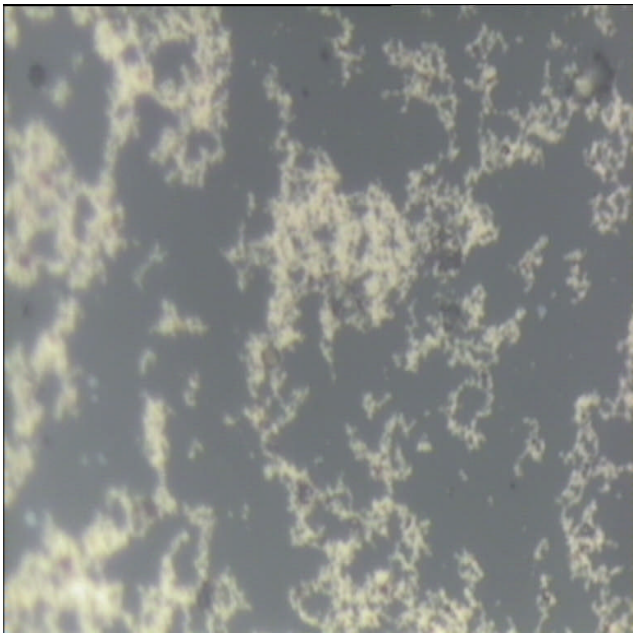

Figure 4.19. Aggregated gold colloid on a microscope slide. A 5 µl drop of a mixture of colloid, compound and 3% NaCl solution was pipetted onto the microscope slide and allowed to evaporate dry before examination under the Raman microscope.

Acetaminophen was initially tested and the spectrum as shown in Figure 4.20 was characteristic of acetaminophen and the result of surface enhancement because no signal could be detected from a 5 µl drop of 0.1 mg/ml solution of acetaminophen left to evaporate dry on a glass microscope slide.

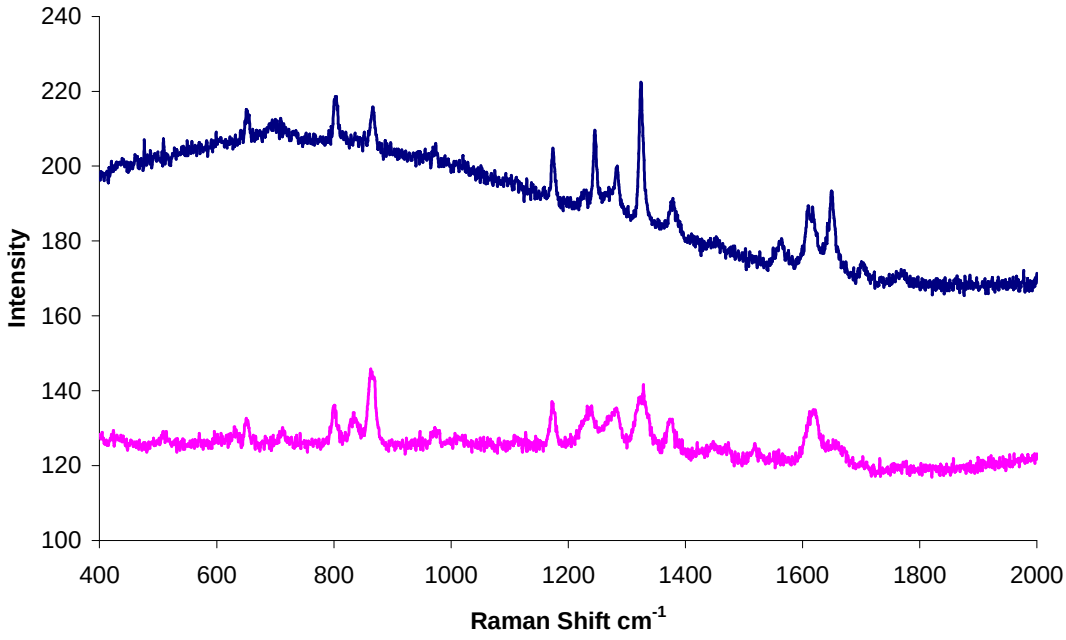

Figure 4.20. Raman spectra for a 0.1 mg/ml acetaminophen solution investigated with the 5 µl drop method. The pink line represents the 20 nm colloid and the blue line represents 5 nm colloidal particles.

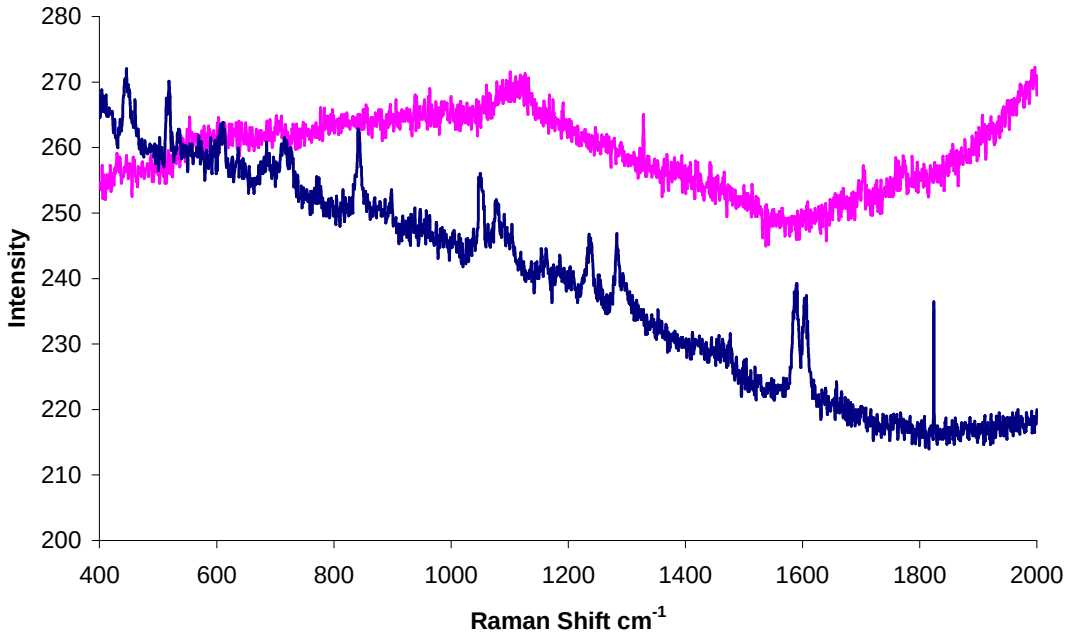

Figure 4.21. Raman spectra for a 0.1 mg/ml diclofenac solution investigated with the 5 µl drop method. The pink line represents the 20 nm colloid and the blue line represents 5 nm colloidal particles.

The pink spectrum representing 20 nm colloidal particles showed none of the characteristic peaks for diclofenac. The blue spectrum representing 5 nm colloidal particles showed the characteristic spectrum of diclofenac. The spectrum is a result of a surface enhancement and the presence of gold colloid because nothing was detectable from a 5 µl drop of 0.1 mg/ml diclofenac left to evaporate dry on a glass microscope slide.

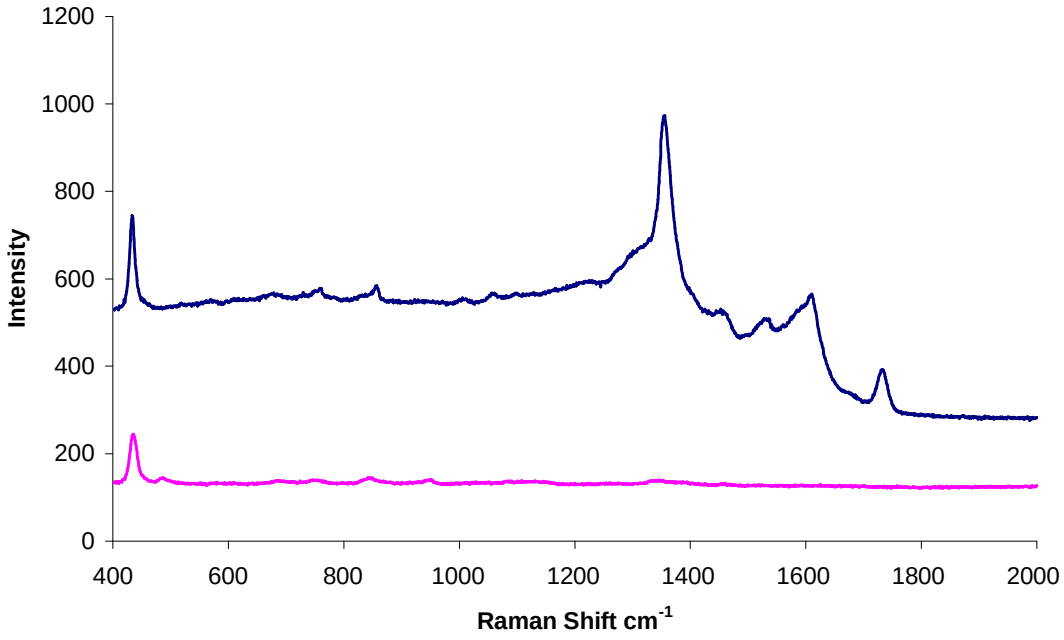

Figure 4.22. Raman spectra for a 0.1 mg/ml trichloroacetic acid solution investigated with the 5 µl drop method. The pink line represents the 20 nm colloid and the blue line represents 5 nm colloidal particles.

Both spectra showed some of the characteristic peaks for trichloroacetic acid. Neither are spectrally complete but the spectrum obtained with 5 nm colloidal particles showed a greater number of characteristic peaks and greater enhancement of signal.

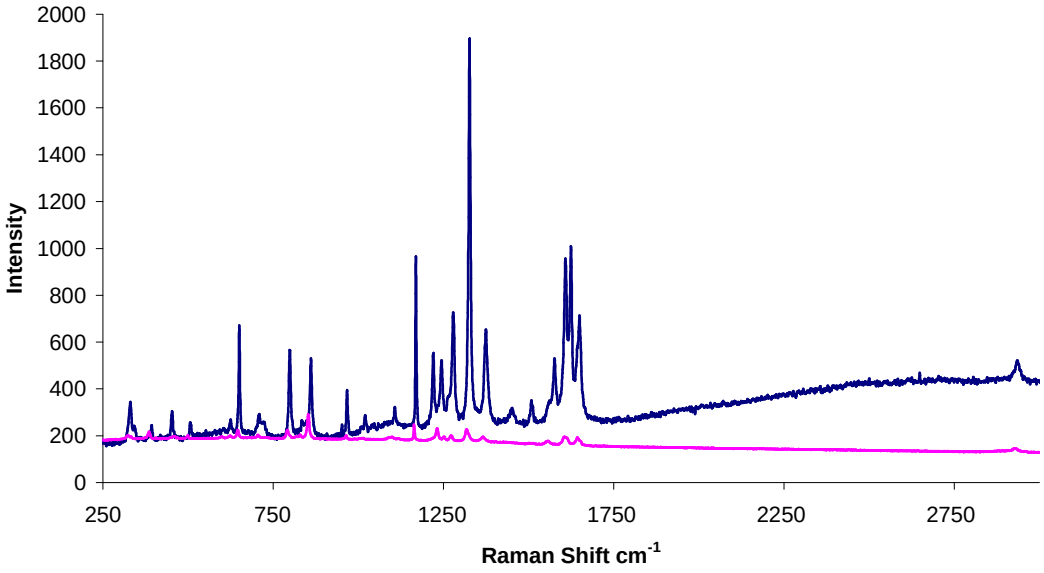

Figure 4.23 Raman spectra for acetaminophen powder (pink) and 0.1 mg/ml acetaminophen solution and 5 nm gold colloidal particles added as 5µl of solution (blue).

Figure 4.23 shows the enhancement of signal for a 5 µl drop of 0.1 mg/ml acetaminophen and 5 nm gold colloidal particles relative to the spectrum of acetaminophen powder on a glass slide. The enhancement of signal was powerful and showed that with the 5 µl drop method a SERS spectrum can be obtained for a low concentration acetaminophen solution allowed to evaporate dry.

SERS with liquid samples

SERS with liquid samples would be advantageous because it would allow the probing of extract from the swabs. The Raman microscope had a liquid sampling accessory which worked in conjunction with a 1 ml cuvette. Solutions containing analyte, gold colloid and 3 % NaCl were pipetted into the cuvette and then analysed on the machine.

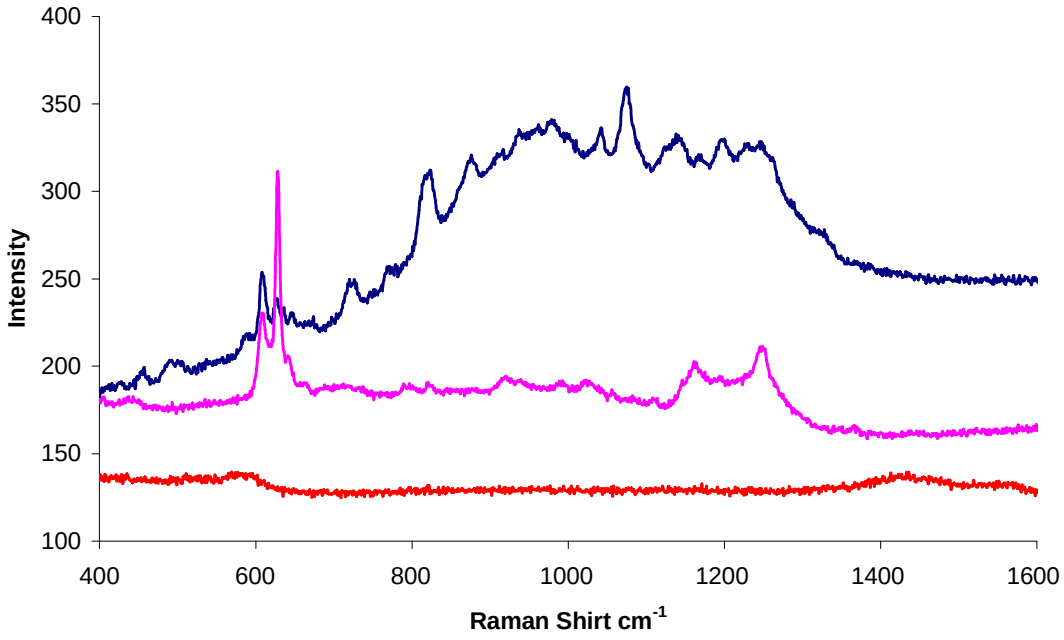

Figure 4.24. Raman spectra for 0.1 mg/ml nicotinic acid mixed with 5 nm gold colloidal particles and 3% NaCl solution (blue), 0.1 mg/ml nicotinic acid mixed with 20 nm gold colloidal particles and 3% NaCl solution (pink) and 0.1 mg/ml nicotinic acid solution (red).

Figure 4.24 showed that SERS was achievable from liquid samples in our measurements as characteristic peaks for nicotinic acid in solutions containing both 5 nm and 20 nm gold colloidal particles were seen. A signal for nicotinic acid could not be collected from a 0.1 mg/ml solution lacking gold colloid and therefore it was concluded that the presence of gold colloid was responsible for the production of signal. Whilst SERS was achievable with nicotinic acid it was not achievable for any of the other compounds tested and this meant that liquid sampling was unsuitable for cleaning verification work because one crucial aspect is generic capability. The technology must be capable of detecting a number of different types of molecules without too much method optimisation for each compound.

4.3.4 SERS on gold colloid impregnated swabs

Impregnation of the swab with gold colloid significantly increased the magnitude of the Raman spectrum. An enhancement of signal was detected for all swabs as shown in Figures 4.25 – 4.30.

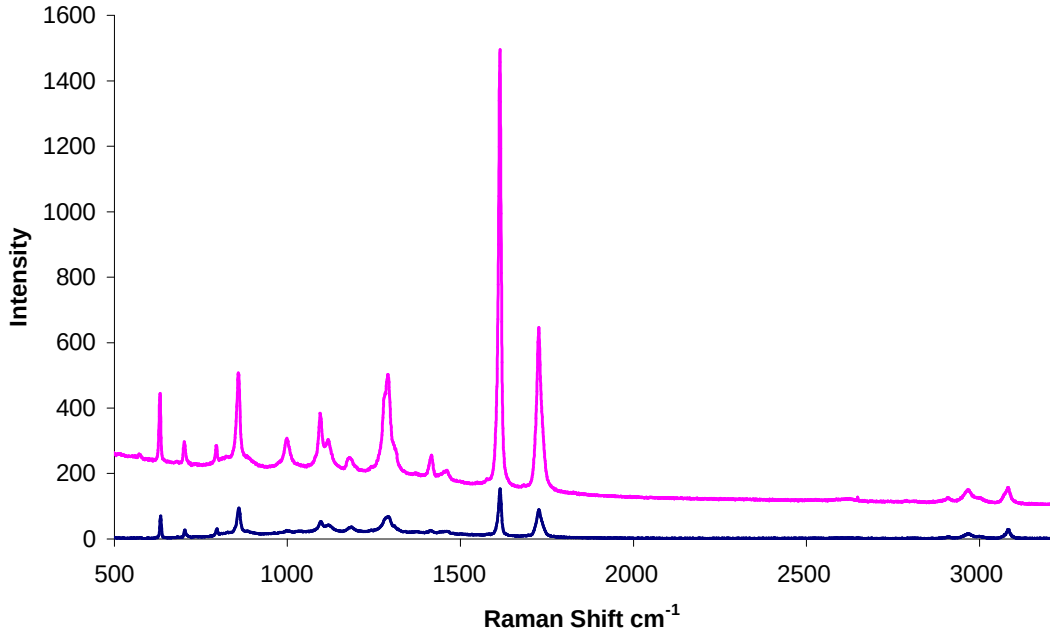

Figure 4.25. Raman spectrum from an Absorbond™ swab (blue) and from an Absorbond™ swab impregnated with gold colloid (pink).

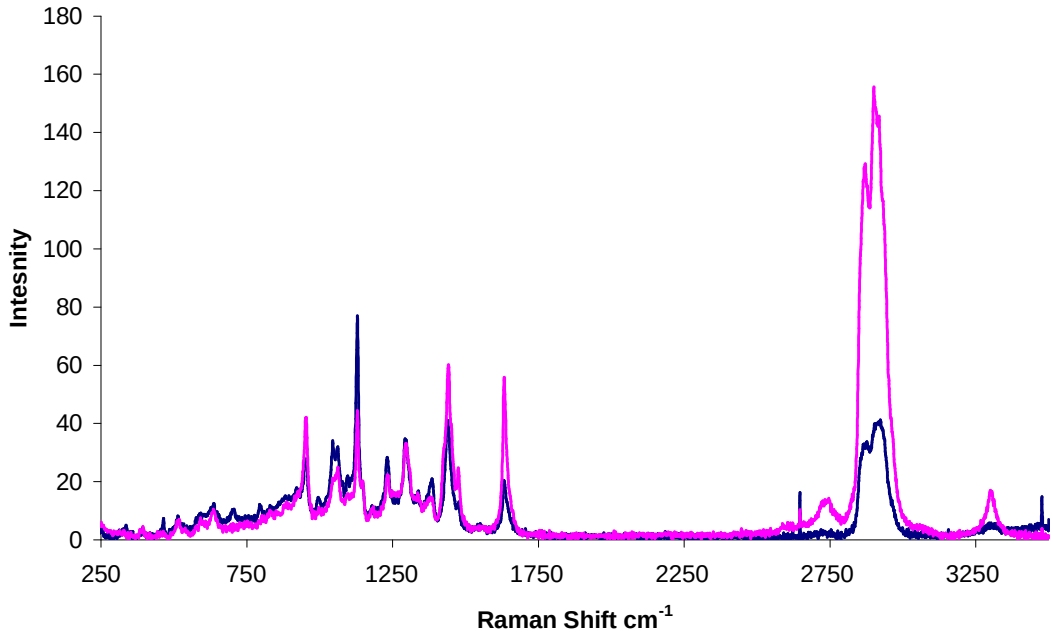

Figure 4.26. Raman spectrum from a MiracleWipe™ swab (blue) and from a MiracleWipe™ swab impregnated with gold colloid (pink).

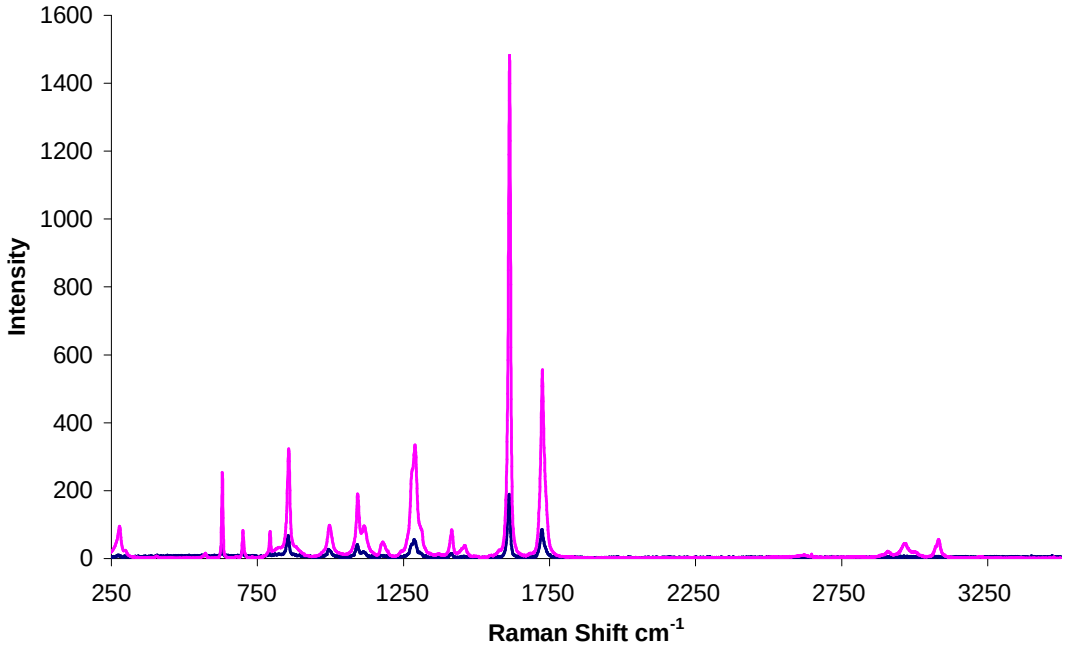

Figure 4.27. Raman spectrum from a Technicloth™ swab (blue) and from a Technicloth™ swab impregnated with gold colloid (pink0.

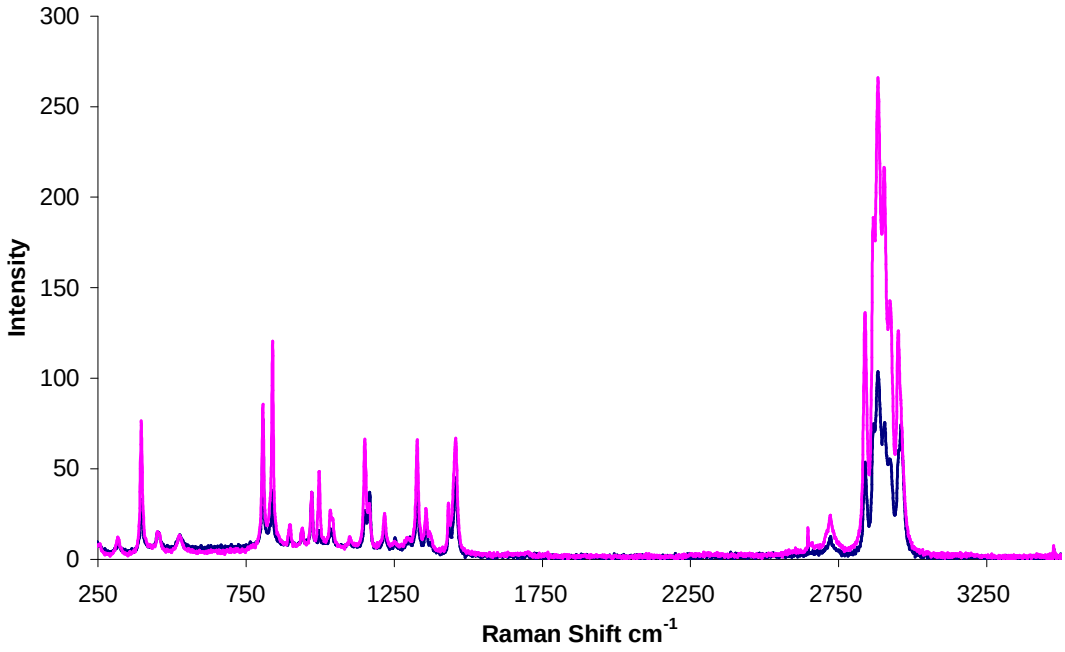

Figure 4.28. Raman spectrum from a Betawipe™ swab (blue) and from a Betawipe™ swab impregnated with gold colloid (pink).

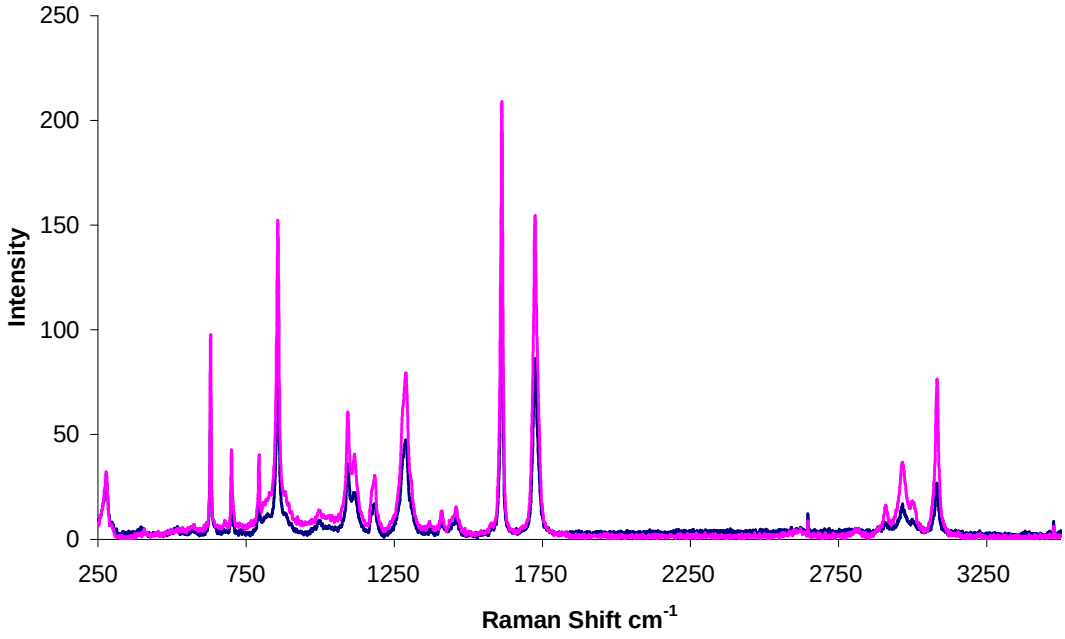

Figure 4.29. Raman spectrum from an Alphawipe™ swab (blue) and from an Alphawipe™ swab impregnated with gold colloid (pink).

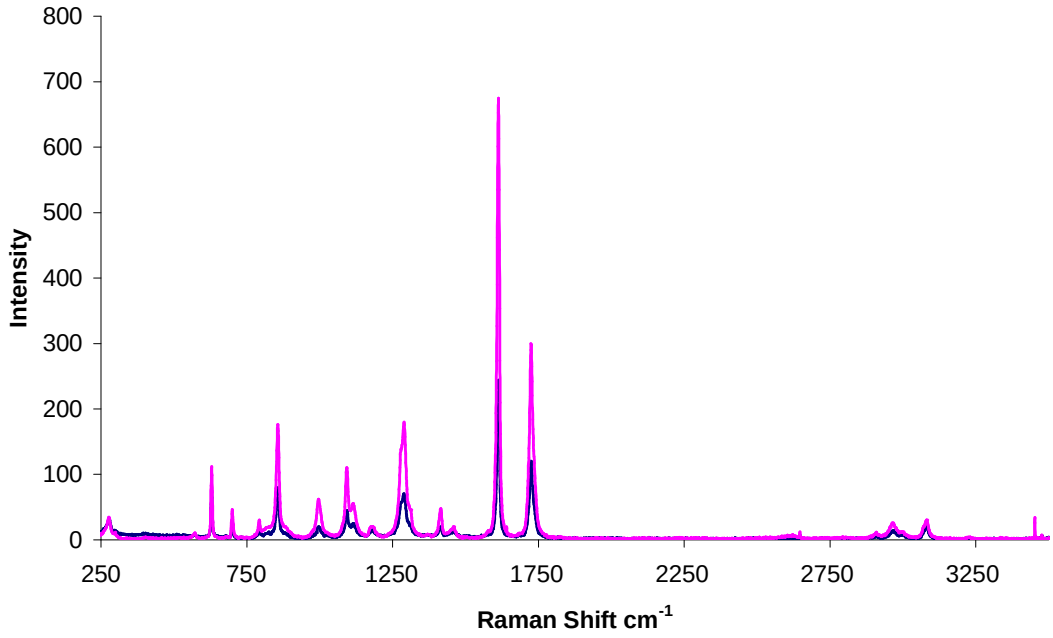

Figure 4.30. Raman spectrum from a Super Polx 1200™ swab (blue) and from a Super Polx 1200™ swab impregnated with gold colloid (pink).

This section showed that it was possible to enhance the Raman spectrum of the swab by impregnating the swab fibres with gold colloid.

4.3.5 SERS on contaminated gold impregnated swabs

This section presents results where gold colloid impregnated swabs were used in an attempt to identify contamination on a stainless steel surface. Figure 4.31 showed an enhanced spectrum from an uncontaminated gold colloid impregnated swab and a spectrum from a gold colloid impregnated swab contaminated with citric acid. Good amplitude in the peaks from the citric acid contaminated swab was seen. A difference in spectrum from the uncontaminated swab was seen and showed contamination was apparent.

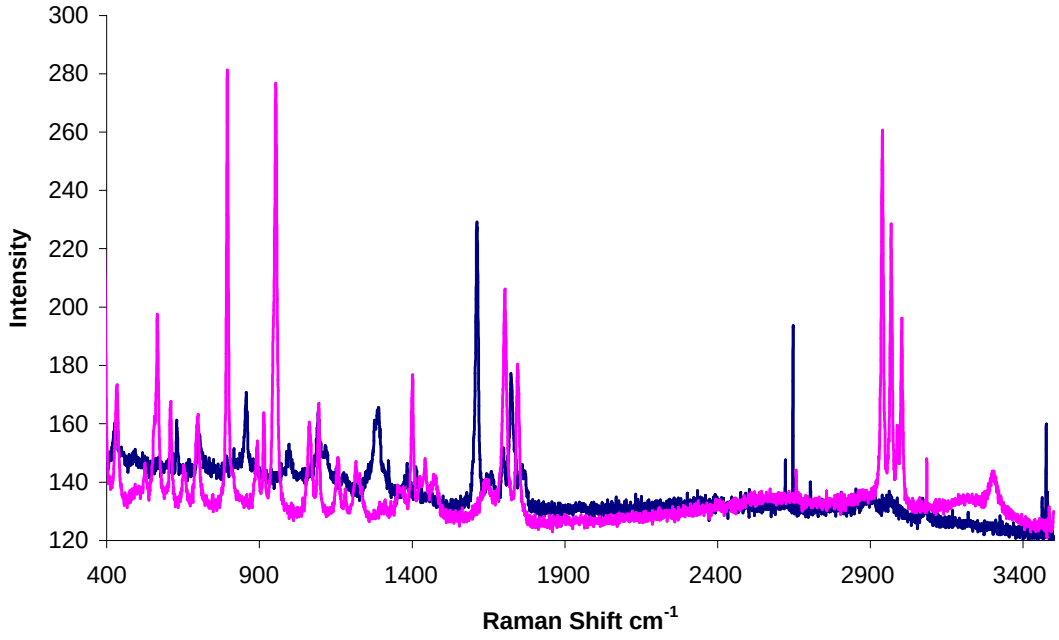

Figure 4.31 Raman spectra from a gold impregnated Texwipe™ swab (blue) and a Texwipe™ swab used to wipe a surface contaminated with citric acid at 111.1 µg/cm^2(pink).

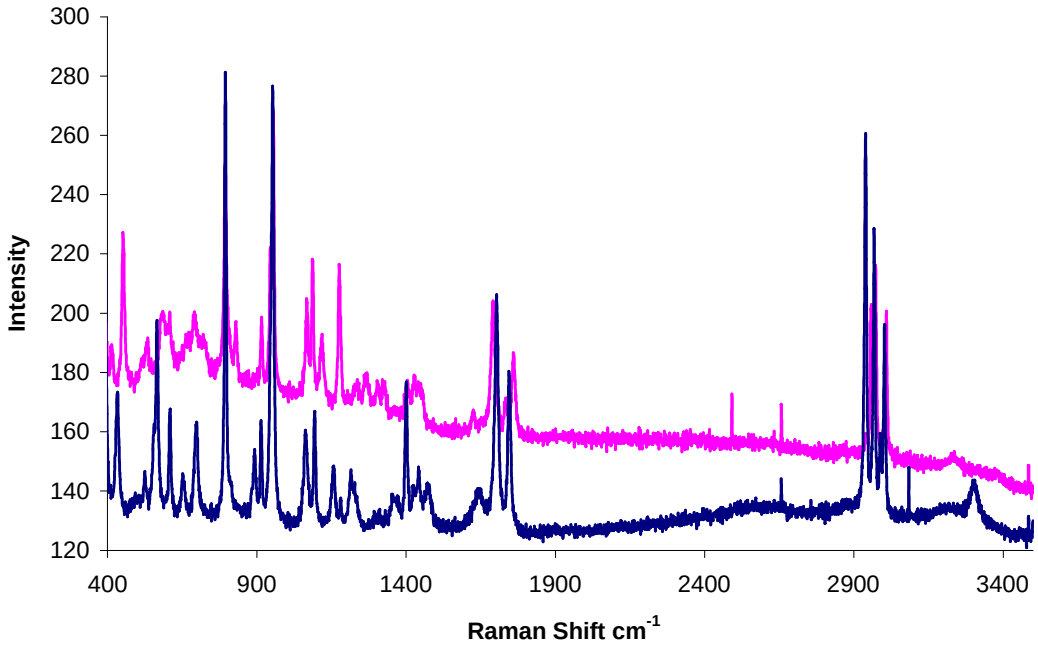

Figure 4.32. Raman spectra from a gold colloid impregnated swab used to wipe a stainless steel surface contaminated with citric acid at 111.1 µg/cm^2 (blue) and a swab used to wipe a stainless steel surface contaminated with citric acid at 111.1 µg/cm^2.

Figure 4.32 shows that a spectrum for citric acid can be enhanced by using a swab impregnated with gold colloid. The spectrum from the gold colloid impregnated swab has greater amplitude in its peaks.

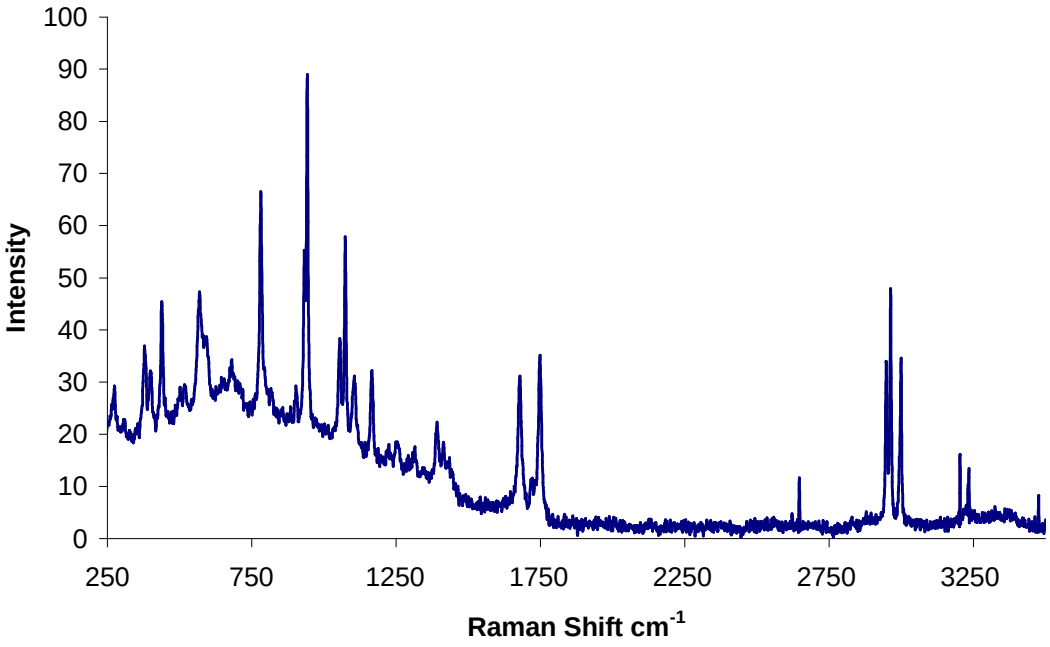

Figure 4.33. Raman spectra from a gold impregnated Betawipe™ swab used to wipe a stainless steel surface contaminated with citric acid at 111.1 µg/cm^2.

Figure 4.33 contained characteristic peaks for citric acid and showed that it was possible to detect contamination in this case. Similar results were obtained with other swabs impregnated with gold colloid (Figures 4.34 & 4.35)

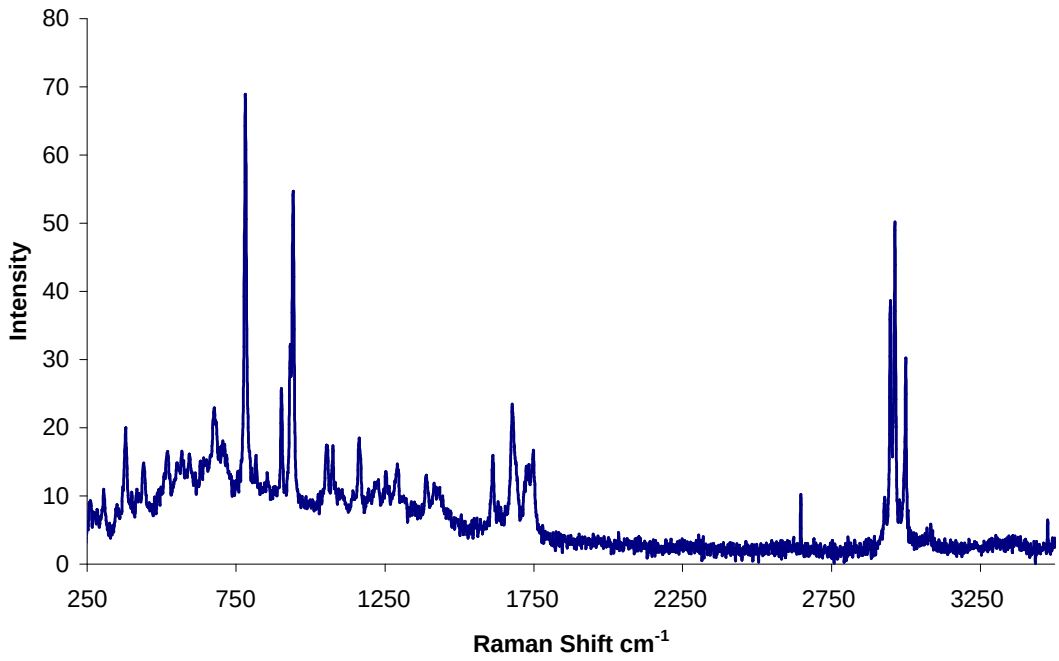

Figure 4.34. Raman spectra from a gold impregnated Alphawipe™ swab used to wipe a stainless steel surface contaminated with citric acid at 111.1 µg/cm^2.

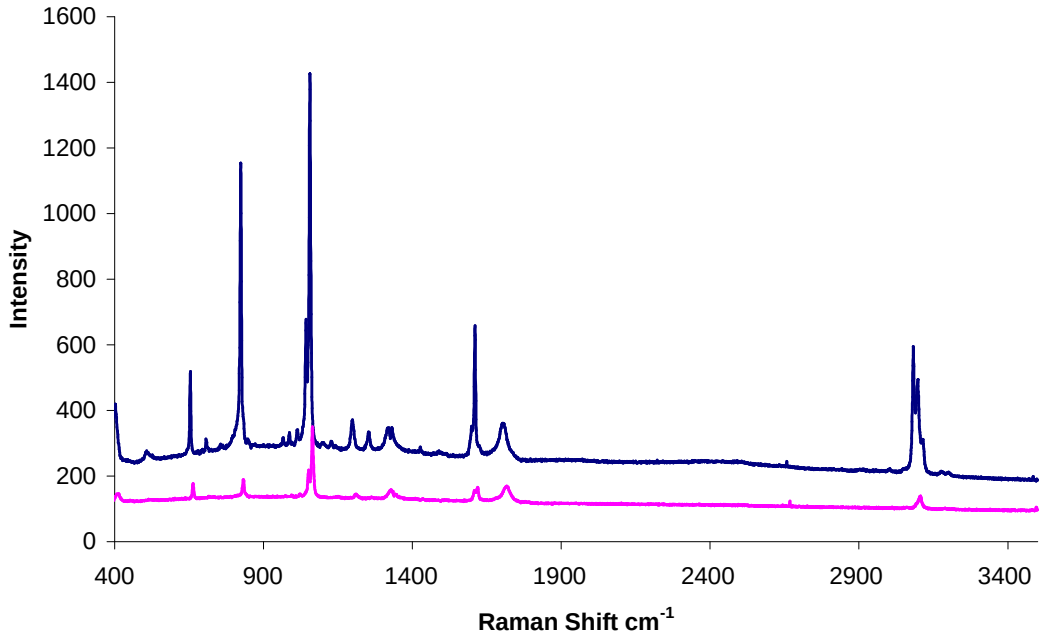

Figure 4.35. Raman spectra from a gold colloid impregnated swab used to wipe a stainless steel surface contaminated with nicotinic acid at 111.1 µg/cm^2 (blue) and a

swab used to wipe a 900 cm^2 stainless steel surface contaminated with nicotinic acid at 111.1 µg/cm^2 (pink).

Thus far, the results in this section have shown a minority of instances where it was possible to visualise contamination on a swab used to wipe a contaminated stainless steel surface. A large number of attempts were made to detect contamination and the results presented in this section represent a few positive examples from many attempts where good Raman spectra were collected. It can be concluded that the heterogeneous nature of the swab creates a problem when trying to collect a Raman spectrum indicative of contamination. The remainder of this section presents some images taken on the Raman microscope that further illustrate the point about sampling difficulties.

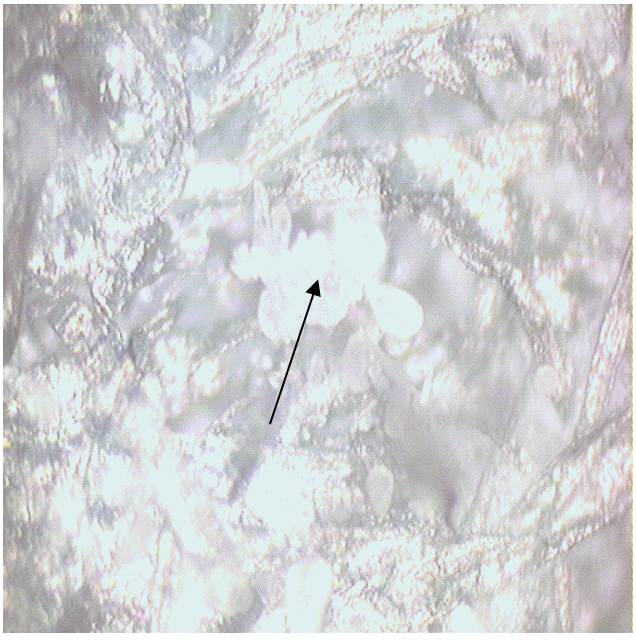

Figure 4.36. An image from a Texwipe™ swab used to wipe a stainless steel surface contaminated with nicotinic acid at 111.1 µg/cm^2. The area in the middle pointed to by the arrow was a deposit of nicotinic acid that had formed on the swab post wiping.

A Raman spectrum for nicotinic acid can be acquired very easily by focusing the laser onto the deposit.

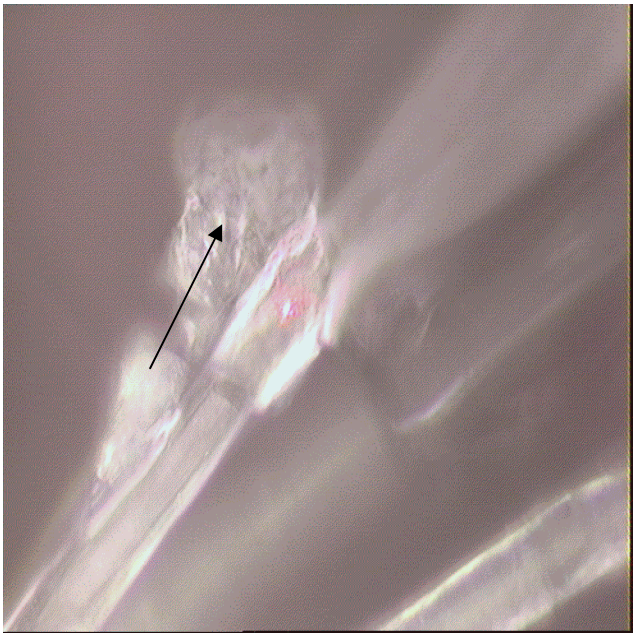

Figure 4.37. An image from a Texwipe™ swab (x50) used to wipe a stainless steel surface contaminated with nicotinic acid at 111.1 µg/cm^2. The pink dot in the centre of the fibre is the laser spot with the filter set to 0.001%. To the left of the laser spot is an area indicated by an arrow. This is another deposit of nicotinic acid and a Raman spectrum for the compound can be acquired in this case by turning the laser filter off and then taking a spectrum.

Whilst some enhancements of signal were seen from gold colloid impregnated swabs the frequency with which contamination was detected did not improve. This was mainly due to the heterogeneous nature of the swab and the need to encounter visible deposits of compound. Impregnating the swab with gold colloid was found not to be a feasible method for achieving a SERS signal from swabs.

Figure 4.38. An image taken of a gold colloid impregnated Texwipe™ swab (x10). The area indicated by the arrow in the centre of the image is an aggregation of gold particles. There are other smaller clusters of gold aggregate in the image. SERS spectra are obtained from these swabs by focusing the laser on areas containing aggregated gold particles.

4.3.6 Sputter coated swabs

In an attempt to improve the homogeneity of the swab surfaces, sputter coating with gold was carried out. The sputter coated swabs were then used to wipe contaminated surfaces.

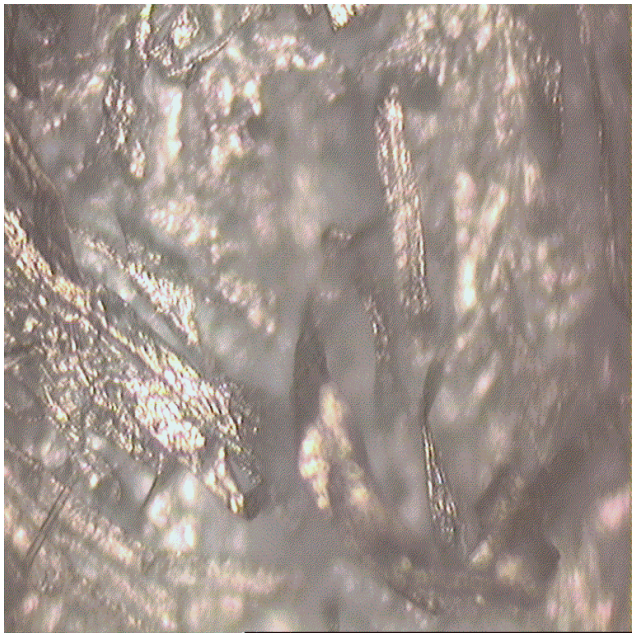

Figure 4.39. An image of a sputter coated Texwipe™ swab (x50). The swab was completely covered in gold meaning that only a certain number of fibres were able to be visualised underneath the gold coating.

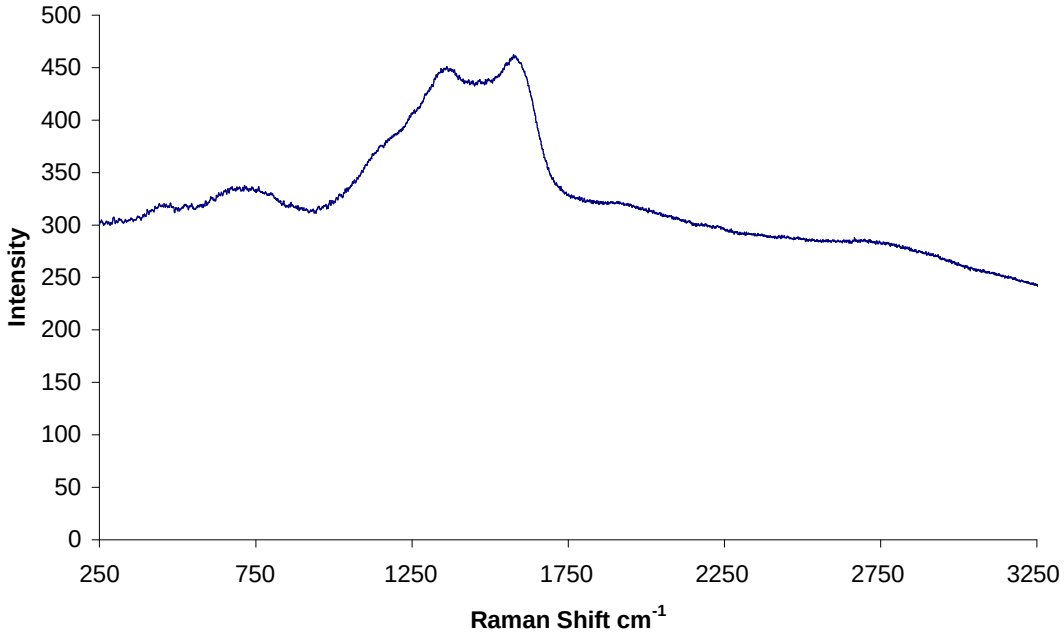

Figure 4.40. Raman spectra from a sputter coated swab used to wipe a surface contaminated with acetaminophen. The spectrum had a high baseline and two broad

unresolved peaks. The spectrum showed fluorescence because of the high amount of gold coverage on the swab surface. In response to this finding the gold coating was reduced by altering the deposition time of the sputter coater from forty seconds to twenty seconds to produce a partially coated swab.

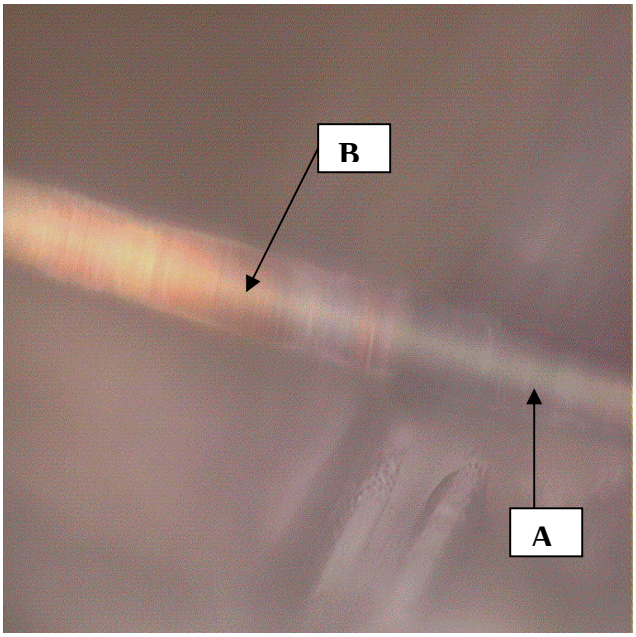

Figure 4.41. An image of a fibre from a partially sputter coated Texwipe™ swab (x50). Raman spectra were taken from the points indicated by arrows A and B.

Figures 4.41 and 4.42 showed how the deposition of gold affects the ability to enhance the spectrum from the swab. A partial coating produced a significant enhancement of signal and this was probably due to the fact that gold and fibre are present under the laser spot.

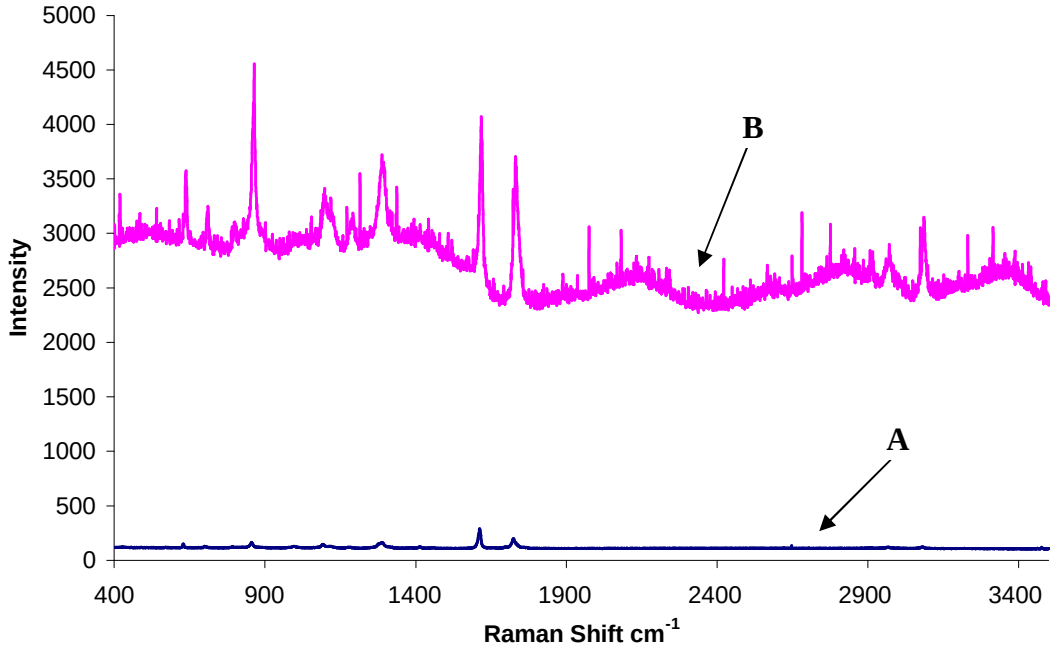

Figure 4.42. Raman spectra from an uncoated section of a Texwipe™ fibre (blue) corresponding to arrow A in the previous figure and from a section of Texwipe™ fibre partially sputter coated in gold (pink) corresponding to arrow B in the previous figure.

Completely sputter coated swabs produced a Raman spectrum high in background fluorescence as shown by figure 4.40 and it was not possible to enhance the background at all in the completely covered swabs or resolve any sign of contamination from swabs used to wipe a contaminated stainless steel surface. Whilst the partially coated swabs produced a significant enhancement of the swab signal it was not possible to detect contamination after wiping a contaminated steel surface.

4.3.7 SERS with nanofabricated substrates from the University of Michigan

SERS spectroscopy was carried out with two different solid substrates. One substrate was received as a gift from Dr Jin-Sung Kim at the University of Michigan and one substrate was purchased from Mesophotonics Ltd and is known as Klarite™.

The substrates provided by Dr Jin-Sung Kim fell into four categories. There were diamond and square substrates where the gold patterning on the surface was either arranged in a square shape or in a diamond shape and there were lift off and non lift off samples. The non lift off samples were composed of a glass layer, a polymer layer and the gold patterning on top and in the lift off sample the polymer layer had been dissolved away to leave the gold patterning on top of the glass layer (see appendix 1).

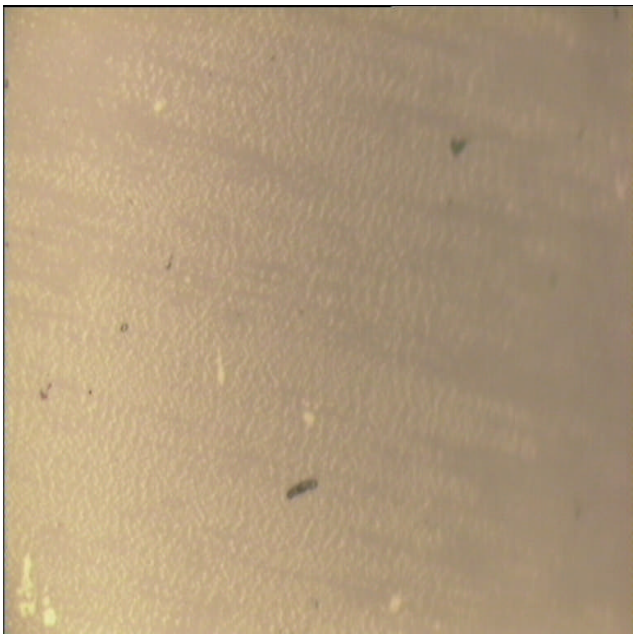

Figure 4.43. Image of the square non lift off substrate (x50). Some patterning or surface roughness was slightly apparent at this magnification.

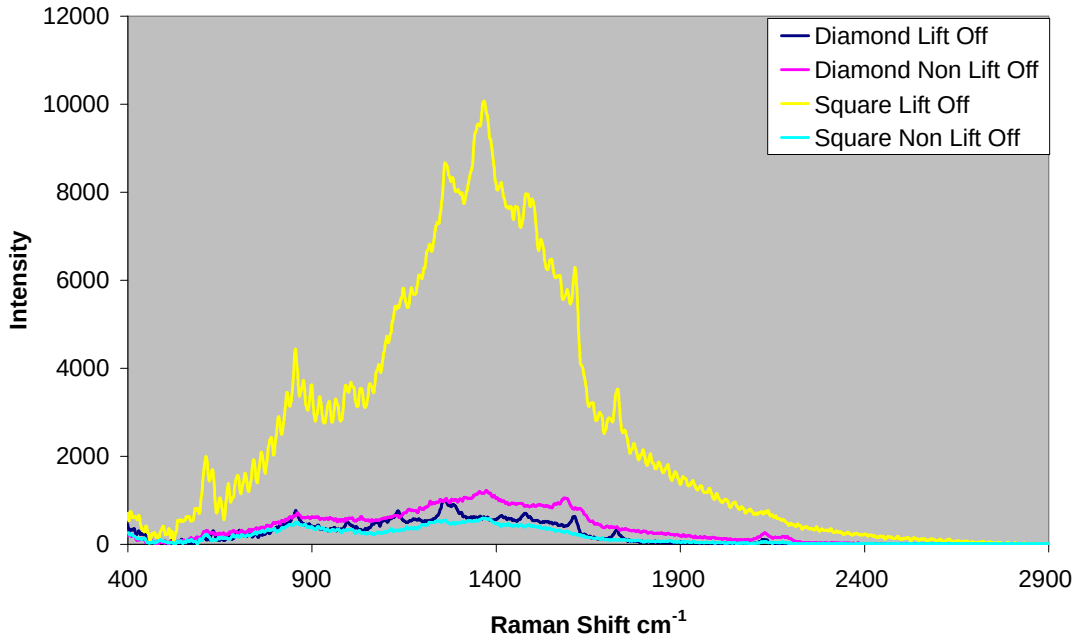

Figure 4.44. Raman spectra from the four SERS substrates after pipetting 5µl of acetaminophen at 100 ppm and allowing to evaporate dry.

It was not possible to detect contamination by acetaminophen diclofenac, ibuprofen and nicotinic acid with any of the substrates (Figures 4.44-4.47). The characteristic peaks in the diamond and square lift off samples (yellow and blue spectra) were from the polymer layer between the glass layer and the gold patterning. The non lift off samples gave a broad unresolved spectrum that did not present any evidence for the presence of compound.

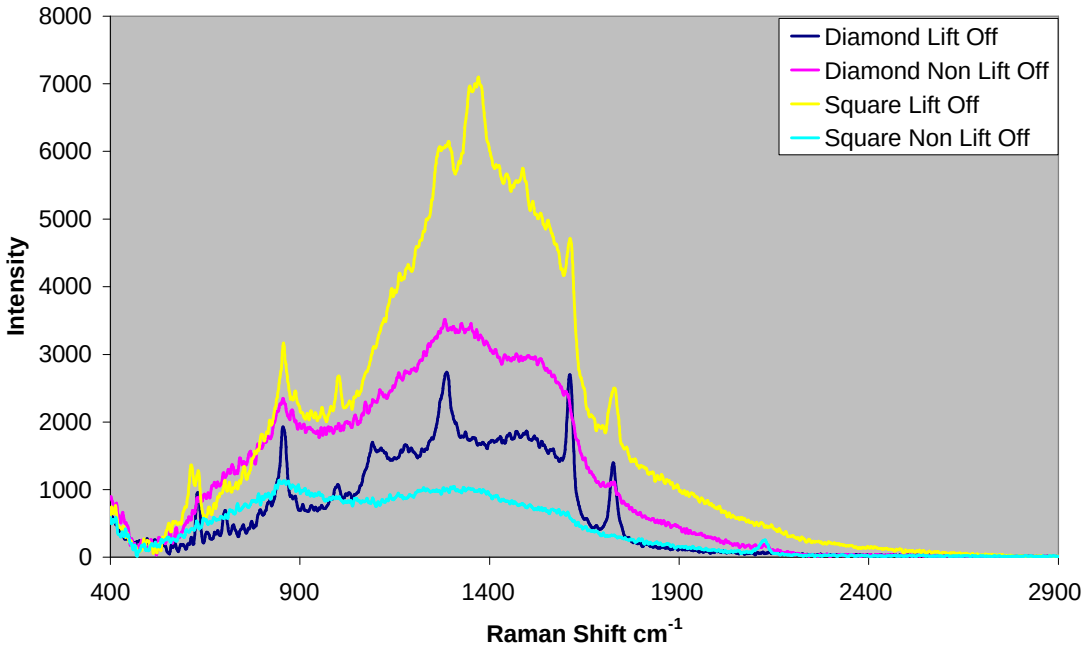

Figure 4.45. Raman spectra from the four SERS substrates after dropping 5µl of diclofenac at 100 ppm and allowing to evaporate dry.

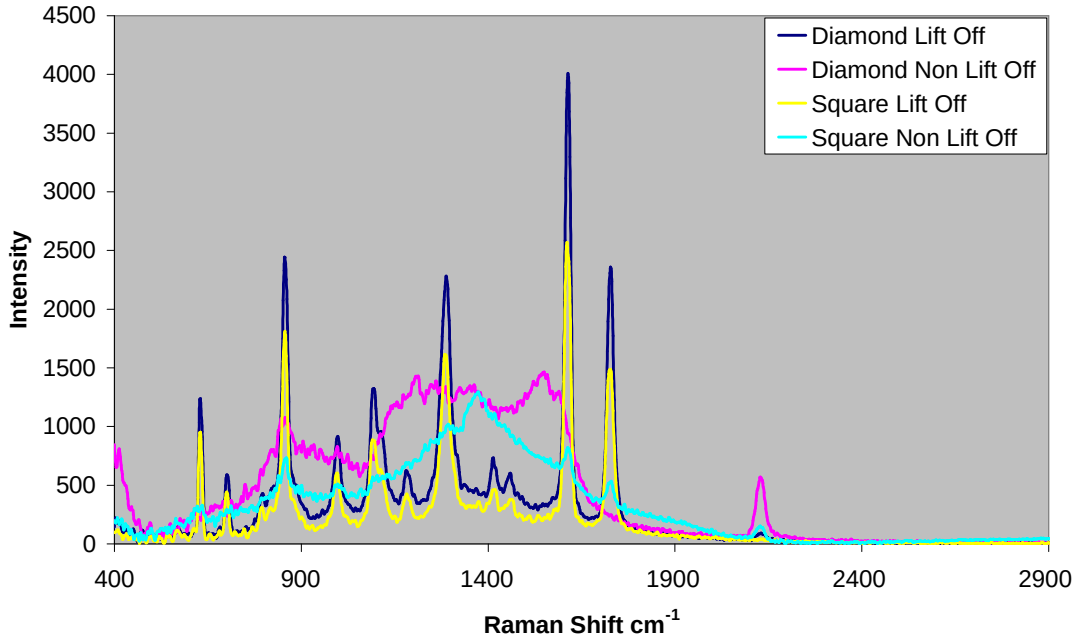

Figure 4.46. Raman spectra from the four SERS substrates after dropping 5µl of ibuprofen at 100 ppm and allowing to evaporate dry.

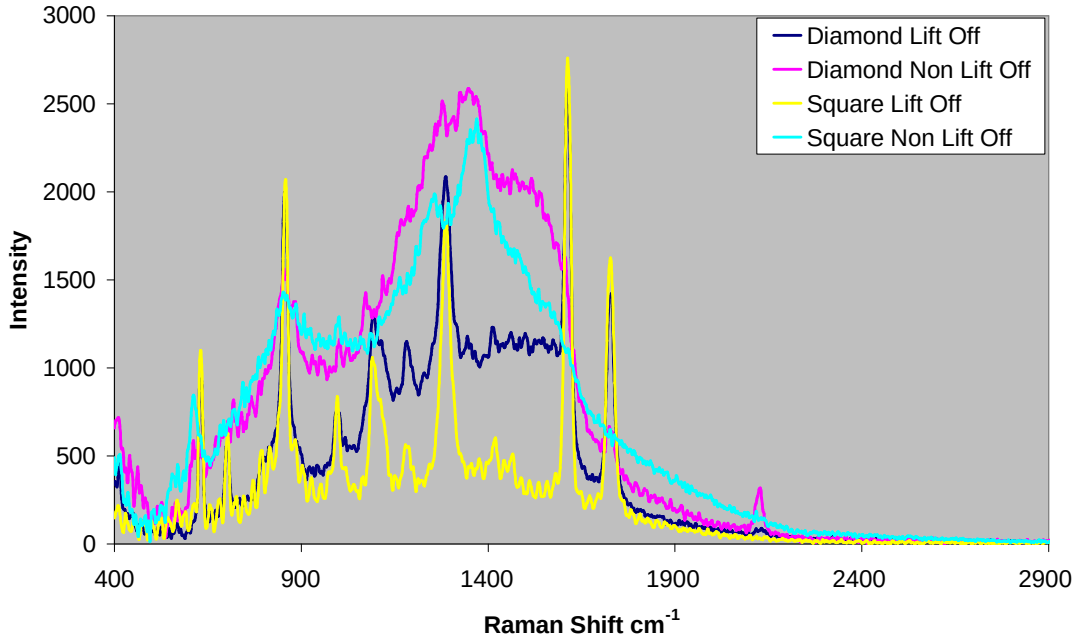

Figure 4.47. Raman spectra from the four SERS substrates after dropping 5µl of nicotinic acid at 100 ppm and allowing to evaporate dry.

The substrates were ineffective in providing an enhancement of signal for the compound of interest introduced onto their surface. No spectra were collected that revealed the presence of compound of interest and the only spectral information was found from non lift off samples where the presence of the polymer between the glass layer and gold patterning was detected.

4.3.8 Klarite™ substrates

Klarite™ substrates are a commercially available SERS substrate. They povide a regular and consistent enhcancement of the SERS signal. To date they have been used for the detection of low levels of particular analytes. In this study they will be used as potential substrates for analysis of cleaning verification samples.

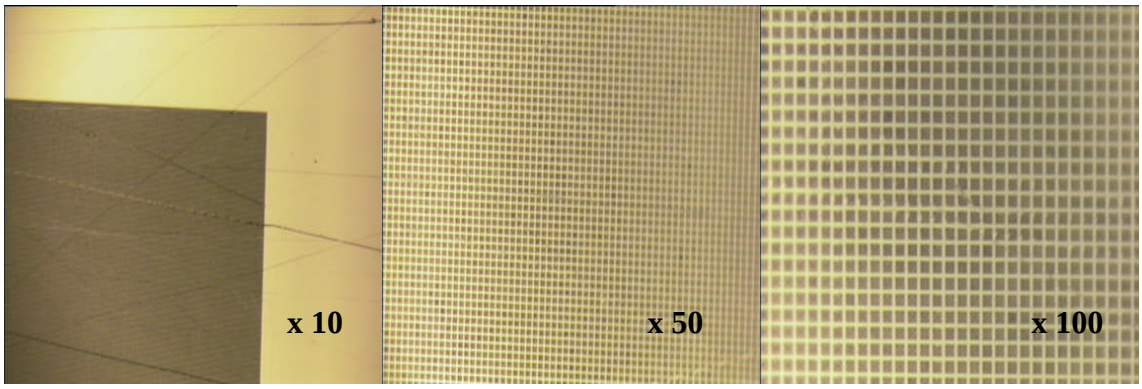

Figure 4.48. Images of the Klarite™ substrate at three different magnifications. Substrate at x10 showing the plain gold border around the SERS area (right), SERS area at x50 magnification (middle) and SERS area at x100 magnification (left).

Acetaminophen

Testing was carried out with solutions of acetaminophen.

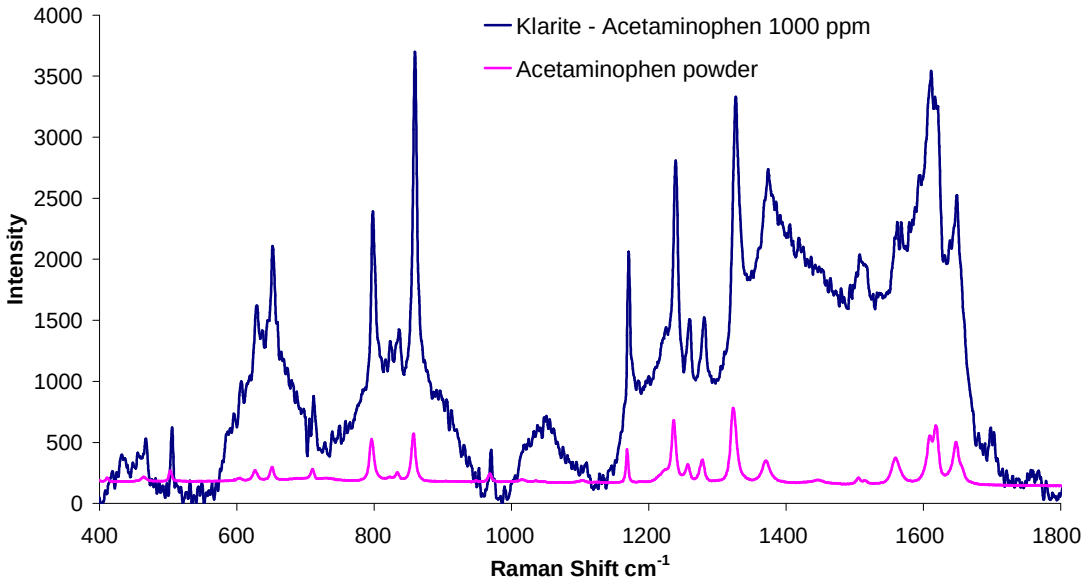

Figure 4.49. Raman spectrum from a dried 5 µl drop of acetaminophen at 1000 ppm taken from the surface of a Klarite™ slide (blue) and neat acetaminophen powder (pink).

The peaks from acetaminophen on the Klarite™ substrate had an extremely high amplitude and the spectrum showed significant enhancement of signal at 1000, 100, 10 and even 1 ppm levels (Figures 4.49 – 4.52).

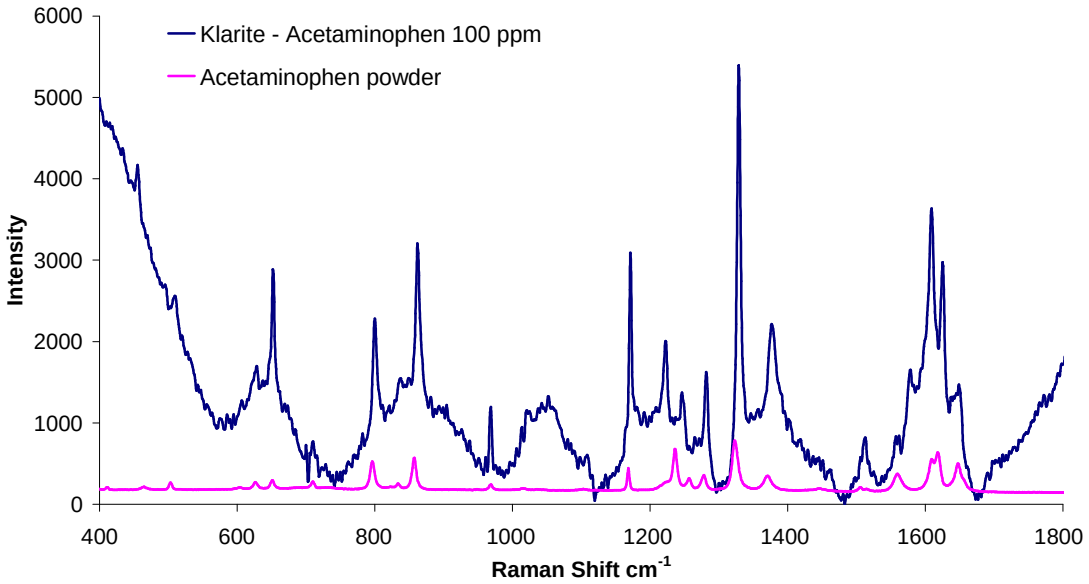

Figure 4.50. Raman spectrum from a dried 5 µl drop of acetaminophen at 100 ppm taken from the surface of a Klarite™ slide (blue) and neat acetaminophen powder (pink).

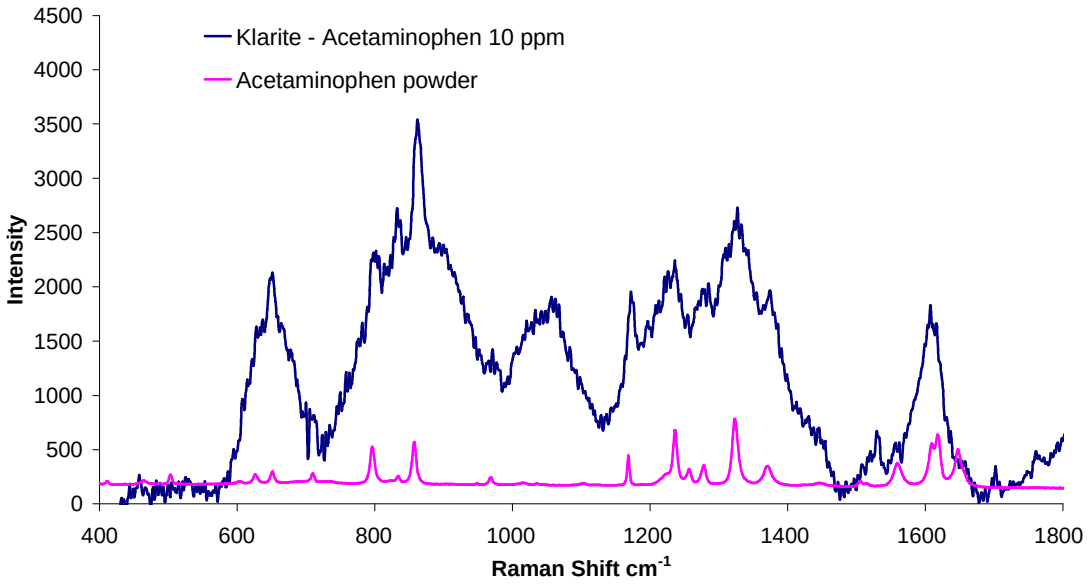

Figure 4.51. Raman spectrum from a dried 5 µl drop of acetaminophen at 10 ppm taken from the surface of a Klarite™ slide (blue) and neat acetaminophen powder (pink).

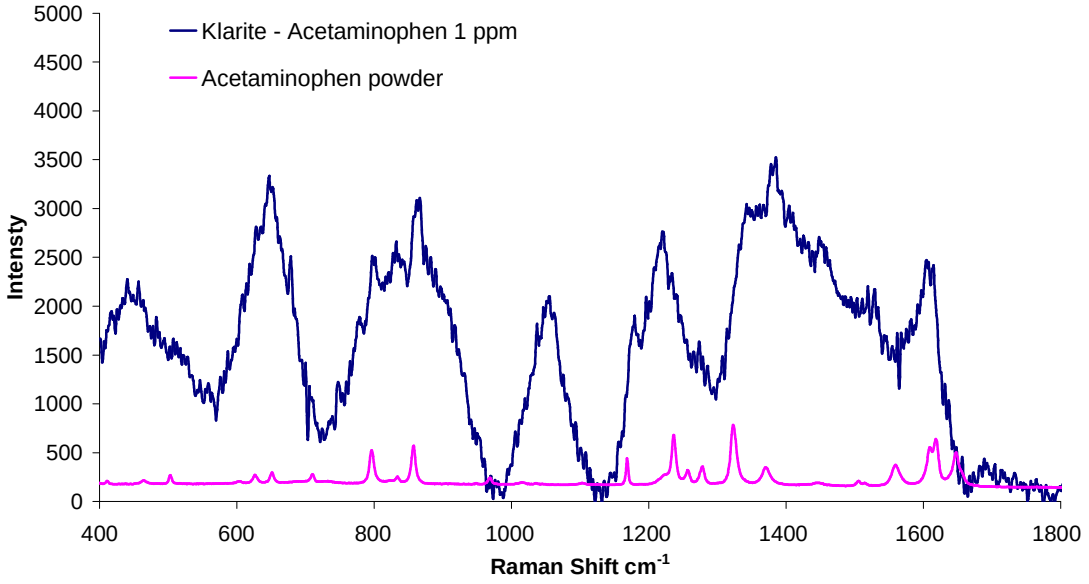

Figure 4.52. Raman spectrum from a dried 5 µl drop of acetaminophen at 1 ppm taken from the surface of a Klarite™ slide (blue) and neat acetaminophen powder (pink).

Further loss of characteristic peaks and amplitude had taken place at 1 ppm but the spectrum still identified acetaminophen as past of a sequence of decreasingly concentrated samples.

Ibuprofen

Similar results to those seen with acetaminophen were obtained for ibuprofen (Figures 4.53-4.56)

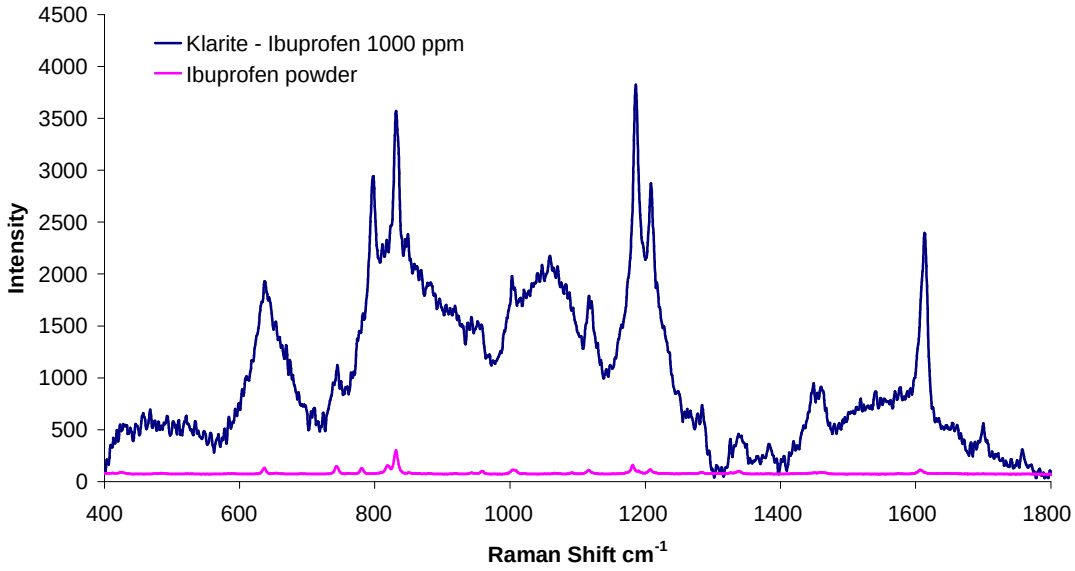

Figure 4.53. Raman spectrum from a dried 5 µl drop of ibuprofen at 1000 ppm taken from the surface of a Klarite™ slide (blue) and neat ibuprofen powder (pink).

The peaks from ibuprofen on the Klarite™ substrate had an extremely high amplitude and the spectrum showed significant enhancement of signal at 1000, 100 and 10 ppm levels.

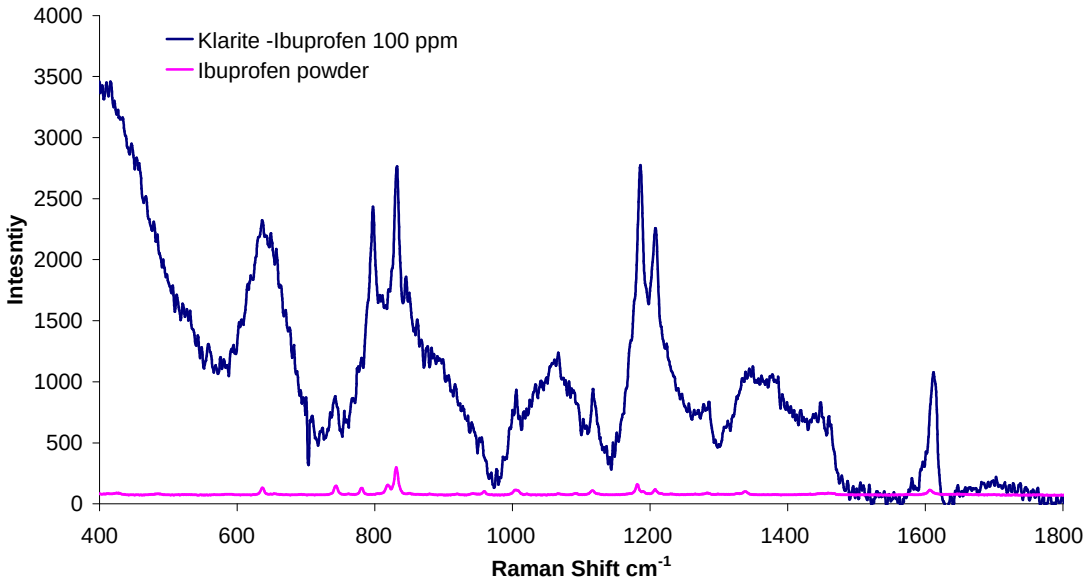

Figure 4.54. Raman spectrum from a dried 5 µl drop of ibuprofen at 100 ppm taken from the surface of a Klarite™ slide (blue) and neat ibuprofen powder (pink).

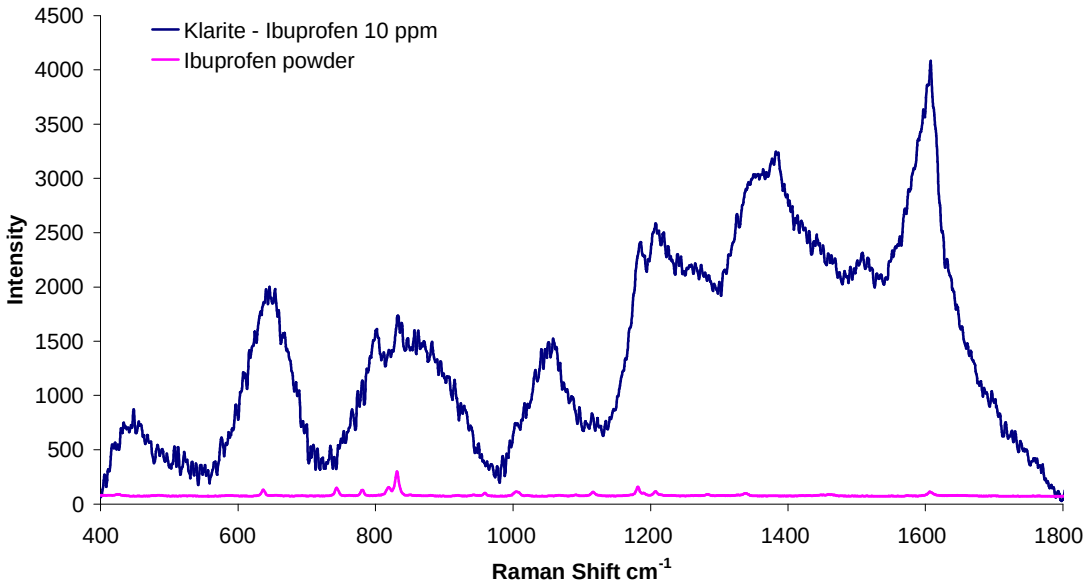

Figure 4.55. Raman spectrum from a dried 5 µl drop of ibuprofen at 10 ppm taken from the surface of a Klarite™ slide (blue) and neat ibuprofen powder (pink).

Four characteristic peaks remained (circled) but definition of those characteristic peaks was greatly reduced for ibuprofen at 10 ppm. A SERS spectrum for ibuprofen was achieved but the point was reached where identification of the sample from this one spectrum alone was not possible.

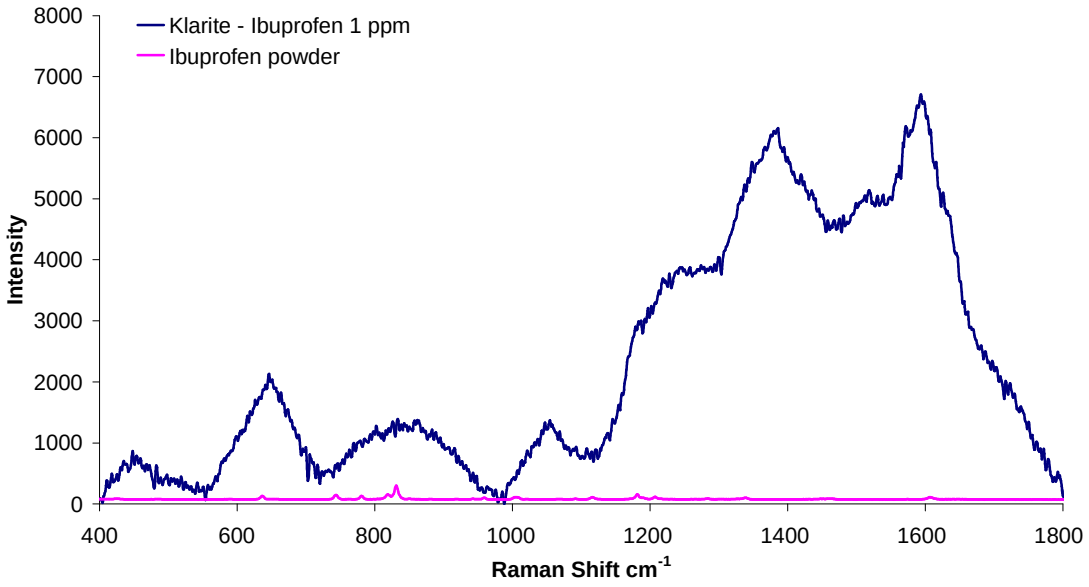

Figure 4.56. Raman spectrum from a dried 5 µl drop of ibuprofen at 10 ppm taken from the surface of a Klarite™ slide (blue) and neat ibuprofen powder (pink).

This spectrum had broad and poorly resolved peaks and taken in isolation would not be identifiable as ibuprofen. The identification of ibuprofen at 1 ppm was not possible.

Diclofenac

Similar results to those obtained for acetaminophen and ibuprofen were obtained for diclofenac (Figures 4.57-4.59)

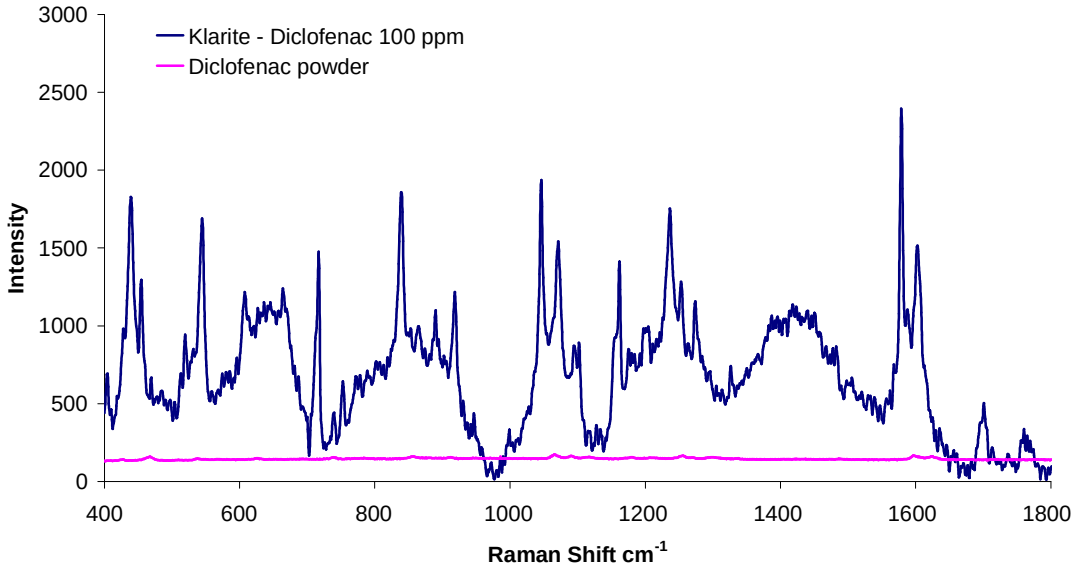

Figure 4.57. Raman spectrum from a dried 5 µl drop of diclofenac at 100 ppm taken from the surface of a Klarite™ slide (blue) and neat diclofenac powder (pink).

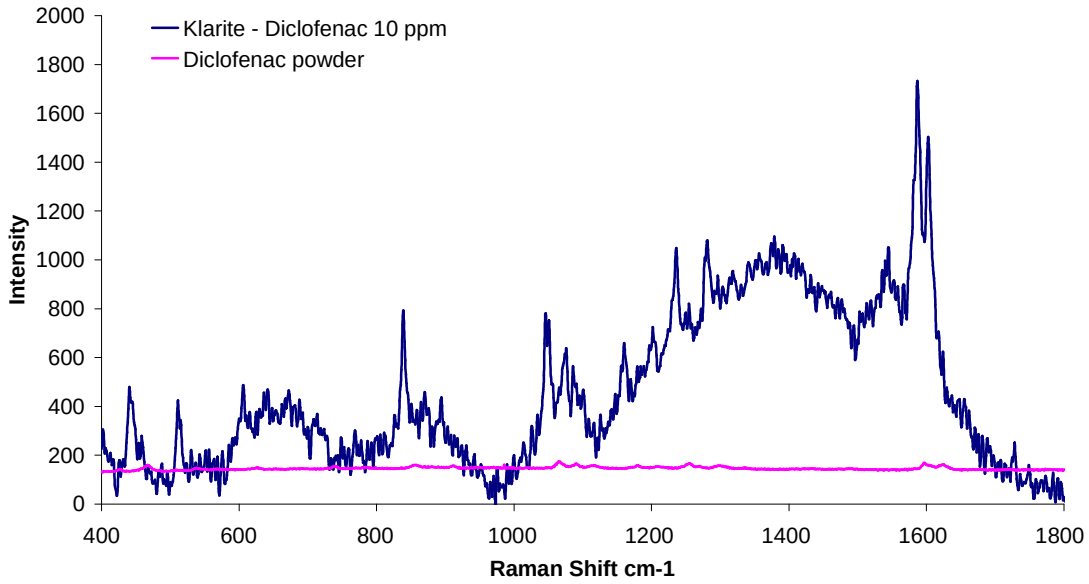

Figure 4.58. Raman spectrum from a dried 5 µl drop of diclofenac at 10 ppm taken from the surface of a Klarite™ slide (blue) and neat diclofenac powder (pink).

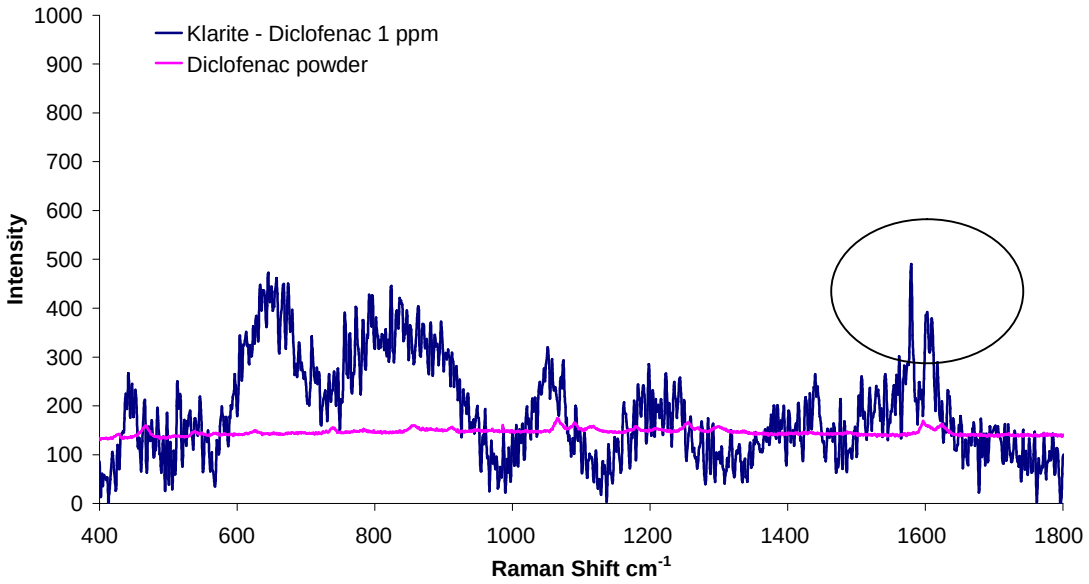

Figure 4.59. Raman spectrum from a dried 5 µl drop of diclofenac at 1 ppm taken from the surface of a Klarite™ slide (blue) and neat diclofenac powder (pink).

The peaks from diclofenac on the Klarite™ substrate had an extremely high amplitude and the spectrum showed significant enhancement of signal at 100, 10 and 1 ppm levels. The spectrum for 10 ppm levels (Figure 4.58) had a poorer signal to noise ratio that had been seen with other spectra originating from the Klarite™ substrate but diclofenac was still easily identifiable on the basis of its characteristic peaks. The spectrum for 1 ppm (Figure 4.59) had an especially poor signal to noise ratio and but for the presence of two poorly resolved peaks (circled) the compound would be unidentifiable as diclofenac.

Klarite™ slides showed regular and consistent enhancements of signal and the Raman spectra presented in this section were taken instantly after sample had dried. Repeats were done to confirm the presence of the compound and ensure the reproducibility of the result but the most impressive aspect of the Klarite™ substrate alongside the magnitude of the signal enhancement was the consistency.

4.3.9 SERS spectra of other compounds with Klarite™ substrates.

To evaluate the generic nature of the Klarite™ substrates Raman spectra were collected for other compounds.

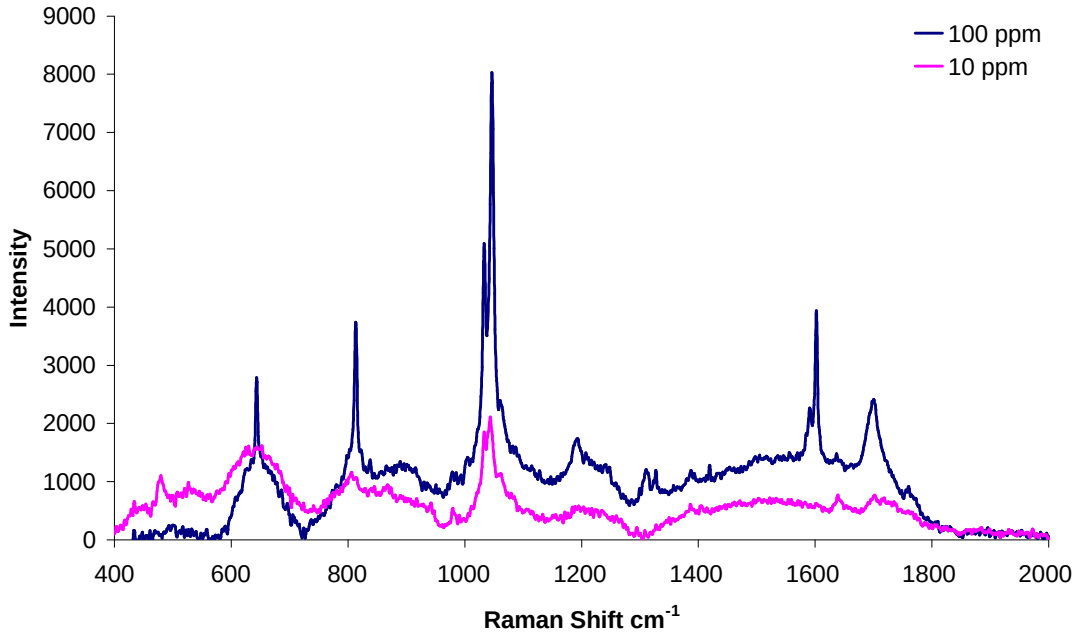

Figure 4.60. Raman spectra of nicotinic acid on a Klarite™ substrate at 100 ppm (blue) and at 10 ppm (pink).

The spectra were characteristic of nicotinic acid and therefore it was possible to detect the compound at 100 and 10 ppm.

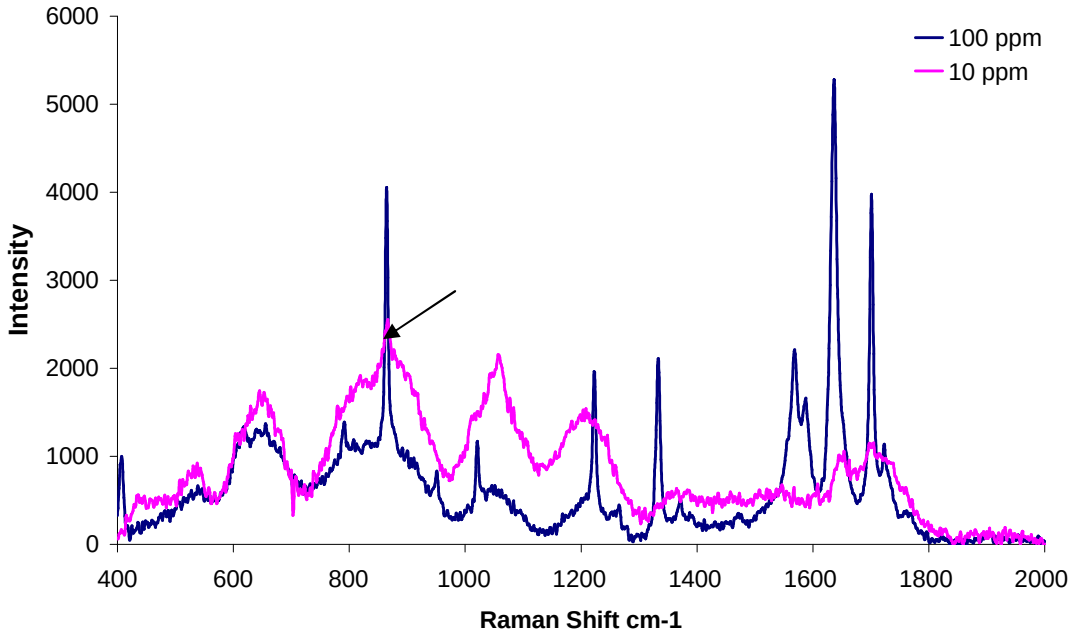

Figure 4.61. Raman spectra of maleic acid on a Klarite™ substrate at 100 ppm (blue) and at 10 ppm (pink).

The spectra at 100 ppm were extremely characteristic of maleic acid, the spectra of 10 ppm is less so with one characteristic peak remaining (arrow).

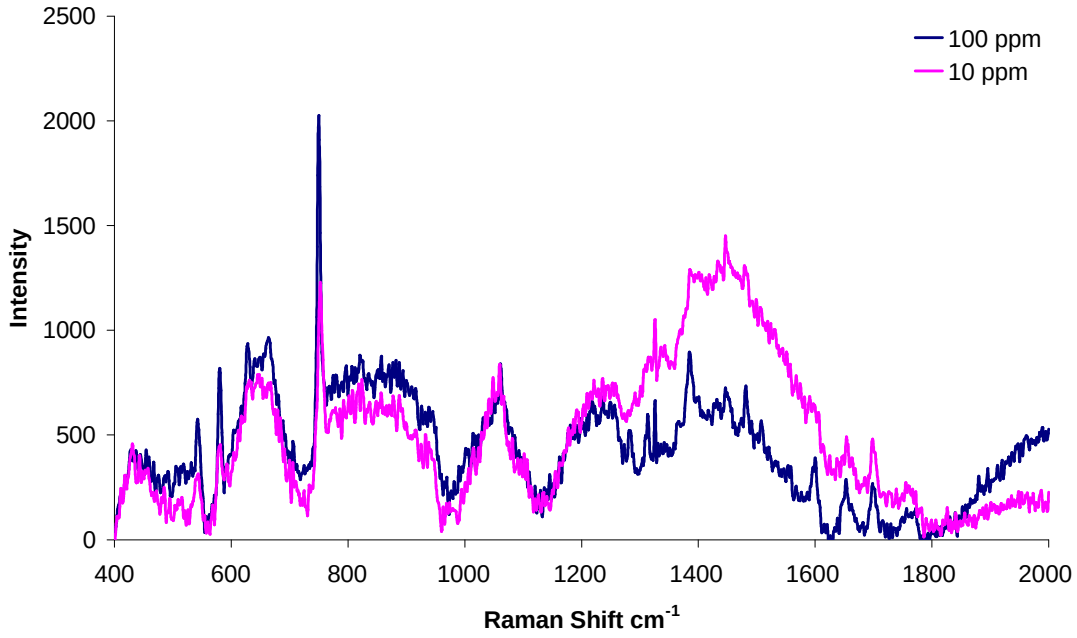

Figure 4.62. Raman spectra of thiamine on a Klarite™ substrate at 100 ppm (blue) and at 10 ppm (pink).

The spectra were characteristic of thiamine and therefore it was possible to detect the compound at 100 and 10 ppm.

4.3.10 Simulation of cleaning verification by SERS with Klarite™ slides

Having shown the Klarite™ slide capable of providing characteristic spectra at concentrations of compound that mimic those encountered in cleaning verification it was decided to simulate the cleaning process. This was done by contaminating a stainless steel surface with a known amount of compound and then analysing the extract from the swab. The swabs were moistened with solvent prior to wiping of the surface. Once the surface had been wiped, the swab was folded into quarters and then 5 µl of the solvent was extracted by pipette and subsequently dropped onto the Klarite™ substrate.

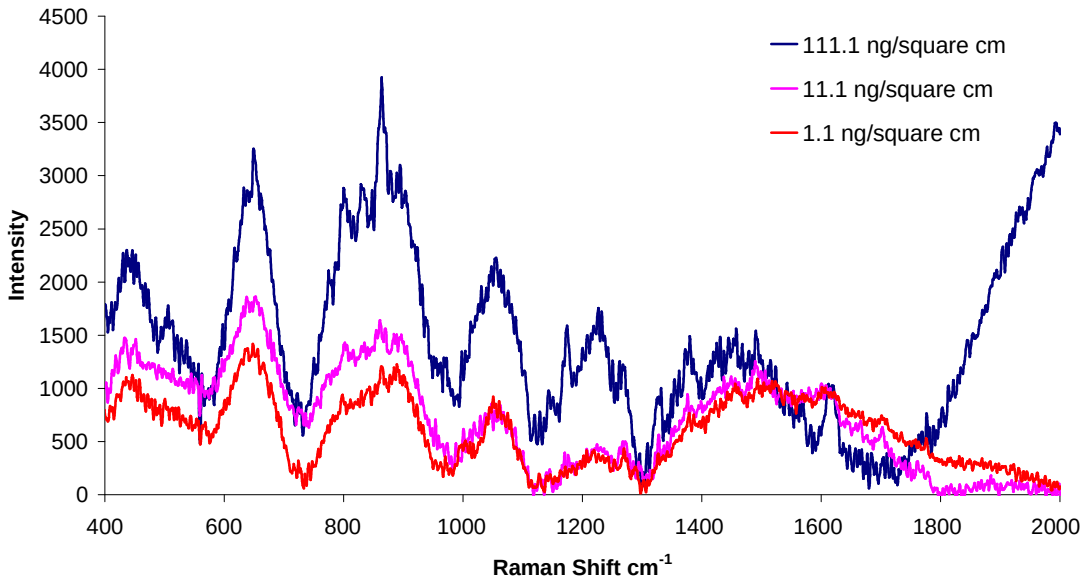

Figure 4.63. Raman spectra for acetaminophen recovered with a Technicloth™ swab from a contaminated steel surface. The surface was contaminated at three different levels: 111.1 ng/cm^2, 11.1 ng/cm^2 and 1.1 ng/cm^2.

The first experiment was performed with acetaminophen (see Figure 4.63). The spectra in this figure showed that it was possible to detect acetaminophen over concentrations relevant to cleaning verification. With highly potent pharmaceutical compounds it is desirable to detect at 5 ng/cm^2 and with acetaminophen it was possible to detect at 1.1 ng/cm^2. The spectra lose resolution as the amount of drug present on the steel surface reduces but with acetaminophen, some of the characteristic peaks were arguable at the lowest level of contamination used in the study.

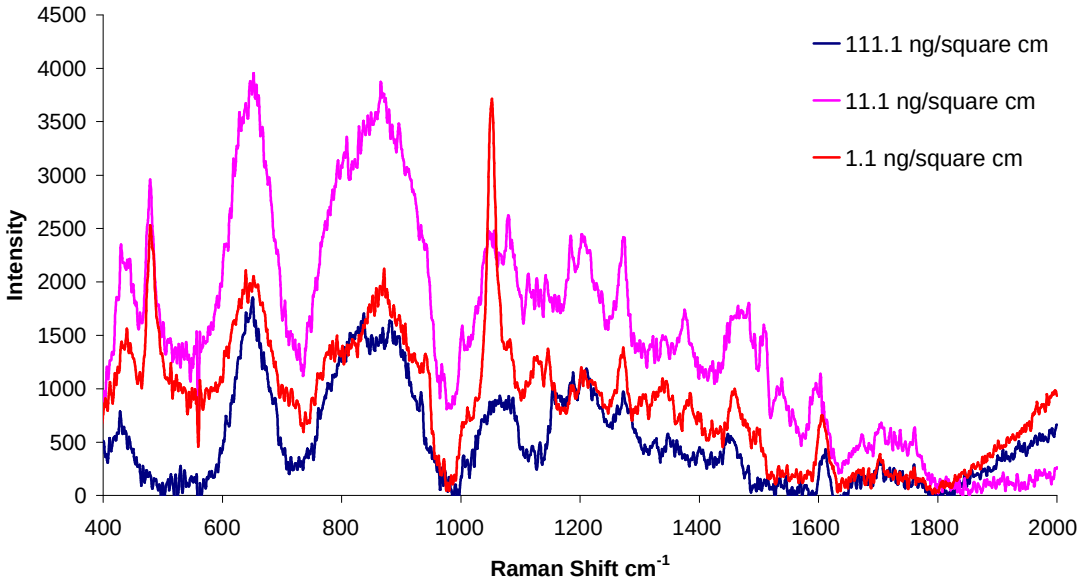

Figure 4.64. Raman spectra for ibuprofen recovered with a Technicloth™ swab from a contaminated steel surface. The surface was contaminated at three different levels: 111.1 ng/cm^2, 11.1 ng/cm^2 and 1.1 ng/cm^2.

Figure 4.64 shows contamination of the surface by ibuprofen. The spectra were less well resolved than those presented earlier for ibuprofen but some of the characteristic peaks remain meaning that the compound was identifiable.

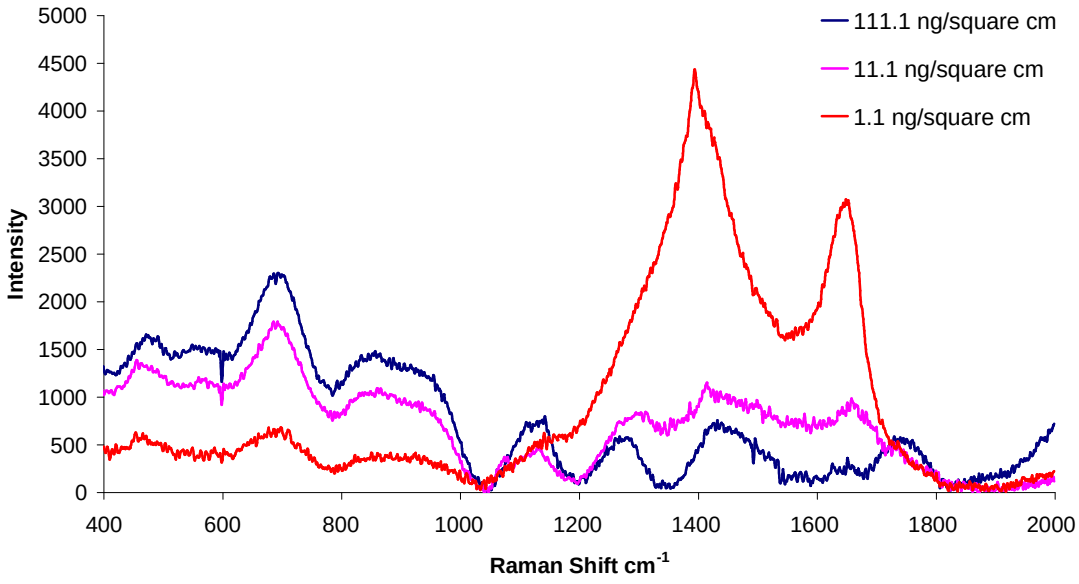

Figure 4.65. Raman spectra for diclofenac recovered with a Technicloth™ swab from a contaminated steel surface. The surface was contaminated at three different levels: 111.1 ng/cm^2, 11.1 ng/cm^2 and 1.1 ng/cm^2.

The spectra fpr diclofenac in Figure 4.65 are less well resolved than the two presented in this section for acetaminophen and ibuprofen. The experiments with diclofenac and Klarite™ substrates in the previous section showed that diclofenac was not as easily detectable as acetaminophen and ibuprofen. In figure 4.65 very few characteristic peaks remain and those that do are broad and unresolved. The compound is identifiable at 111.1 ng/cm^2 by the presence of two peaks just after 1600 nm. These peaks remain in the other two spectra but for diclofenac at 1.1 ng.cm^2 the peak is very broad.

4.3.11 Summary of results chapter

The series of experiments that make up this chapter are summarised below in a diagram which depicts the order of experiments and direction taken during the study.

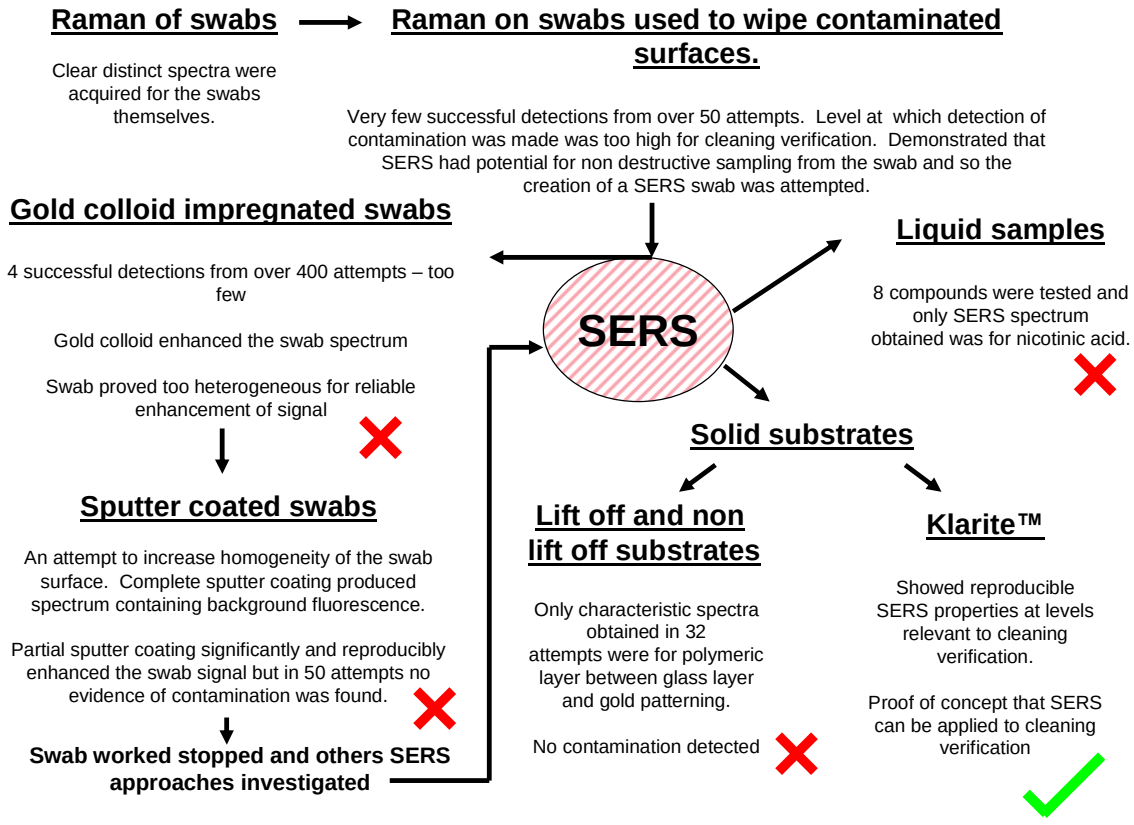

Figure 4.66. Schematic representation of the experimentation carried out for this chapter.

4.4 Discussion

Absorbond™, Technicloth™, Alphawipe™, Super Polx™ and Texwipe™ all showed highly similar Raman spectra. These swabs were composed of polyester, cellulose and cotton. MiracleWipe™ displayed a different Raman spectrum and is made from nylon. Betawipe™ also had a different Raman spectrum and is made from polypropylene. The swabs all showed significant numbers of distinct Raman peaks. An aim of these experiments was to compare swab spectra to see if any were less active because the presence of fewer interfering peaks might result in it being easier to discriminate peaks owing to contamination. All seven swabs showed significant activity in conjunction with Raman spectroscopy and therefore no swab could be identified as particularly useful but the spectra were highly reproducible and the major peaks identified and noted for the use in the rest of the study.

Beneath the Raman microscope all of the swabs had significant depth and therefore different fibres could be focused upon to obtain a characteristic Raman spectrum. Focusing the laser spot onto individual fibres produced clearer Raman spectra with a higher intensity and a more favourable signal to noise ratio. The surface heterogeneity of the swabs meant that poor quality Raman spectra for the swabs could also be obtained. The act of sampling proved critical in determining the quality of the Raman spectrum produced.

Raman spectra for contamination could be seen when the swab was used to wipe a surface contaminated at a level of 111.1 $\mu g/cm^2$. The problem is one of sensitivity with Raman spectroscopy not being a sensitive enough technique to determine the

presence of contaminating residues in actual cleaning verification work. The spectra and images presented in the section on Raman spectra from contaminated swabs represented a few positive spectra from many attempts. The images of residue in close proximity to swab fibres were found rarely and therefore the process of detecting contamination from swabs by Raman spectroscopy is an incredibly inefficient process. To progress the idea of measuring contamination by directly probing the swab it was necessary to improve the sensitivity of the system and this was carried out by investigating SERS.

Initially it was necessary to prove that SERS was achievable for a range of drugs and substrates. This was done by using mixtures containing gold colloid, drug and NaCl solution. The drops were placed on a microscope slide and allowed to evaporate dry. Once dry, the remaining residue was probed under the microscope and Raman spectra taken. An enhancement of signal was found to be the case and with the 5 µl method, SERS spectra for nicotinic acid, trichloroacetic acid, diclofenac and acetaminophen were collected. All spectra showed clear characteristic peaks for the compounds of interest and compared well to reference spectra. Gold colloidal particles of mean diameter 5 nm and 20 nm were used and it was found that the aggregates of 5 nm particles tended to perform better. Figure 4.23 which presented a SERS spectrum for acetaminophen showed a particularly impressive enhancement of signal.

SERS was also carried out on liquid samples in order to see if it was possible to acquire characteristic spectra for low levels of compound in solution. It was possible to obtain a SERS spectra for nicotinic acid when in solution with aggregated gold

colloid but the result came about through large amounts of experimentation. Several other compounds were also tested but without success.

Having demonstrated that a surface enhancement of signal was possible as a result of having gold colloid present, the swabs were impregnated with aggregates of gold colloid. The spectra from gold impregnated swabs were all much stronger with higher intensities than the spectra of ordinary swabs. Some swabs showed greater levels of signal enhancement than others but the experiments showed that it was possible to consistently enhance the spectrum of the swab by introducing aggregates of gold colloid amongst the swab fibres.

With this information in mind, testing was carried out by swabbing a contaminated surface and then examining under the Raman microscope for contamination. Contamination was detected on three swabs but modest enhancements of signal were seen with the Texwipe™, Betawipe™ and Alphawipe™. A significant enhancement of signal was seen for nicotinic acid on a gold colloid impregnated Texwipe™. Again, one of the main problems encountered was due to sampling. Many spectra were taken in order to obtain the results presented and the overwhelming majority were characteristic for the swab rather than residue of the contaminating species. The heterogeneous nature of the swab in combination with the relatively small amount of residue present and the diffuse nature of colloidal aggregates throughout the swab meant that the system was not suitable to reveal contamination in the desired manner. It was concluded that by increasing the homogeneity of the swab surfaces it might proven easier to detect contamination.

In an attempt to add homogeneity to the system, the swabs were sputter coated with gold. The rationale behind this approach was the heterogeneous nature of the swab in combination with the complete gold coverage offered by the sputter coating system might offer more suitable conditions from which to gain a reproducible SERS signal from the swab. Initial experimentation with completely sputter coated swabs was unsuccessful because the only spectra attainable contained significant levels of background fluorescence through which none or very few peaks were resolvable. It was concluded that the fluorescence was due to the thick gold coating. A partial sputter coating of the swab was then tested and this was carried out by altering the deposition time of the sputter coater so that gold coverage of the surface would be incomplete. Testing with partially coated fibres showed that an enhancement of signal could be achieved if the correct area of the swab was sampled from. The enhancement of signal was significant and provided convincing evidence that a significant surface enhancement of signal from the swab surface was possible with sputter coating. However, after wiping contaminated surfaces with partially sputter coated swabs, it was not possible to produce any spectra indicative of contamination on the swab.

At this point it was decided to change the focus of the study away from the swab because experimentation had shown it too heterogeneous on the microscopic scale to produce consistent and significant enhancement of signal. A significant enhancement of signal indicative of contamination was seen rarely throughout the experiments previously discussed and this was not the ideal basis for a technique aimed for industrial application, particularly a process where a wide range of drug compounds would require detection. A generic system was required and the results obtained from

experiments designed to produce a SERS swab showed that obtaining a SERS spectrum for the compound of interest was too time consuming a process.

The focus of the study was switched from the swab to solid SERS substrates. Substrates were provided as a gift from a lab at the University of Michigan and Klarite™ substrates were purchased from Mesophotonics Ltd.

The substrates from the lab at the University of Michigan were unsuccessful in revealing contamination. A 5 µl drop of drug in solution was pipetted onto the surface and allowed to evaporate dry before investigation under the Raman microscope. Acetaminophen, ibuprofen, diclofenac and nicotinic acid were tested and it was not possible to detect any contamination because no characteristic spectra were obtained.

The substrates were classified as either lift off or non lift off. A lift off sample contained the gold patterning on a glass substrate and the non lift off substrates had a layer of polymer between the glass and gold patterning. It was possible to detect peaks characteristic of the polymer in the non lift off samples where as the lift off samples produced broad unresolved spectra.

5 µl of solution containing compound of interest was pipetted onto a Klarite™ substrate. Acetaminophen showed excellent enhancement of signal and very strong SERS spectra were detected for the compound at concentrations of 1000 ppm, 100 ppm and 10 ppm. Characteristic peaks for the compound were also present at 1 ppm and the compound was identifiable. Identification of acetaminophen on the basis of

the 1 ppm spectrum alone would have been difficult but in sequence with the other spectra it was identifiable. All the spectra had good amplitude of peaks and a good signal to noise ratio. SERS spectra were collected for ibuprofen at concentrations of 1000 ppm, 100 ppm and 10 ppm. Identification of the compound was possible and the spectra showed good amplitude of peaks and good signal to noise ratio. SERS spectra were also collected for diclofenac at concentrations of 100 ppm, 10 ppm and 1 ppm. Again the compound was easily identifiable at 100 and 10 ppm but at 1 ppm two characteristic peaks remained meaning identification was possible but the unfavourable signal to noise ratio meant the peaks were poorly resolved.

As mentioned previously, experiments were carried out by dropping a 5 µl drop onto the Klarite™ surface and allowing it to dry prior to inspection under the Raman microscope. The crucial difference between the results presented for the Klarite™ substrates and other substrates and methods used in an attempt to produce SERS spectra in this study was that the spectra presented from Klarite™ were the result of one collection. The Klarite™ substrate had proven to be a highly consistent enhancer of Raman signal and therefore was useful for demonstrating the potential of SERS for analysis of cleaning verification samples.

SERS spectra were also obtained at 100 ppm and 10 ppm for thiamine, maleic acid and nicotinic acid and this showed the generic nature of the Klarite™ substrate as a signal enhancer. Generic capability is a well known problem with many SERS substrates with some not working for particular compounds. The Klarite™ substrates provided a reliable and quick enhancement of signal compared to the other SERS

strategies employed in the study were large amounts of time were invested to obtain a small number of spectra indicative of contamination.

By contaminating a surface, wiping with a swab, extracting 5 µl of solution from that swab, depositing on the Klarite™ surface and then analysing, it was possible to detect acetaminophen, ibuprofen and diclofenac at levels of contamination relevant to cleaning verification. Acetaminophen and ibuprofen could be identified by eye at 111.1 ng/cm ^{2} and evidence of contamination was visible for the two compounds at 11.1 ng/cm^2 and 1.1 ng/cm^2 . An often quoted worst case scenario for cleaning verification work is 5 ng/cm^2. In this study it was possible to detect at levels close to that and so the potential of SERS for cleaning verification was therefore demonstrated. To take this work further and definitively prove the capability of SERS with well defined detection limits for compounds it will be necessary to employ chemometric techniques.

Some basic chemometric analysis was performed on the data produced from Klarite™ slides and swabs used to wipe a contaminated surface. The Savitzky-Golav smoothing filter was applied to smooth spectra and principal component analysis (PCA) was carried out on the data from acetaminophen and ibuprofen to see if spectra from the two drugs could be differentiated.

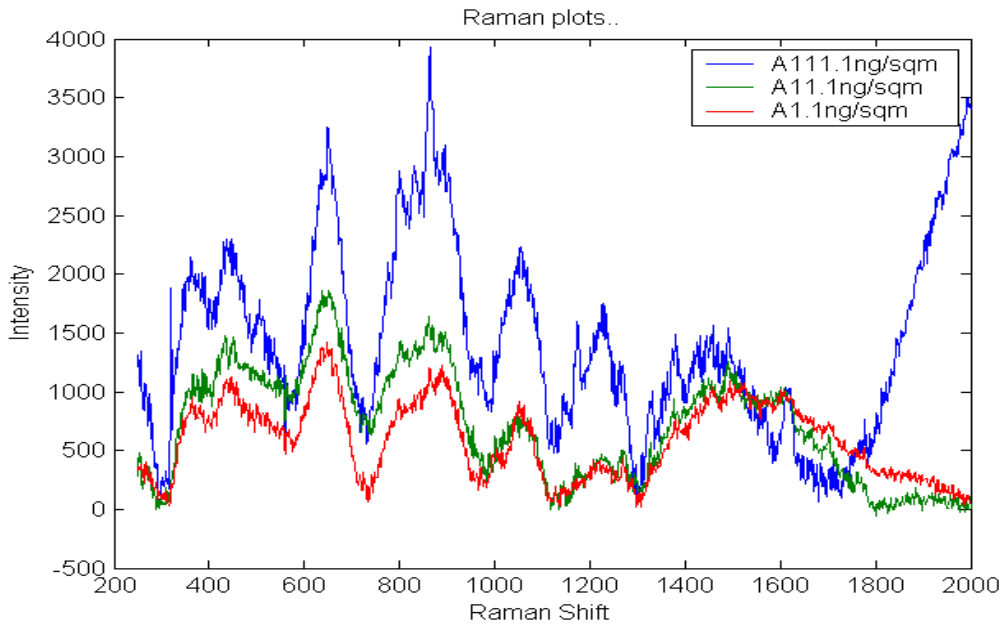

Figure 4.67. Raman spectra for 5µl extracts from swabs used to wipe a surface contaminated with acetaminophen at 111.1 ng.cm^2, 11.1 ng/cm^2 and 1.1 ng/cm^2.

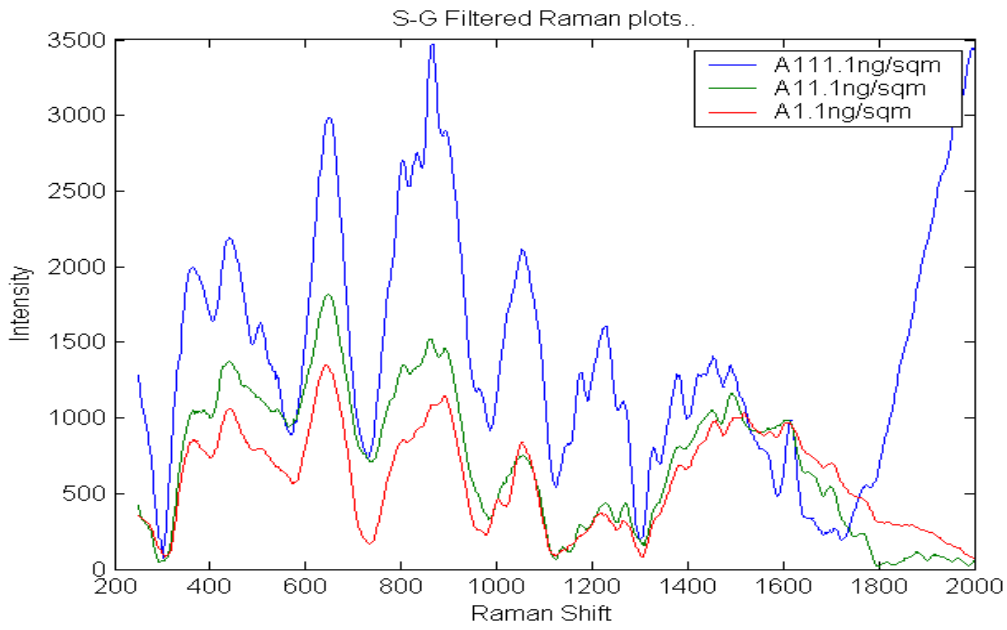

Figure 4.68. Raman spectra smoothed with the Savitzky-Golav smoothing filter for 5µl extracts from swabs used to wipe a surface contaminated with acetaminophen at 111.1 ng.cm^2, 11.1 ng/cm^2 and 1.1 ng/cm^2.

Figure 4.69 shows how samples of acetaminophen (A – green circle) can be differentiated from ibuprofen (B – red circle).

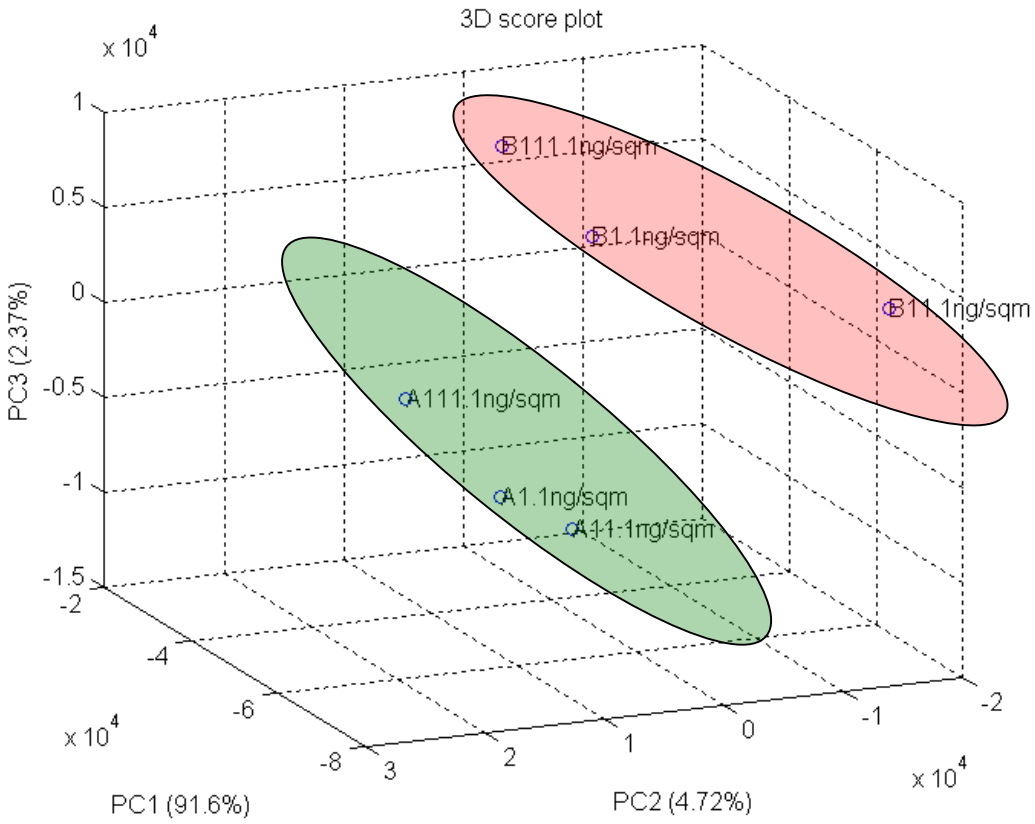

Figure 4.69. Three dimensional plot of PCA scores from SERS spectra of acetaminophen and ibuprofen recovered from a stainless steel surface.

The results presented in this chapter are novel in terms of the application of SERS for cleaning verification work. The idea of detecting contamination directly from the swab represents an elegant solution to the problem of cleaning verification but the attempts made to modify the swab in order for it to produce a SERS signal revealing of contamination were unsuccessful. Current technologies such as infrared and near infrared which spectroscopically probe a surface have been shown to be quite effective on flat surfaces. Curved surfaces, depressions and pipes are much more

difficult to sample from. By analysing the swab it is possible to detect contamination from all points of the equipment train. The results presented in this chapter showed that it was possible to enhance the Raman signal from a swab and in some instances detect contamination. Unfortunately, the detection of contamination occurred too infrequently to form the basis of an industrial process. Potential future work to circumnavigate these problems could include the production of more homogenous swabs to improve sampling, or making swabs from polymer so that gold can be reacted to give a more homogenous coating thus increasing the number of SERS "hot spots" necessary for the enhancement of signal.

Should it not prove possible to develop a SERS swab for cleaning verification then as shown in this chapter it is possible to use SERS substrates to produce the necessary enhancement of signal for swab extract analysis. A myriad of options exist for producing a SERS system for cleaning verification work and potential ideas include, a SERS surface used in conjunction with a portable or laboratory Raman system, SERS vials in which the inside of the vial is coated with an enhancing gold or silver substrate or tip based SERS in which fibre optic tips are coated with gold particles so that surfaces can be probed. The disadvantages with analysis of swab extract is that further processing steps and complexity are introduced into the process. HPLC is a time consuming process but it is important to be mindful of the need for simplicity in the replacement technology.

Another important aspect of cleaning verification work to be considered is the quantitative aspect. If SERS is to be implemented as a technology for cleaning verification the method must be quantitative. The field of quantitative SERS work is

growing and a key aspect is sampling. Reproducibility is a key aspect of sampling with quantitative SERS and one method of ensuring good reproducibility and of producing samples amenable to quantitative work is to ensure all of the sample is covered by the laser spot. Future work based on results in this chapter could include experimentation with smaller volumes than 5 µl on the Klarite™ slide and different sizes of laser spot.

An important aspect of Raman microscopy and therefore SERS by Raman microspectroscopy is that of sampling. Numerous options exist when looking at samples and taking Raman spectra; these include acquisition time, number of acquisitions, laser strength and objective. The microscope used during this investigation had three objectives and they were: x 10, x 50 and x 100. Acquisition times employed were between five and thirty seconds and the maximum number of acquisitions was five. It is possible to improve the quality of a Raman spectrum by adjusting the acquisition time and number of acquisitions. The overriding aim of this chapter was to speed up the cleaning verification process and that was kept in mind when selecting the acquisition time and number of acquisitions with very few samples taking more than two attempts to obtain a spectrum. The Klarite™ substrates came with clear instructions about their use from the manufacturer. High objectives were not recommended because of the tendency for the laser to damage the substrate surface through these objectives. The use of five to ten second accumulation times was also recommended when using Klarite™ slides so as to not go over the maximum count of Raman scattered photons and flood the CCD. In deciding how best to produce a spectrum, the strength of the laser can be an important factor. Using the laser at full power can give the most well defined spectrum with good peak amplitude

but it is also possible to obtain background fluorescence and in the case of SERS measurements flood the CCD. With SERS measurements the signal can be so intense from the laser on full power that it was necessary to drop the laser power in order to resolve the spectrum.

SERS offers a number of advantages over other technologies currently employed within the cleaning verification field. It has sensitivity and specificity similar to HPLC whilst possessing the rapid detection times of spectroscopic techniques, ion mobility spectroscopy and total organic carbon analysis. This study has shown SERS detection with Klarite™ slides was possible at levels of contamination encountered within the industrial cleaning verification scenario. Future work would involve the formulation of a portable/handheld Raman system for analysis of cleaning directly from the manufacturing equipment itself.

5 Optical detection of genotoxic impurities

This chapter presents an introduction to the compound known as 2,6-diphenyl-4-(2,4,6-triphenyl-1-pyridinio)phenolate or Reichardt's dye. Additional introductory information on genotoxic impurities of specific importance to the experiments undertaken is also presented. Results are presented that showed Reichardt's dye as a potential candidate dye for use in the optical sensing of alkylating agents present as genotoxic impurities in pharmaceutical formulations.

5.1 Introduction

The importance of genotoxic impurities, the limits for genotoxic impurities, the current analytical methods used for genotoxic impurity detection and the need for improved analytical techniques were discussed in the introductory section to the thesis. The main aim of this chapter is to develop a sensitive and rapid assay system for alkylating agents (a class of genotoxic impurities). The methods described in the literature which are commonly employed for detection of these compounds in industrial settings are traditional analytical chemistry techniques such as HPLC and GC/MS. The aim of this chapter was to develop an optical system based on fluorescent/UV-visible dyes that can quantify alkylation by alkylating agents.

5.1.1 Reichardt's Dye

Reichardt's dye (figure 5.1) also known as 2,6-diphenyl-4-(2,4,6-triphenyl-1-pyridinio)phenolate is a well known solvatochromic dye and has been used in several experiments to determine the polarity of solvents or a medium. The dye or related molecules are sometimes referred to in the literature as betaine dyes.

The zwitterionic compound known as Reichardt's dye exhibits one of the largest observed solvatochromic effects of any known organic molecule. Charge-transfer absorption wavelength shifts amount to several hundred nanometers in going from a polar solvent ($\lambda_{abs\ max} \approx 453$ nm in water) to a non polar solvent ($\lambda_{abs\ max} \approx 925$ nm in hexane) (Fletcher *et al.,* 2001).

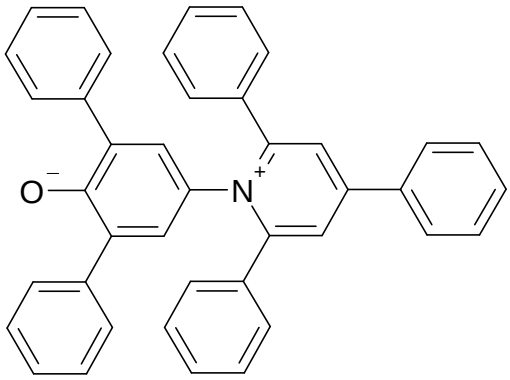

Figure 5.1. 2,6-diphenyl-4-(2,4,6 triphenylpyridinio)phenolate, also known as Reichardt's dye or Reichardt's betaine.

Et (30) values are defined as molar transition energies (kcal mol^{-1}) for the longest wavelength, intramolecular charge transfer UV-visible absorption band of the dissolved standard betaine dye. The values are known for more than three hundred solvents and numerous binary solvent mixtures and they have found many applications in analytical chemistry (Linert *et al.,* 1992). The term solvatochromism describes a shift in an electronic absorption band of a molecule in response to changes in polarity of its solvational cage. The shift results from physical intermolecular solvent-solute interactions (dipole-dipole, dipole induced, hydrogen bonding, etc) which alter the energy difference between the electronic ground and excited states of the absorbing species. Reichardt's dye exhibits one of the largest solvatochromic

effects observed and this results from the highly dipolar zwitterionic ground state and the less polar excited state, brought about by the intramolecular charge transfer from the phenoxide group into the pyridinium moiety occurring on the absorption of light. In the ground state the positive charge on the pyridinum group is delocalized and sterically shielded, while the phenoxide moiety has a highly basic electron donating capacity (Krech & Pehrsson, 1997)

The solvatochromic abilities of the dye and related dyes are extremely well documented. Paley & Harris, 1991 synthesised a number of different but related dye molecules to utilise the dyes solvatochromic properties in order to investigate second-harmonic generation. Dickert *et al.,* 2000 utilised Reichardt's dye and related dyes as optochemical sensor materials. By measuring in UV-visible region the solvatochromic effect of the dye was monitored in response to the presence of various solvents in the gaseous phase. They were able to immobilise the dye by a sol gel process and under mild conditions produce a sensor system with optically transparent, highly porous and stable layers.

Reichard *et al.,* 2001 synthesised three new "fluorophillic" fluorine and perfluoroalkyl substituted N-phenolate betaine dyes (figure 5.2).

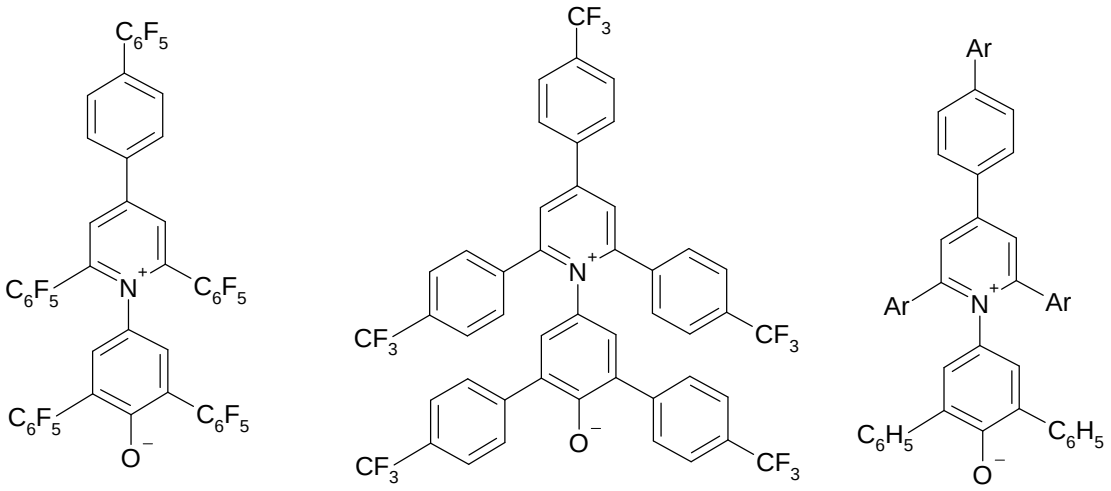

Figure 5.2. The three dyes prepared by Reichardt *et al.*, 2001.

The new dyes performed well and extended the Et (30) scale to new solvents of interest and therefore increased the supply of solvatochromic indicator dyes. The newly synthesised dyes were particularly useful for the determination of Et (30) values of more acidic solvents, polymers and surfaces where the normal dye is protonated. In spite of the introduction of fluorine and perfluoroalkyl substituents Et (30) values are still lacking for perfluoroalkanes because lack of solubility means UV-vis spectroscopy is not possible (Reichardt *et al.*, 2001).

Krech & Rose-Pehrsson, 1997 were able to incorporate Reichardt's dye into several polymer films of differing polarity and sorbency. The polymers employed were: polyisobutylene, polypichlorohydrin, polyvinyl pyrrolidone and polystyrene. Solutions of the dye in methanol or chloroform were mixed with a stock solution of polymer and sprayed onto a surface. Reversible and reproducible changes in the absorption maximum of the dye were observed when the polymer films were exposed to a series of vapours of different polarities. The incorporation of environment sensitive dyes into various polymeric films could produce a low cost sensor array with

in situ detection capabilities for several analyte vapours (Krech & Rose-Pehrsson, 1997).

Imai & Chujo, 2000 investigated the potential use of Reichardt's dye with organic-inorganic polymer hybrids. These hybrids are the molecular composite of organic polymers and a three dimensional siloxane network. They are prepared by the sol-gel reaction of alkoxsilanes in the presence of organic polymers such as poly (2-methyl-2-oxazoline) and poly (N-vinylpyrrolidone). The solvatochromic polymer was prepared by attaching Reichardt's dye to a side chain of poly (2-methyl-2-osazoline). Reichardt's dye was also used in the experiment to dope sol-gel glasses and it was found that the dye containing organic-inorganic hybrids and the dye doped glass performed almost as well as the dye on it's own for solvatochromic changes. In the organic-inorganic polymer hybrid the local polarity was affected by the tetramethoxysilane to methyltrimethoxysilane ratio and the presence of organic polymer. The authors concluded that better control of the microenvironment around the dye molecules was possible (Imai & Chujo, 2000).

Reichardt's dye was used by Fletcher *et al.,* 2001 in part of a study on ionic liquids and their potential as alternative solvents. The authors investigated the change in the longest wavelength intramolecular charge-transfer π-π^*absorption band of Reichardt's dye in bmim PF_6(the ionic liquid of interest) and selected solvents at ambient conditions (figure 5.3).

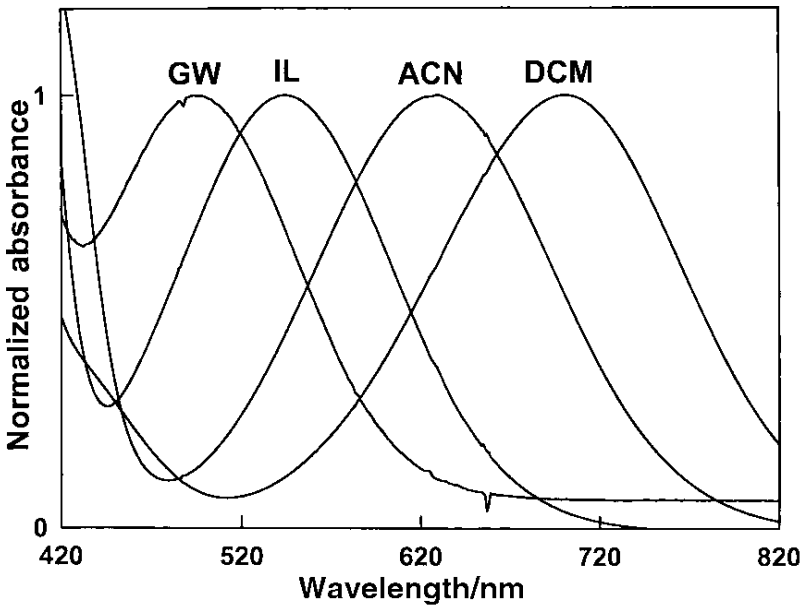

Figure 5.3. Longest wavelength intramolecular charge-transfer π-π^*absorption band of Reichardt's betaine dye in 90 wt % glycerol in water (GW), bmimPF_6 (IL), acetontirile (ACN) and dichloromethane (DCM) under ambient conditions.

Linert *et al.,* 1992 and Carreno *et al.,* 1999 used the decrease in the solvatochromic long wavelength UV-visible absorption band of Reichardt's dye when reacted with iodomethane to make observations about the kinetics of the reaction mechanism, looking at parameters such as the substituent, solvent and temperature dependence of the reaction (figure 5.4).

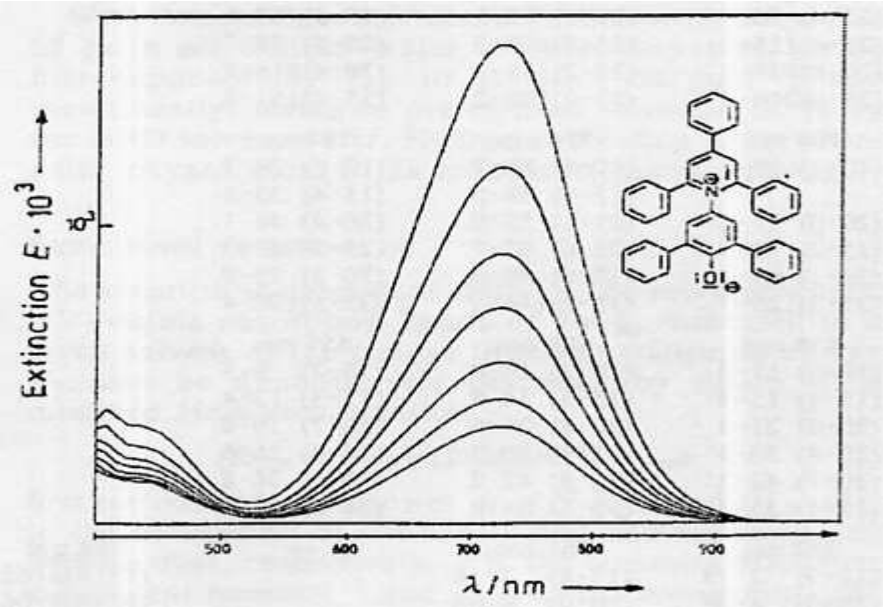

Figure 5.4. Decrease of solvatochromic, long wavelength UV-visible absorption band of Reichardt's dye during methylation with iodomethane in chloroform at 19.9°C. The first spectrum was recorded sixty seconds from the reaction commencing and the other spectra were recorded at 200 second intervals (Linert *et al.*, 1992).

5.1.2 Reichardt's dye and genotoxic impurities

In this section of the project we have employed Reichardt's dye for the direct measurement of alkylation reactions. Figure 5.3 shows the lateral shift in the longest wavelength intramolecular charge-transfer π-π^*absorption band as a result of solvatochromic changes. Figure 5.4 shows a decrease in the solvatochromic long wavelength UV-visible absorption band as a result of alkylation. It is therefore anticipated that alkylation of the dye will result not in a shift of wavelength but in a reduced absorption maximum. The proposed reaction would operate by an SN2 mechanism and take place at the phenoxide moiety. Observing a decrease in the solvatochromic long wavelength UV-visible absorption band should indicate that

alkylation of Reichardt's dye has taken place. It is also known that the dye molecule is active with fluorescence spectroscopy. Fluorescence is a potentially sensitive spectroscopic technique and so fluorescence spectroscopy will also be investigated as a potential method for measuring alkylation of Reichardt's dye. Additionally, to gain further confirmation of alkylation of Reichardt's dye and to confirm the products of the reactions; investigations were carried out with NMR spectroscopy.

Experimental work for this chapter involved attempting to quantify the alkylation of Reichardt's dye and two related dye molecules with fluorescence spectroscopy and UV-vis spectroscopy (figure 5.5). NMR experiments were also carried out to confirm alkylation of Reichardt's dye. The assay was then tested with drug samples to see if sample interference is a problem and whether sample preparation and clean up is necessary; as it is with many of the analytical methods currently employed by the pharmaceutical industry to measure genotoxic impurities. Making extra sample processing redundant would be a big advantage to any analytical system and in this case it would be desirable if the drug substances did not interfere with the dye. Were this proven to be the case, drug samples for alkylating agent testing could be dissolved immediately and testing carried out.

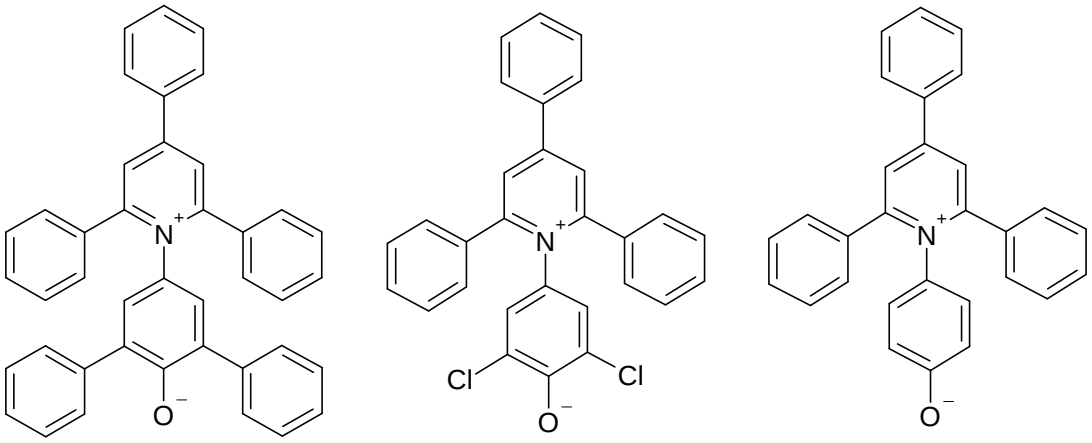

Figure 5.5. The three betaine dyes to be investigated experimentally. 2,6-diphenyl-4-(2,4,6-triphenyl-1-pyridinio)phenolate (Reichardt's dye - left), 2,6-dichloro-4-(2,4,6-triphenyl-1-pyridinio)phenolate (centre) and 1-(4-hydroxyphenyl)-2,4,6-triphenylpyridinium hydroxide inner salt (right).

5.1.3 Other candidate dye molecules

The azo dyes 4-phenylazophenol and Fat Brown B were also considered for testing because it was suspected they too may have susceptibility to alkylation.

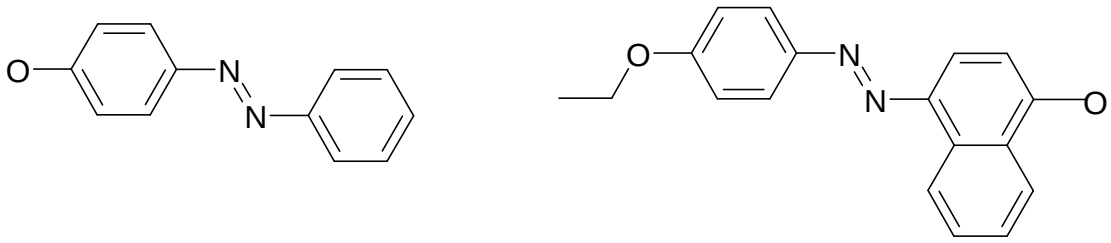

Figure 5.6. 4-phenylazophenol (left) and Fat brown B (right).

5.1.4 Alkylating agents under investigation

The classes of alkylating agent used in this study:

1) Alkyl halides.

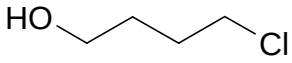

4-chloro-1-butanol

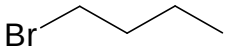

1-bromobutane

2) Sulfonate esters

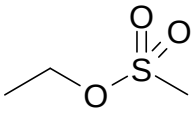

ethyl methane sulfonate

3) Diazonium salts

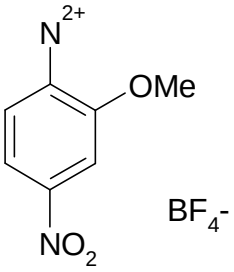

Fast Red B

4-chloro-1-butanol is an extremely important and common genotoxic impurity because it originates as a result of a reaction between hydrochloric acid and the solvent tetrahydrofuran (figure 5.7). This reaction is frequently employed in the pharmaceutical manufacturing process.

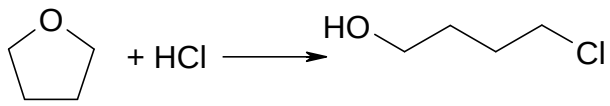

(THF)

Figure 5.7. Summarising 4-chloro-1-butanol formation as a result of the reaction between tetrahydrofuran (THF) and hydrochloric acid.

1-Bromobutane is not a common genotoxin but it has been included in the study as an additional alkyl halide to help develop an understanding of the alkylation of Reichardt's dye.

Ethyl methane sulfonate is a common genotoxic impurity and belongs to the class of alkylating agents know as sulfonate esters. These impurities arise from the use of sulfonic acids such as methane sulfonic acid, benzene sulfonic acid and ρ-toluene sulfonic acid (Calon & Richoll 2005). The likelihood of producing sulfonate esters as impurities is increased if solvent or intermediates with an alcohol group are present during synthesis (Taylor *et al.*, 2005).

Fast Red B is a diazonium compound and is representative of a class of compounds normally used as reaction intermediates during the synthetic stages of drug production, they are sometimes utilised when trying to introduce an N-N coupling into a molecule.

Experiments in this chapter were carried out at concentrations of alkylating agent relevant to industrial situations. As previously stated in the introductory chapter the limit for genotoxic impurities in a drug for which a patient is taking for a period of greater than one year is 1.5 µg of genotoxic impurities per day. This limit increases

for drugs which are taken for shorter amounts of time and can go up to 120 µg of genotoxic impurities per day when the drug is taken for no longer than a month (McGovern & Jacobsen-Kram, 2006). For experiments in this chapter, alkylating agents were initially tested in parts per million ranges similar to those investigated by pharmaceutical companies 0-100 ppm. For experiments where drug is dissolved alongside the dye and alkylating agent; alkylating agents were present in µg/ml. The reason for this is that it is then easier to relate the amounts of genotoxic impurity to the amount of drug dissolved alongside the alkylating agent and dye. If the dissolved drug were a lifetime drug, provided the daily maximum dose was dissolved, no more than 1.5 µg of genotoxic impurities should be present.

5.2 Materials & Methods

4-chloro-1-butanol, 1-bromobutane, ethyl methane sulfonate, Fast Red B, 4-phenylazophenol, Fat Brown B, 2,6-diphenyl-4-(2,4,6-triphenyl-1-pyridinio)phenolate, 2,6-dichloro-4-(2,4,6-triphenyl-1-pyridinio)phenolate and 1-(4-hydroxyphenyl)-2,4,6-triphenylpyridinium hydroxide inner salt, acetaminophen, ibuprofen and diclofenac were purchased from Sigma (Poole, Dorset, UK). N,N-dimethylformamide (DMF) and Acetonitrile (ACN) were purchased from Fisher.Scientific (Loughborough, UK)

Fluorescence measurements were carried out on an RF-5001PC spectrofluorimeter (Shimadzu, Milton Keynes UK) and UV-vis measurements were carried out on a UV2100 UV-visible spectrophotometer (Shimadzu, Milton Keynes UK). Samples measured using fluorescence spectroscopy were excited at 347 nm collected at 693 nm.

400 µM stock solutions of 2,6-diphenyl-4-(2,4,6-triphenyl-1-pyridinio)phenolate, 2,6-dichloro-4-(2,4,6-triphenyl-1-pyridinio)phenolate and 1-(4-hydroxyphenyl)-2,4,6-triphenylpyridinium hydroxide inner salt were prepared in Acetonitrile or N,N-dimethylformamide. 40 µM stock solutions of Fat Brown B and 4-Phenylazophenol were prepared in acetonitrile or N.N-dimethylformamide. 1000 ppm stock solutions of 4-chloro-1-butanol, 1-bromobutane, ethyl methane sulfonate and Fast Red B were prepared in acetontirile or N.N dimethylformamide. Appropriate dilutions of alkylating agents were subsequently made for experimentation.

400 µM Dye solutions were mixed with solutions of alkylating agent in 18 ml glass vials. Volumes of dye and alkylating agent were always mixed in a 1:1 fashion thus giving a final dye concentration of 200 µM. Analysis was then carried on the spectrofluorimeter or on the UV-vis spectrophotometer. Clean pipette tips were used for every transfer of solution and the cuvette was washed out with solvent and dried with tissue paper between each reading. Samples in glass vials requiring heat were placed in a 5000 ml beaker containing 50 mls of water and heated on a hot plate for 4 hours. A thermometer was used to ensure a temperature in the water of 85^{o}C.

Dye samples containing drug for the drug interference experiments were made to concentrations of 10.0 or 100.0 mg/ml of acetaminophen, ibuprofen or diclofenac. To create buffer solutions of pH 5.0, 7.0 and 9.0 monosodium phosphate monohydrate and disodium phosphate were weighed out using approximate calculations and then adjusted to final concentrations using a pH meter.

NMR spectroscopy was carried out using a Jeol ECX 400 NMR spectrometer (Jeol, Welwyn Garden City, UK). Deuterated DMF was purchased from Goss Scientific (Great Baddow, Essex, UK).

5.3 Results

Results are presented that establish the potential use of reichardt's dye for the optical detection of genotoxic impurities.

5.3.1 Visual changes of the dyes in response to the addition of 1-bromobutane and 4-chloro-1-butanol.

Visual changes in Reichardt's dye were initaly observable to the eye at high concentrations of alkylating agent. Figures 5.8-5.10 show photgraphs of bleaching by 4-chloro-1-butanol and 1-bromobutane.

Figure 5.8. 200 µM 2,6-diphenyl-4-(2,4,6-triphenyl-1-pyridinio)phenolate (left), 200 µM 2,6-diphenyl-4-(2,4,6-triphenyl-1-pyridinio)phenolate and 500 ppm 4-chloro-1-butanol (middle) and 200 µM 2,6-diphenyl-4-(2,4,6-triphenyl-1-pyridinio)phenolate and 500 ppm 1-bromobutane (right).

Figure 5.9. 200 µM 2,6-dichloro-4-(2,4,6-triphenyl-1-pyridinio)phenolate (left), 200 µM 2,6-dichloro-4-(2,4,6-triphenyl-1-pyridinio)phenolate and 500 ppm 4-chloro-1-butanol (middle) and 200 µM 2,6-dichloro-4-(2,4,6-triphenyl-1-pyridinio)phenolate and 500 ppm 1-bromobutane (right).

Figure 5.10. 200 µM 1-(4-hydroxyphenyl)-2,4,6-triphenylpyridinium hydroxide inner salt (left), 200 µM 1-(4-hydroxyphenyl)-2,4,6-triphenylpyridinium hydroxide inner salt and 500 ppm 4-chloro-1-butanol (middle) and 200 µM 1-(4-hydroxyphenyl)-2,4,6-triphenylpyridinium hydroxide inner salt and 500 ppm 1-bromobutane (right).

To the eye, all three dyes showed significant bleaching in the presence of 4-chloro-1-butanol. The dye colour was completely lost in the presence of 4-chloro-1-butanol at 500 ppm indicating complete alkylation of the dye by the compound.

2,6-diphenyl-4-(2,4,6-triphenyl-1-pyridinio)phenolate and 2,6-dichloro-4-(2,4,6-triphenyl-1-pyridinio)phenolate showed a slight lightening in colour in response to the presence of 1-bromobutane at 500 ppm. This indicated a partial alkylation of the dye molecules in solution by 1-bromobutane.

1-(4-hydroxyphenyl)-2,4,6-triphenylpyridinium hydroxide inner salt changed colour from purple to brown in the presence of 500 ppm 1-bromobutane. This means a solvatochromic change occurred alongside the partial bleaching which took place .

5.3.2 Fluorescent response to the addition of 1 –Bromobutane and 4-Chloro-1-butanol.

Changes in the dyes appearance in response to the addition of 1-bromobutane and 4-chloro-1-butanol were measured using fluorescence spectroscopy (figures 5.11 – 5.14).

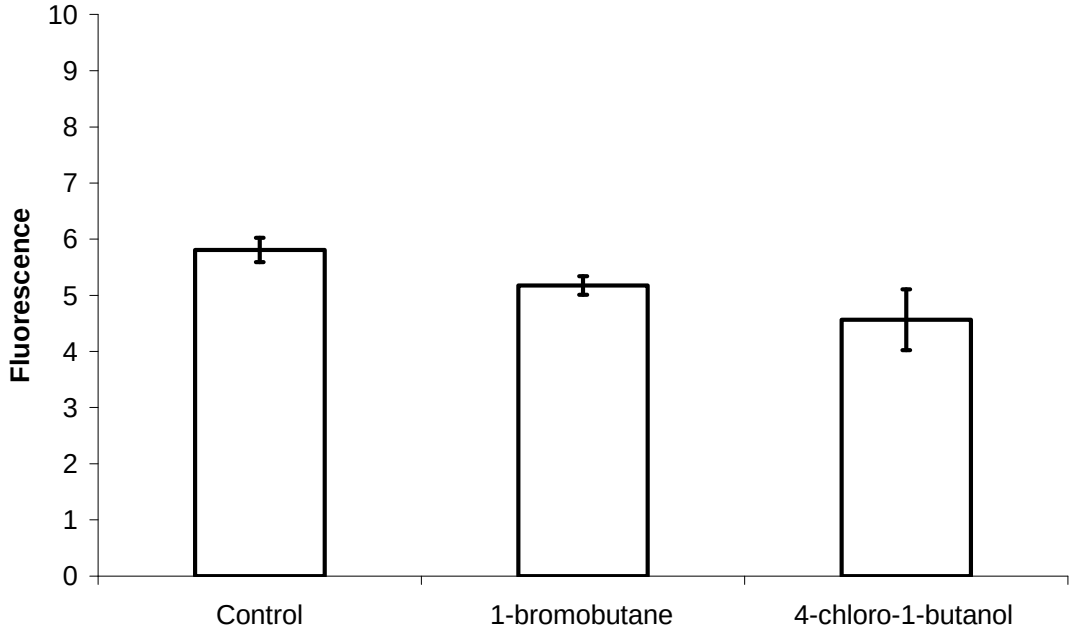

Figure 5.11. Changes in fluorescence of 2,6-diphenyl-4-(2,4,6-triphenyl-1-pyridinio)phenolate in response to the addition of 35 ppm of 1-bromobutane or 4-chloro-1-butanol. n = 9.

The dye was present at a concentration of 200 µM and fluorescence decreased slightly in the presence of 1-bromobutane at 35 ppm. 4-Chloro-1-butanol caused a more significant decrease in fluorescence with a drop from 5.8 in the control to 4.6 AU.

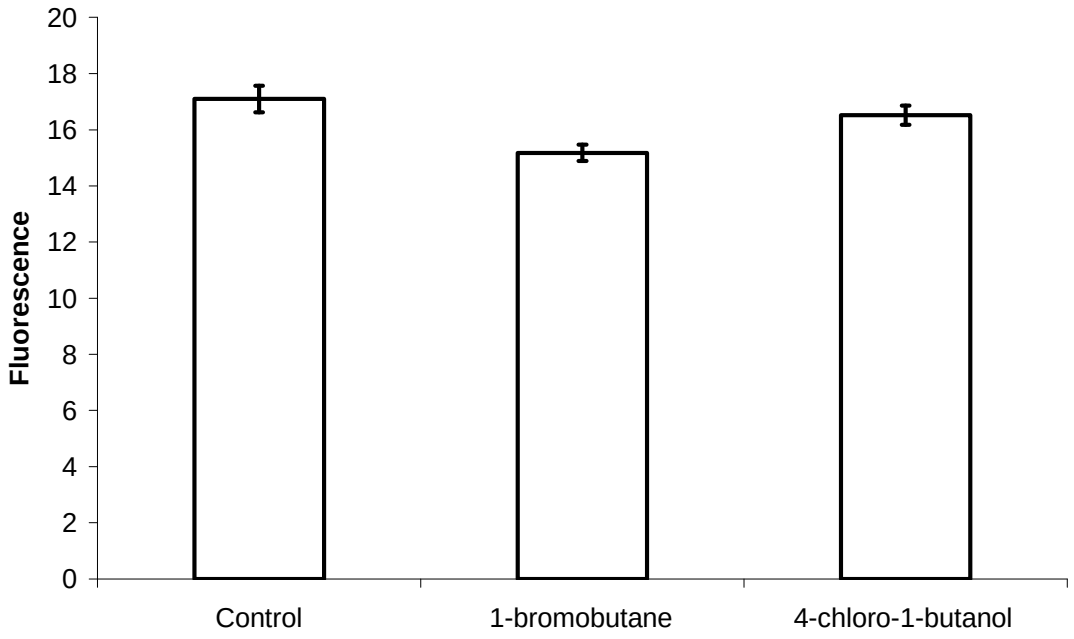

Figure 5.12. Changes in fluorescence of 2,6-diphenyl-4-(2,4,6-triphenyl-1-pyridinio)phenolate in response to the addition of 35 ppm of 1-bromobutane and 4-chloro-1-butanol. n = 10

The dye was present at a concentration of 2 µM and fluorescence decreased slightly in the presence of 1-bromobutane at 35 ppm going from 17.1 in the control sample to 15.2 AU in the sample containing 1-bromobutane at 35 ppm. 4-Chloro-1-butanol at 35 ppm caused a smaller decrease in fluorescence with a drop from 17.1 in the control to 16.5 AU.

When attempting to create an optical sensor system such as this one it is preferable to have maximum possible distinction so that changes due to alkylation can be easily determined and quantified. Diluting the dye from 200 µM to 2 µM caused the fluorescence intensity to increase from the approximate range of 5-6 AU to the approximate range of 15-20 AU. Increasing the fluorescence intensity will make changes in fluorescence that result from alkylation more apparent.

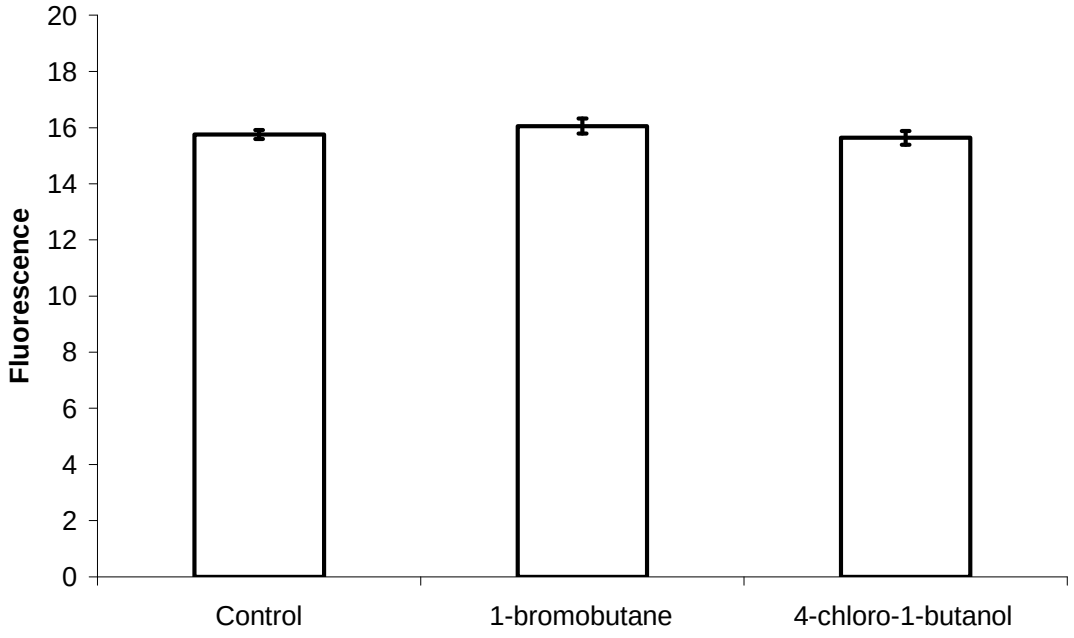

Figure 5.13. Changes in fluorescence of 2,6-dichloro-4-(2,4,6-triphenyl-1-pyridinio)phenolate in response to the addition of 35 ppm of 1-bromobutane and 4-chloro-1-butanol. n = 10

The dye is present at a concentration of 2 µM and fluorescence increased slightly in the presence of 1-bromobutane at 35 ppm going from 15.8 in the control sample to 16.1 AU in the sample containing 1-bromobutane at 35 ppm. 4-chloro-1-butanol at

35 ppm caused a small decrease in fluorescence with a drop from 15.8 in the control to 15.7 AU.

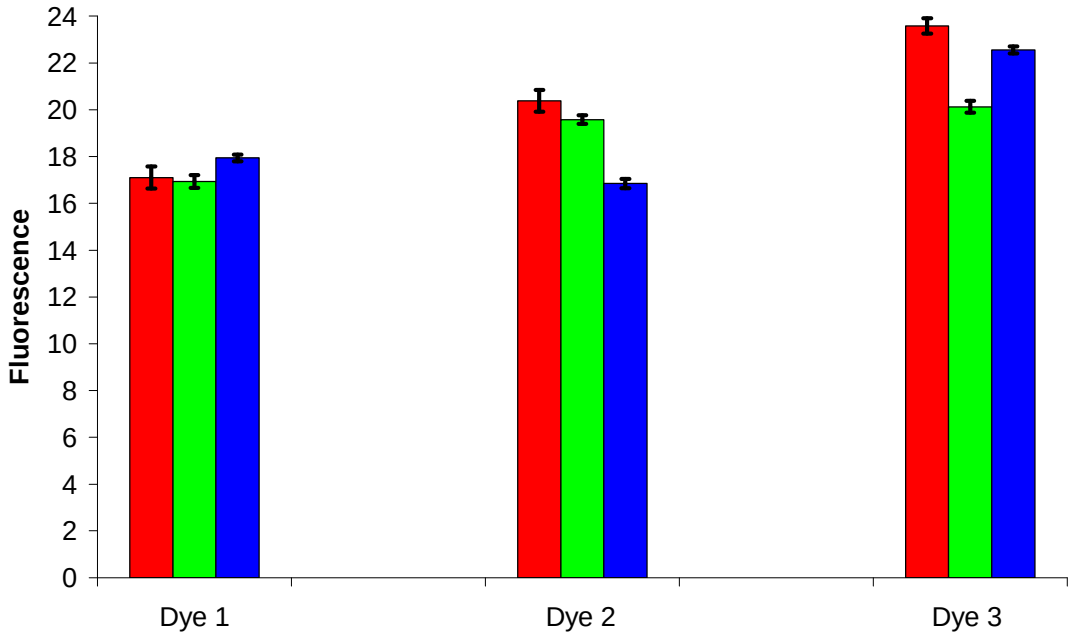

Figure 5.14. Changes in fluorescence of 2,6-diphenyl-4-(2,4,6-triphenyl-1-pyridinio)phenolate (dye 1), 2,6-dichloro-4-(2,4,6-triphenyl-1-pyridinio)phenolate (dye 2) and 1-(4-hydroxyphenyl)-2,4,6-triphenylpyridinium hydroxide inner salt (dye 3) in response to the addition of 35 ppm of 1-bromobutane and 4-chloro-1-butanol. n =3. The red columns indicate control measurements where dye is present in solvent, the green columns represent fluorescence when 1-bromobutane is present at 35 ppm and the blue columns represent fluorescence when 4-chloro-1-butanol is present at 35 ppm.

All three dyes showed different responses to the addition of 1-bromobutane and 4 – chloro-1-butanol. 2,6-diphenyl-4-(2,4,6-triphenyl-1-pyridinio)phenolate (dye 1 – black) showed a very slight decrease in fluorescence (17.1 to 16.93) when 1-

bromobutane was present at 35 ppm but a slight increase in fluorescence (17.1 to 17.9 AU) when 4-chloro-1-butanol was present at 35 ppm. 2,6-dichloro-4-(2,4,6-triphenyl-1-pyridinio)phenolate (dye 2 – blue) showed a small decrease in fluorescence when 1-bromobutane was present at 35 ppm (20.4 to 19.6 AU) and a larger decrease in fluorescence (20.4 to 16.8 AU) when 4-chloro-1-butanol was present at 35 ppm. 1-(4-hydroxyphenyl)-2,4,6-triphenylpyridinium hydroxide inner salt (dye 3 - pink) showed a decrease (23.6 to 20.1 AU) in fluorescence when 1-bromobutane was present at 35 ppm and a smaller decrease in fluorescence (23.6 to 22.6 AU) when 4-chloro-1-butanol was present at 35 ppm.

The data presented in this section failed to show a significant correlation between the presence of 1-bromobutane and 4-chloro-1-butanol and changes in the fluorescent response of the dye. Some of the data showed decreases in fluorescence in response to the presence of the two alkylating agents but the magnitude of the decreases were small and to produce a reliable sensor system it is desirable to have more significant changes in the parameter being measured.

Changes in the appearance of the dye resulting from alkylation were far more apparent to the eye than by using fluorescence detection. The conclusion from this section of work was that fluorescence spectroscopy does not represent a particularly sensitive or reproducible measurement technique for alkylation of the three dyes 2,6-diphenyl-4-(2,4,6-triphenyl-1-pyridinio)phenolate, 2,6-dichloro-4-(2,4,6-triphenyl-1-pyridinio)phenolate and 1-(4-hydroxyphenyl)-2,4,6-triphenylpyridinium hydroxide inner salt.

5.3.3 Use of UV-vis spectroscopy to measure changes in dye absorption in response to the addition of alkylating agent.

The UV-vis absorbance spectra were recorded for the three dyes in the presence of 4-chloro-1-butanol and 1-bromobutane. Results are presented in figures 5.15 – 5.17.

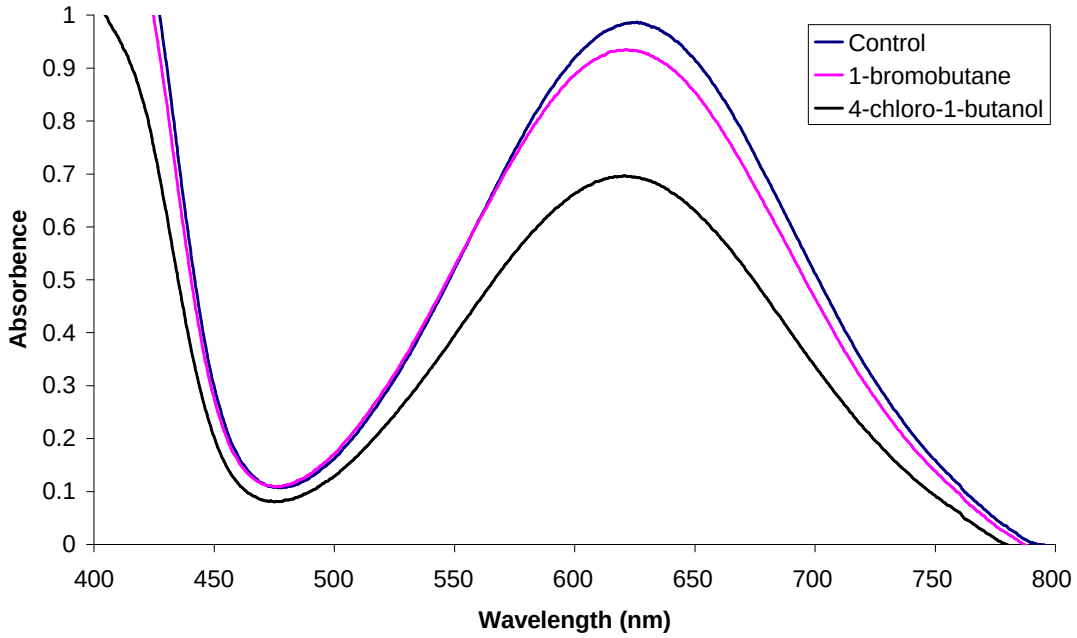

Figure 5.15. Changes in absorbance of 2,6-diphenyl-4-(2,4,6-triphenyl-1-pyridinio)phenolate at 200 µM (blue) in response to the presence of 50 ppm of 1-bromobutane (pink) and 4-chloro-1-butanol (black).

The control sample of 2,6-diphenyl-4-(2,4,6-triphenyl-1-pyridinio)phenolate at 200 µM showed a maximum absorption of 0.986 AU. The maximum absorption in response to the addition of 50 ppm of 1-bromobutane changed to 0.933 AU and to 50 ppm of 4-chloro-1-butanol the maximum absorption changed to 0.695 AU.

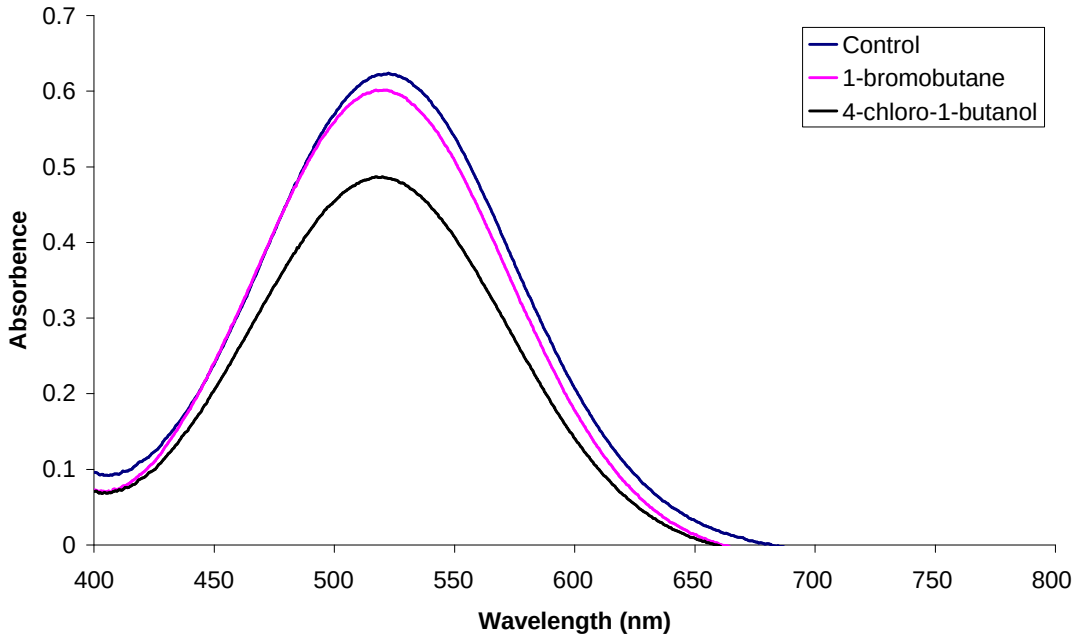

Figure 5.16. Changes in absorbance of 2,6-dichloro-4-(2,4,6-triphenyl-1-pyridinio)phenolate (blue) in response to the presence of 50 ppm of 1-bromobutane (pink) and 4-chloro-1-butanol (black).

The control sample of 2,6-dichloro-4-(2,4,6-triphenyl-1-pyridinio)phenolate at 200 µM showed a maximum absorption of 0.624 AU. The maximum absorption in response to the addition of 50 ppm of 1-bromobutane changed to 0.602 AU and in response to the addition of 50 ppm of 4-chloro-1-butanol changed to 0.486 AU.

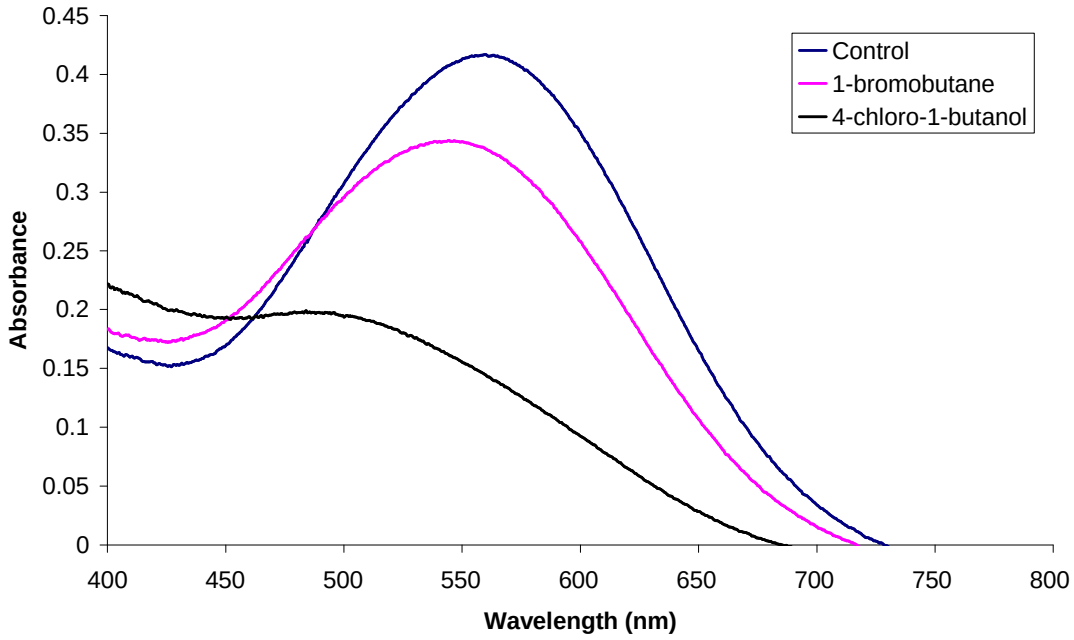

Figure 5.17. Changes in absorbance of 1-(4-hydroxyphenyl)-2,4,6-triphenylpyridinium hydroxide inner salt (blue) in response to the presence of 50 ppm of 1-bromobutane (pink) and 4-chloro-1-butanol (black).

The control sample of 1-(4-hydroxyphenyl)-2,4,6-triphenylpyridinium hydroxide inner salt at 200 µM showed a maximum absorption of 0.416 AU and changed in response to the addition of 50 ppm of 1-bromobutane to 0.343 AU and to 0.198 AU in response to the addition of 50 ppm of 4-chloro-1-butanol. This loss in absorption would suggest some alkylation of the dye by 1-bromobutane and 4-chloro-1-butanol.

The wavelength of the absorption maximum changed significantly for 1-(4-hydroxyphenyl)-2,4,6-triphenylpyridinium hydroxide inner salt. The control sample maximum was at 559.5 nm where as for 1-bromobutane and 4-chloro-1-butanol it was found at 541.5 nm and 480.5 nm respectively.

This significant change in the wavelength of the absorption maximum for 1-(4-hydroxyphenyl)-2,4,6-triphenylpyridinium hydroxide inner salt suggests a solvatochromic change is taking place alongside alkylation.

To try and detect a solvatochromic effect and therefore help confirm whether changes in absorbance were due to alkylation of the dye rather than the aforementioned solvatochromic effect, the dyes under normal circumstances were compared to dye samples where cyclohexane was present at 25 ppm. 25 ppm was selected because it is a concentration around which a pharmaceutical company would look for the presence of alkylating agents. Cyclohexane was chosen because of its similarity in size and solubility to 1-bromobutane and 4-chloro-1-butanol.

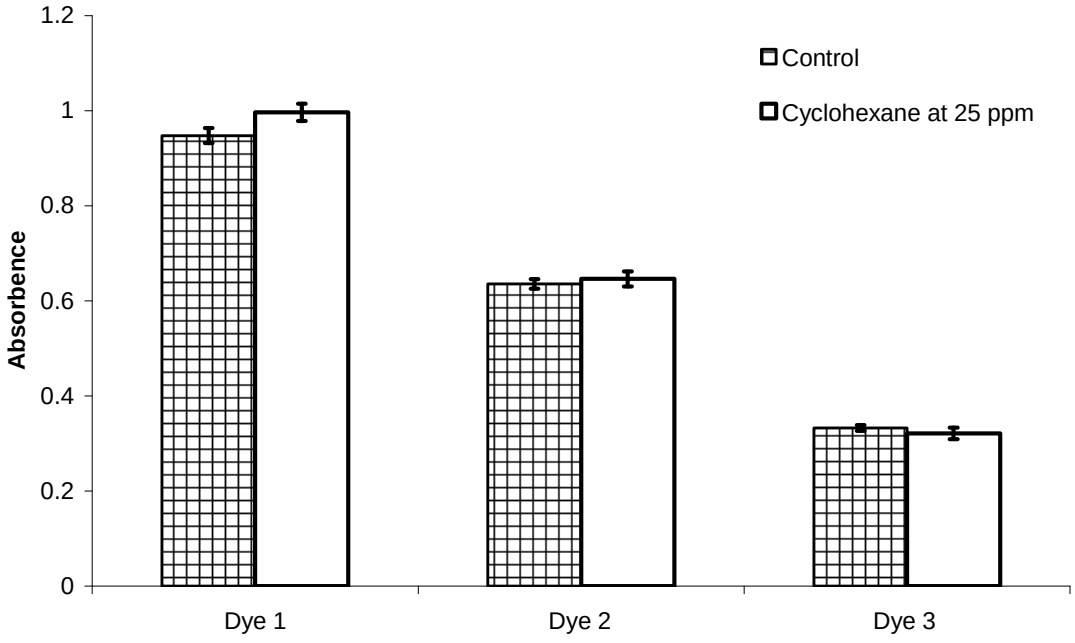

Figure 5.18. Changes in absorbance for all three dyes in response to the addition of 25 ppm of cyclohexane.

For 2,6-diphenyl-4-(2,4,6-triphenyl-1-pyridinio)phenolate the presence of cyclohexane at 25 ppm caused an increase from the control value of 0.945 to 0.996 AU. For 2,6-dichloro-4-(2,4,6-triphenyl-1-pyridinio)phenolate the presence of cyclohexane at 25 ppm caused an increase from the control value of 0.636 to 0.646 AU. For 1-(4-hydroxyphenyl)-2,4,6-triphenylpyridinium hydroxide inner salt the presence of cyclohexane at 25 ppm caused a decrease from the control value of 0.333 to 0.321 AU.

Cyclohexane caused a slight increase in absorption for 2,6-diphenyl-4-(2,4,6-triphenyl-1-pyridinio)phenolate and 2,6-dichloro-4-(2,4,6-triphenyl-1-pyridinio)phenolate where as a slight decrease for 1-(4-hydroxyphenyl)-2,4,6-triphenylpyridinium hydroxide inner salt was observed.

The results help show that when a drop in absorbance is detected in response to the addition of 1-bromobutane or 4-chloro-1-butanol it can be said with confidence that the change is due to alkylation of the dye rather than a solvatochromic effect.

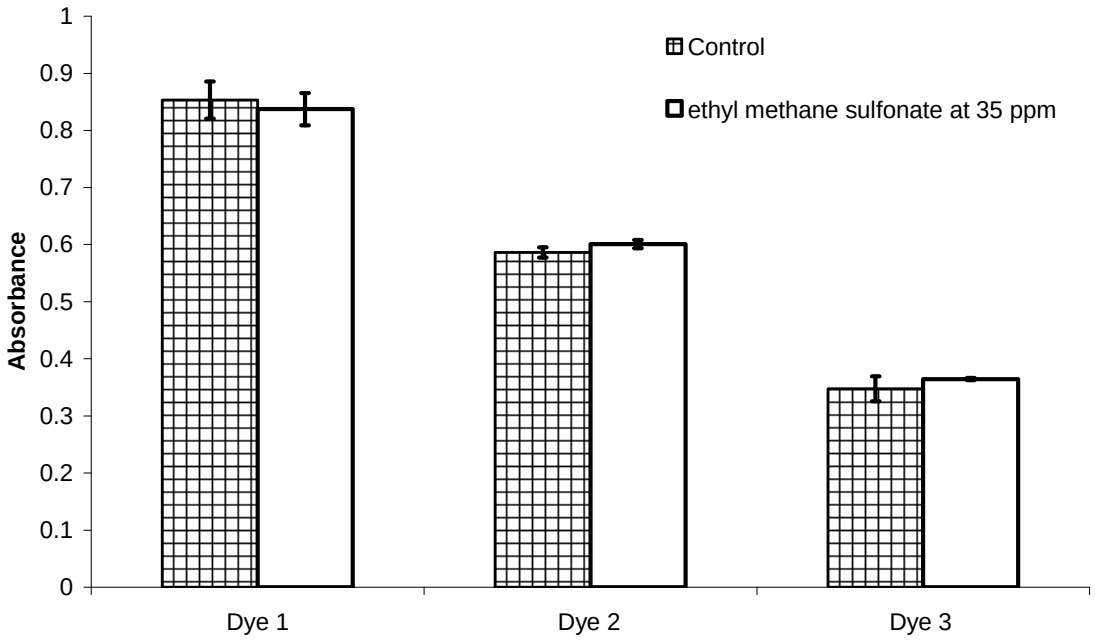

Figure 5.19. Changes in absorbance for all three dyes in response to the addition of 35 ppm of ethyl methane sulfonate.

For 2,6-diphenyl-4-(2,4,6-triphenyl-1-pyridinio)phenolate the presence of ethyl methane sulfonate at 35 ppm caused a decrease from the control value of 0.853 to 0.837 AU. For 2,6-dichloro-4-(2,4,6-triphenyl-1-pyridinio)phenolate the presence of ethyl methane sulfonate at 35 ppm caused an increase from the control value of 0.586 to 0.601 AU. For 1-(4-hydroxyphenyl)-2,4,6-triphenylpyridinium hydroxide inner salt the presence of ethyl methane sulfonate at 35 ppm caused an increase from the control value of 0.348 to 0.365 AU.

Ethyl methane sulfonate at 35 ppm caused a slight decrease in absorbance for 2,6-diphenyl-4-(2,4,6-triphenyl-1-pyridinio)phenolate and slight increases for 2,6-dichloro-4-(2,4,6-triphenyl-1-pyridinio)phenolate and 1-(4-hydroxyphenyl)-2,4,6-

triphenylpyridinium hydroxide inner salt. Ethyl methane sulfonate at 35 ppm was found to have no evidence of an alkylating effect.

The results presented in this section showed that the UV-vis spectrum of the dyes changed in the fashion shown by Figure 5.4 when Reichardt's dye was reacted with iodomethane. Therefore it can be suggested that alkylation was responsible for the change in dye appearance. The addition of cyclohexane as a similarly sized but non alkylating agent did not produce the response seen in the presence of alkylating agents. The change in absorbance was very small which also shows that the introduction of molecules of similar molecular weight and solubility at the 35 ppm level did not induce solvatochromic changes. Ethyl methane sulfonate was also tested in the way that 4-chloro-1-butanol and 1-bromobutane were and in all three dyes there was no evidence of alkylation.

5.3.4 Linearity of the assay and assay conditions.

In the previous section, the dyes were shown to undergo alkylation and present a change in absorbance when measured by UV-vis spectroscopy. In this section results are presented where a range of concentrations of alkylating agent are reacted with dye in order to see if a linear relationship can be established.

In the case of combinations of dye and alkylating agent that do not produce linear responses, the reaction conditions will be varied to determine whether a linear response to the presence of a particular alkylating agent can be established.

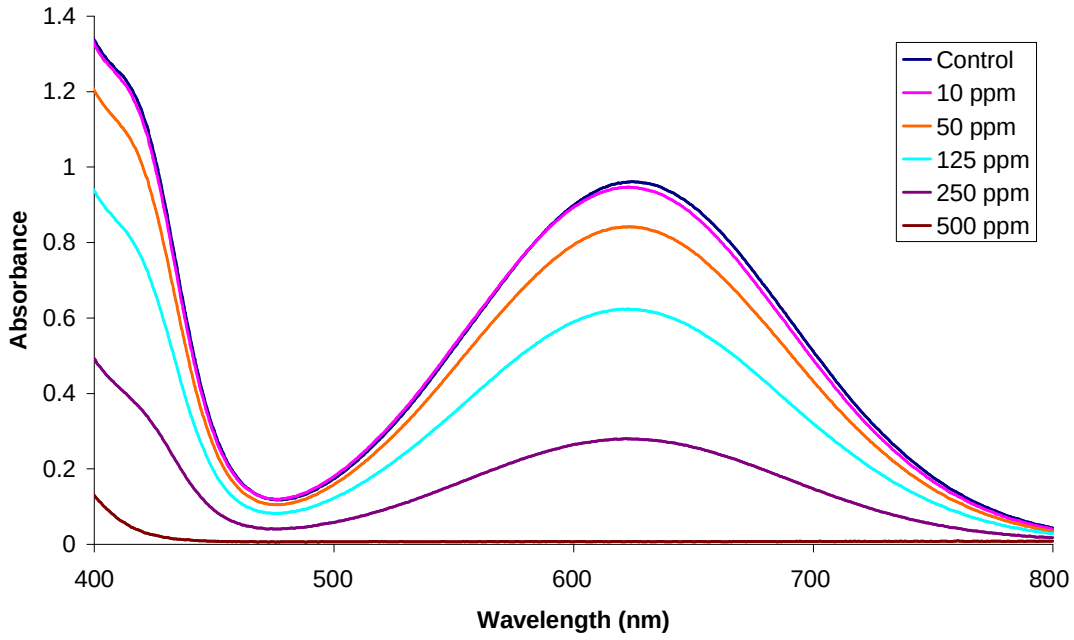

Figure 5.20. Changes in absorbance for 2,6-diphenyl-4-(2,4,6-triphenyl-1-pyridinio)phenolate in response to the addition of 4-chloro-1-butanol at 0 ppm (blue), 10 ppm (pink), 50 ppm (orange), 125 ppm (sky blue), 250 ppm (purple) and 500 ppm (brown).

The graph showed absorbance decreasing in a proportional manner to increasing concentration of 4-chloro-1-butanol. The absorption maxima can be taken and plotted to form the basis of a linear assay for 4-chloro-1-butanol using 2,6-diphenyl-4-(2,4,6-triphenyl-1-pyridinio)phenolate.

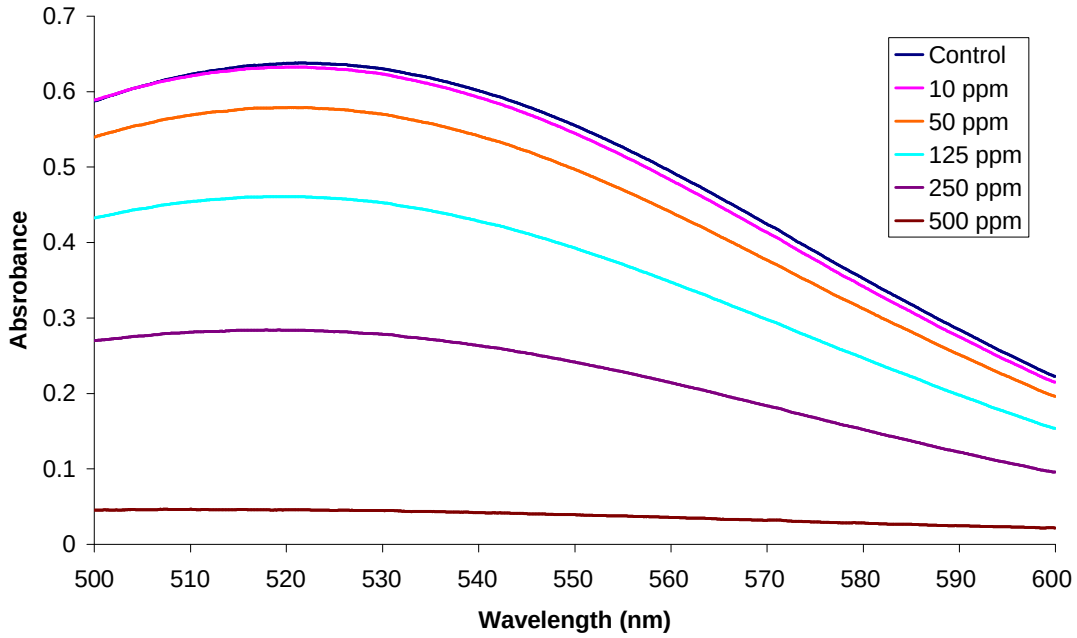

Figure 5.21. Changes in absorbance for 2,6-dichloro-4-(2,4,6-triphenyl-1-pyridinio)phenolate in response to the addition of 4-chloro-1-butanol at 0 ppm (blue), 10 ppm (pink), 50 ppm (orange), 125 ppm (sky blue), 250 ppm (purple) and 500 ppm (brown).

The graph showed absorbance decreasing in a proportional manner to increasing concentration of 4-chloro-1-butanol. Again, the absorption maxima can be taken and plotted to form the basis of a linear assay for 4-chloro-1-butanol using 2,6-dichloro-4-(2,4,6-triphenyl-1-pyridinio)phenolate.

The following plots show the absorption maxima on the y-axis and concentration of alkylating agent on the x-axis. The bars represent standard deviation and all experiments were carried out in triplicate.

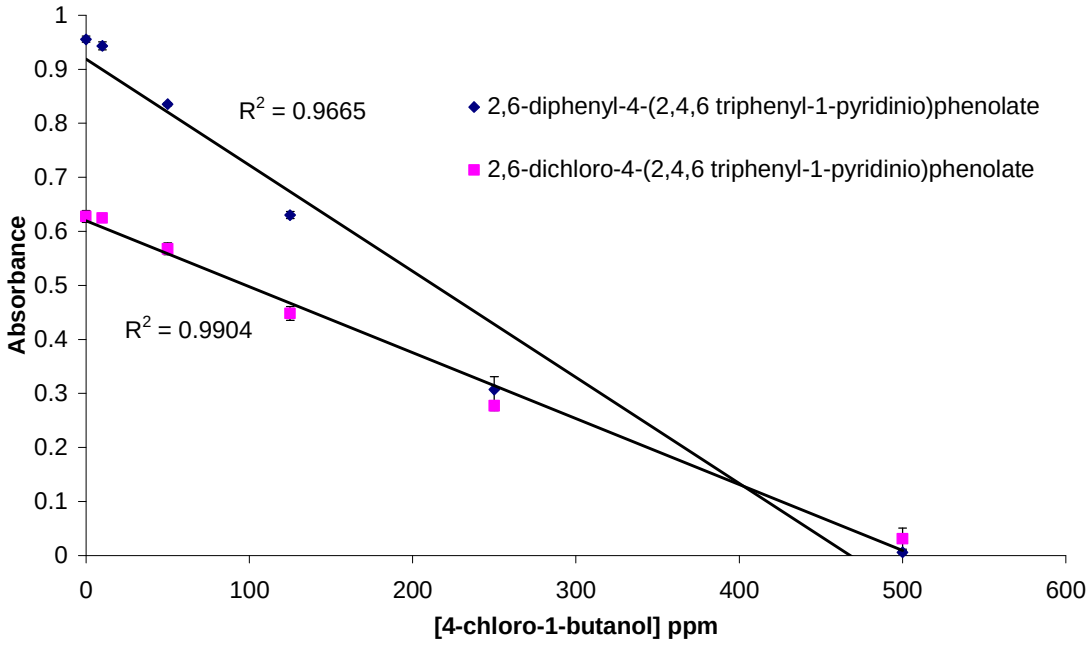

Figure 5.22. Changes in absorbance at 618 nm for 2,6-diphenyl-4-(2,4,6-triphenyl-1-pyridinio)phenolate (blue) and 2,6-dichloro-4-(2,4,6-triphenyl-1-pyridinio)phenolate (pink) in response to the addition of 4-chloro-1-butanol at the concentrations of 0 ppm, 10 ppm, 50 ppm, 125 ppm, 250 ppm and 500 ppm.

2,6-diphenyl-4-(2,4,6-triphenyl-1-pyridinio)phenolate showed good linearity with an R^2 value of 0.9665 but that value was affected by the last point at 500 ppm which lies beyond the range where 4-chloro-1-butanol induced partial bleaching of the dye. The graph showed the linear nature of the response but a lower and equally extensive range of concentrations must be subjected to similar experimentation in order to fully how linear the assay can become.

2,6-dichloro-4-(2,4,6-triphenyl-1-pyridinio)phenolate showed excellent linearity with an R^2 value of 0.9904. The figure showed that 2,6-diphenyl-4-(2,4,6-triphenyl-1-

pyridinio)phenolate was less sensitive to 4-chloro-1-butanol but that the dye can form the basis of a linear assay for that particular alkylating agent.

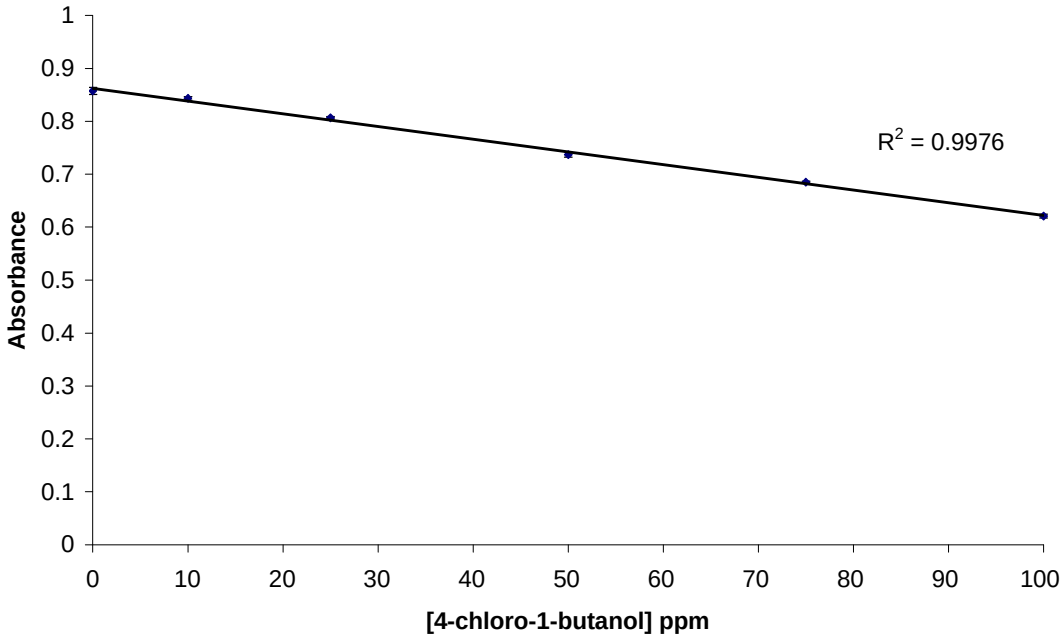

Figure 5.23. Changes in absorbance at 618 nm for 2,6-diphenyl-4-(2,4,6-triphenyl-1-pyridinio)phenolate in response to the addition of 4-chloro-1-butanol at the concentrations of 0 ppm, 10 ppm, 25 ppm, 50 ppm, 75 ppm and 100 ppm.

Over the range of 0 to100 ppm 2,6-diphenyl-4-(2,4,6-triphenyl-1-pyridinio)phenolate showed excellent linearity in response to the presence of 4-chloro-1-butanol with an R^2 value of 0.9976.

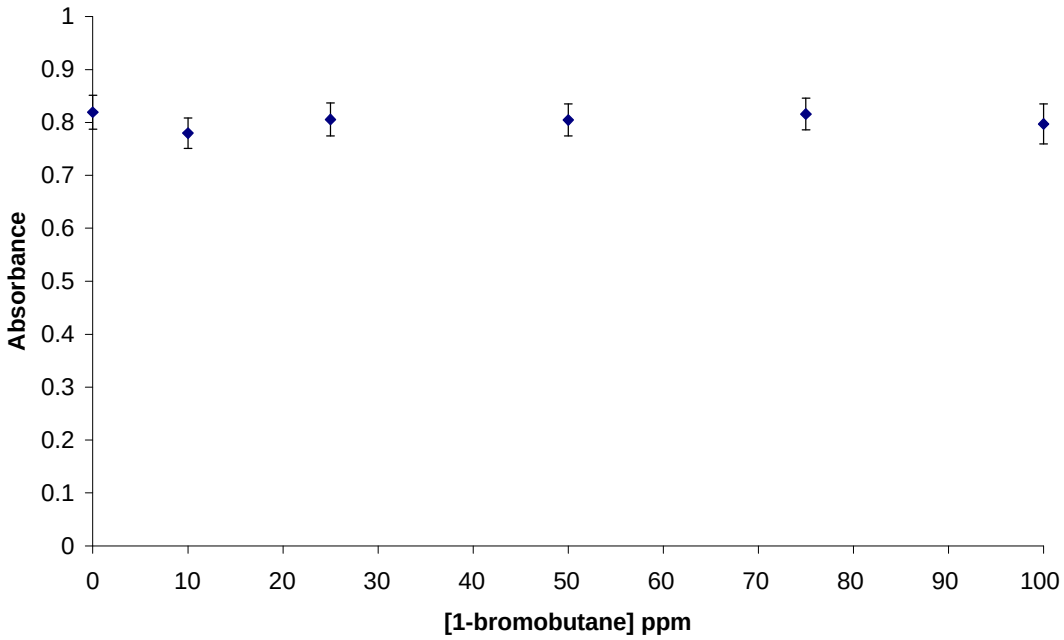

Figure 5.24. Changes in absorbance at 618 nm for 2,6-diphenyl-4-(2,4,6-triphenyl-1-pyridinio)phenolate in response to the addition of 1-bromobutane at the concentrations of 0 ppm, 10 ppm, 25 ppm, 50 ppm, 75 ppm and 100 ppm

Over the range of 0 to 100 ppm 2,6-diphenyl-4-(2,4,6-triphenyl-1-pyridinio)phenolate showed no discernable reactivity with 1-bromobutane. Bleaching of the dye did not take place and so 1-bromobutane did not alkylate the dye compound.

Over the range of 0 to 100 ppm 2,6-diphenyl-4-(2,4,6-triphenyl-1-pyridinio)phenolate showed no discernable reactivity with ethyl methane sulfonate. Bleaching of the dye did not take place and so ethyl methane sulfonate did not alkylate the dye compound.

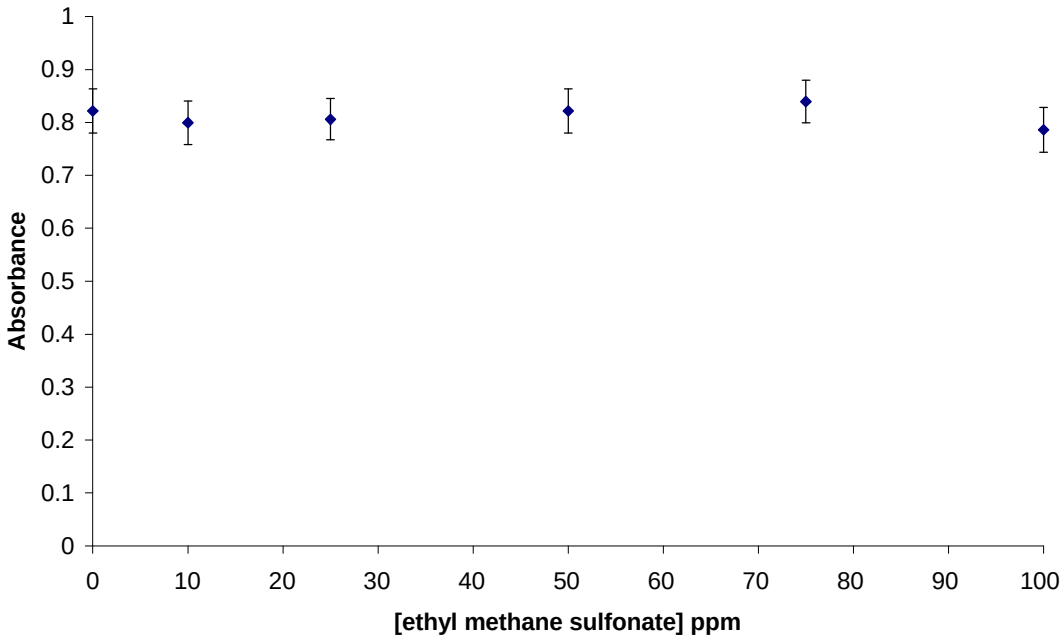

Figure 5.25. Changes in absorbance at 618 nm for 2,6-diphenyl-4-(2,4,6-triphenyl-1-pyridinio)phenolate in response to the addition of ethyl methane sulfonate at the concentrations of 0 ppm, 10 ppm, 25 ppm, 50 ppm, 75 ppm and 100 ppm

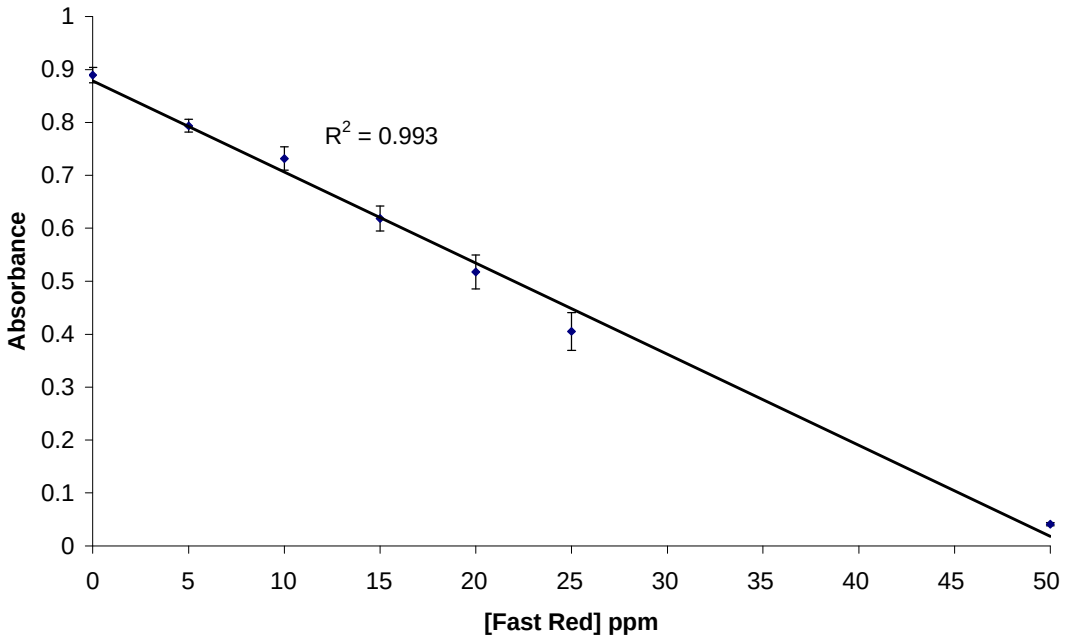

Figure 5.26. Changes in absorbance at 618 nm for 2,6-diphenyl-4-(2,4,6-triphenyl-1-pyridinio)phenolate in response to the addition of the diazonium compound Fast Red B at the concentrations of 0 ppm, 10 ppm, 25 ppm, 50 ppm, 75 ppm and 100 ppm.

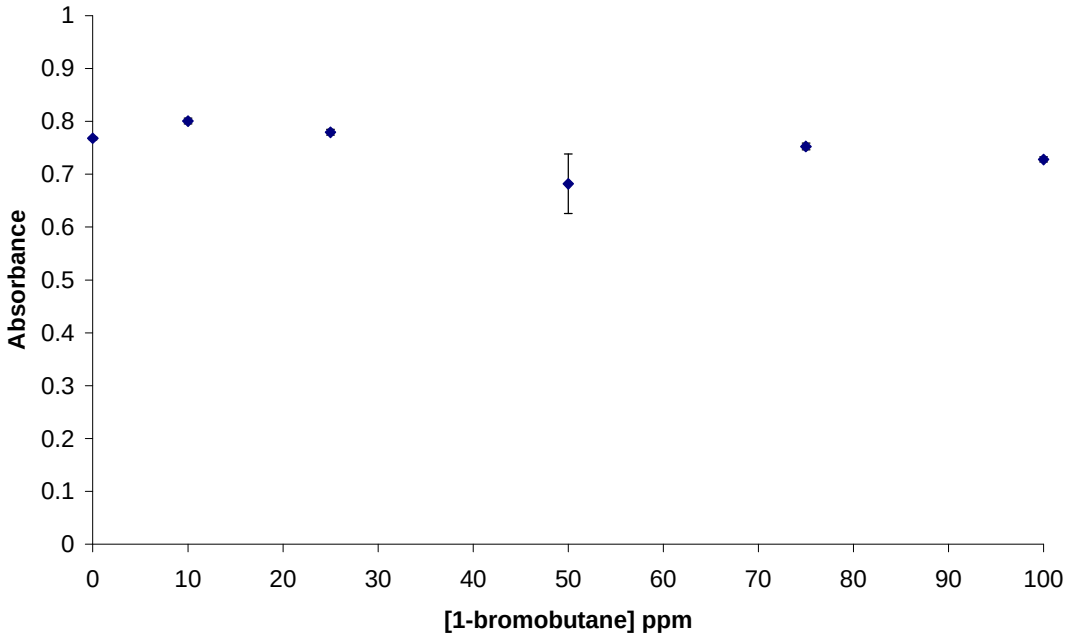

Figure 5.27. Changes in absorbance at 618 nm for 2,6-diphenyl-4-(2,4,6-triphenyl-1-pyridinio)phenolate in response to the addition of 1-bromobutane at the

concentrations of 0 ppm, 10 ppm, 25 ppm, 50 ppm, 75 ppm and 100 ppm at 85^{o}C for 4 hours.

Over the range of 0 to 100 ppm and after 4 hours at 85^{o}C, 2,6-diphenyl-4-(2,4,6-triphenyl-1-pyridinio)phenolate showed no discernable reactivity with 1-bromobutane. Bleaching of the dye did not take place and so 1-bromobutane did not alkylate the dye under these reaction conditions.

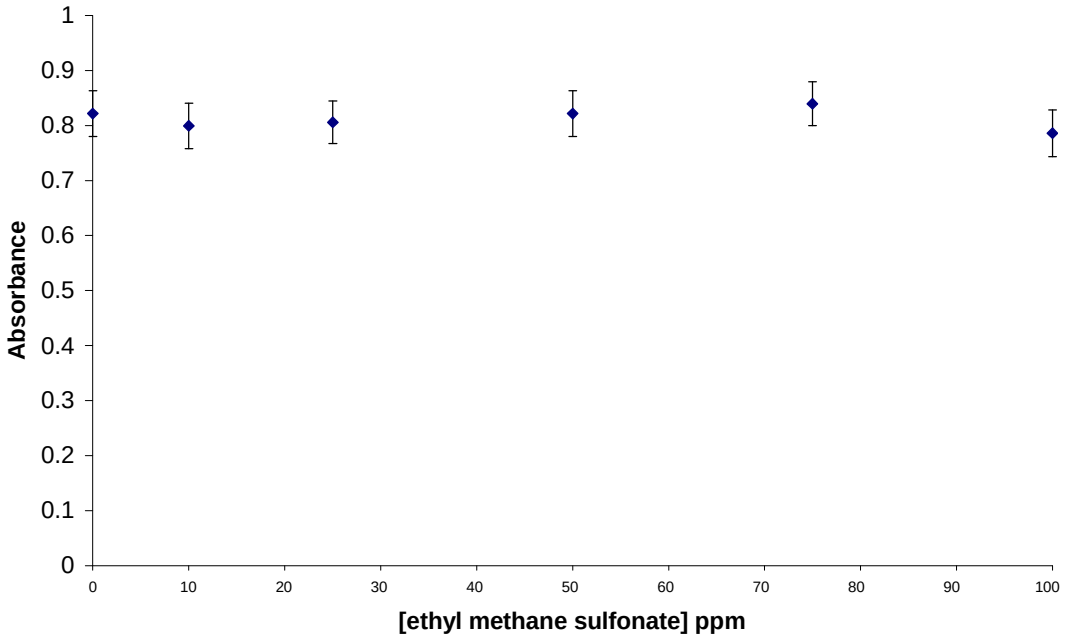

Figure 5.28. Changes in absorbance for 2,6-diphenyl-4-(2,4,6-triphenyl-1-pyridinio)phenolate in response to the addition of ethyl methane sulfonate at the concentrations of 0 ppm, 10 ppm, 25 ppm, 50 ppm, 75 ppm and 100 ppm at 85^{o}C for 4 hours.

Over the range of 0 to 100 ppm and after 4 hours at 85^{o}C, 2,6-diphenyl-4-(2,4,6-triphenyl-1-pyridinio)phenolate showed no discernable reactivity with ethyl methane

sulfonate. Bleaching of the dye did not take place and so ethyl methane sulfonate did not alkylate the dye under these reaction conditions.

Acetonitrile had been used as a solvent and had proven useful in the reactions between 2,6-diphenyl-4-(2,4,6-triphenyl-1-pyridinio)phenolate and 4-chloro-1-butanol and Fast Red B. These reactions showed excellent linearity over a range of concentrations that are industrially relevant without any heating or the use of any sort of catalyst. 1-Bromobutane and ethyl methane sulfonate would not react with the dye in acetonitrile under normal conditions or over a four hour time period at 85^{o}C.

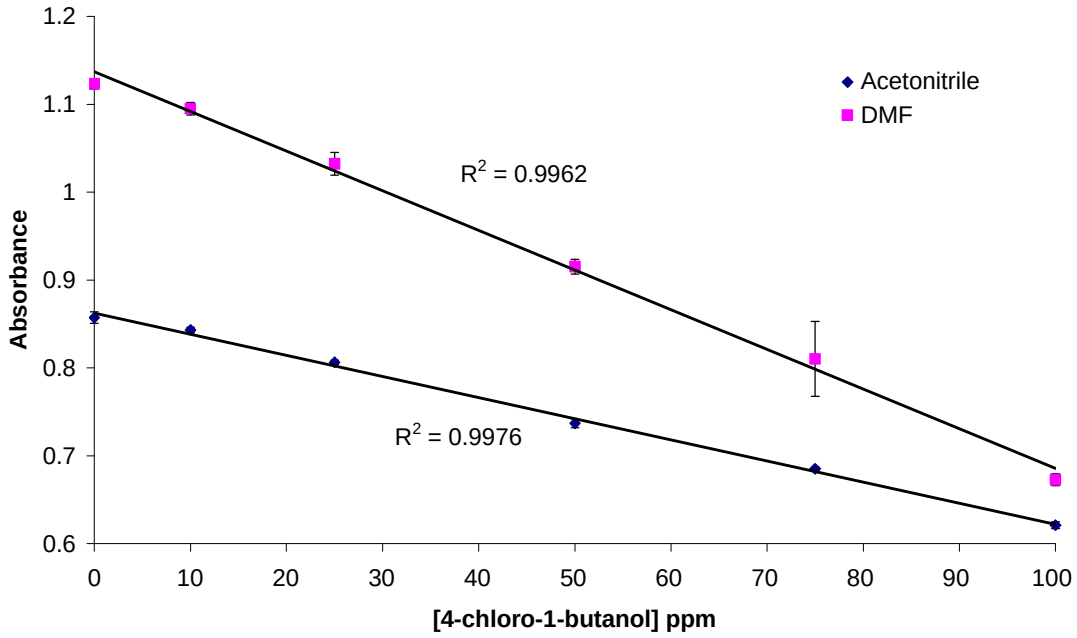

Figure 5.29. Changes in absorbance for 2,6-diphenyl-4-(2,4,6-triphenyl-1-pyridinio)phenolate in response to the addition of 4-chloro-1-butanol at the concentrations of 0 ppm, 10 ppm, 25 ppm, 50 ppm, 75 ppm and 100 ppm in acetonitrile (blue – 618 nm) in DMF (pink – 624 nm).

Both assays showed excellent linearity (R^2 values of 0.9976 in acetonitrile and 0.9962 in DMF) but the assay in DMF showed greater separation of the data points over the concentration range of 0 to 100 ppm. Acetonitrile was identified as a potentially useful solvent for this work because it has low activity in the UV-vis region and therefore would not attenuate the UV beam too heavily. DMF is well known as a good solvent for SN2 reactions and so it was also tested as a potential solvent.

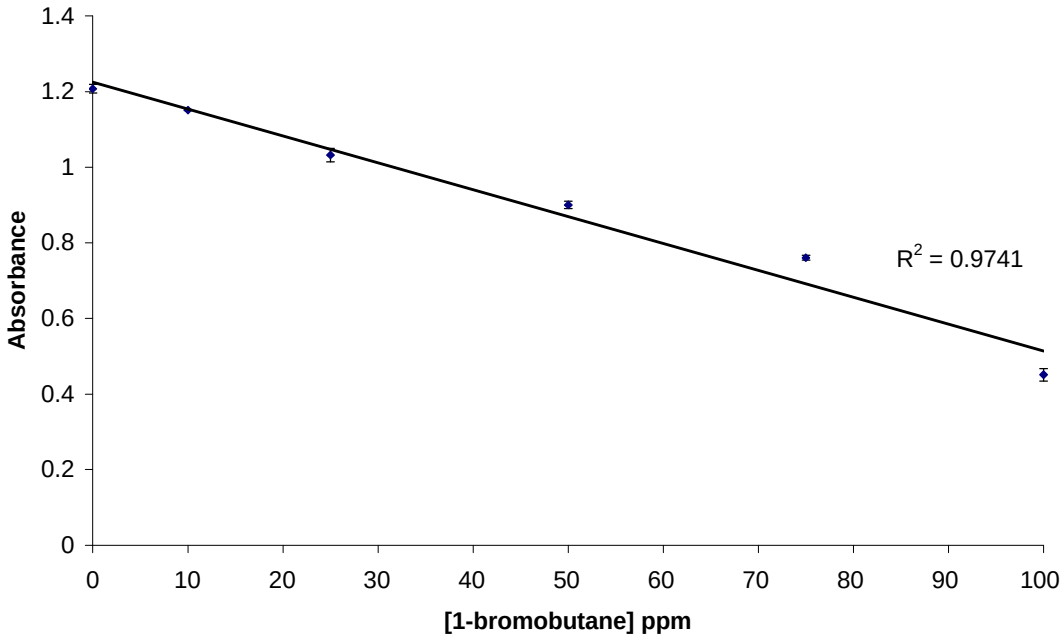

Figure 5.30. Changes in absorbance at 624 nm for 2,6-diphenyl-4-(2,4,6-triphenyl-1-pyridinio)phenolate in response to the addition of 1-bromobutane at the concentrations of 0 ppm, 10 ppm, 25 ppm, 50 ppm, 75 ppm and 100 ppm at 85^{o}C for 4 hours in DMF in the presence of the catalyst tetrabutylammonium iodide at 200 µM.

2,6-diphenyl-4-(2,4,6-triphenyl-1-pyridinio)phenolate showed good linearity in response to the presence of 1-bromobutane producing an R^2 value of 0.9741.

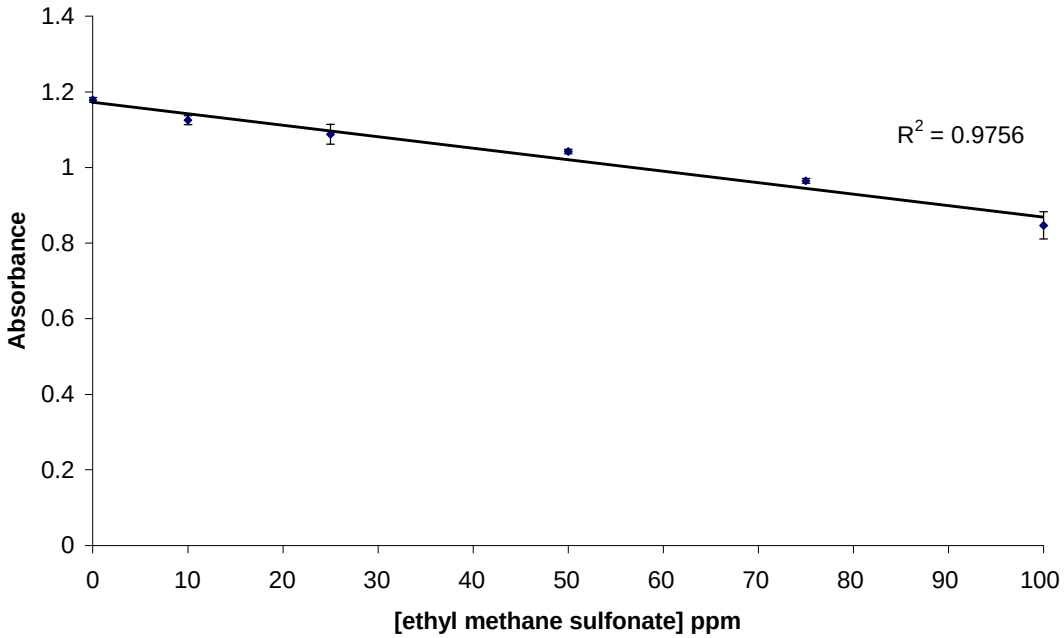

Figure 5.31. Changes in absorbance at 624 nm for 2,6-diphenyl-4-(2,4,6-triphenyl-1-pyridinio)phenolate in response to the addition of ethyl methane sulfonate at the concentrations of 0 ppm, 10 ppm, 25 ppm, 50 ppm, 75 ppm and 100 ppm at 85^{o}C for 4 hours in DMF in the presence of the catalyst tetrabutylammonium iodide at 200 µM.

2,6-diphenyl-4-(2,4,6-triphenyl-1-pyridinio)phenolate showed good linearity in response to the presence of 1-bromobutane producing an R^2 value of 0.9756.

It was then necessary to check if heat and the catalyst tetrabutylammonium iodide had affected the rate of the reaction and so the reactions were repeated but at 0, 50 and 100 ppm. Measurements were made where the samples were not heated, where catalyst was not added but heat was present and where catalyst and heat were both present.

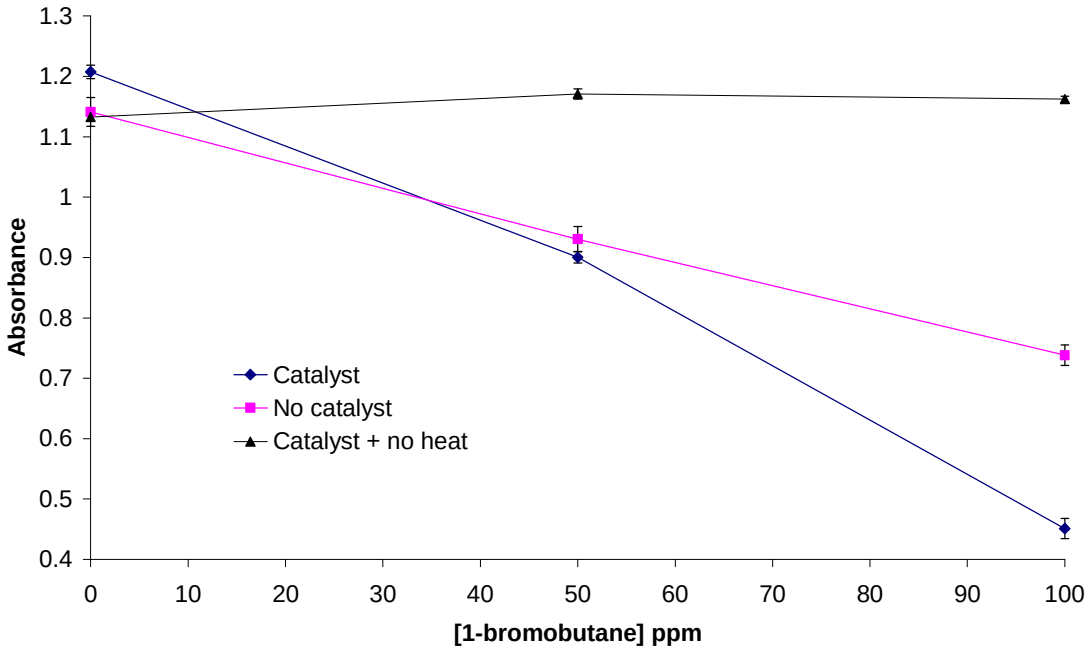

Figure 5.32. Changes in absorbance at 624 nm for 2,6-diphenyl-4-(2,4,6-triphenyl-1-pyridinio)phenolate in response to the addition of 1-bromobutane at the concentrations of 0 ppm, 50 ppm and 100 ppm at 85^{o}C for 4 hours in DMF in the presence of the catalyst tetrabutylammonium iodide at 200 µM (blue), with no catalyst present (pink) and with tetrabutylammonium iodide present for 4 hours but with no heat (black).

The graph showed no decrease in absorbance when 1-bromobutane was added at 50 or 100 ppm but not heated over the 4 hour time course (black). Absorbance decreased when the sample was heated at 85^{o}C for four hours (pink) but the absorbance decrease was greatest after four hours at 85^{o}C of in the presence of tetrabutylammonium iodide. Therefore it can be concluded that for 1-bromobutane the catalyst tetrabutylammonium iodide sped up the alkylation of 2,6-diphenyl-4-(2,4,6-triphenyl-1-pyridinio)phenolate.

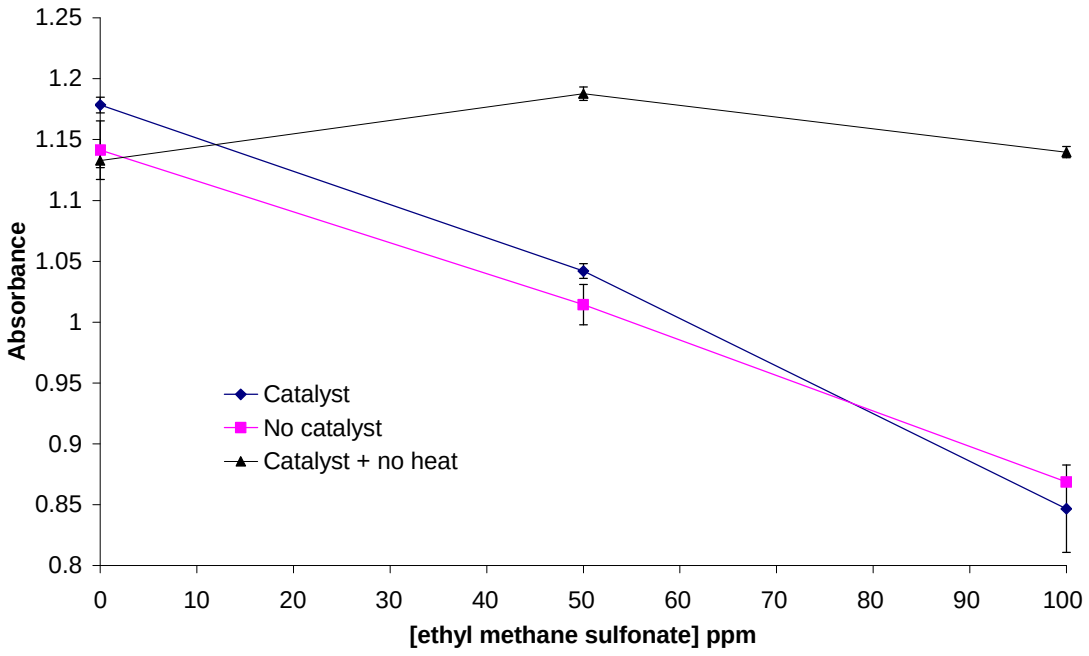

Figure 5.33. Changes in absorbance at 624 nm for 2,6-diphenyl-4-(2,4,6-triphenyl-1-pyridinio)phenolate in response to the addition of ethyl methane sulfonate at the concentrations of 0 ppm, 50 ppm and 100 ppm at 85^{o}C for 4 hours in DMF in the presence of the catalyst tetrabutylammonium iodide at 200 µM (blue), with no catalyst present (pink) and with tetrabutylammonium iodide present for 4 hours but with no heat (black).

A decrease in absorbance was not observed when ethyl methane sulfonate was added at 50 or 100 ppm but not heated over the 4 hour time course (black). Absorbance decreased when the sample was heated at 85^{o}C for four hours (pink) and absorbance decreased similarly after four hours at 85^{o}C of in the presence of tetrabutylammonium iodide. Therefore it can be concluded that for ethyl methane sulfonate, the catalyst tetrabutylammonium iodide did not have an effect on the alkylation of 2,6-diphenyl-4-(2,4,6-triphenyl-1-pyridinio)phenolate.

5.3.5 Reactions of Azo dyes with alkylating agents.

Reichardt's dye reacted well with 4-chloro-1-butanol and Fast Red B giving linear response to changes in concentration with high R^2 values. 1-Bromobutane and ethyl methane sulfonate showed linear responses in DMF after heating to 85^{o}C for four hours. Also, the addition of tetrabutylammonium iodide increased the reaction of 1-bromobutane and 2,6-diphenyl-4-(2,4,6-triphenyl-1-pyridinio)phenolate.

4-pheynlazophenol and Fat Brown B were tested with the alkylating agents to see if a linear assay could be produced, in particular for 1-bromobutane and ethyl methane sulfonate that did not rely on heating or the presence of catalyst.

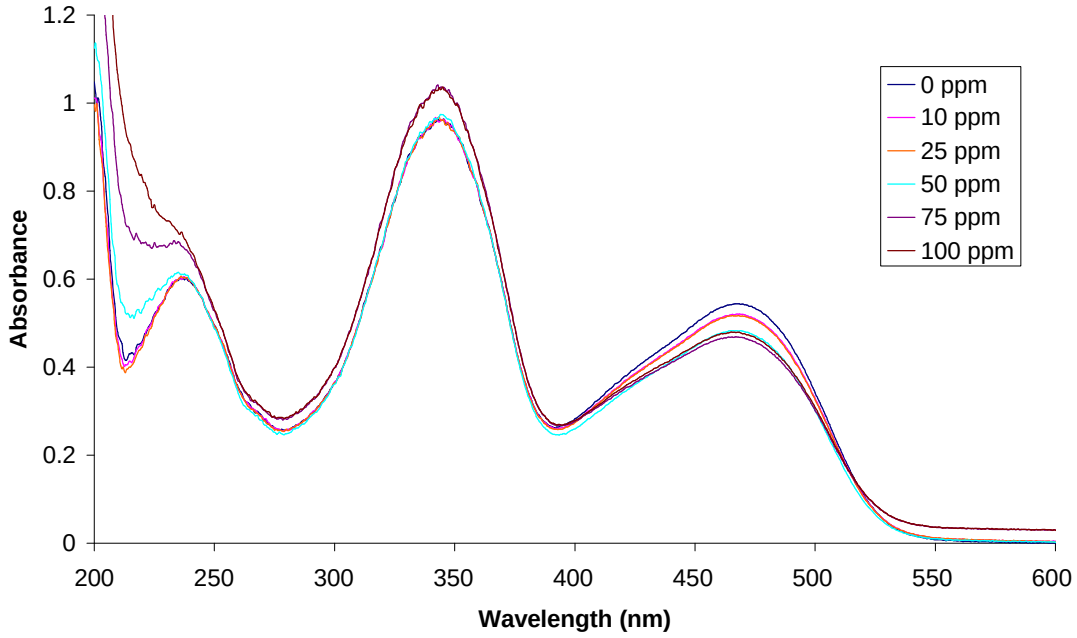

Figure 5.34. Changes in absorbance for 4-phenylazophenol in response to the addition of 4-chloro-1-butanol at 0 ppm, 10 ppm 25 ppm, 50 ppm, 75 ppm and 100 ppm.

The UV-vis spectra for 4-phenylazophenol did not present a linear decrease in absorbance in response to increasing concentrations of 4-chloro-1-butanol like Reichardt's dye.

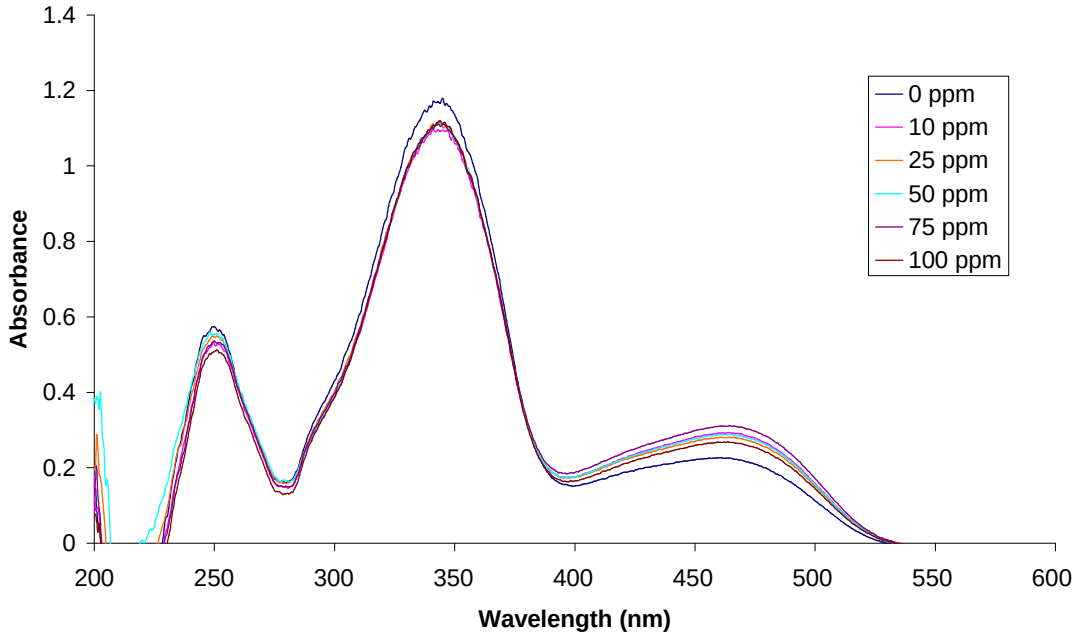

Figure 5.35. Changes in absorbance for 4-Phenylazophenol in response to the addition of 1-bromobutane at 0 ppm, 10 ppm, 25 ppm, 50 ppm, 75 ppm and 100 ppm

The UV-vis spectra for 4-phenylazophenol did not present a linear decrease in absorbance in response to increasing concentrations of 1-bromobutane like Reichardt's dye had displayed. The changes in absorbance did not follow step with the concentration increases and so 4-phenylazophenol was not be tested further.

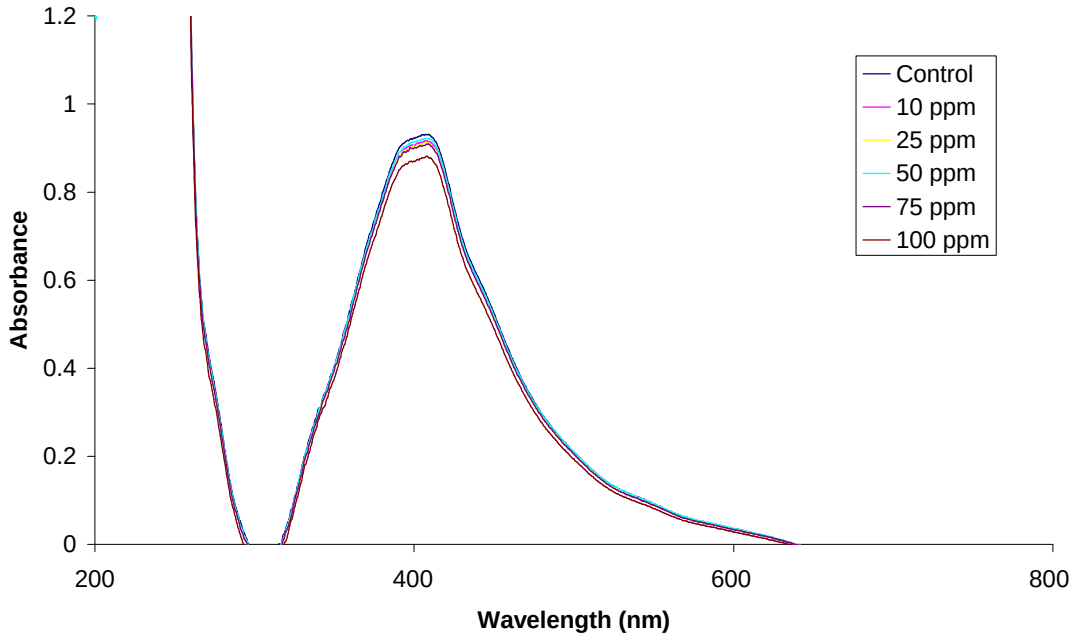

Figure 5.36. Changes in absorbance for Fat Brown B in response to the addition of 1-Bromobutane at 0 ppm, 10 ppm 25 ppm, 50 ppm, 75 ppm and 100 ppm

The UV-vis spectra for Fat Brown B did not present a linear decrease in absorbance in response to increasing concentrations of 1-bromobutane like Reichardt's dye had. The changes in absorbance were not in step with the changes in concentration of 1-bromobutane and the separations between absorption maxima were very small in comparison to other changes observed in this study.

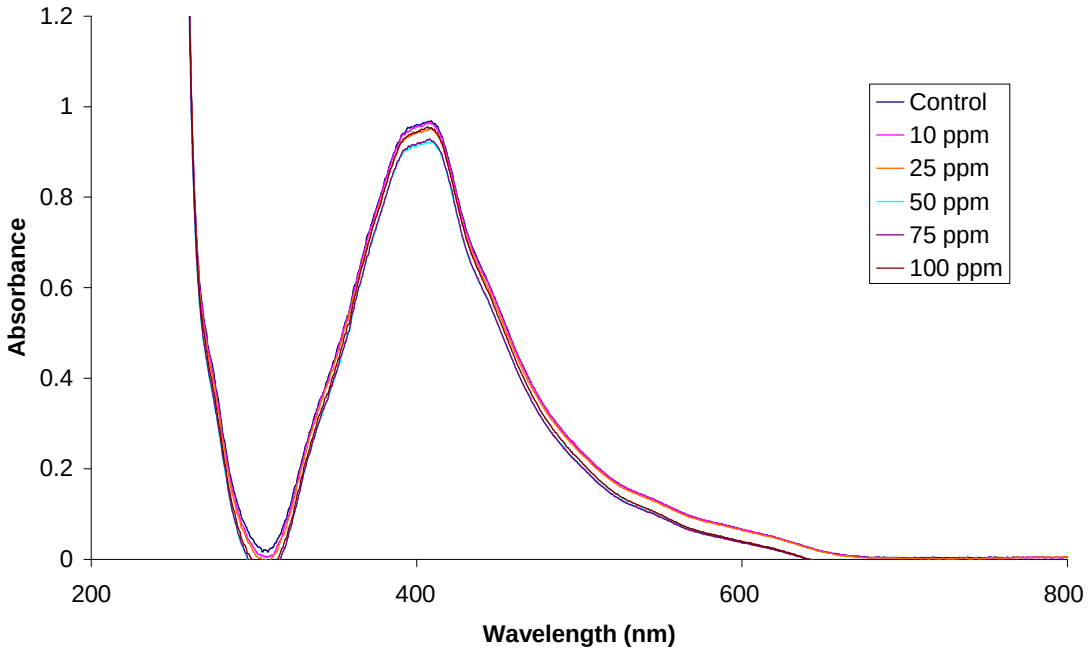

Figure 5.37. Changes in absorbance for Fat Brown B in response to the addition of ethyl methane sulfonate at 0 ppm, 10 ppm 25 ppm, 50 ppm, 75 ppm and 100 ppm.

The UV-vis spectra for Fat Brown B did not present a linear decrease in absorbance in response to increasing concentrations of ethyl methane sulfonate like Reichardt's dye. The changes in absorbance were not in step with the changes in concentration of ethyl methane sulfonate and the separation between absorption maxima was also very small.

The azo dyes 4-phenylazophenol and Fat Brown B were found to be unsuitable for the UV-vis spectrophotometric detection of alkylation and work with the two compounds was terminated at this point.

5.3.6 NMR spectroscopy on the reactions between 2,6-diphenyl-4-(2,4,6-triphenyl-1-pyridinio)phenolate and the alkylating agents 4-chloro-1-butanol and ethyl methane sulfonate

Confirmation of the products of the reaction was necessary to ensure that it was indeed alkylation of the dye that was responsible for the bleaching. It was known from the paper by Reichardt *et al.,* 1992 that a decrease in the UV absorption maximum for Reichardt's dye was observed when the dye was alkylated by iodomethane. As shown in the results section of this chapter, the decrease in the absorption maximum was observed when Reichardt's dye was reacted with the alkylating agents used in this study. The objective of this study is to produce a sensor for industrial implementation. Therefore it was prudent practice to carry out NMR spectroscopy in order to confirm the products of the reaction.

4-chloro-1-butanol and ethyl methane sulfonate were the two alkylating agents of most industrial importance and therefore their reactions with 2,6-diphenyl-4-(2,4,6-triphenyl-1-pyridinio)phenolate were investigated.

2,6-diphenyl-4-(2,4,6-triphenyl-1-pyridinio)phenolate

An NMR spectrum of Reichardt'sdye was recorded and is presented in figure 5.38.

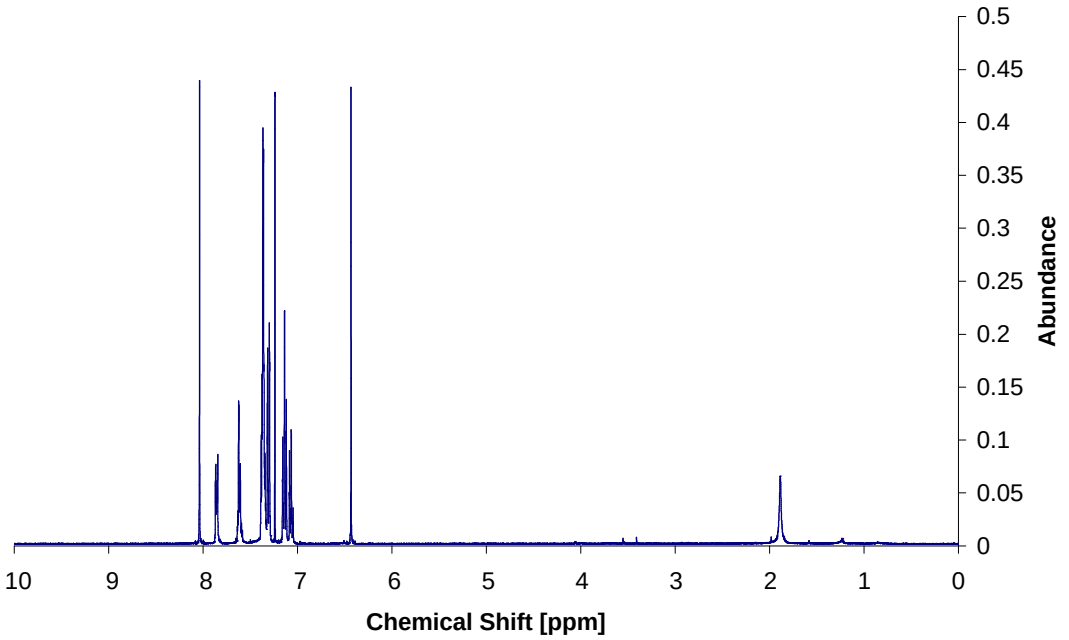

Figure 5.38. ^{1}H NMR spectrum of 2,6-diphenyl-4-(2,4,6-triphenyl-1-pyridinio)phenolate in deuterated chloroform .

All the peaks owing to the dye were seen in the region between 6.0 and 9.0 ppm. With proton NMR this is the region in which phenyl groups are seen and with the dye being composed entirely of phenyl groups this was the region where its characteristic peaks were seen.

4-chloro-1-butanol and 2,6-diphenyl-4-(2,4,6-triphenyl-1-pyridinio)phenolate.

4-chloro-1-butanol and 2,6-diphenyl-4-(2,4,6-triphenyl-1-pyridinio)phenolate were reacted together in methanol. The product of the reaction was isolated and then investigated with NMR spectroscopy by dissolving in deuterated DMF.

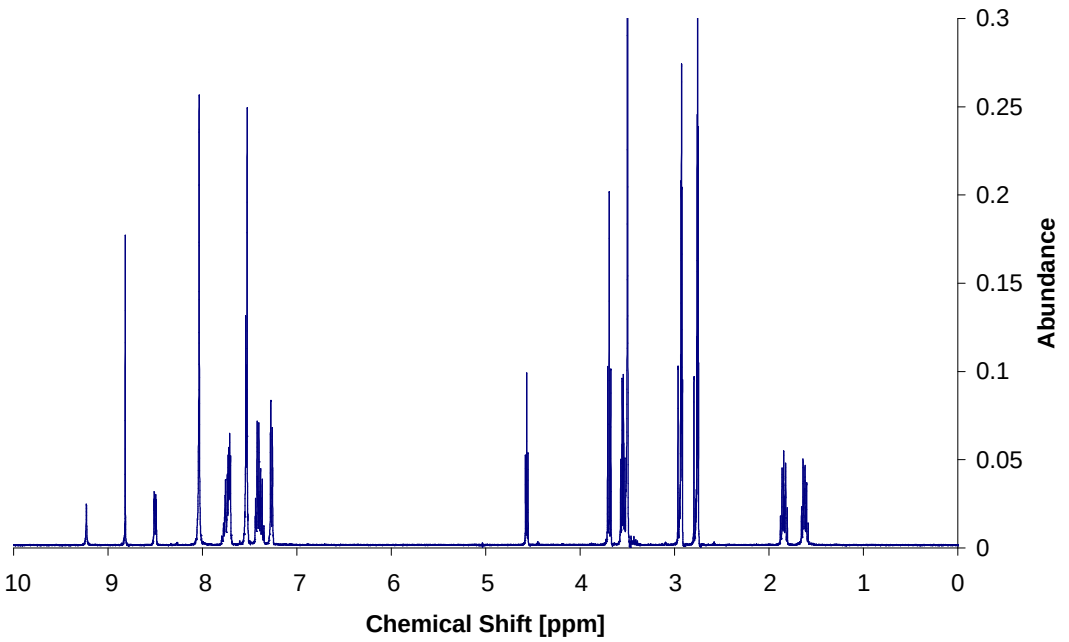

Figure 5.39. ^{1}H NMR spectrum of the product from the reaction between 4-chloro-1-butanol and 2,6-diphenyl-4-(2,4,6-triphenyl-1-pyridinio)phenolate.

The peaks between 7 and 9.5 ppm belonged to the dye molecule because they were present in the phenyl region. Between 0 and 4.5 ppm the peaks from the 4 carbon chain added to the dye by 4-chloro-1-butanol were found. The two large peaks between 2.8 and 3 ppm were due to the solvent (DMF) and the large peak at approximately 3.5 ppm was due to water.

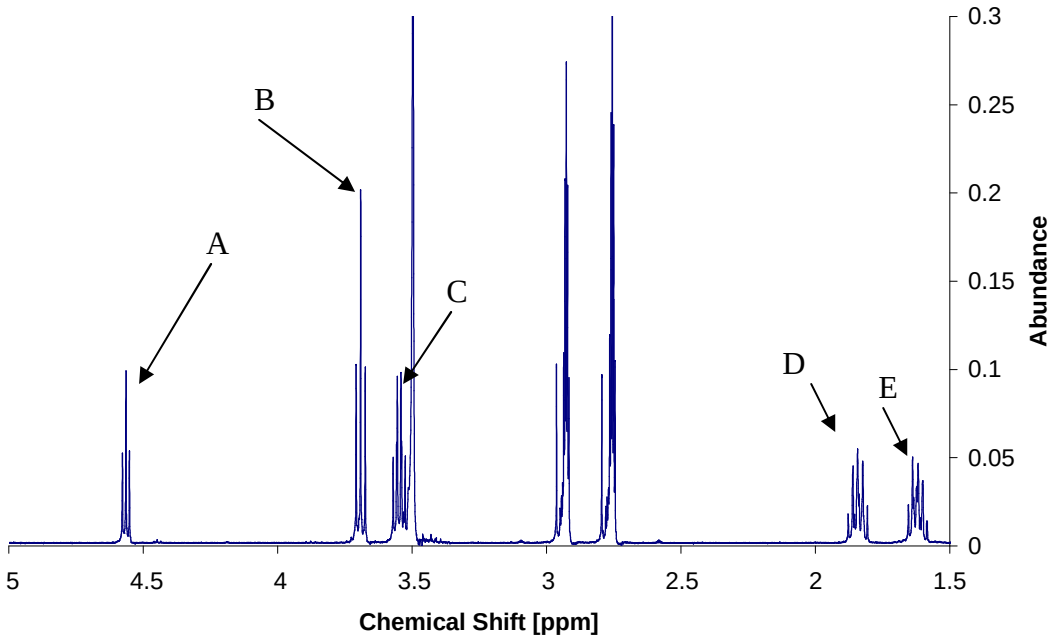

Figure 5.40. A zoomed in version of the previous ^{1}H NMR spectrum between 5 and 1.5 ppm from the product of the reaction between 4-chloro-1-butanol and 2,6-diphenyl-4-(2,4,6-triphenyl-1-pyridinio)phenolate.

As previously stated, the large peaks between 2.8 and 3 ppm were due to solvent (DMF) and the large peaks at 3.5 were due to water. The other five peaks labelled by arrows were due to the four carbon chain added to 2,6-diphenyl-4-(2,4,6-triphenyl-1-pyridinio)phenolate by 4-chloro-1-butanol. The integrals of the five labelled peaks were all very similar.

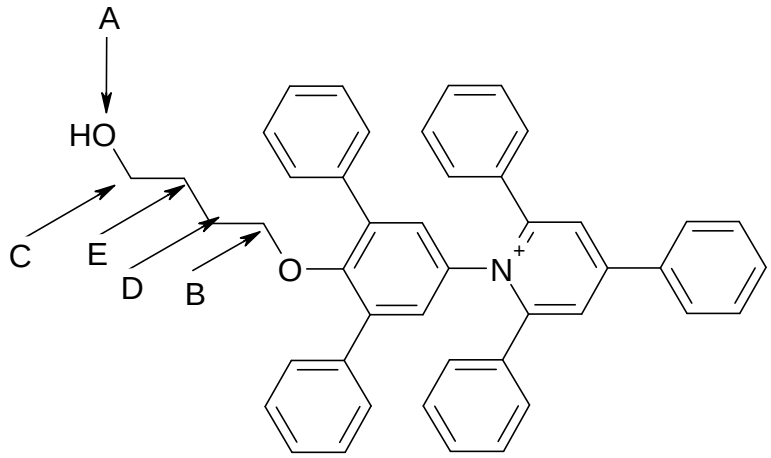

Figure 5.41. The alkylated product of the reaction between 4-chloro-1-butanol and 2,6-diphenyl-4-(2,4,6-triphenyl-1-pyridinio)phenolate. The arrows correspond to the peaks highlighted in Figure 5.40.

From the proton NMR spectra presented, peaks D and E cannot be identified with certainty but it can be said with absolute certainty that they are both due to the points of the molecule indicated by either arrows D and E. Both peaks are due to the CH_2 groups in the middle of the for carbon chain. Peak A is in the position expected of an OH group and is a triplet which is indicative of being next to a CH_2 group, peak B is a triplet which indicates it can only be next to a CH_2 and therefore it must be in the position indicated by arrow B and peak C is difficult to resolve but is not a triplet and is indicative of having a CH_2 on one side and an OH on the other.

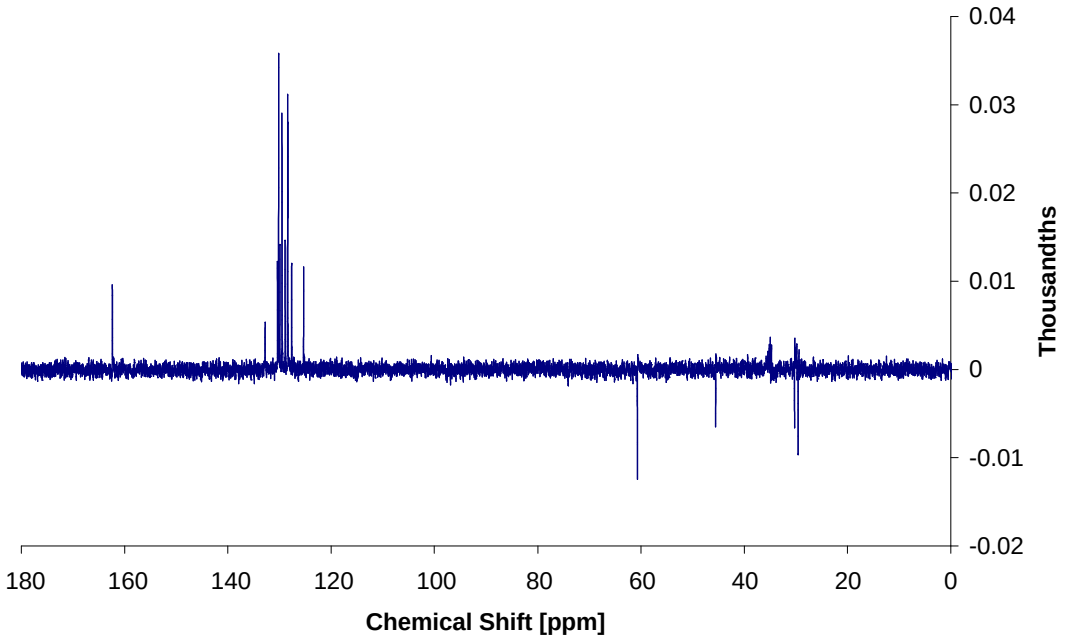

Figure 5.42. ^{13}C NMR spectrum from a dept 135 experiment on the product of 4-chloro-1-butanol and 2,6-diphenyl-4-(2,4,6-triphenyl-1-pyridinio)phenolate.

A dept 135 experiment eliminates the solvent peaks and produces a result where CH and CH_3 groups point upwards and CH_2 groups point downwards. From this spectrum the CH groups of the dye present in the region between 120 and 140 ppm were observed and four signals pointing downwards in the region of 20 to 60 ppm were seen, indicating the presence of four CH_2 groups.

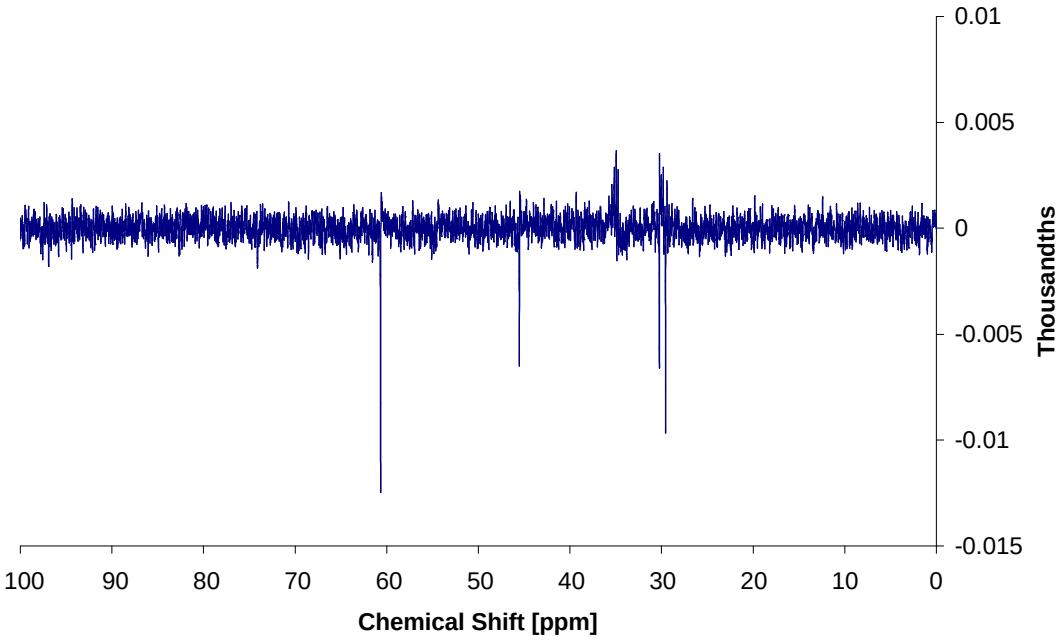

Figure 5.43. ^{13}C NMR spectrum from a dept 135 experiment on the product of 4-chloro-1-butanol and 2,6-diphenyl-4-(2,4,6-triphenyl-1-pyridinio)phenolate between 0 and 100 ppm..

This spectrum is a zoomed in view of the previous one and shows in greater detail the presence of the four peaks which helped confirm the presence of four CH_2 groups that were added to the dye molecule by alkylation.

Ethyl methane sulfonate and 2,6-diphenyl-4-(2,4,6-triphenyl-1-pyridinio)phenolate.

The reaction between 2,6-diphenyl-4-(2,4,6-triphenyl-1-pyridinio)phenolate and ethyl methane sulfonate was slower than the reaction between 2,6-diphenyl-4-(2,4,6-triphenyl-1-pyridinio)phenolate and 4-chloro-1-butanol and required heating up to

85°C over a four hour time course. Proton NMR was used to study the progress of the reaction in deuterated DMF and identify the products.

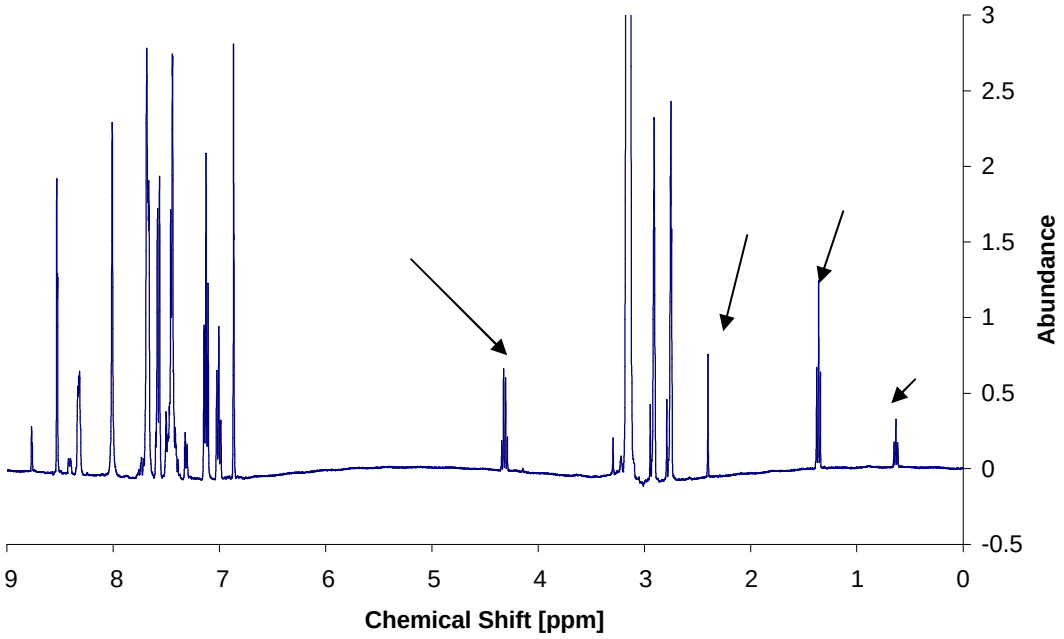

Figure 5.44. ^{1}HNMR spectrum five minutes after the beginning of the reaction between 2,6-diphenyl-4-(2,4,6-triphenyl-1-pyridinio)phenolate and ethyl methane sulfonate.

The spectrum showed the presence of the dye molecule between 6 and 9 ppm. This is the region where phenyl groups are apparent in ^{1}HNMR spectroscopy. The peaks owing to ethyl methane sulfonate and the beginnings of new peaks formed during the reaction were found between 0 and 4.5 ppm and are indicated by the arrows present. The two large peaks between 2.8 and 3.0 ppm were due to the solvent (DMF) and the large peak at approximately 3.1 ppm was due to water.

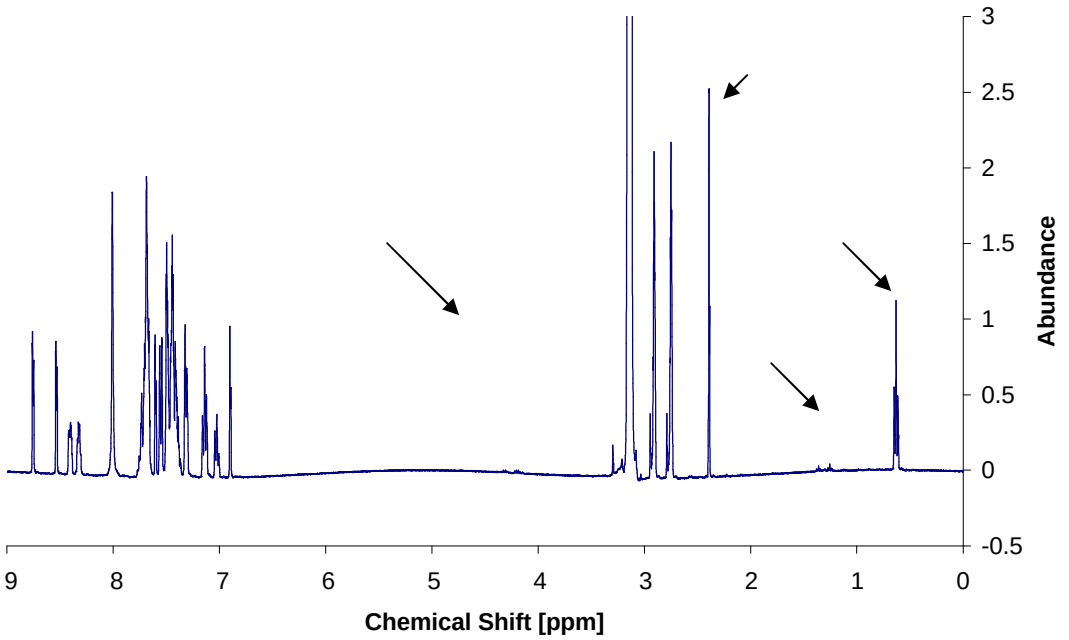

Figure 5.45. ^{1}H NMR spectrum four hours after the beginning of the reaction between 2,6-diphenyl-4-(2,4,6-triphenyl-1-pyridinio)phenolate and ethyl methane sulfonate.

This spectrum is from a time point when the reaction was complete. The arrows help to illustrate how the peaks in the region between 0 and 4.5 ppm changed during the course of the reaction. We saw the emergence of two peaks at approximately 0.6 and 2.4 ppm and the disappearance of two peaks at approximately 4.4 and 1.4 ppm.

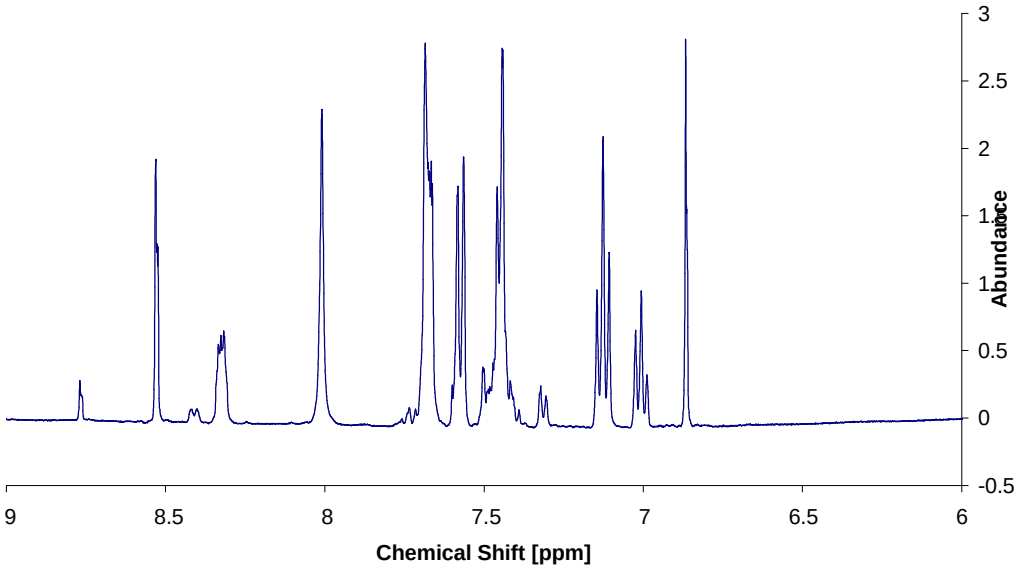

Figure 5.46. ^{1}H NMR spectrum five minutes after the beginning of the reaction between 2,6-diphenyl-4-(2,4,6-triphenyl-1-pyridinio)phenolate and ethyl methane sulfonate.

This proton NMR spectrum presents a zoomed in view of the phenyl region in which the dye spectrum was found. At the beginning of the reaction a series of sharp and well defined peaks can be seen.

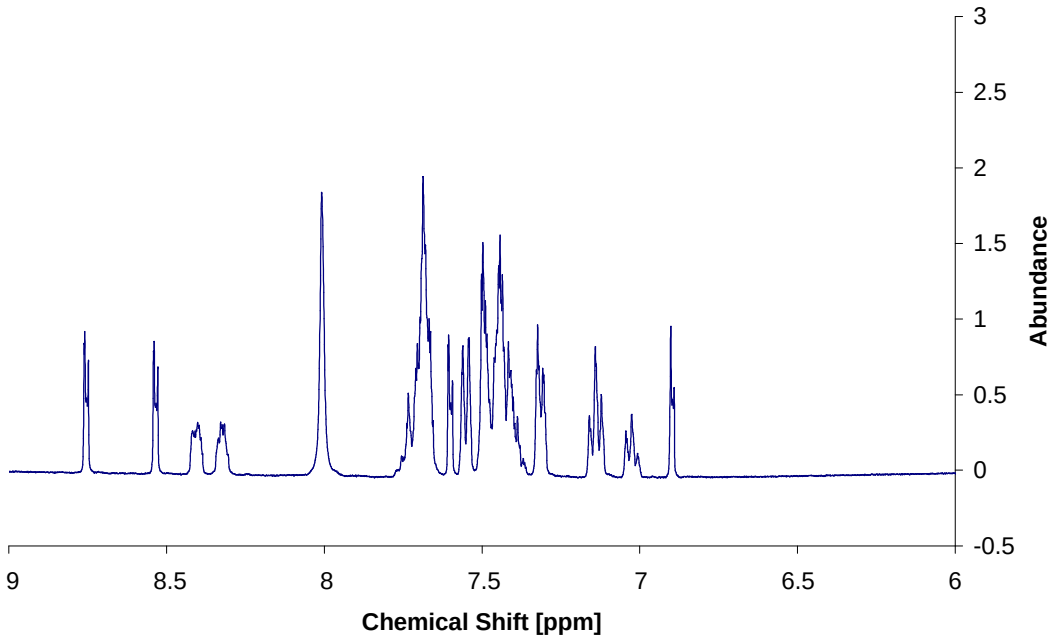

Figure 5.47. ^{1}H NMR spectrum four hours after the beginning of the reaction between 2,6-diphenyl-4-(2,4,6-triphenyl-1-pyridinio)phenolate and ethyl methane sulfonate.

This proton NMR spectrum presents a zoomed in view of the phenyl region in which the dye spectrum was found and at the end of the reaction it was found that the number of peaks had doubled whilst the integrals for the peaks had approximately halved. This doubling of the peaks and halving of the integrals was indicative of the formation of two species. In this case the production of alkylated dye was observed with NMR and the ratio of ethyl methane sulfonate and 2,6-diphenyl-4-(2,4,6-triphenyl-1-pyridinio)phenolate employed during the reaction meant that it ended with an approximate 50:50 ratio of alkylated and unalkylated product as there was only enough ethyl methane sulfonate used to alkylate half of the dye molecules present..

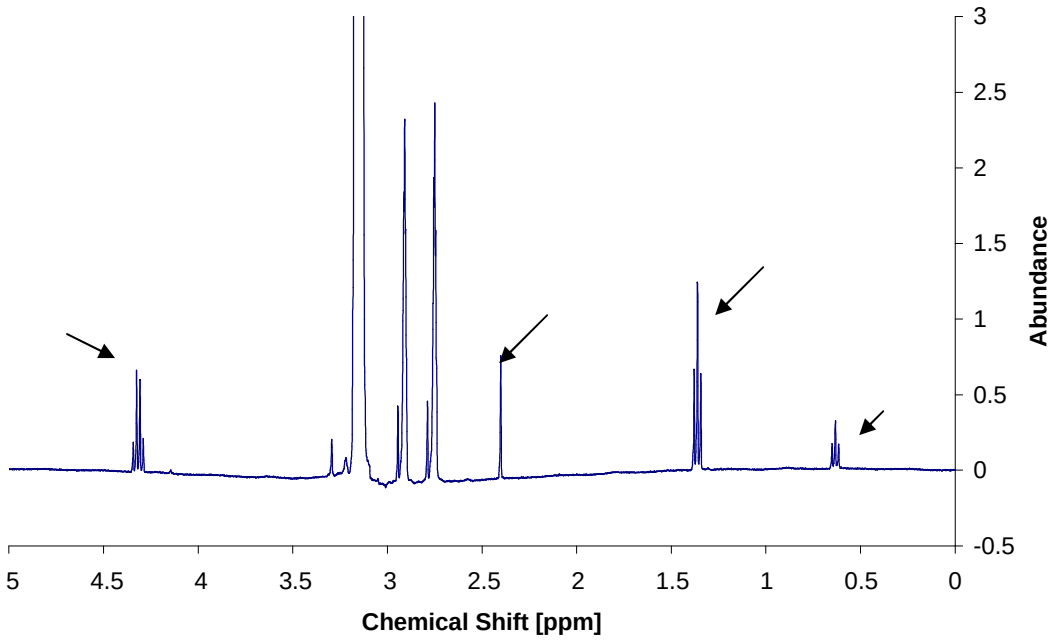

Figure 5.48. ^{1}H NMR spectrum five minutes after the beginning of the reaction between 2,6-diphenyl-4-(2,4,6-triphenyl-1-pyridinio)phenolate and ethyl methane sulfonate.

This spectrum showed the early stages of the reaction between 2,6-diphenyl-4-(2,4,6-triphenyl-1-pyridinio)phenolate and ethyl methane sulfonate and in this region four peaks have been highlighted.

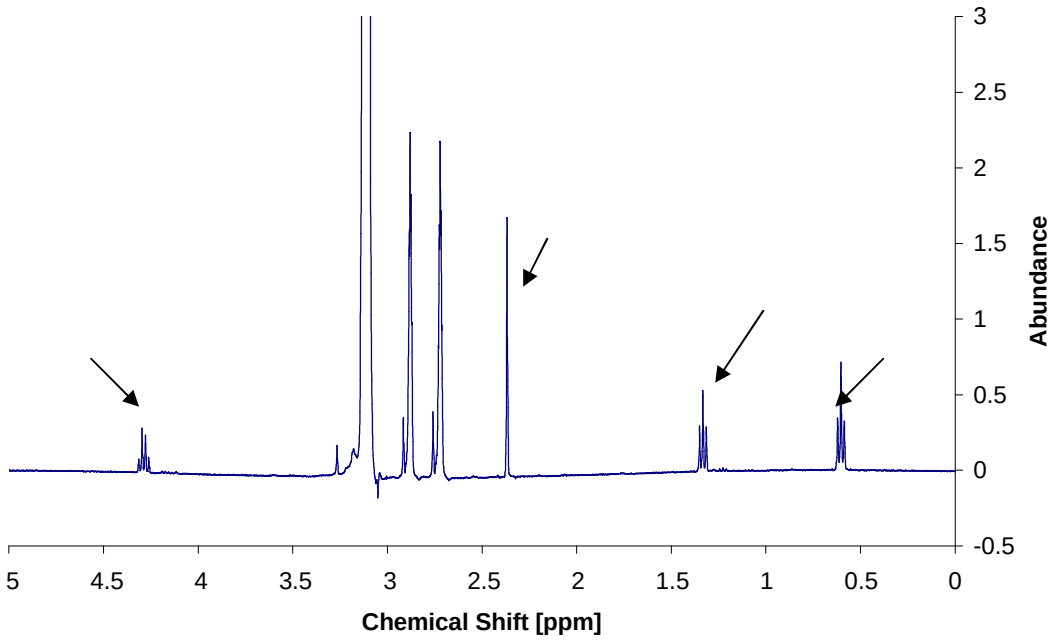

Figure 5.49. ^{1}H NMR spectrum one hour after the beginning of the reaction between 2,6-diphenyl-4-(2,4,6-triphenyl-1-pyridinio)phenolate and ethyl methane sulfonate.

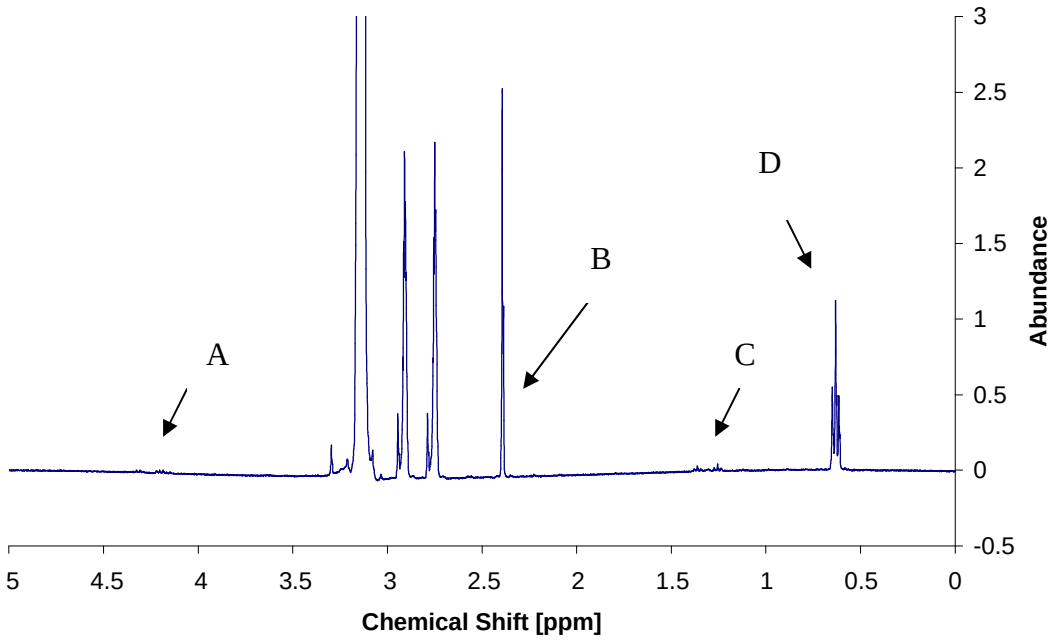

Figure 5.50. ^{1}H NMR spectrum four hours after the beginning of the reaction between 2,6-diphenyl-4-(2,4,6-triphenyl-1-pyridinio)phenolate and ethyl methane sulfonate.

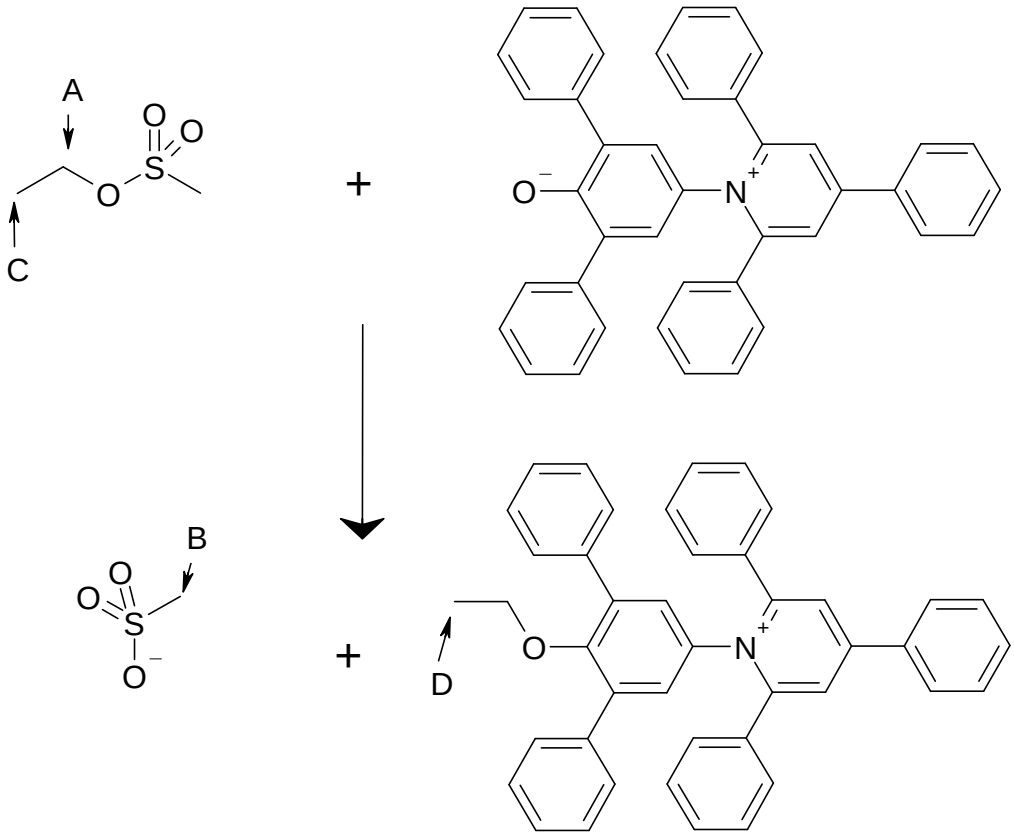

Figure 5.51. Ethyl methane sulfonate, 2,6-diphenyl-4-(2,4,6-triphenyl-1-pyridinio)phenolate and the products of their reaction. The labelled arrows in this figure correspond to the peaks highlighted by labelled arrows in figure 5.50.

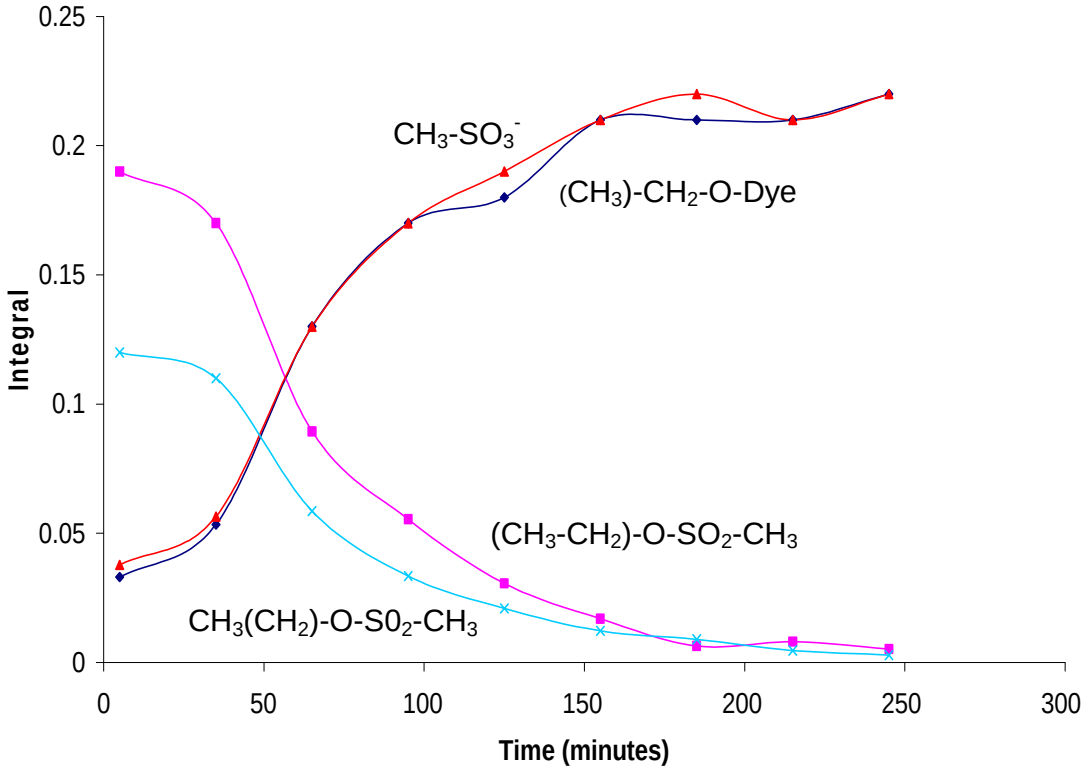

Figure 5.52. The relationship between integrals of four selected peaks over the four hour time period for which the reaction between 2,6-diphenyl-4-(2,4,6-triphenyl-1-pyridinio)phenolate and ethyl methane sulfonate was carried out.

The plot of the integrals of the peaks highlighted in Figures 5.50 and 5.51 over time shows how the peaks owing to ethyl methane sulfonate diminished and how the peaks owing to the two products grew.

Summary of NMR findings

The product of the reaction between 2,6-diphenyl-4-(2,4,6-triphenyl-1-pyridinio)phenolate and 4-chloro-1-butanol was isolated and investigated with NMR spectroscopy. ^{1}H NMR, a ^{13}C dept experiment and an HMQC confirmed the alkylated product as shown in Figure 5.41. The reaction between 2,6-diphenyl-4-

(2,4,6-triphenyl-1-pyridinio)phenolate and ethyl methane sulfonate was slower and could be tracked in an NMR tube. ^{1}H NMR showed the disappearance of peaks from ethyl methane sulfonate and the appearance of peaks from the alkylated dye and the methyl sulfonate ion.

The importance of this section lies in the confirmation of the chemistry of the reaction. It is therefore possible to proceed with certainty that the bleaching of the dye is a result of alkylation by 4-chloro-1butanol and ethyl methane sulfonate.

5.3.7 Summary of results

With the proof of alkylation of 2,6-diphenyl-4-(2,4,6-triphenyl-1-pyridinio)phenolate by ethyl methane sulfonate and 4-chloro-1-butanol from NMR spectroscopy the results of the reactions between 2,6-diphenyl-4-(2,4,6-triphenyl-1-pyridinio)phenolate and the 4-chloro-1-butanol, 1-bromobutane, ethyl methane sulfonate and Fast Red B are summarised below.

The two most industrially relevant alkylating agents used in the study were 4-chloro-1-butanol and ethyl methane sulfonate. 1-bromobutane was used to help show a generic element to the alkyl halide detection and Fast Red B was representative of the diazonium salts. Diazonium salts are becoming less frequently used in chemical syntheses because of their associated alkylating behaviour as trace impurities.

The table shows the assays which established linearity for each alkylating agent and the reaction conditions necessary to achieve linearity.

Table 5.1. Summarising outcomes of testing with alkylating agents and 2,6-diphenyl-4-(2,4,6-triphenyl-1-pyridinio)phenolate. Green boxes indicate the successful establishment of a linear change in absorbance in response to addition of alkylating agent over the concentration range of 0-100 ppm. Red boxes indicate that it was not possible to establish a linear change in absorbance in response to the addition of alkylating agents over the concentration range of 0-100 ppm.

Alkylating Agent	**ACN**	**DMF**	**Heat and DMF**	**Catalyst**	**R^2**
4-Cb	Yes	Yes	N/A	N/A	0.9962
1-Bb	No	No	Yes	Yes	0.9741
EMS	No	No	Yes	No	0.9756
FR B	Yes	Yes	N/A	N/A	0.9930

5.3.8 Measurement of alkylation in the presence of drug compounds.

Following on from the initial development of linear assays for 4-chloro-1-butanol and ethyl methane sulfonate it was then decided to investigate the changes in absorbance when drug was dissolved in the appropriate solvent. This would provide insight into whether preparation would be necessary for industrial samples or whether pharmaceutical formulations could be simply dissolved and assayed. 100 per cent pure acetaminophen was used for testing.

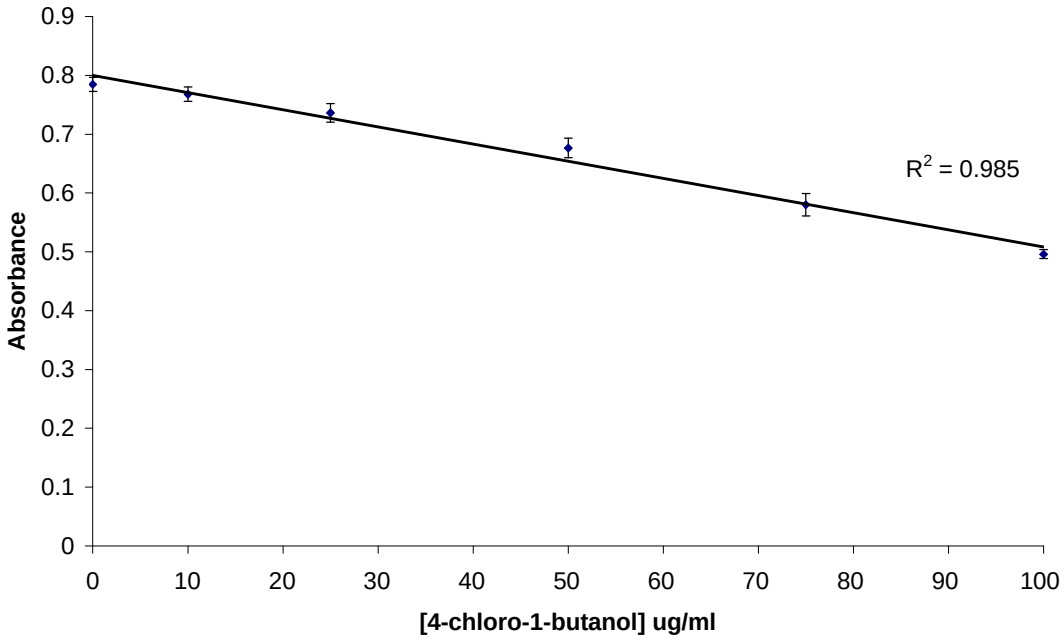

Figure 5.53. Changes in absorbance at 624 nm for 2,6-diphenyl-4-(2,4,6-triphenyl-1-pyridinio)phenolate in response to increasing concentrations of 4-chloro-1-butanol when acetaminophen is present at a concentration of 10 mg/ml.

This figure showed that 2,6-diphenyl-4-(2,4,6-triphenyl-1-pyridinio)phenolate was capable of maintaining its linear change in absorbance in response to increasing concentrations of 4-chloro-1-butanol with acetaminophen present at 10 mg/ml.

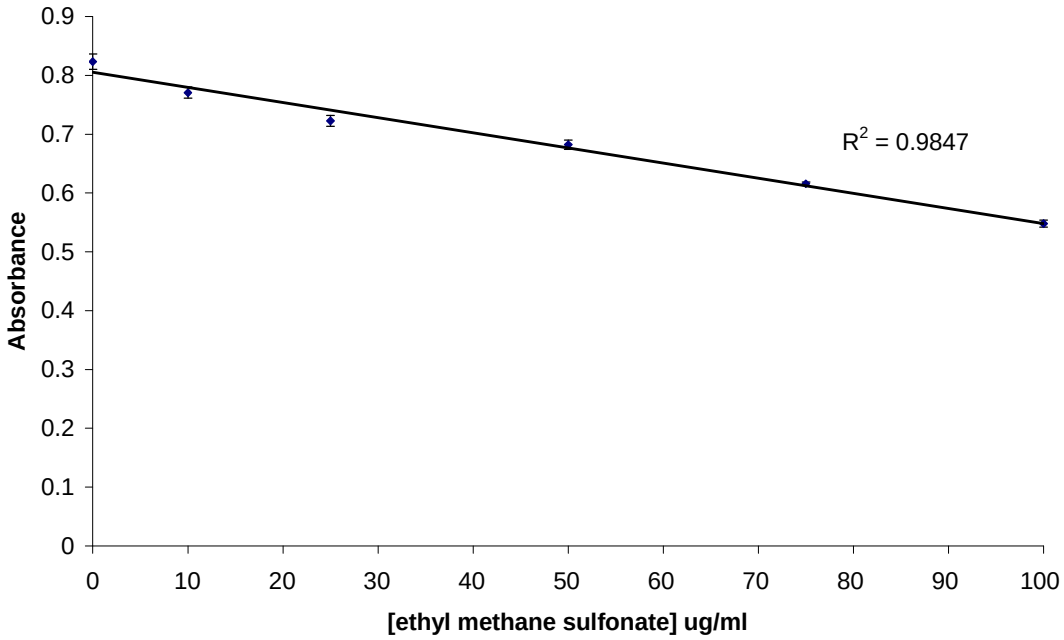

Figure 5.54. Changes in absorbance at 624 nm for 2,6-diphenyl-4-(2,4,6-triphenyl-1-pyridinio)phenolate in response to increasing concentration of ethyl methane sulfonate when acetaminophen is present at a concentration of 10 mg/ml. The samples were heated at 85^{o}C for 4 hours before UV-vis analysis was carried out.

This figure showed that 2,6-diphenyl-4-(2,4,6-triphenyl-1-pyridinio)phenolate was capable of maintaining its linear change in absorbance in response to increasing concentrations of ethyl methane sulfonate with acetaminophen at 10 mg/ml.

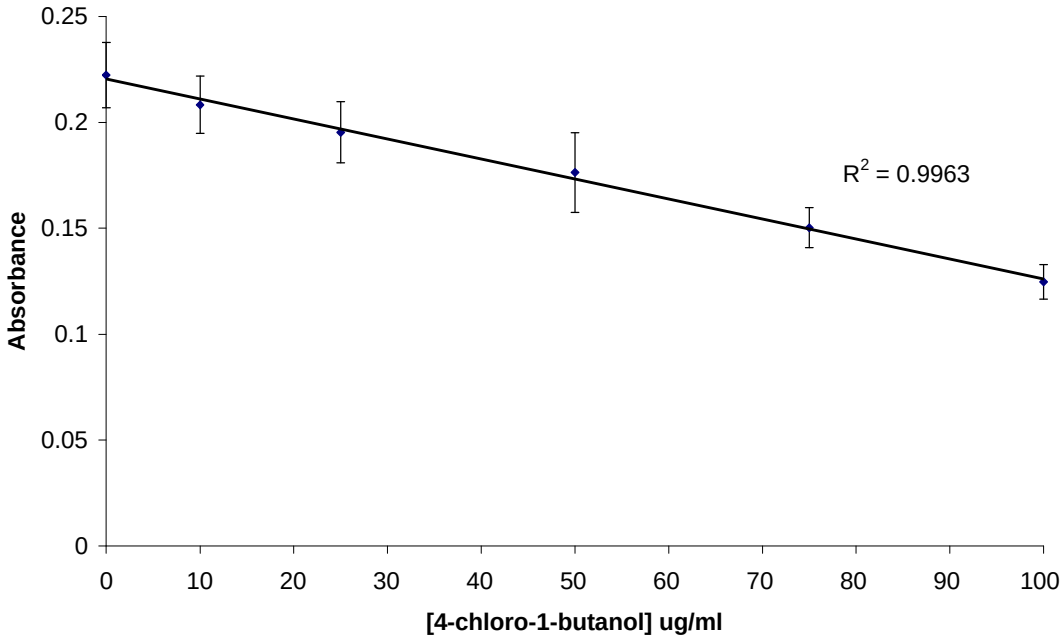

Figure 5.55. Changes in absorbance at 624 nm for 2,6-diphenyl-4-(2,4,6-triphenyl-1-pyridinio)phenolate in response to increasing concentration of 4-chloro-1-butanol when acetaminophen is present at a concentration of 100 mg/ml.

This figure showed that 2,6-diphenyl-4-(2,4,6-triphenyl-1-pyridinio)phenolate maintained its linear response to the addition of 4-chloro-1-butanol at 100mg/ml of acetaminophen.

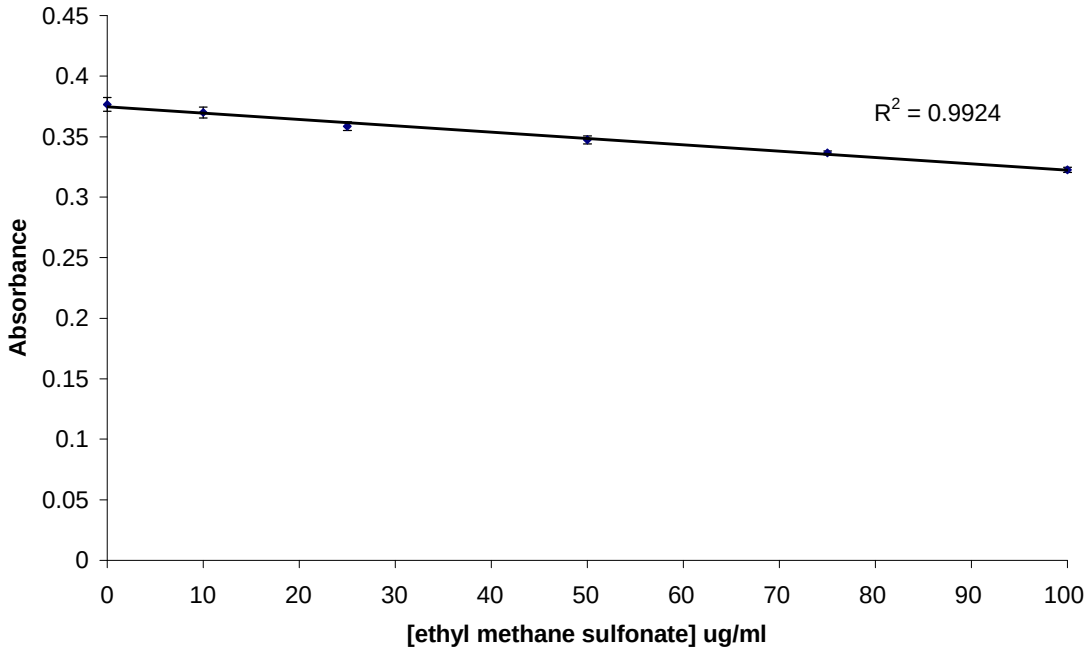

Figure 5.56. Changes in absorbance at 624 nm for 2,6-diphenyl-4-(2,4,6-triphenyl-1-pyridinio)phenolate in response to increasing concentration of ethyl methane sulfonate when acetaminophen is present at a concentration of 100 mg/ml. The samples were heated at 85^{o}C for 4 hours before UV-vis analysis was carried out.

This figure shows that 2,6-diphenyl-4-(2,4,6-triphenyl-1-pyridinio)phenolate maintained its linear response to the addition of ethyl methane sulfonate at 100mg/ml of acetaminophen.

The linearity of the assay seemed to remain but R^2 values were poorer in the presence of acetaminophen at 10 mg/ml and 100 mg/ml. The increase in concentration of acetaminophen from 10 mg/ml to 100 mg/ml caused the overall absorbances to decrease meaning that the magnitude of the change was also smaller. It can therefore be concluded that the presence of acetaminophen, particularly at a concentration of 100 mg/ml was having a deleterious effect on the assay.

In light of this finding it was decided to investigate possible explanations for the loss of the assay's resolution and linearity. Acetaminophen is slightly acidic and it was postulated that a pH effect might explain the changes in dye behaviour. Whilst the experiments involving acetaminophen were carried out, ibuprofen (more acidic compound) was also investigated. At concentrations of 10 mg/ml and 100 mg/ml ibuprofen bleached the dye. This bleaching was reversed when base was added so in this case it was found that the slightly more acidic ibuprofen was affecting the dye. Also the presence of water in the assay as an impurity in the acetaminophen was another possible explanation for the decreased performance. It was therefore decided to investigate effects of apparent pH and water on dye behaviour.

5.3.9 Effects of apparent pH on dye behaviour in the presence of 4-chloro-1-butanol

The molecule 2,6-diphenyl-4-(2,4,6-triphenyl-1-pyridinio)phenolate is extremely sensitive to its environment, Having already shown that the assay for 4-chloro-1-butanol and ethyl methane sulfonate does not work as well in acetaminophen as it did in earlier experiments it was decided to investigate the effect of apparent pH on dye bleaching.

Initial experiments were run in 95% DMF and 5% water with phosphate buffer dissolved in the water to provide different pH values. Testing was carried out with 5% water on it's own and phosphate buffers set at pH 5.0, 7.0 and 9.0.

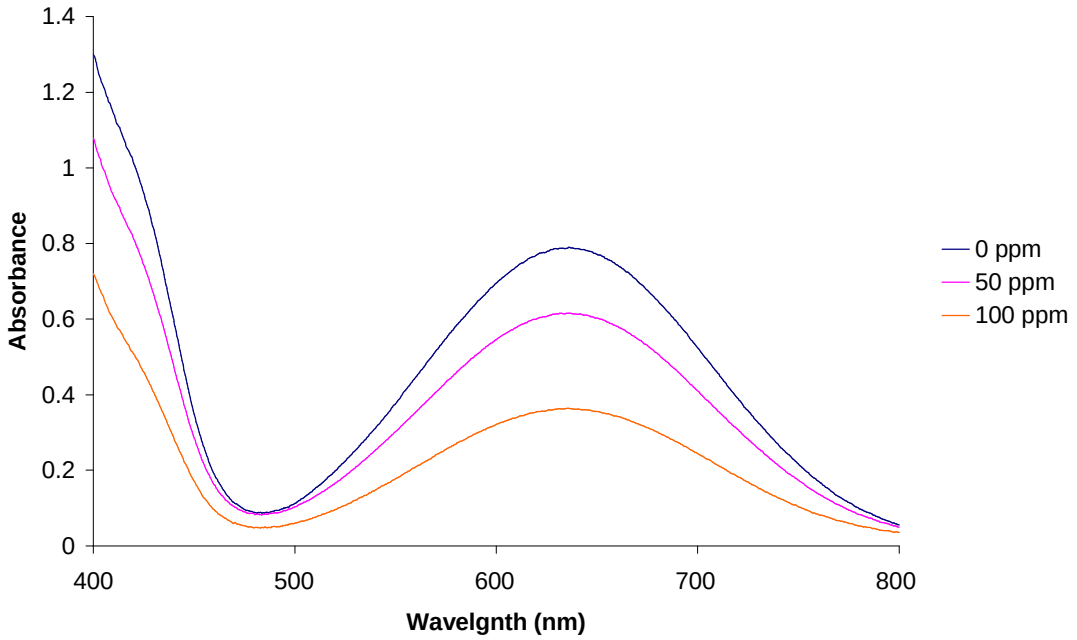

Figure 5.57. UV spectrum showing the effect of 4-chloro-1-butanol on the absorption maximum of 2,6-diphenyl-4-(2,4,6-triphenyl-1-pyridinio)phenolate in 95 % DMF and 5% water. Blue = 0 ppm, pink = 50 ppm ad orange = 100 ppm.

Under the conditions described, 4-chloro-1-butanol reduced the absorption maximum in a fashion similar to that already seen in this study.

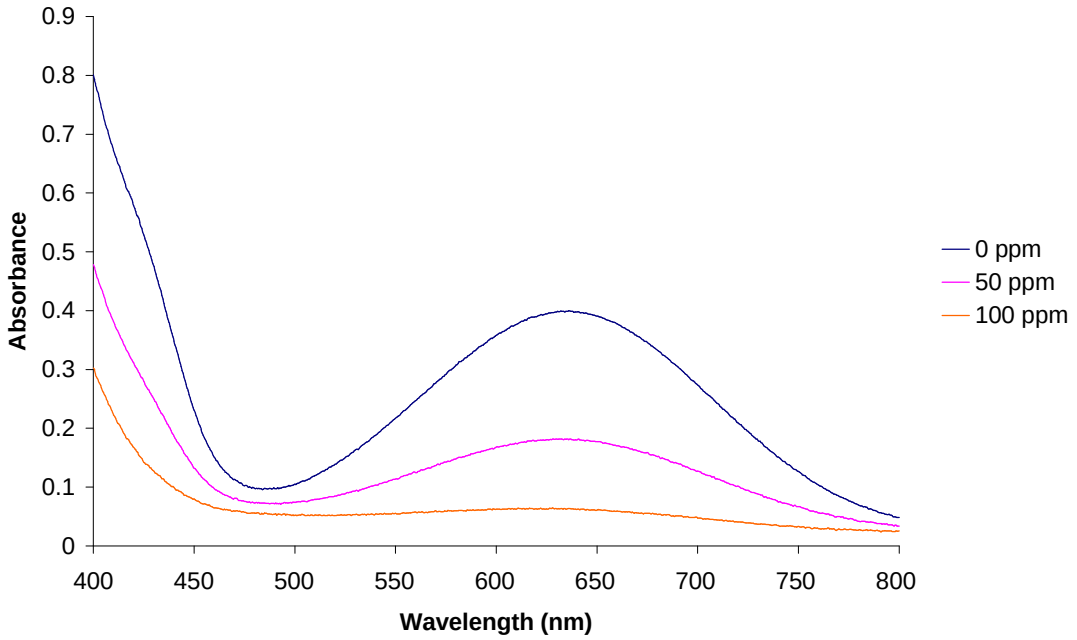

Figure 5.58. UV spectrum showing the effect of 4-chloro-1-butanol on the absorption maximum of 2,6-diphenyl-4-(2,4,6-triphenyl-1-pyridinio)phenolate in 95 % DMF and 5% phosphate buffer solution at pH 7.0. Blue = 0 ppm, pink = 50 ppm ad orange = 100 ppm

2,6-diphenyl-4-(2,4,6-triphenyl-1-pyridinio)phenolate had a smaller absorption maximum to begin with but the maximum reduced in the presence of 4-chloro-1-butanol in a fashion similar to that already observed in this study.

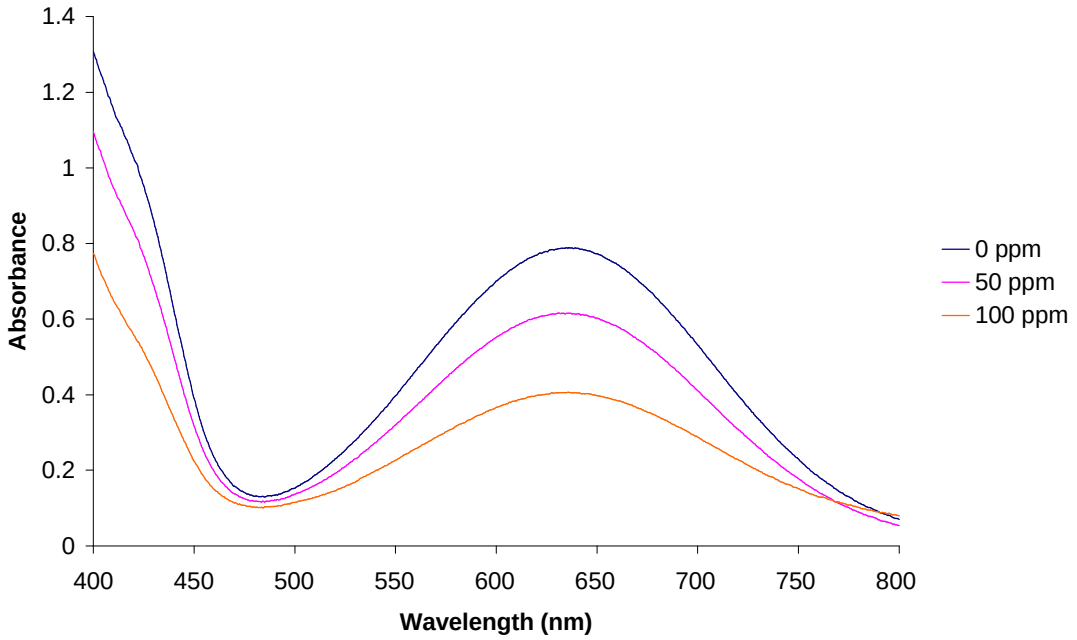

Figure 5.59. UV spectrum showing the effect of 4-chloro-1-butanol on the absorption maximum of 2,6-diphenyl-4-(2,4,6-triphenyl-1-pyridinio)phenolate in 95 % DMF and 5% phosphate buffer solution at pH 9.0. Blue = 0 ppm, pink = 50 ppm ad orange = 100 ppm

At pH 9.0, 2,6-diphenyl-4-(2,4,6-triphenyl-1-pyridinio)phenolate had an absorption maximum similar to that observed for 5% water. The absorption maximum reduced in the presence of 4-chloro-1-butanol in typical fashion.

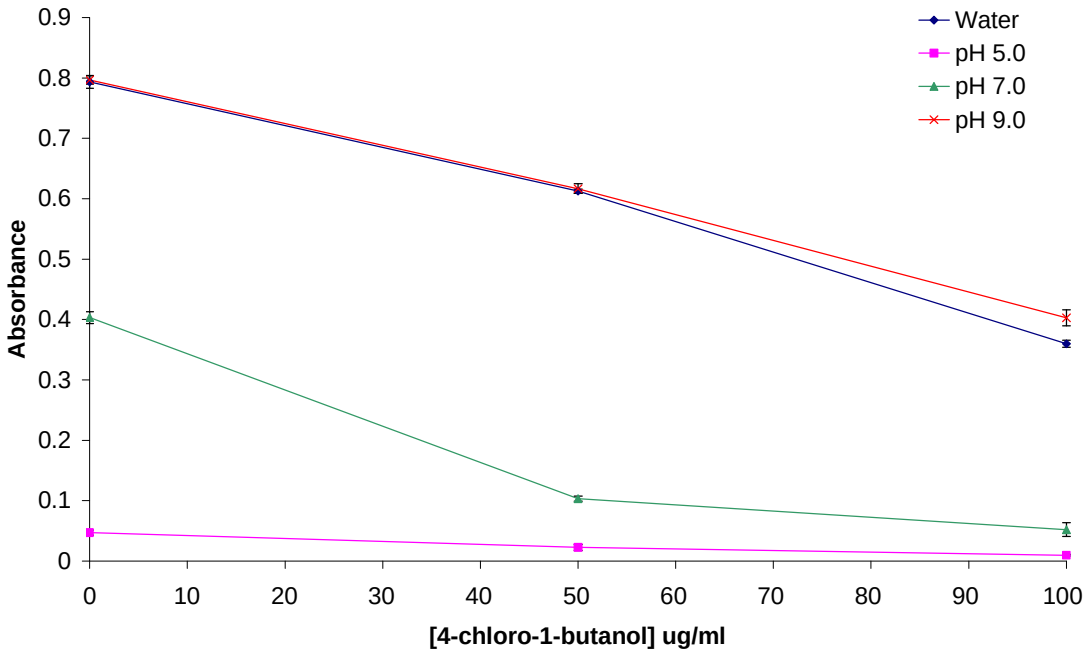

Figure 5.60. The changing absorbance maximum of 2,6-diphenyl-4-(2,4,6-triphenyl-1-pyridinio) phenolate in the presence of 4-chloro-1-butanol in four different pH environments.

The addition of buffer at pH 5.0 had a profound effect. The dye bleached completely and therefore it was not possible to detect alkylation by 4-chloro-1-butanol using UV-vis spectroscopy. To confirm the reversibility of the bleaching by phosphate buffer at pH 5.0, a drop of organic base was added and the dye regained its colour.

The addition of 5% water and the addition of phosphate buffer at pH 9.0 produced a similar response with the dyes' absorbance decreasing in a fashion similar to that seen in earlier experiments.

Having shown apparent pH to have an effect on the dyes' behaviour it was decided to manipulate the pH conditions in the presence of drug compounds in order to see if dye

performance could be improved. Previous experiments had shown acetaminophen to affect the dyes behaviour and a likely explanation was the drugs' effect on the apparent pH. Acetaminophen is weakly acidic and at 100 mg/ml especially would have caused a pH effect on the dye. Ibuprofen was also tested but it was found to strongly bleach the dye when present at a concentration of 100 mg/ml. The addition of organic base restored colour and so in the light of these experiments which showed apparent pH manipulation may benefit the assay, it was decided to investigate the possibility of pH manipulation in the presence of acetaminophen in an attempt to improve the robustness of the assay in the presence of drug compounds.

Alkylation and apparent pH effects in the presence of acetaminophen

Due to the high concentrations of drug present in the system (10 mg/ml or 100 mg/ml) it was not possible to continue this line of enquiry with phosphate buffer. The DMF to water ratio was 95% to 5% and dissolving the phosphate compounds in water at the necessary concentrations would not have been possible. It was therefore decided to use an organic base and triethylamine was selected. Concentrations of 0.662 M and 0.066 M were selected because these gave an equimolar ratio with acetaminophen at 100 mg/ml and 10 mg/ml.

The assay for 4-chloro-1-butanol was tested with acetaminophen present at 10 mg/ml and 100 mg/ml and with triethylamine present at 0.066 M and 0.662 M concentrations.

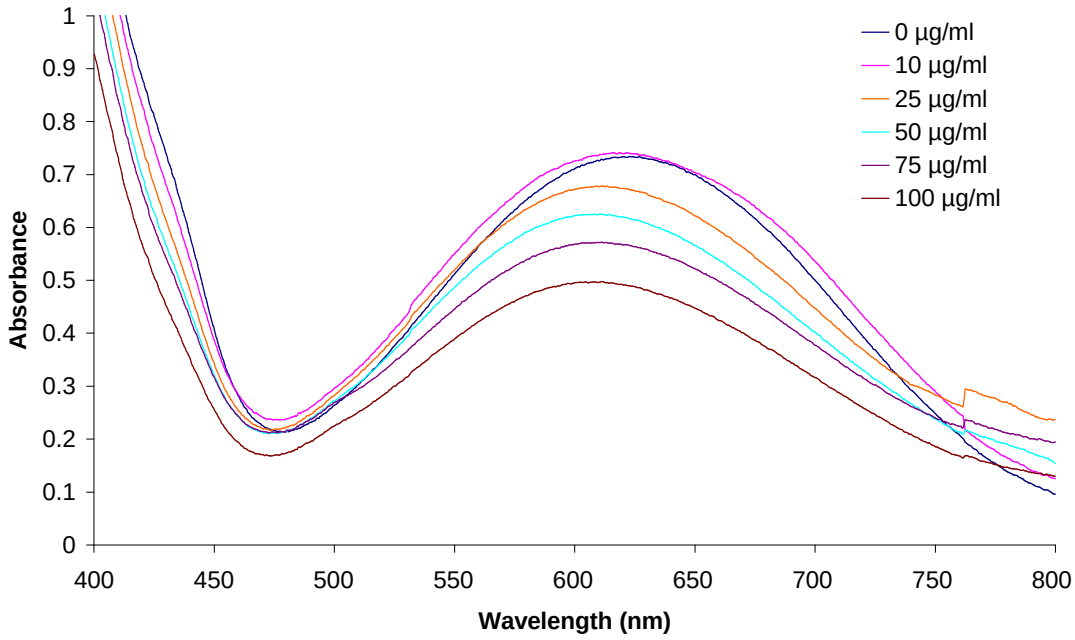

Figure 5.61. UV-vis spectrum showing the effect of 4-chloro-1-butanol on the absorption maximum of 2,6-diphenyl-4-(2,4,6-triphenyl-1-pyridinio) phenolate with acetaminophen present at 10 mg/ml and triethylamine present at a concentration of 0.066 M.

This UV spectrum showed that the UV absorption maximum for 2,6-diphenyl-4-(2,4,6-triphenyl-1-pyridinio) phenolate reduced as the concentration of 4-chloro-1-butanol increased.

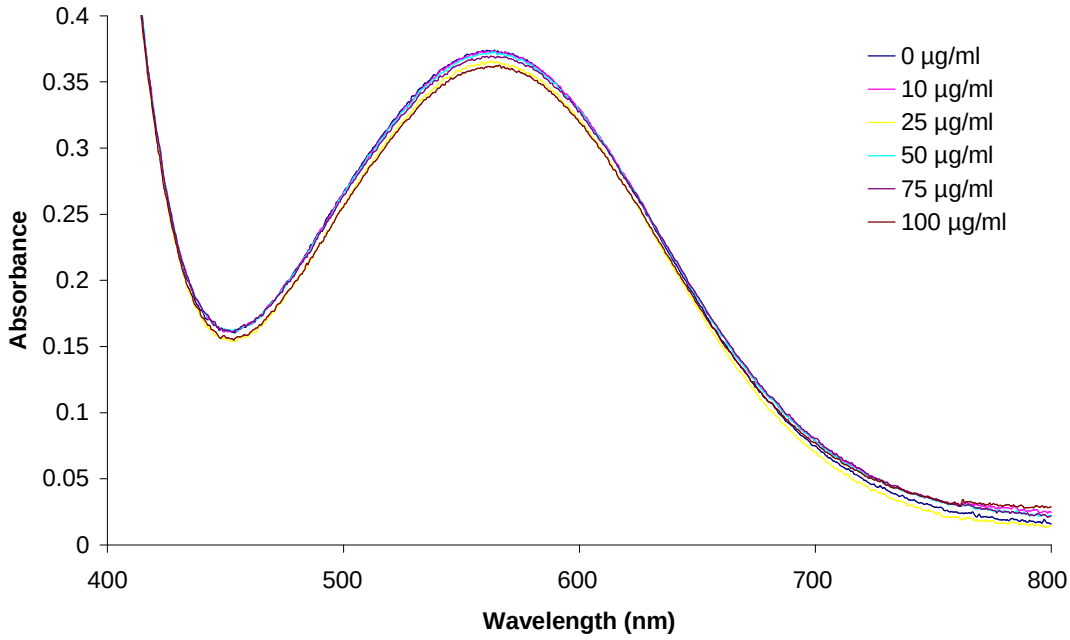

Figure 5.62. UV-vis spectrum showing the effect of 4-chloro-1-butanol on the absorption maximum of 2,6-diphenyl-4-(2,4,6-triphenyl-1-pyridinio) phenolate with acetaminophen present at 100 mg/ml and triethylamine present at a concentration of 0.662 M.

The UV absorption maximum for 2,6-diphenyl-4-(2,4,6-triphenyl-1-pyridinio) phenolate did not reduce as markedly as it had in previous assays and the decreases were not uniform and concentration dependant as they had been shown to be in other cases. There was a significant difference between 0 ppm and 100 ppm which implied alkylation of 2,6-diphenyl-4-(2,4,6-triphenyl-1-pyridinio) phenolate was taking place but the system was less reliable at measuring the alkylation.

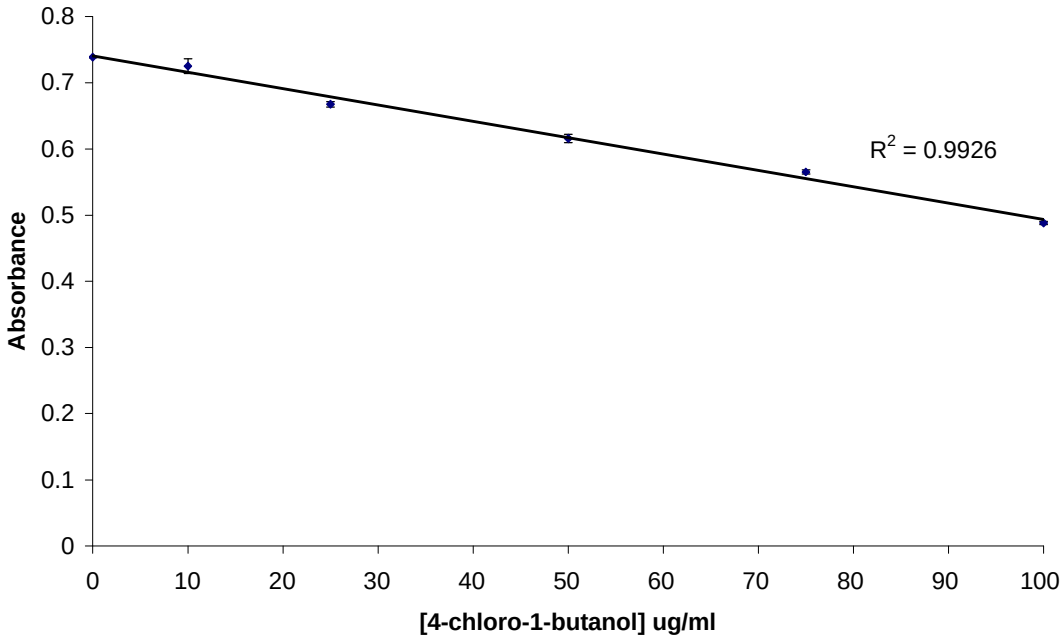

Figure 5.63. The effect of 4-chloro-1-butanol on the absorption maximum of 2,6-diphenyl-4-(2,4,6-triphenyl-1-pyridinio) phenolate in the presence of acetaminophen at 10 mg/ml and triethylamine at 0.066 M.

At 10 mg/ml of acetaminophen the presence of triethylamine produced a plot with an R^2 value of 0.9926 which therefore had good linearity. Earlier experimentation showed the assay had reasonable linearity and good preservation of concentration dependant drops in absorbance so the performance of triethylamine at 10 mg/ml of acetaminophen was not as critical as for 100 mg/ml where drug interference represents a more profound effect.

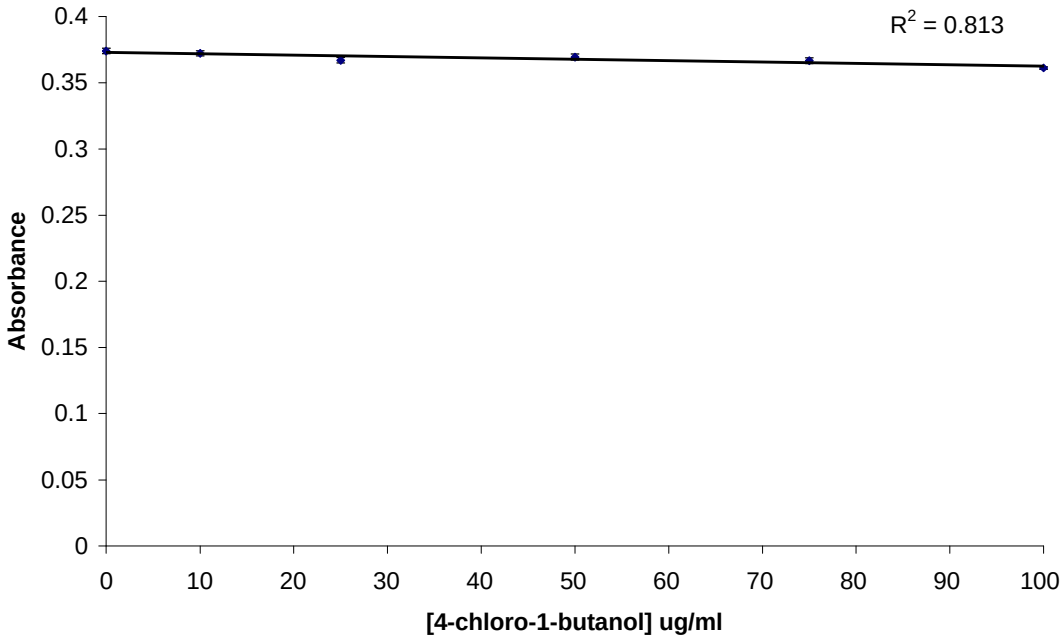

Figure 5.64. The effect of 4-chloro-1-butanol on the absorption maximum of 2,6-diphenyl-4-(2,4,6-triphenyl-1-pyridinio) phenolate in the presence of acetaminophen at 100 mg/ml and triethylamine at 0.662 M.

It can be seen that the presence of triethylamine did not improve linearity of the assay or increase the concentration dependant drops in absorbance. An R^2 value of 0.813 represents poor linearity and so it was found that the presence of triethylamine did not improve the robustness of the assay in the presence of acetaminophen.

A potential problem with 4-chloro-1-butanol and the presence of base is that the molecule can cyclise to THF and therefore it was decided to test the assay with ethyl methane sulfonate in order to ensure that we weren't observing a lessened effect due to THF formation from 4-chloro-1-butanol. It was also hypothesised that the presence of water might aid proton exchange and improve the reaction.

Therefore experiments were carried out with 4-chloro-1-butanol and ethyl methane sulfonate where 0.662 M triethylamine was ever present and in which some samples contained 5% water.

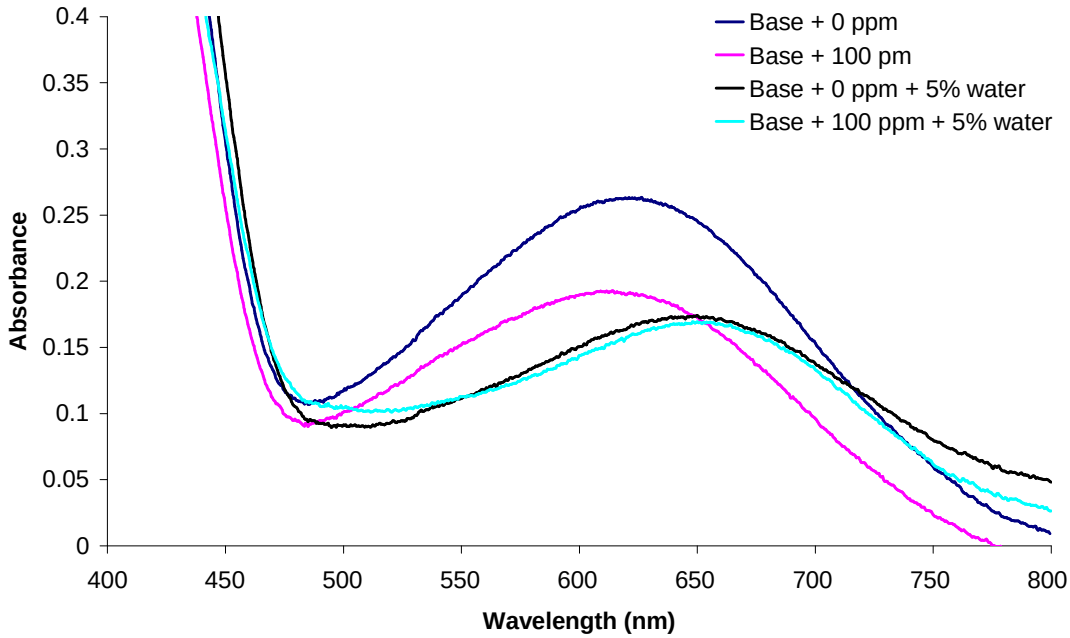

Figure 5.65. UV-vis spectrum showing the effect of 4-chloro-1-butanol on the absorption maximum of 2,6-diphenyl-4-(2,4,6-triphenyl-1-pyridinio) phenolate in the presence of 100 mg/ml acetaminophen, 0.662 M triethylamine and 5 % water.

The UV spectrum showed that when 100 mg/ml acetaminophen and 0.662 M triethylamine were present, 100 µg/ml 4-chloro-1-butanol caused a reduction in the absorption maximum. The presence of 5% water reduced the overall drop in absorption maximum.

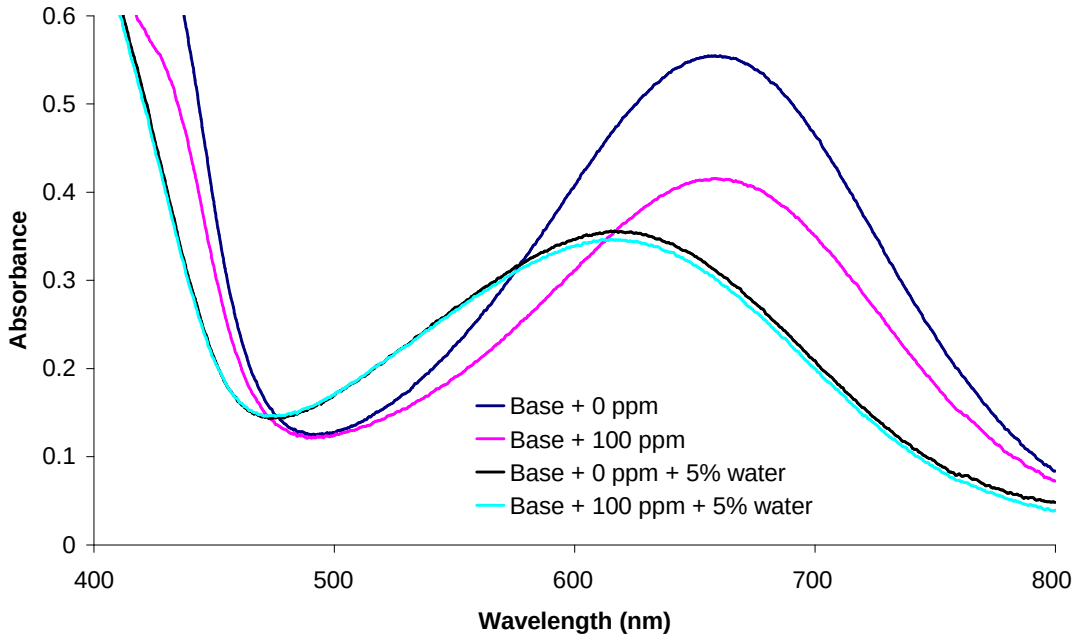

Figure 5.66. UV-vis spectrum showing the effect of ethyl methane sulfonate on the absorption maximum of 2,6-diphenyl-4-(2,4,6-triphenyl-1-pyridinio) phenolate in the presence of 0.662 M triethylamine and 5 % water.

The UV spectrum showed that when 100 mg/ml acetaminophen and 0.662 M triethylamine were present, 100 µg/ml ethyl methane sulfonate caused a reduction in the absorption maximum. The presence of 5% water reduced the overall drop in absorption maximum.

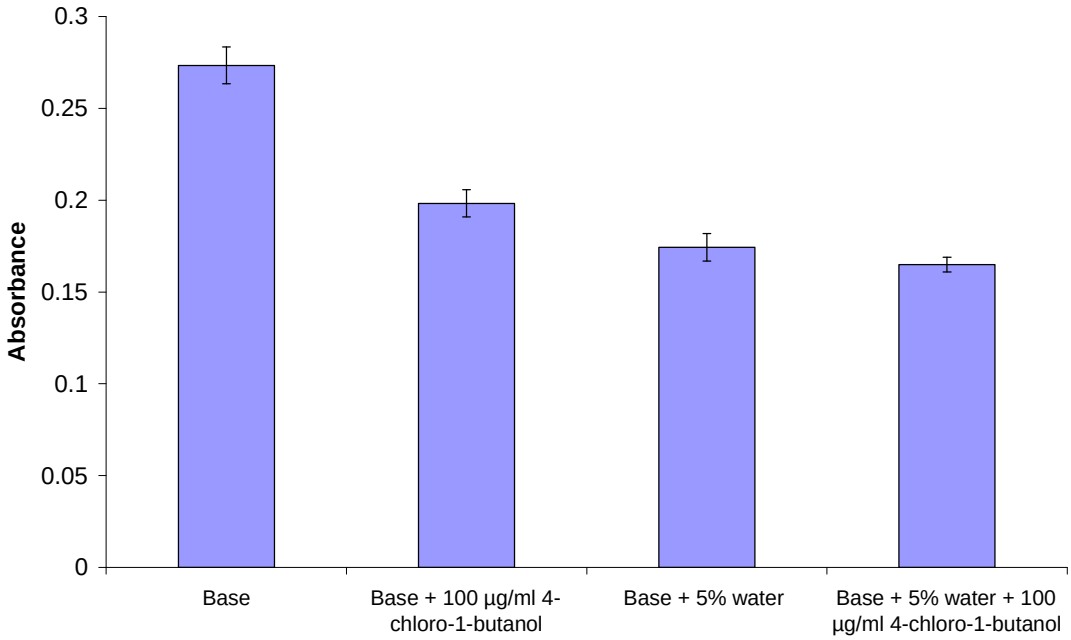

Figure 5.67. Summary of the effect of 4-chloro-1-butanol on the absorption maximum of 2,6-diphenyl-4-(2,4,6-triphenyl-1-pyridinio) phenolate in the presence of 0.662 M triethylamine and 5% water. Bars represent standard deviation (n = 3).

It can be seen that the presence of water at 5% reduced the size of the drop in absorption maximum of 2,6-diphenyl-4-(2,4,6-triphenyl-1-pyridinio) phenolate as a result of alkylation by 4-chloro-1-butanol.

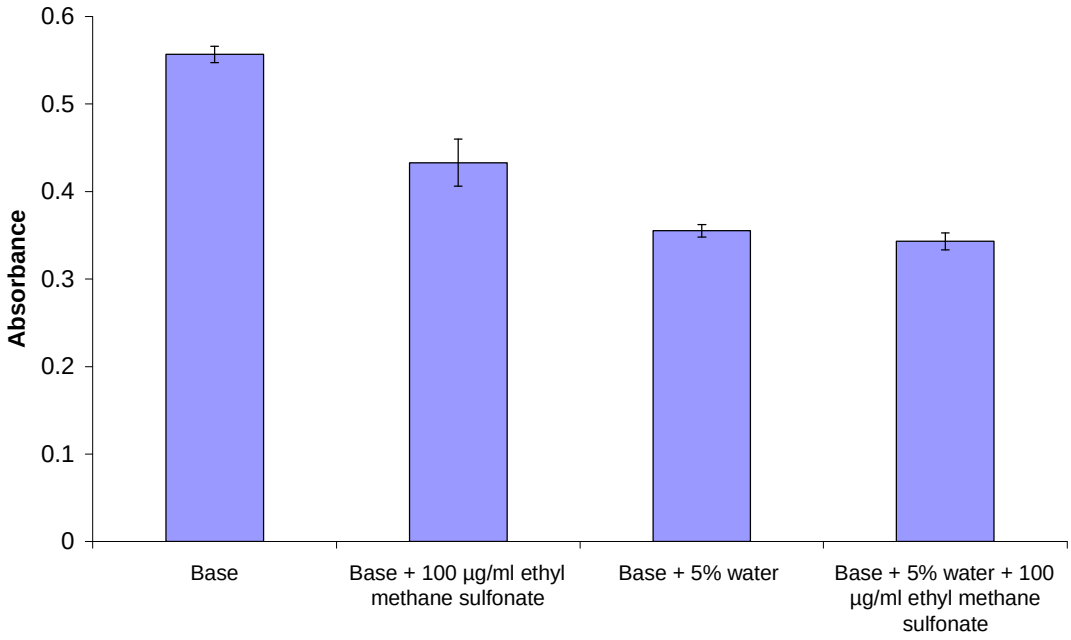

Figure 5.68. Summary of the effect of ethyl methane sulfonate on the absorption maximum of 2,6-diphenyl-4-(2,4,6-triphenyl-1-pyridinio) phenolate in the presence of 0.662 M triethylamine and 5% water. Bars represent standard deviation (n = 3).

It can be seen that the presence of water at 5% reduced the size of the drop in absorption maximum of 2,6-diphenyl-4-(2,4,6-triphenyl-1-pyridinio) phenolate as a result of alkylation by 4-chloro-1-butanol.

It can be seen that water caused the absorption maximum of 2,6-diphenyl-4-(2,4,6-triphenyl-1-pyridinio) phenolate to decrease and then reduce in a smaller manner than usual in the presence of 4-chloro-1-butanol or ethyl methane sulfonate. Therefore it can be concluded that rather than aiding proton exchange as was originally hypothesised, in combination with drug and base, water somehow inhibits the reaction between 2,6-diphenyl-4-(2,4,6-triphenyl-1-pyridinio) phenolate and 4-chloro-1-butanol and ethyl methane sulfonate.

It has been shown that the presence of drug compound at 100 mg/ml has an adverse effect on the linearity of the assay and the magnitude of the alkylation induced changes to the absorption maximum of 2,6-diphenyl-4-(2,4,6-triphenyl-1-pyridinio) phenolate.

It was shown that when dye was present alone it was possible to manipulate the assay by altering the apparent pH with phosphate buffer. However, when it becomes necessary to buffer in the presence of interfering drug compounds such as acetaminophen it is no longer possible to buffer with the phosphate system and so it is necessary to use a base.

Triethylamine was selected as a base and it was found that it did not make a significant difference to the linearity of the assay in the presence of 100 mg/ml of acetaminophen.

2,6-diphenyl-4-(2,4,6-triphenyl-1-pyridinio) phenolate is extremely sensitive to its local environment and it was found that in the presence of 100 mg/ml acetaminophen and 0.662 M triethylamine the addition of 5% water adversely effected the reaction so that only very small changes in the absorption maximum of 2,6-diphenyl-4-(2,4,6-triphenyl-1-pyridinio) phenolate could be observed. Therefore, the tendency for the assay to worsen in the presence of acetaminophen could possibly be explained by a pH effect and also the presence of water as an impurity within the drug especially at a concentration as high as 100 mg/ml. It should also be remembered that when it was attempted to test with ibuprofen rather than acetaminophen, 2,6-diphenyl-4-(2,4,6-

triphenyl-1-pyridinio) phenolate was completely bleached by the acidic nature of ibuprofen but colour could be restored by the addition of organic base.

Therefore it can be concluded that changes in apparent pH and the aqueous and solvent environment of the dye have an effect on its performance when used to measure alkylation by 4-chloro-1-butanol and ethyl methane sulfonate. Further testing would be required to identify the optimum conditions for the measurement of alkylation by 4-chloro-1-butanol and ethyl methane sulfonate or should that testing prove unsuccessful it may be necessary to introduce a preparation step involving a technique such as solid phase extraction to remove drug compounds.

5.4 Discussion

Fluorescence spectroscopy and UV-vis spectroscopy were tested for the quantification of alkylation of the betaine dyes by alkylating agents. Fluorescence spectroscopy demonstrated small changes in fluorescence in the presence of alkylating agents but the changes were not shown in as reproducible a fashion as UV-vis spectroscopy. Dilution of the dyes in an attempt to increase the fluorescence signal did not increase the magnitude of the changes resulting from alkylation and it did not help to make fluorescence detection a suitable technique for measurement of alkylation. Fluorescence is potentially a sensitive technique but is often more suited to measuring gains in fluorescence. The problem in this case could be self quenching by the dye or the changes in fluorescence levels of the dye due to alkylation being too small for accurate detection.

UV-vis spectroscopy performed much better when it came to quantifying alkylation of the dyes. From UV-vis spectra it was possible to detect loss in absorbance as a result of alkylation of the dye and using the technique it was possible to investigate the potential of Reichardt's dye and the related dyes for the detection of alkylating agents.

4-Chloro-1-butanol alkylated all the dyes used in the study and changes in the absorption maximum for the dye were pronounced. 2,6-diphenyl-4-(2,4,6-triphenyl-1-pyridinio)phenolate showed excellent linearity in the presence of 4-chloro-1-butanol at different concentrations. The reaction proceeded rapidly at room temperature with colour changes observable by eye taking place within one or two seconds of mixing

dye 4-chloro-1-butanol. The reaction proceeded well in acetonitrile and DMF but showed a greater overall drop in absorbance in DMF.

Fast Red B, the diazonium salt also showed good reactivity with 2,6-diphenyl-4-(2,4,6-triphenyl-1-pyridinio)phenolate and the presence of the compound at different concentrations caused the absorption maximum of the dye to change in a linear fashion. The reaction proceeded within seconds of mixing dye with Fast Red B.

1-Bromobutane is an alkyl halide like 4-chloro-1-butanol but reactivity between the alkylating agent and the dyes was less pronounced than for 4-chloro-1-butanol. The reaction did not proceed at all in acetonitrile where as heating at 85^{o}C for four hours in DMF caused the reaction to proceed. As with 4-chloro-1-butanol and Fast Red B, a linear plot could be made which showed a decrease in absorption in response to the presence of 1-bromobutane at different concentrations. Additionally, it was found that the catalyst tetrabutlyammonium iodide increased the rate of the reaction so that the changes in absorbance were greater over the equivalent time period.

Ethyl methane sulfonate was also unreactive with the betaine dyes in acetonitrile. As with 1-bromobutane the, reaction between ethyl methane sulfonate and 2,6-diphenyl-4-(2,4,6-triphenyl-1-pyridinio)phenolate could be made to proceed by heating the reaction mixture up to 85^{o}C for a period of four hours. The presence of tetrabutylammonium iodide did not increase the rate of the reaction. The change in absorbance could be plotted in a linear fashion as with the other compounds.

The experiments where alkylating agent and dye were reacted alone in either acetonitrile and DMF showed that the dye 2,6-diphenyl-4-(2,4,6-triphenyl-1-pyridinio)phenolate would undergo alkylation. The change in absorbance was proportional to the concentration of alkylating agent present and so a linear plot could be produced.

It was established through one of the series of results presented in this chapter that the compound 2,6-diphenyl-4-(2,4,6-triphenyl-1-pyridinio)phenolate could be used as a sensitive assay for the alkylating agents: 4-chloro-1-butanol, 1-bromobutane, ethyl methane sulfonate and Fast Red B. 4-Chloro-1-butanol and Fast Red B reacted with 2,6-diphenyl-4-(2,4,6-triphenyl-1-pyridinio)phenolate instantly and at room temperature giving visible colour changes that could be quantified spectrophotometrically. 1-Bromobutane and ethyl methane sulfonate were found to react less well with 2,6-diphenyl-4-(2,4,6-triphenyl-1-pyridinio)phenolate and to produce the linear assay seen for 4-chloro-1-butanol and Fast Red B, the reaction conditions needed to include heating at 85^{o}C for four hours in DMF. 1-Bromobutane's reaction was also slightly sped up by the presence of tetrabutlyammonium iodide. The extra conditions required for 1-bromobutane and ethyl methane sulfonate prompted the study to look at the azo dyes 4-phenylazophenol and Fat Brown B. Both dyes performed similarly in that some changes to the eye could be seen when alkylating agents were present but spectrophotometrically the changes were much less easy to interpret. The data presented in this chapter on the azo dyes showed that the changes in response to presence of alkylating agents were small in comparison to the betaine dyes and those changes did not always appear in the step wise fashion needed to construct a linear

assay. After testing with 4-chloro-1-butanol for the purposes of comparison and then 1-bromobutane and ethyl methane sulfonate it was found that 4-phenylazophenol and Fat Brown B were not as useful as the betaine dyes for the detection and potential quantification of alkylating agents. These results provided the basis for a sensitive and quantitative assay for alkylating agents. The next challenge was to determine if the dyes would undergo the alkylation in the presence of drug sample. The dyes working in the presence of drug would be very useful to the final assay because sample preparation would be unnecessary. The drug is often provided to the analytical scientists within a company in powder form and then analysis will take place. If the drug can be dissolved straight away and then subjected to the assay for genotoxins it would represent a significant time saving.

The experiments where acetaminophen was dissolved at 10 mg/ml showed that the linearity of the assay was maintained in the presence of acetaminophen. The absorbance values were much smaller and the overall change in absorbance maxima at 100 mg/ml of acetaminophen. The failure of the assay to work at 100 mg/ml of acetaminophen resulted in the investigation of apparent pH as a possible means of stabilising it. Acetaminophen is mildly acidic and at the concentration of 100 mg/ml was found to be bleaching 2,6-diphenyl-4-(2,4,6-triphenyl-1-pyridinio)phenolate and when ibuprofen was tried it was found to cause complete bleaching. The bleaching was reversible with the addition of base and was due to a pH effect. It was therefore decided to investigate the possibility of buffering so that dye performance could be maintained in the presence of drug. It was found that the use of phosphate buffer did affect dye performance. At pH 5.0 the dye bleached meaning that no measurements could be carried out (addition of organic base restored colour), at pH 7.0 and 9.0 the

dye's performance improved indicating that in slightly basic conditions performance was better. It was not possible to use phosphate buffer when dissolving drug because of the problem of getting the buffers into solution at such high concentration so it was decided to try triethylamine as an organic base in a 1:1 ratio with acetaminophen. It was found that the presence of triethylamine at an equimolar ratio to acetaminophen at 100 mg/ml did not restore the assay. It was found that whilst absorbances changed in response to alkylating agent in a concentration dependant fashion the assay performed very poorly for 100 mg/ml of acetaminophen. It was also found that the presence of 5% water alongside acetaminophen also worsened the assay which may suggest that when drug is added the presence of water as an impurity and the effect on apparent pH may be responsible for the assay not working. The advantage of being able to dissolve large amounts of drug lies in the fact that it increases the amount of genotoxic impurity available for measurement.

To set the importance of this work into a context, the European Medicines Agency released a statement on the 21st of June 2007 in which it was recommended to the European Commission that the authorisation for the marketing of a drug called Viracept be suspended due to the presence of a genotoxic impurity at levels deemed unsafe. The suspension was subsequently lifted on the 20th of September 2007 after the new production methods and product checks from the manufacturing company had been reviewed by the agency. Incidents such as this one highlight the importance of genotoxic impurities and illustrate the idea that a recall or suspension of authorisation can have a very negative effect on a company. A generic and easy to operate assay for alkylating agents would be a very useful tool to the pharmaceutical industry and an extra fail safe for patient welfare.

In the light of results presented in this chapter, further work that could be done to enhance the understanding and potential of this system would be to look at the reaction between dye and alkylating agent in the presence of drug by NMR. Testing can also be carried out with other drugs to see if a universal assay system for alkylating agents can be developed. Other refinements to the system could involve the production of a sensor which may involve the dye covalently attached to a polymer or present in a sol/gel type sensor.

5.5 Conclusions

In this chapter the idea of genotoxic impurities was introduced. Reichardt's dye (2,6-diphenyl-4-(2,4,6-triphenyl-1-pyridinio)phenolate) was identified as a potentially useful dye molecule for the optical detection of alkylating agents. Testing was carried out with 4-chloro-1-butanol, 1-bromobutane, ethyl methane sulfonate and Fast Red B which showed the optimum reaction conditions to detect the presence of the alkylating agents at different concentrations. 2,6-diphenyl-4-(2,4,6-triphenyl-1-pyridinio)phenolate was found to be the most suitable dye molecule of the three investigated. As the two most industrially relevant impurities, NMR was carried out on the reactions of 4-chloro-1-butanol and ethyl methane sulfonate with Reichardt's dye and the alkylated dye product of the reaction was confirmed. Testing of the dye and alkylating agent in the presence of acetaminophen at 10 mg/ml and 100 mg/ml was carried out and this showed the linearity of the assay remained to some degree but the drug was interfering with the assay.

6 Overall Discussion and Future Work

The work of Chapter 3 was been aimed at gaining understanding of particular elements of the swabbing process. Swab sampling is a critical aspect of the cleaning verification process. It is of paramount importance that a pharmaceutical company can accurately estimate the amount of material remaining on its manufacturing equipment. At present many companies have validated processes for a particular drug in combination with a particular swab and analytical technique. Understanding does not go much further beyond a particular swab, drug and solvent combination producing adequate recoveries. Companies at present do not know what is their optimum combination of swab, solvent and drug. The results presented in Chapter 3 demonstrate how compound recovery can be affected by the combination of swab, solvent and drug. It was shown that recoveries varied in some instances from forty eight percent to eighty eight percent.

The literature in the cleaning verification field often makes fairly general claims about what type of swabs should be used. This work puts some of those claims into context because it has produced typical recoveries for different swab, solvent and drug combinations and also quantified the process of debris generation. We have shown that the extraction procedure is generally efficient and that the remaining drug is left behind on the surface of interest rather than remaining unextracted from the swab. It was found that in line with manufacturers' claims, debris generation was low. This is an important confirmation, particularly for swabs that are marketed for applications in clean room environments.

The section of the study which shed light on the swabbing process and demonstrated that the critical feature of the swabbing process – recovery, can be affected

significantly by the swab, solvent and drug combination was also particularly useful for Chapter 4 and the SERS enquiry.

Another aspect of the swabbing process on which important light was shed was error. All swab sampling was carried out by one person in order to minimise variation but the results showed that a certain amount of error is inherent in the swabbing process. It was also shown that certain combinations of swab, solvent and drug had smaller errors which again is a very important point because it shows that companies can reduce the amount of error in their swabbing process by choosing a proven combination of swab, solvent and drug.

Cleaning verification itself is a growing field because there is currently a more widespread desire within the pharmaceutical industry to deviate away from an HPLC driven cleaning verification process. This is because other analytical techniques which offer faster analysis times and potential portability are starting to emerge as serious alternatives to HPLC. Companies producing this new generation of analytical technology are tending to focus on total organic carbon analysis, ion mobility spectroscopy and UV analysis. In this study, we have provided evidence to support the idea that surface enhanced Raman spectroscopy is a potentially useful analytical technique capable of meeting the sensitivity requirement for cleaning verification work and having the advantages of specificity, portability and rapid analysis times. The use of commercially available Klarite™ SERS slides to measure swab extracts proved a successful approach. This section of the project has received commercial funding to continue. It is hoped that through our work, the SERS approach can be

optimised further in combination with chemometric analysis to offer a very credible alternative to HPLC analysis of cleaning verification samples.

In terms of further experiments for SERS and cleaning verification a number of options exist. In many ways the capability of the technique is limited by the reproducibility of the SERS effect. By employing the commercially available Klarite™ SERS substrates it has been shown that analysis of cleaning verification samples can be carried out. With analysis of cleaning samples being an industrial process of importance it is essential that the SERS effect is reproducible. As has already been said the reproducibility comes from he highly ordered nano-architecture of the Klarite™ slide. Advances in SERS and SERS substrates will only improve the techniques' amenability to the problem of cleaning verification. As was discussed in the literature review, tip-enhanced Raman spectroscopy is a technique of immense promise, particularly in combination with fibre optic cable that would allow for portable sampling and direct measurement from contaminated surfaces. Our attempts to produce a SERS swab were the beginning in a potential line of enquiry that may yield a sampling device capable of directly detecting contamination of manufacturing equipment.

As has already been said, genotoxic impurities are a subject of growing importance within the field of pharmaceutical manufacturing. Until now their analysis has relied on the traditional techniques of analytical chemistry. In this study, a potential optical sensor for commonly occurring alkylating impurities has been developed on the basis of the molecule known as Reichardt's dye. The assay was developed by dissolving

the dye in organic solvent and testing the effect of various alkylating agents and varied conditions.

The findings showed that in ordinary circumstances where Reichardt's dye and alkylating agent were present in solvent, the reaction proceeded efficiently and could be used to form the basis of a linear assay. It then became apparent that the presence of drug alongside Reichardt's dye and alkylating agent had an adverse effect on the linearity on the assay. The absorption maximum of Reichardt's dye also reduced significantly in the presence of acetaminophen and the alkylaton induced changes in absorption maximum reduced in size in the presence of acetaminophen and caused poorer separation of absorption maxima between different concentrations of alkylating agent. It was established through experimentation that apparent pH might have been affecting the performance of Reichardt's dye. The introduction of phosphate buffer at pHs 5.0, 7.0 and 9.0 in 5% water showed that the absorption maximum of Reichardt's dye was affected by apparent pH. Unfortunately it was not possible to buffer reactions where drug was present with phosphate buffer and so the base triethylamine was used. It was found that the presence of triethylamine did not stabilise the reaction when acetaminophen was present.

The work on Reichardt's dye and alkylating agents showed clear potential for the development of an optical sensor for genotoxic impurities. The problem of drug interference would need further investigation and there are a number of ways by which this could be done. It was clear that apparent pH and water had an adverse effect on dye performance so other solvent conditions could be investigated. Reichardt's dye could be investigated as a sensor through inclusion of the molecule in

polymer films or through covalent attachment to polymeric fibres. The dye's performance may differ in these conditions and so drug interference may prove less problematic. Through inclusion in a sensor type device it may prove possible to increase the overall sensitivity of the assay by having large amounts of dye present in a relatively small area. Should it not prove possible to circumnavigate the problem of drug interference then the assay would still work in combination with an appropriately chosen separation column or through solid phase extraction which is the predominantly employed technique when cleaning up samples for genotoxic analysis.

In summary this project has addressed issues associated with the production of pharmaceuticals. Through experimentation the understanding of the swabbing process has been increased, surface enhanced Raman spectroscopy has been shown as a technique of promise for the analysis of cleaning verification samples and a simple and rapid linear assay for alkylating agents has been developed that through further refinement may turn out to be an industrially implementable system.

7 References

Aldrich, D. S. & Smith, A. S., (1999). Pharmaceutical application of infrared microspectroscopy. Applied Spectroscopy Reviews. **34,** (no 4), 275-327

Argentine, M.D., Owens, P.K. & Olsen, B.A., (2007). Strategies for the investigation and control of process related impurities in drug substances. Advanced Drug Delivery Reviews. **59**, 12-28

Aroca, R.F., Alvanez_Puebla, R.A., Pieczonka, N., Sanchez-Cortes, S., & Garrcia-Ramos, J.V., (2005) Surface Enhanced Raman scattering on colloidal nanostructures. Advances in Colloid and Interface Sciences. **116**, 45-61.

Bazzaoui, E.A., Bazzoui, M., Aubard, J., Lomas, J.S., Felidj, N., & Levi, G., (2001). Surface-enhanced Raman scattering study of polyalkylthiophenes on gold electrodes and in silver colloids. Synthetic Metals. **123**, 299-309.

Bley, H. & Behrning, S., (2001). FT-IR spectroscopy for quantifying surface cleanliness. Research & Development **1**, (S), 41-44

Brolo, A.G., Irish, D.E., & Lipowski, J., (1997) Surface Enhance Raman spectra of Pyradine and pyrazine on a Au(210) single-crystal electrode. Journal of Physical Chemistry. **101**, 3906-3909.

Bugay, D. E., (2001). Characterisation of the solid state spectroscopic techniques. Advanced Drug Delivery Reviews. **48,** 43-65

Callon, I. & Richoll, S.M.,(2005). Determination of methyl and ethyl esters of methanesulfonic, benzenesulfonic and p-toluenesulfonic acids in active pharmaceutical ingredients by solid-phase microextraction (SPME) coupled to GC/SIM-MS. Journal of Pharmaceutical and Biomedical Analysis. **39**(3-4), 477-485

Campion, A., & Kambhampandi, P., (1998). Surface-enhanced Raman scattering. Chemical Society Reviews. **27**, 241-250.

Cao, Y., & Li, Y.S., (1999). Constructing surface roughness of silver for surface-enhanced Raman scattering by self-assembled monolayers and selective etching process. Applied Spectroscopy, **53**, 540-546.

Carreno, L., Carrasco, N., & Rezende, M.C., (1999). Kinetics of methylation of a solvatochromic vinylogous α-pridone in different solvents. International Journal of Chemical Kinetics. **31**(11), 819-825.

Chen, K., Leona, M., Vo-Dinh, K.C., Yan, F., Wabuyele, M.D., & Vo-Dinh, T., (2005). Application of surface-enhanced Raman scattering (SERS) for the identification of anthraquinone dyes used in works of art**.** Journal of Raman Spectroscopy. **37**(4), 520 – 527.

Ciurczak, E. W., (1998). Validation of spectroscopic methods in pharmaceutical analyses. Pharmaceutical Technology. **22** (no 3), 92-102

Ciurczak, E. W. & Drennen, J, K., (2002). Applications of near infrared spectroscopy. In Near-infrared applications in Biotechnology, 349-366. Edited by R Raghavachari. (Dekker, NewYork).

Cooper, D. W. (1996). Reducing Pyrogens in Cleanroom Wiping Materials. Pharmaceutical Engineering. **16** (no 4) 1-4.

Cooper, D. W. (1997). Cleaning, validating and monitoring aseptic fill areas. Pharmaceutical Technology Asia. **Sep/Oct**. 1-6.

Cutmore, E. A. & Skett, P. W. (1992). Applications of FT-Raman spectroscopy to a range of compounds of pharmaceutical interest. Spectrochimica Acta **49A,** (no 5/6), 809-818

Dickert, F.L., Geiger, U., Lieberzeit, P., & Reutner, U., (2000). Solvatochromic betaine dyes as optochemical sensor materials: detection of polar and non polar vapours. Sensors and Actuators B. **70**, 263-269.

Dou, X., Jung, Y.M., Cao, Z., & Ozaki, Y., (1999). Surface-enhanced Raman scattering of biological molecules of metal colloid II: effects of aggregation of gold colloid and comparison effects of pH of glycine solutions between gold and silver colloids. Applied Spectroscopy. **53,** (No 11), 1440-1447.

FDA (1993). FDA guide to inspections of validated cleaning processes.

Fabriciova, G., Garcia-ramos, J.V., Miskovsky, P., & Sancez-Cortes, S., (2004). Adsorption and acidic behaviour of anthraquinone drugs quinizarin and danthron on Ag nanoparticles studied by Raman spectroscopy. Vibrational Spectroscpy. **34**, 273-281.

Faulds, K., Littleford, R.E., Graham, D., Dent, G., & Ewen-Smith, W., (2004). Comparison of surface-enhanced resonance Raman scattering from unaggregated and aggregated nanoparticles. Analytical Chemistry. **76**, 592-598.

Fletcher, K.A., Storey, I.A., Hendirck, A.E., Pandey, S., & Pandey, S., (2001) Behaviour of the solvatochromic probes Reichardt's dye, pyrene, dansyamide, Nile Red and 1-pyrenecarbaldehyde within the room-temperature ionic liquid bmimPF_6. Green Chemistry. **3**, 210-215.

Findley, P. W. & Bugay, D, E. (1998). Raman Spectroscopy for the study of pharmaceutical crystal forms. Journal of Pharmaceutical and Biomedical Analysis. **16,** 921-930

Freeman, R.G., Hommer, M.B., Grabar, K., Jackspon, M.A., & Natan, M.J., (1996). Ag-clad Uu nanoparticles: novel aggregation, optical and surface enhanced Raman scattering properties. Journal of Physical Chemistry. **100**, 718-724.

Frens, G., (1973). Controlled nucleation for the regulation of the particle size in monodisperse gold suspensions. Nature Physical Science. **241**, 20 - 23

Gavlick, W. K., Ohlemeir, L.A. & Kaiser, H. J., (1995). Analytical strategies for cleaning residue determination. Pharmaceutical Technology **19,** 136-144

Gonzalez, F. & Pous, R. (1995). Quality control in manufacturing processes by near infrared spectroscopy. Journal of Pharmaceutical and Biomedical Analysis **13** (No 4/5), 419-423

Gunzler, H. & Gremlich, H. U. (2002). IR spectroscopy: an introduction. (Wiley. Weiheim).

Hollas, M. (1995). Basic Atomic and Molecular Spectroscopy. (Royal Society of Chemistry. McGraw-Hill. London)

Hossain, M.K., Shibamoto, K., Ishioka, K., Kitajima, M., Mitani, T., & Nakashima, S., (2006). 2D nanostructure of gold nanoparticles: an approach to SERS active substrates. Journal of Luminescence. **122-123**, 792-795.

Imai, Y. & Chujo, Y., (2000). Solvatochromic Characterization of Organic-Inorganic Polymer Hybrids with Pyridinium *N*-Phenolate Betaine Dyes. Macromolecules **33** (8), 3059 -3064.

Jacobson-Kram, D. & McGovern, T., (2007). Toxicological overview of impurities in pharmaceutical products. Advanced Drug Delivery Reviews. **59**, (No. 1), 38-42

Jenkins, K. M. & Vanderweilen, A. J. (1994). Cleaning validation: an overall perspective. Pharmaceutical Technology. **18,** 60-73

Jenkins, K.M., Vanderweilen, A.J., Armstrong J.A., Leonard, L.M., Murphy, G.P. & Piros, N.A. (1996). Application of total organic carbon analysis to cleaning validation. Journal of Pharmaceutical Science and Technology. **50,** (No 1), 6-15.

Kaiser, H. J., Tirey, J. F. & LeBlanc, D. A. (1999). Measurement of organic and inorganic residues from surfaces. Journal of validation technology. **6,** (no 1).

Kaiser, H.J. & Minowitz, M. (2001). Analyzing cleaning samples: what method? Journal of Validation Technology. **7**, (No 3), 2-12.

Kirkland, D. & Snodin, D., (2004). Setting limits for genotoxic impurities in drug substances: Threshold-based and pragmatic approaches. International Journal of Pharmaceutical Medicine. **18**: 197-207

Klinkenberg, R., Streel, B. & Ceccato, A. (2003). Development and validation of a liquid chromatographic method for the determination of amlodipine residues on manufacturing equipment surfaces. Journal of pharmaceutical and Biomedical Analysis. **32,** 345-352

Kneipp, K., Kneipp, H., Manoharan, R., Hanlon, E.B., Itzkan, I., Dasari, R.R., & Feld, M.S., (1998). Extremely large enhancement factors in surface-enhanced raman scattering for molecules on colloidal gold clusters. Applied Spectroscopy. **52,** (no 12), 1493-1497.

Kneipp, K., Kneipp, H., Manoharan, R., Itzkan, I., Dasari, R.R., & Feld, M.S., (1998). Surface-enhanced Raman scattering (SERS) – a new tool for single molecule detection and identification. Bioimaging. **6**, 104-110.

Kneipp, K., wang, Y., Kneipp, H., Perelman, L.T., Manoharan, R., Itzkan, I., Dasari, R.R., & Feld, M.S., Single molecule detection using surface-enhanced Raman scattering. Physical Review Letters. (**78**, no 9), 1667-1670.

Krech, J.H., & Rose -Pehrsson, S.L., (1997) Detection of volatile organic compounds in the vapor phase using solvatochromic dye-doped polymers. Analytica Chimica Acta. **341**, (No 1), 53-62.

Kuncicky, D.M., Prevo, B.G. and Velev, O.D., (2006). Controlled assembly of SERS substrates templated by colloidal crystal films. Journal of Materials Chemistry. **16**(13), 1197–1296.

Lakowicz, J. R. (1999). Principles of fluorescence spectroscopy. (Kluwe, New York.)

Lee, V.Y. & Farquharson, S., (1999). Surface-enhanced Raman sensor for trace chemical detection in water. Proceedings of SPIE. **3857:** November, 76-84.

Leopold, N., Cinta-Pinzaru, S., Baia, M., Antonescu, E., Cozar, O., Kiefer, W., & Popp, J., (2005). Raman and surface-enhanced Raman study of thiamine at different pH values**.** Vibrational Spectroscopy. **39**, (Issue 2), 169-176.

Li, H. & Slugget, G.W., (2005). Development and validation of a sensitive GC-MS method for the determination of trace levels of an alkylating reagent in a β-lactam active pharmaceutical ingredient. Journal of Pharmaceutical and Biomedical Analysis. **39**, 486-494.

Li, Y., Bachmann, K.A. & Cameron, B.D., (2003). In vivo cytochrome p450 drug metabolizing enzyme characterization by surface enhanced Raman spectroscopy. Proceedings of SPIE. **4967**, 179-184.

Linert, W., Straus, B., Herlinger, E., & Reichardt, C., (1992). Alkylation of pyridinium-N-phenoxide betaine dyes with iodomethane: substituent, solvent and temperature dependence. Journal of Physical Chemistry. **5**, 275-284.

Liu, L. & Pack, B.W. (2007). Cleaning verification assays for highly potent compounds by high performance liquid chromatography mass spectrometry: strategy, validation, and long-term performance. Journal of Pharmaceutical and Biomedical Analysis. **43** (4), 1206-1212.

Maruyama, Y., Ishikawa. M., & Futamata, M., (2001) Single molecule detection with SERS. Analytical Sciences. **17**, 1181-1183.

McCreery, R. L. (2000). Raman spectroscopy for chemical analysis. (Wiley & Sons, Chichester).

McGovern, T.M. & Jacobson-Kram, D., (2006). Regulation of genoxotxic and carcinogenic impurities in drug substances and products. Trends in Analytical Chemistry. **25**, 790-795.

Mehta, N.K., Goenaga-Polo, J., Hernandez-Rivera, S. P., Hernandez, H., Thomson, M. A. & Melling, P. J. (2002). Development of an in situ spectroscopic method for cleaning validation using mid-IR fiber optics. *Bio Pharm,* May 36-42

Mieza, T., Lunn, M. J., Keely, F. J., George, R. C. & Bodemiller, J. R., (1999). Cleaning level acceptance criteria and a high pressure liquid chromatography procedure for the assay of Meclizine Hydrochloride residue in swabs collected from pharmaceutical manufacturing equipment surfaces. Journal of Pharmaceutical and Biomedical Analysis. **19,** 747-756

Miscoscio, K. (1997). Choosing the correct swab for cleaning validation. Cleanrooms. **January**, 1-4.

Moreira, A. B., Dias, I. L.T., Graciliano, O. N., Zagatto, E. A.G. & Kubota, L. T. (2004). Solid-phase fluorescence spectroscopy for the determination of acetylsalicylic acid in powdered pharmaceutical samples. Analytica Chimica Acta. **523,** 49-52

Moskovits, M., (2005) Surface-enhanced Raman spectroscopy: a brief retrospective. Journal of Raman Spectroscopy. **36**, 485-496.

Müller, L., Mauthe, R.J., Riley, C.M., Andino, M.M., De Antonis, D., Beels, C., DeGeorge, J., De Knaep, A.G.M., Ellison, D., Fagerland, J.A., Frank, F., Fritschel, B., Galloway, S., Harpur, H., Humfrey, C.D.M., Jacks, A.S., Jagota, N., Mackinnon, J., Mohan, G., Ness, D.K., O'Donovan, M.R., Smith, M.D., Vudathala, G., & Yotti, L., (2006). A rationale for determining, testing and controlling specific impurities in pharmaceuticals that possess potential for genotoxicity. Regulatory Toxicology and Pharmacology. **44**, 198-211.

Munro, C.H., Smith, W.E., Garner, M., Clarkson, J., & White, P.C. (1995). Characterisation of a surface of a citrate reduced colloid optimised for use as a substrate for surface enhanced Raman resonance scattering. Langmuir. **11**, 3712-3720.

Myers, T., Kasica, T. & Chirai S. (1997). Approaches to cycle development for clean-in-place processes. Journal of Parenteral Medicine. **41,** (no 1), 9-15

Nozal, M. J., Bernal, M. J., Toribio L, Jimenez, J. J. & Martin M. T. (2000). Validation of acetylsalicylic acid recovery and determination of residues on various surfaces by high performance liquid chromatography. Journal of Chromatography, **870,** 69-75

Nozal, M. J., Bernal, J. L., Toribio, L, Martin, M. T. & Diez, F. J. (2002). Development and validation of an LC assay for sumatriptan succinate residues on surfaces in the manufacture of pharmaceuticals. Journal of Pharmaceutical and Biomedical Analysis, **30,** 285-291

O'Neal, P.D., Motamedi, M. & Lin, W.C., (2003). Feasibility study using surface enhanced Raman spectroscopy for the quantitative detection of excitatory amino acids. Journal of Biomedical optics. **8**(1), 33-39.

Pal, A., Pal, T. Stokes, D. & Vo Dinh, T., (2003). Photochemically prepared gold nanoparticles: a substrate for surface enhance Raman scattering. Current Science. **84**, (no 10), 1342-1346.

Paley, S.M., & Harris, M.J. (1991). Synthesis and characterisation of some pyridinium-N-phenoxide betaine dyes for second-harmonic generation. Journal of Organic Chemistry. **56**, 568-574.

Pavia, D. L., Lampman, G. M. & Kriz, G. S. (2001). Introduction to Spectroscopy 3rd Edition. (Thomson Learning, London).

Pettinger, B., Ren, B., Picardi, G., Schuster, R., & Ertk, G., (2005). Tip-enhanced Raman spectroscopy (TERS) of malachite isothiocyanate at Au(111): bleaching behaviour under the influence of high electromagnetic fields. Journal of Raman Spectroscopy. **36**, 541-550.

Quagliano, L.G. (2004). Surface enhanced Raman scattering to study surface contamination on semiconductors. Surface Science **566-568**, 875-879.

Reichardt, C., Eschener, M., & Schafer, G., (2001). Syntheses and UV-visible spectroscopic properties of new 'flurophillic' fluorine- and perfluoroalkyl-substituted solvatochromic pyridinium N-phenolate betaine dyes. Journal of Physical Organic Chemistry. **14**, 737-751.

Sanchez-Cortes, S., Vasina, M. Francioso, J.V. & Garcia-Ramos, J.V., (1998). Raman and surface-enhanced Raman scpectroscopy of dithiocarbamate fungicides. Vibrational Spectroscopy. **17**, 133-144.

Severdia, A. G, (1995). Transmission FT-IR spectroscopy applied to the determination of hydrocarbon residues on pharmaceutical process equipment. Applied Spectroscopy. **49**(4), 540-541

Sharma, A. & Shuman, S. G. (1999). Introduction to fluorescence spectroscopy. (Wiley, Chichester).

Shifflet, M.J. & Shapiro, M. (2002). Development of Analytical Methods to Accurately and Precisely Determine Residual Active Pharmaceutical Ingredients and Cleaning Agents on Pharmaceutical Surfaces. American Pharmaceutical Review. **4**, 35–39.

Simonovska, B., Andrensek, S., Vovk, I. & Prosek, M. (1999). High performance thin-layer chromatography method for monitoring norflaxin residues on pharmaceutical equipment surfaces. Journal of Chromatography. **862,** 209-215

Sommer, A. J. & Hardgrove, M. (2000). Attenuated total internal reflection infrared microspectroscopy for the analysis of trace solutes in aqueous solutions. Vibrational Spectroscopy. **24,** 93-100

Somsen, G. W., Gooijer, C., Velthorst, N. H. & Brinkman, U. A. Th (1998). Coupling of column liquid chromatography and Fourier transform infrared spectrometry. Journal of Chromatography. **811,** 1-34

Stokes, D.L., Chi, Z., & Vo-Dinh, T., (2004). Surface-enhanced-Raman-scattering-inducing nanoprobe for spectrochemical analysis. Applied Spectroscopy. **58**, (no 3), 292–298.

Stuart, B. (2004). Infrared spectroscopy: fundamentals and approaches. (Wiley, Chichester).

Sun, X., Dong, S., & Wang, E., (2005). One-step preparation of highly concentrated well-stable gold colloids by direct mix of polyelectrolyte and $HAuCl_4$ aqueous solutions at room temperature. Journal of Colloid and Interface Science. **288,** (issue 1), 301-303.

Taylor, T.E., Gosliong, M. & Pearce, A., (2005). Low level determination of ρ-toluenesulfonate and benzenesulfonate esters in drug substance by high performance liquid chromatography/mass spectrometry. Journal of Chromatography A. **1119**, 231-237.

Trachta, G., Schwarze, B., Sagmuller, B., Brehm, G. & Schneider, S., (2004). Combination of high-performance liquid chromatography and SERS detection applied to the analysis of drugs in human blood and urine. Journal of Molecular Structure. **693**, 175-185.

Urbas, A. A., & Lodder, R. A., (2003). *In situ* spectroscopic cleaning. *NIR news.* **14, (**no 2) 8-10

Valeur, B. (2002). Molecular fluorescence. (Wiley, Weinheim).

Valvis, I.I. & Champion W.L. (1999). Cleaning and decontamination of potent compounds in the Pharmaceutical industry. Organic Process Research & Development. **3**, 44-52.

Viets, C., & Hill, W., (2004). Fibre-optic SERS sensors. The internet Journal of Vibrational Spectroscopy. **4**, edition 2.

Wang, Y., Li, Y.S., Zhang, Z., & An, D., (2003). Surface-enhanced Raman scattering of some water insoluble drugs in silver hydrosols. Spectrochimica Acta part A. **59**, 559-594.

Wargo, D..J. & Drennen, J. K. (1995). Near-infrared spectroscopic characterisation of pharmaceutical powder blends. Journal of Pharmaceutical and Biomedical Analysis. **14,** 1415-1423

Williams, D. H. & Fleming, I. (1995). Spectroscopic methods in organic chemistry. (Mc Graw-Hill. Berkshire).

Wold, S., (1987). Principal Component Analysis. Chemometrics and Intelligent Laboratory Systems. **2**, 37 – 52.

Xu, H., & Kall, M., (2003). Polarization-dependant Surface-enhanced Raman spectroscopy of isolated silver nanoaggregates. ChemPhysChem. **4**, 1001-1005.

Yoon, W. I., Jee, R. D., Charvill, A., Lee, G. & Moffat, A. C. (2004). Application of near-infrared spectroscopy to the determination of the sites of manufacture of proprietary products. Journal of Pharmaceutical and Biomedical Analysis. **34,** 933-944.

Zeller, A.O. (1993). Cleaning validation and residue limits: a contribution to current discussions. Pharmaceutical Technology **October**. 70-80.

8 Appendices

8.1 Appendix 1 – fabrication of SERS nanostructures by Dr Jin-Sung Kim (University of Michigan)

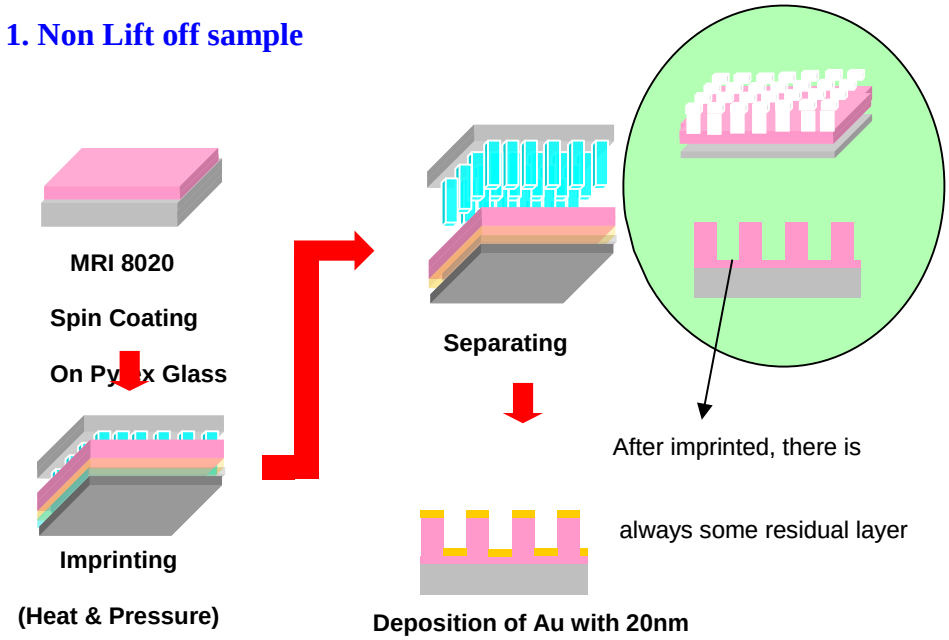

2. Lift off sample